The Dissertation Committee for Babatunde Adegboyega Oyenekan certifies that this is the approved version of the following dissertation:

Modeling of Strippers for CO_2 Capture by Aqueous Amines

Committee:

Gary Rochelle, Supervisor

Thomas F. Edgar

Keith P. Johnston

Kamy Sepehrnoori

R. Bruce Eldridge

Frank Seibert

Modeling of Strippers for CO_2 Capture by Aqueous Amines

by

Babatunde Adegboyega Oyenekan, B.Sc.; M.S.

Dissertation

Presented to the Faculty of the Graduate School of

the University of Texas at Austin

in Partial Fulfillment

of the Requirements

for the Degree of

Doctor of Philosophy

The University of Texas at Austin

May 2007

To My Family

Acknowledgments

I would like to thank Dr. Gary Rochelle for his support, insights and encouragement during this work. His direction has exposed me to a wide variety of topics. He has provided me with opportunities that have developed me both professionally and personally by attending numerous national and international meetings. I will always cherish the chance to interact with numerous industrial sponsors.

Aspen Technology's in kind support of the Aspen Plus and Aspen Custom Modeler used in this work is appreciated.

The three executive assistants to the Rochelle group during my stay here made my academic career at UT a lot easier. Thank you Jody Lester, Lane Salgado and Maeve Cooney.

I have had the pleasure of interacting professionally and personally with a number of past students in Dr. Rochelle's research group, including Dr. Mohammed Al-Juaied, Dr. Tim Cullinane, Dr. George Goff, Ian Wilson, Akin Alawode, Chuck Okoye, John McLees and current students: Eric Chen, Marcus Hillard, Ross Dugas, Andrew Sexton, Jason Davis, Bob Tsai, David VanWagener, Jorge Plaza, Sepideh Ziaii Fashami and Qing Xu. Thank you for your friendship and contributions during the weekly group meetings.

Thank you Dr. Frank Seibert your time and interest in my research and professional development. I would like to thank Chris Lewis, Robert Montgomery and

Steve Briggs at The Pickle Research Campus (PRC) for their help especially during the pilot plant campaigns and in answering questions I had concerning operations at the PRC.

I had the pleasure of taking classes and learning from some excellent faculty members including Professors Benny Freeman, Bruce Eldridge, Kamy Sepehrnoori, Mukul Sharma and Krishan Malik. I thank Professor Michael Poehl for the opportunity to serve as a teaching assistant for the Senior Plant Design course twice under his tutelage.

I would like to take my friends and roommates at different times – Azubuike Egwuenu, Rotimi Ojifinni and Babatunde Oguntade. Thanks for your help and encouragement. You guys made my life a lot easier.

I appreciate the prayers, love, care, concern and motivation of my family – Mrs. Anne Adetoun Oyenekan, Dr. and Mrs. Lanre Oyenekan, Mr. And Mrs. Akinola Ishola, Mrs. Olajumoke Lewis, Mrs. Adetola Olusoga, Dr. and Mrs. Sola Labinjo, Mr. and Mrs. Ojeme, Mr. and Mrs. Kayode Savage, Olubiyi, Adetola, Olanrewaju, Omolara, Oluwagbemisayo, Funmi and Adedolapo.

I would like to thank my wife, Olamide. She has been very supportive, understanding and a constant source of encouragement. Thank you for adding to my life by being a part of it. Thanks for taking good care of our daughter, Opemipo.

Finally, I am grateful to the Almighty God for His wisdom, knowledge, understanding, guidance and direction. I thank Him for the gift of life and the strength to carry out this work.

This dissertation was prepared with the support of the U.S. Department of Energy, under Award No. DE-FC26-02NT41440. However, any opinions, findings, conclusions, or recommendations expressed herein are those of the authors and do not necessarily reflect the views of the DOE.

Modeling of Strippers for CO_2 Capture by Aqueous Amines

Publication No._____

Babatunde Adegboyega Oyenekan, Ph.D.

The University of Texas at Austin, 2007

Supervisor: Gary T. Rochelle

This work evaluates stripper performance for CO_2 capture using seven potential solvent formulations and seven stripper configurations. Equilibrium and rate models were developed in Aspen Custom Modeler (ACM). The temperature approach on the hot side of the cross exchanger was varied between 5 – 10^{o}C.

The results show that operating the cross exchanger at a 5^{o}C approach results in 12% energy savings for a 7m MEA rich solution of 0.563 mol/mol Alk and 90% CO_2 removal. For solvents with ΔH_{abs} < 60 kJ/gmol CO_2, stripping at 30 kPa is more attractive than stripping at 160 kPa. Normal pressure (160 kPa) favors solvents with high heats of desorption. The best solvent and process configuration, matrix with MDEA/PZ, offers 22% and 15% energy savings over the baseline and improved baseline, respectively, with stripping and compression to 10 MPa. The energy requirement for stripping and

compression to 10 MPa is about 20 % of the power output from a 500 MW power plant with 90% CO_2 removal.

Rate model results show that a 'short and fat' stripper requires 7 to 15% less equivalent work than a 'tall and skinny' one. The optimum stripper design could be one that operates between 50% and 80% flood at the bottom. Stripping at 30 kPa and 160 kPa require 230 s and 115 s of effective packing volume to get an equivalent work 4% greater than the minimum. Stripping at 30 kPa with $\Delta T = 5^{o}C$ was controlled by mass transfer with reaction in the boundary layer and diffusion (88% resistance at the rich end and 71% resistance at the lean end) and mass transfer with equilibrium reactions (84% resistance at the rich end and 74% resistance at the lean end) at 160 kPa.

The model was validated with data obtained from pilot plant experiments at the University of Texas with 5m K^+/2.5m PZ and 6.4m K^+/1.6m PZ under normal pressure and vacuum conditions using Flexipac AQ Style 20 structured packing. Foaming was experienced during tests. The effective packing height was 5.09m for 5m K^+/2.5m PZ and 6.47m for 6.4m K^+/1.6m PZ.

Contents

List of Tables

List of Figures

Nomenclature

A = cross sectional are of column [m^2]

act = activity of water regressed from Aspen Plus

act1, act2, act3 = activity expression constants

Alk = total alkalinity [mol K^+ + (2*mol PZ)]

a_T = specific dry packing area [m^2/m^3]

a_w = specific wetted area of packing [m^2/m^3]

Cp = heat capacity of liquid [kJ/mol-K]

$C_{p,i}$ = heat capacity of component i [kJ/mol K]

D_G = diffusivity of the gas [m^2/s]

D_L = diffusivity of the liquid [m^2/s]

d_p = nominal packing diameter [m]

E_{mv} = Murphree section efficiency defined in terms of partial pressures [-]

f = fractional flood at bottom [-] = $\frac{u_g}{u_{g,flood}}$

g = acceleration due to gravity [m^2/s]

g_{CO2} = mole rate of CO_2 [gmoles/s]

G_o = gas rate [kg/m^2-s]

H = height [m]

H_p = pump head [m]

h_{seg} = height of segment [m]

H_{vap} = heat of vaporization of water [45 kJ/mol]

k = ratio of heat capacity at constant pressure to that at constant volume (c_p/c_v)

K_{CO2} = equilibrium constant for CO_2 [kPa]

k_g = gas phase mass transfer coefficient [kmol/Pa-m^2-s]

K_G = overall mass transfer coefficient based on the gas phase [kmol/Pa-m^2-s]

k_g'' = liquid phase mass transfer coefficient based on a partial pressure driving force due to kinetics[kmol/Pa-m^2-s]

k_l = liquid phase mass transfer coefficient [m/s]

K_y = overall mass transfer coefficient in mole fraction units [kmol/m^2-s]

k_y' = liquid phase mass transfer coefficient in mole fraction units [kmol/m^2-s]

L = liquid flow rate [moles]

L = Liquid rate [gmoles/s]

ldg = [mol CO_2/(mol MEA + mol K^+ + mol 2 PZ + mol MDEA + KS-1]

L_o = liquid rate [kg/m^2-s]

m = slope of equilibrium line [Pa-m^3/kmol]

M_L = molecular weight of the liquid , 25.5 [g/gmol]

mol Alk = [mol MEA + mol K^+ + mol 2 PZ + mol MDEA + mol KS-1]

n_{CO2} = mole of CO_2 [moles]

$n_{CO2,product}$ = mole of CO_2 in N_2 rich stream [moles]

$n_{CO2,removed}$ = mole of CO_2 in CO_2 stream [moles]

N_{CO2} = flux of CO_2 [kmol/m^2-s]

n_{H2O} = mole of H_2O [moles]

n_{N2} = mole of nitrogen [moles]

$n_{N2,product}$ = mole of nitrogen in N_2 rich stream [moles]

$n_{N2,removed}$ = mole of nitrogen in CO_2 stream [moles]

P = reboiler pressure [kPa]

P_1, P_2 = initial and final pressures for ideal compression [kPa]

P_{CO2} = partial pressure of CO_2 in the bulk gas [kPa]

P_{CO2}* = equilibrium partial pressure of CO_2 [kPa]

P_{CO2i} = partial pressure of CO_2 at the gas/liquid interface [kPa]

P_n = partial pressures on sections n [kPa]

P_n* = equilibrium partial pressure leaving section n [kPa]

P_{n-1} = partial pressures sections n-1 [kPa]

Polyeff = polytropic efficiency = 0.75

P_T = total pressure of a segment [kPa]

Q = reboiler duty [kJ/gmol CO_2]

Q_{des} = Heat of desorption of CO_2 [kJ/gmol CO_2]

$Q_{H2O,gen}$ = Heat of steam generation [kJ/gmol CO_2]

Q_{sens} = Sensible heat required to heat rich solution to reboiler

R = universal gas constant [J/K-mol]

T = temperature [K] or [^{o}C]

T_{reb} = reboiler temperature [K] or [^{o}C]

T_{ref} = reference temperature [298.15 K]

u_g = superficial velocity of the gas [m/s]

$u_{g,flood}$ = superficial velocity of the gas at flood [m/s]

V = Vapor flow rate [moles]

v_L = liquid velocity [m/s]

W_{comp} = isentropic work of compression [kJ/gmol CO_2]

W_{eq} = equivalent work [kJ/gmol CO_2]

W_{ideal} = ideal work of compression [kJ/gmol CO_2]

W_{min} = theoretical minimum thermodynamic work [kJ]

$W_{min\ CO2\ removed}$ = work associated with the CO_2 stream [kJ]

$W_{min,flue\ gas}$ = work associated with the flue gas [kJ]

$W_{min,normalized}$ = theretical minimum thermodynamic work per gmol CO_2 removed [kJ/gmol CO_2]

$W_{min,product}$ = work associated with the N_2 rich stream [kJ]

W_{pump} = pump work [kJ/gmol CO_2]

$W_{reboiler}$ = equivalent work of reboiler [kJ/gmol CO_2]

x_{CO2} = mole fraction of CO_2 in flue gas [-]

$x_{CO2,product}$ = mole fraction of CO_2 in N_2 rich stream [-]

$x_{CO2,removed}$ = mole fraction of CO_2 in CO_2 stream [-]

x_{N2} = mole fraction of N_2 in flue gas [-]

$x_{N2,product}$ = mole fraction of N_2 in N_2 rich stream [-]

$x_{N2,removed}$ = mole fraction of N_2 in CO_2 stream [-]

X_{CO2} = CO_2 liquid mole fraction [mol CO_2/(mol amine + mol CO_2 + mol H_2O)]

X^o_{amine} = CO_2 free amine mole fraction [mol amine / (mol amine + mol H_2O)]

y = mole fraction in the vapor phase [-]

Greek Symbols

γ = CO_2 loading [mol CO_2/(mol MEA + mol K^+ + mol 2 PZ + mol MDEA + mol KS-1)]

ΔH = heat of absorption/desorption [kJ/gmol CO_2]

ΔP = pressure drop [=] kPa/m

ΔP_{flood} = pressure drop at flood , 1.63 kPa/m

ΔT = Temperature approach in cross exchanger [K]

η_p = pump efficiency [-]

μ_g = viscosity of the gas [Pa-s]

μ_l = viscosity of the liquid [Pa-s]

ρ_g = density of the gas [kg/m^3]

ρ_l = density of the liquid [kg/m^3]

σ_c = critical surface tension of the packing, 0.075 N/m

σ_L = surface tension of the packing, 0.04 N/m

τ = effective packing volume = $\frac{\text{volume of packing}}{\text{liquid rate}}$ [s]

Superscripts

L = liquid phase

V = vapor phase

Subscripts

i = component

j = segment j

j-1 = segment j-1 (segment above j)

j+1 = segment j+1 (segment below j)

Chapter 1 : Introduction

This chapter introduces the problem of CO_2 emissions from fossil fuel combustion. Coal-fired power plants are large point sources of CO_2 emissions in the United States and as such prime targets to reducing CO_2 emissions. Aqueous absorption/stripping is an important technological option for CO_2 capture from combustion gas. The problems associated with the implementation of this technology in coal-fired power plants are outlined and solutions suggested. The research problem is presented and the objectives and scope of this work are outlined.

1.1. Global Warming

The United States relies on fossil fuels for more than 85% of its energy needs. Future energy consumption projections suggest that the consumption of fossil fuels will be a significant portion of the energy mix for the next thirty years. Figure 1-1 shows the projected energy consumption from different sources through 2030. The combustion of

fossil fuels has increased the atmospheric concentrations of greenhouse gases (primarily CO_2). The earth's surface temperature increased by 0.6 ± 0.2 ^oC in the 20th century. This phenomenon is termed "global warming".

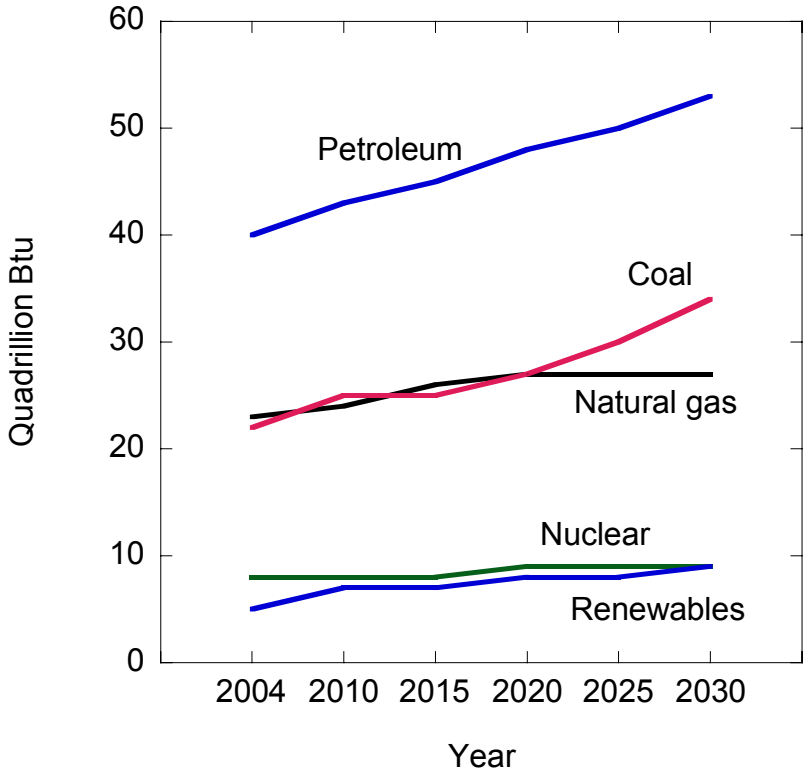

Figure 1-1: United States Projected Energy Consumption (2004 – 2030) (USEIA 2006)

Models referenced by the Intergovernmental Panel on Climatic Change (IPCC) suggest that the surface temperatures of the earth might increase by 1.5 – 5.8^oC between 1990 and 2100 if this trend is not curbed. If this situation is not addressed, rising sea levels and changes in the amount and pattern of precipitation will be experienced. This could lead to floods, droughts, heat waves, hurricanes and tornados with dire effects on

the quality of human life and severe economic and financial losses. Combating global warming and climatic change becomes necessary. In the United States in 2004, CO_2 accounted for 84.6% of the total greenhouse gas emissions, the balance being methane, CH_4 (7.9%), nitrous oxide, N_2O (5.5%) and halogenated compounds (2%). Fossil fuel combustion accounted for 94% of the CO_2 emissions in the United States in 2004 (USEPA 2006).

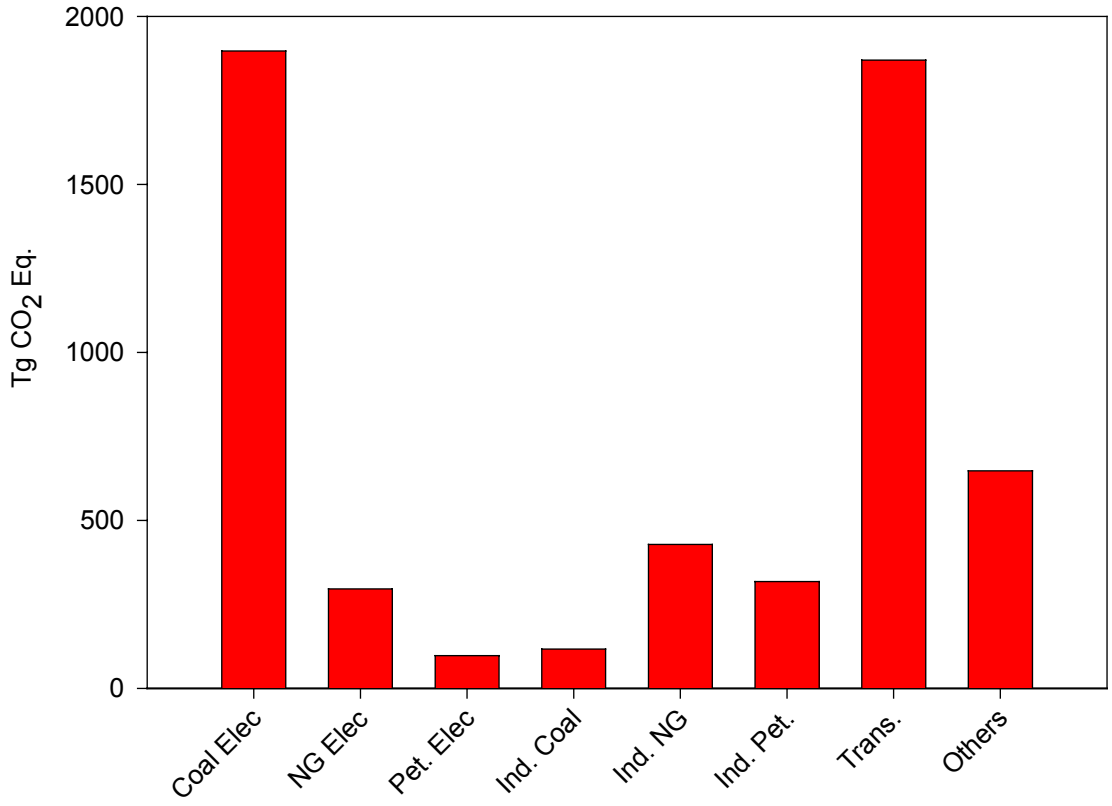

Figure 1-2: 2004 U.S. CO_2 emissions by sector (USEPA 2006)

Figure 1-2 shows the U.S. CO_2 emissions by sector in 2004. Coal-fired power plants and transportation contributed significantly to the overall emissions in 2004. Since the emissions by transportation are small point sources from vehicles and jet planes reducing emissions by transportation can only be achieved by the use of improved efficiency internal combustion engines. Coal-fired plants because of their number and large sizes are prime targets for reducing CO_2 emissions. The focus of this work is therefore CO_2 capture from coal-fired power plants.

1.2. CO_2 sequestration from a coal-fired power plant

CO_2 sequestration consists of two major activities. The first, capture, involves the separation of CO_2 from large point sources such as power plants, iron and steel plants and cement manufacturing plants while the second, storage, involves the injection of the captured CO_2 into geological or oceanic reservoirs for large timescales, typically hundreds of years. Power plants by virtue of their large sizes and significant emissions of CO_2 are prime candidates for CO_2 capture.

The system for CO_2 sequestration is shown in Figure 1-3. In a coal-fired power plant, coal is burned in air in a boiler producing hot gases and heat. The heat converts water in tubes lining the boiler walls into steam. The steam is used to run the turbines that generate electricity while the hot flue gases go through a particulate removal system, mainly an electrostatic precipitator (ESP) or bag house to remove the fly ash (particulates), a flue gas desulfurization (FGD) system to remove SO_2. The flue gases are

then sent to the absorption/stripping system for CO_2 capture. The concentrated CO_2 from the capture unit is then compressed and sent to disposal.

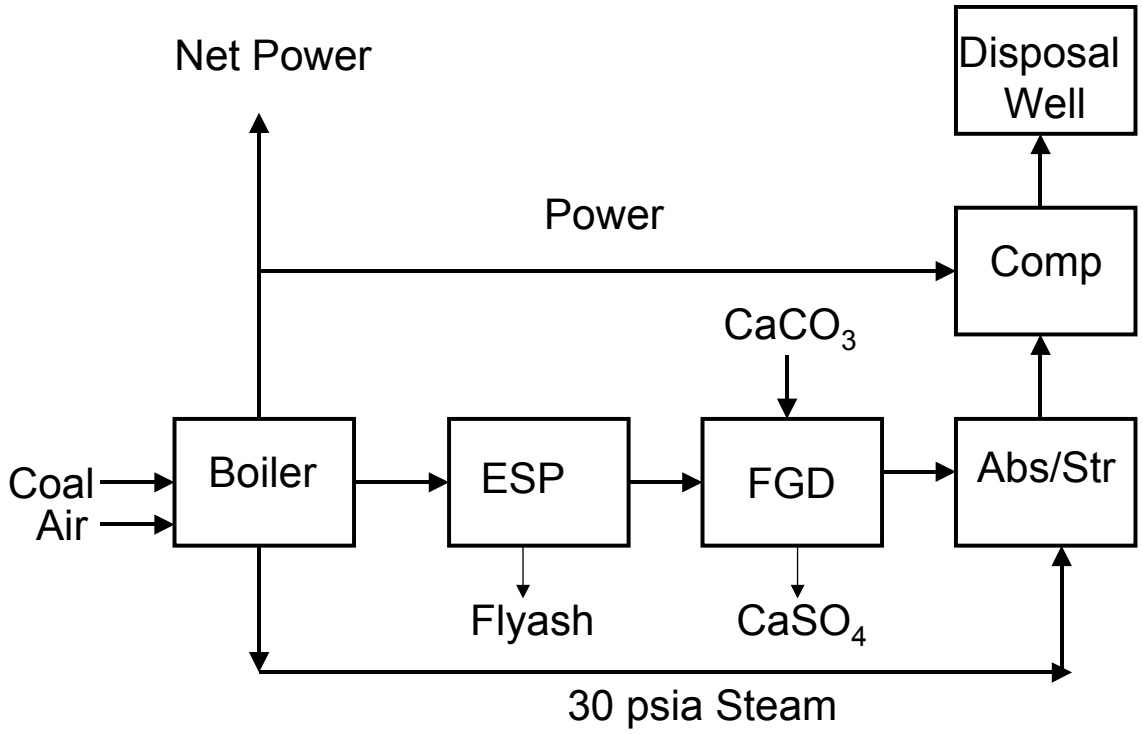

Figure 1-3: System for CO_2 Sequestration

Low-pressure (LP) steam withdrawn from the boiler is condensed in the reboiler in the stripping operation. This reduces the amount of steam that can be used in the low pressure turbine to generate electricity. Electric power is also used to drive the blowers, pumps and compressors in the process and this reduces the net power production from the plant.

1.3. Absorption/Stripping for CO_2 Capture

Aqueous absorption/stripping is one of the post-combustion methods for CO_2 capture that can be retrofitted to the tail end of a power plant and can be incorporated into new ones. This process has been widely used in natural gas processing and in syngas and ammonia production (Sartori, Ho et al. 1985; Weiland, Chakravarty et al. 1985; Goldstein, Brown et al. 1986; Vickery, Campbell et al. 1988; Bosch 1989; Veldman and Ball 1991; Sandall, Rinker et al. 1993). Figure 1-4 shows a typical flow diagram of the process. The system consists of two columns, the absorber, in which the CO_2 is absorbed into an amine solution via fast chemical reaction and a stripper where the amine is regenerated and then sent back to the absorber for further absorption. Prior to CO_2 removal, particulates, sulfur dioxide and NO_x are removed from the flue gas. The flue gas from the power plant is typically cooled before the absorber from 150^{o}C to 55^{o}C, its adiabatic saturation temperature, or to 40^{o}C if cooling water is used. A blower is used to drive the flue gas into the base of the first column, the absorber, in which the CO_2 reacts with the lean amine solution flowing from the top. The treated gas exits at the top of the tower. Typical target CO_2 removal efficiency is 90% though efficiencies ranging from 70% to 99% could be achieved in a well-designed absorber (Oyenekan and Rochelle 2006).

The exiting liquid, the rich solution, is then pumped through a cross heat exchanger and heated to a higher temperature by the lean solution from the stripper. If the sum of the equilibrium partial pressure of CO_2 and water in the rich solution is higher

than the operating pressure of the stripper, flashing occurs at the stripper inlet, desorbing some of the CO_2. Further desorption occurs within the contactor (a series of trays or height of packing) by normal mass transfer and some desorption occurs in the reboiler.

Water vapor generated in the reboiler provides the latent and sensible heat required for desorption of CO_2 and represents the diluent gas needed to keep the partial pressure of CO_2 in the gas phase low enough for stripping to take place. Gaseous CO_2 and water vapor exit the top of the stripper where water is condensed. The condensed water is then sent to the top stage of the stripper. The lean solution, the solution exiting the stripper at the bottom, is sent through a cross heat exchanger, a filter and cooled before it is sent to the absorber for further absorption.

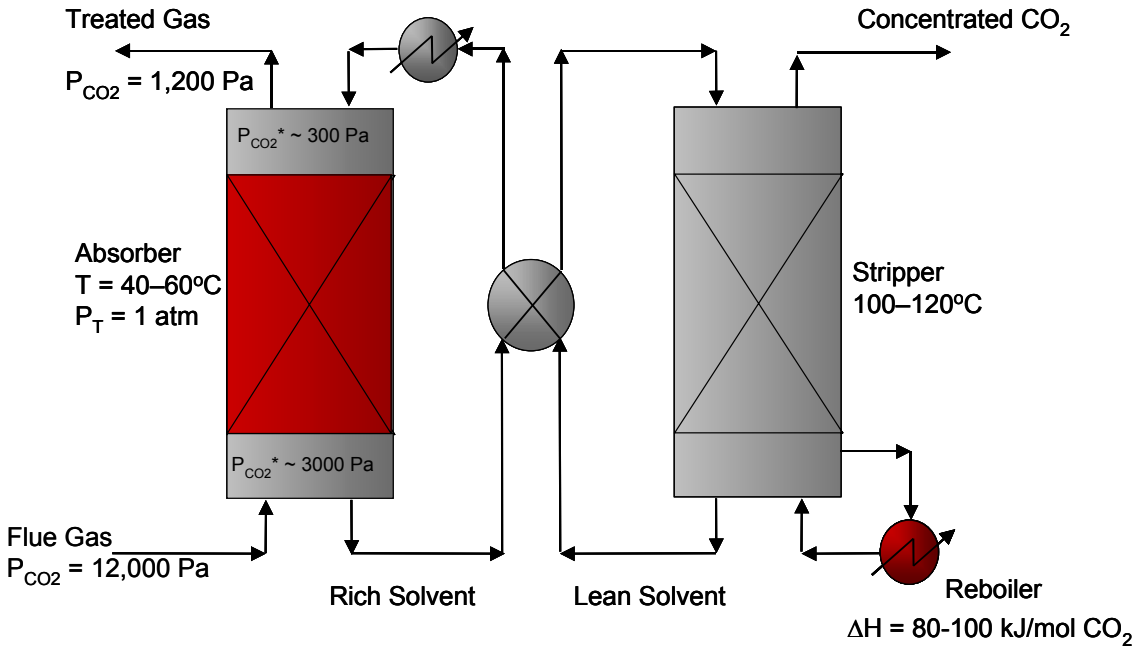

Figure 1-4: Typical absorber/stripper configuration

Even though high removal efficiencies can be obtained using absorption/stripping, the costs of implementation are high. If applied to a coal-fired power plant, this may reduce the power output by 20-30% (Rochelle 2003). For the technology to be commercially and economically viable, the high capital cost (columns, pumps, exchangers and initial solvent) and operating cost (reboiler duty, pump circulation rate, solvent make-up) should be reduced. However this must be done without compromising the system performance. This is accomplished by good solvent selection and the use of new process configurations. Since there exists limited public information on stripper design and operation, modeling becomes a very useful tool in the design of stripping columns and solving operational problems.

1.3.1. Solvent Selection for CO_2 Capture

The industrial state-of-the-art solvent is 7m (30-wt%) monoethanolamine (MEA). This solvent is demonstrated technology (Rochelle 2003). MEA is economic relative to other amines and possesses good reaction rates with CO_2. Practical problems with this technology include high-energy requirement for stripping, amine degradation, and corrosion and high capital costs.

Alternative solvents to monoethanolamine are being proposed. Desirable properties of these solvents include lower energy consumption, equivalent or better mass transfer rates with CO_2 and less degradation and corrosion than MEA. The important alternative solvents are promoted K_2CO_3 (Cullinane, Oyenekan et al.; Cullinane 2002; Cullinane and Rochelle 2004; Cullinane 2005), promoted MEA (Dang 2000; Okoye

2005), promoted tertiary amines (Bishnoi 2000; Aroonwilas and Veawab 2006; Idem, Wilson et al. 2006) and mildly hindered amines (Mitsubishi Heavy Industries). Fluor has developed an improved MEA process (MEA with some corrosion inhibitors). Mitsubishi Heavy Industries (MHI) and Kansai Electric Power Co. Inc. have developed the solvent KS-1 (Mimura, Simayoshi et al. 1997; Yagi, Mimura et al. 2006).

There are also other solvent screening and development activities around the world. The Research Institute of Innovation Technology for the Earth (RITE) have developed some solvents (Shimizu, Onoda et al. 2006) and Svendsen and co-workers (Ma'mum, Svendsen et al.; Hoff, Mejdell et al. 2006) have screened other solvents. Amino acid salts have been tested for gas absorption/ membrane hybrid applications at TNO, Netherlands (Feron and ten Asbroek; Versteeg, Kumar et al. 2002). The potential use of ionic liquids for CO_2 capture has also been evaluated (Bates, Mayton et al. 2002; Dixon, Muldoon et al. 2005).

1.3.2. Stripper modeling

Absorption / stripping with aqueous amines is an important technological option for CO_2 capture from combustion gas. Quantitative models based on our understanding of the vapor-liquid equilibrium and mass transfer rates can provide optimal design of economic processes. Optimal stripper design is critical because the stripping energy requirement accounts for 80% of the operating cost. The energy requirement for CO_2 capture and storage includes contributions for stripping, pumping of liquids and compression of the gas to the final pressure. These activities represent parasitic losses to

the power plant as the steam condensed in the reboiler and energy required to run blowers, pumps and compressors are taken from the power plant. Modeling will provide a detailed understanding of the stripper operation and mass transfer with chemical reaction at stripper conditions.

Table 1-1 summarizes previous studies that involve stripper modeling for both gas purification and CO_2 capture. A number of studies include absorption/stripping (Suenson, Georgakis et al. 1985; Escobillana, Saez et al. 1991; Alatiqi, Sabri et al. 1994; Desideri and Paolucci 1999; Freguia and Rochelle 2003; Aroonwilas 2004; Alie, Backham et al. 2005; Jassim and Rochelle 2006), others include only the stripper (Tobiesen, Svendsen et al. 2005; Oyenekan and Rochelle 2006; Oyenekan and Rochelle 2006). There are three approaches used in addressing mass transfer in strippers - the equilibrium approach such as that employed by previous authors (Oyenekan and Rochelle 2006; Oyenekan and Rochelle 2006), mass transfer with equilibrium reaction (Weiland, Rawal et al. 1982; Freguia and Rochelle 2003; Tobiesen, Svendsen et al. 2005; Tobiesen and Svendsen 2006), and mass transfer with diffusion and reaction in the liquid boundary layer as used in this work.

1.3.3. Research Needs

Most studies in absorption/stripping operations have been focused on absorption. There are very few studies of stripping operations. There is a need for more information in the open literature on stripping operations. This will help in the fundamental design of stripping columns and aid in solving operational problems encountered in stripping.

Most strippers are constructed based on experience; as such stripper design is an art rather than a science. Since the stripping operation usually determines the economics of absorption/stripping operations, minimizing the energy requirement for stripping is vital.

In a power plant, the steam used to run the reboiler will be extracted from the power plant. This constitutes an energy loss to the power plant. For CO_2 sequestration, the CO_2 will be compressed to the desired pressure for final use or storage. This presents opportunities in energy integration with the power plant.

Stripper modeling is required to quantify the performance of different solvents and process configurations under different operating conditions. This will provide some guidance to those engaged in solvent development, process design and development. Rate-based modeling allows for insight into the fundamental mechanisms of mass transfer and could help predict the operation of a constant diameter column as well as aid in the design of columns with variable diameter at constant percent flood.

An understanding of stripping operations, particularly for CO_2 capture, is lacking. An understanding of the stripping operation will help in the development of energy saving concepts and reduce the energy penalty to the power plant. This will also help in the design of large-scale commercial systems. This work focuses on quantifying the performance of different classes of solvents and process configurations for CO_2 capture.

Table 1-1: Previous stripper modeling studies

Reference	Solvent	Platform/Application	Method	Conclusions
(Weiland, Rawal et al. 1982)	Aqueous MEA	In-house simulator. First model to predict stripper operation from equilibrium data and physicochemical properties. Used to verify pilot plant data.	Equilibrium reaction.	Stripping operations are liquid phase controlled at the rich end and gas phase controlled at the lean end.
(Escobillana, Saez et al. 1991)	Aqueous MEA	In-house simulator. Used to verify pilot plant data. Applied to sieve trays.	Equilibrium reactions.	An adjustable parameter, equivalent mean bubble diameter used to fit model to pilot plant data. Temperature drops at extreme point in column fit pilot plant data.
(Desideri and Paolucci 1999)	30 wt% MEA	Aspen Plus. Performance of a CO_2 removal and liquefaction system.	Equilibrium reactions.	Increasing the liquid to gas ratio reduced the heat duty per ton of recovered CO_2.
(Freguia 2002; Freguia and Rochelle 2003)	30 wt% MEA	Aspen Plus. Studied the effect of changing operating variables on stripper performance	Equilibrium reactions.	10% reduction in steam consumption over the base case, which was commercial plant data.
(Alie, Backham et al. 2004)	30 wt% MEA	Aspen RateFrac. Studied effect of CO_2 concentrations in flue gas. Developed procedure for solving	Equilibrium reactions.	Solution of decoupled flowsheet served as starting point for convergence of entire flowsheet. Minimum reboiler duty was at a lean

		the process flowsheet.		loading of 0.25 mol CO_2/mol MEA.
(Aroonwilas 2004)	30 wt% MEA	In-house mechanistic mass transfer and hydrodynamic model. Split flow configuration.	Equilibrium reactions.	Using the split flow scheme can reduce reboiler duty.
(Tobiesen and Svendsen 2004; Tobiesen, Svendsen et al. 2005; Tobiesen, Mejdell et al. 2006; Tobiesen and Svendsen 2006)	30 wt% MEA	Fortran 90 model. Studied effect of adding an organic compound and varying parameters on energy requirements.	Equilibrium reactions.	Desorption process is sensitive to reboiler temperature. Addition of organic compound reduced stripper temperatures but increased reboiler duty.
(Oyenekan and Rochelle 2005; Oyenekan and Rochelle 2006; Oyenekan and Rochelle 2006)	30 wt% MEA, 5m K^+/2.5m PZ, Generic Solvents	Aspen Custom Modeler (ACM). Simple, vacuum and multipressure strippers were evaluated.	Equilibrium stage model.	Vacuum stripper attractive for solvents with low ΔH_{abs}, Optimum generic solvent has $\Delta H_{abs} \geqslant$ 20 kcal/gmol CO_2.
(Jassim and Rochelle 2006) (Fisher, Beitler et al. 2005)	30 wt% MEA	Aspen Plus (Freguia 2002; Freguia and Rochelle 2003)). Evaluated Simple and multipressure configurations with vapor recompression.	Equilibrium reactions.	Multipressure required 3-11% less equivalent work than simple stripping. Economics showed multipressure reduced CO_2 capture costs by 9.8% over the simple case.

1.3.4. Objectives and Scope

This work accomplishes the following scientific and practical objectives:

1. Compare the energy performance of different solvents for absorption/stripping in CO_2 capture applications.
2. Propose and quantify the performance of innovative stripper configurations.
3. Propose optimum operating stripper pressure for different solvents and process configurations.
4. Quantify mass transfer phenomenon at stripper conditions.
5. Validate the stripper model with data from a pilot plant.

The scope of this work is to develop rigorous stripper models for different classes of solvents in Aspen Custom Modeler (ACM). The vapor-liquid equilibria in the model were regressed from a variety of sources (Mitsubishi Heavy Industries; Posey, Tapperson et al. 1996; Suzuki, Iwaki et al. 1999; Freguia 2002; Cullinane 2005). Approximate representations of mass transfer with chemical reaction in the liquid boundary layer and diffusion are used in the model. The model accounts for gas and liquid mass transfer resistances as well as flash and reboiler mass transfer. Equilibrium models are used to evaluate the performance of different process configurations.

Objective 1 is satisfied by developing an equilibrium model in Aspen Custom Modeler (ACM) and carrying out simulations at normal pressure (160 kPa) with 7m monoethanolamine (MEA) and four classes of alternative solvents. These classes of

solvents have different properties and as such the results also help to characterize generic solvents.

Objective 2 is satisfied with simulating different solvents and process configurations based on the analyses of the results from objective 1. Analyzing the results of objectives 1 and 2 satisfies objective 3. Developing a rate-based model for the solvents satisfies objectives 4.

Analyzing results from a pilot plant at The University of Texas and refining the model with the data collected satisfies objective 5.

1.3.5. Dissertation Outline

Chapter 2 summarizes the different solvents used for CO_2 capture and outlines advantages and disadvantages of the baseline solvent, 7m monoethanolamine (MEA). The baseline configuration is described and results of equilibrium model simulations of 7m MEA with a simple stripper (160 kPa), vacuum stripper (30 kPa), and multipressure stripper (280/212/160 kPa) are presented. Ways of reducing energy requirements are identified and methods presented.

Chapter 3 presents the equilibrium model developed in Aspen Custom Modeler and presents model results for four innovative process configurations (matrix, internal exchange, multipressure with split feed, and flashing feed) and seven representative solvent formulations.

Chapter 4 gives details of the rate-based model and presents the model results stripping with 5m K^+/2.5m PZ equipped with IMTP #40 random packing. The mass transfer phenomenon at stripper conditions is quantified.

Chapter 5 presents results from pilot plant tests with 5m K^+/2.5m PZ and 6.4m K^+/1.6m PZ with the absorber and stripper equipped with Flexipac AQ Style 20 structured packing. The ACM model was validated with results from the pilot plant tests.

Chapter 6 presents conclusions from this work and recommendations for future work.

Chapter 2 : Baseline Analysis and Modeling Results

This chapter summarizes the different solvents used for CO_2 capture and outlines advantages and disadvantages of the baseline solvent, 7m monoethanolamine (MEA). The baseline configuration is described and results of equilibrium model simulations of 7m MEA with a simple stripper (160 kPa), vacuum stripper (30 kPa), and multipressure stripper (280/212/160 kPa) are presented. Ways of reducing energy requirements are identified and methods presented.

2.1. Solvents for CO_2 Capture

Solvents used for CO_2 capture can be divided into two categories – physical and chemical solvents. Physical solvents such as Selexol and Rectisol are typically used to remove high pressure CO_2 (Rochelle, Bishnoi et al. 2001; Kirk Othmer Encyclopedia of Chemical Technology 2004; Cullinane 2005). Natural gas and coal-fired power plant flue gases contain low concentrations of CO_2, typically 3-6 mol % and 10-15 mol %

respectively at atmospheric pressure. The chemical solvents used are aqueous solutions of potassium carbonate, K_2CO_3, promoted potassium carbonate, and aqueous alkanolamines. The aqueous alkanolamines fall into four categories: primary amines (e.g. monoethanolamine, MEA), secondary amines (e.g. diethanolamine, DEA and piperazine, PZ), tertiary amines (e.g. methyl diethanolamine, MDEA) and hindered amines (e.g. 2-amino-2-methyl-1-propanol, AMP).

The main solvent properties to be exploited in reducing the energy requirements for absorption/stripping are; (a) the heat of absorption (ΔH_{abs}) (b) the capacity of the solvent and (c) the rates of reaction of the solvent with CO_2.

The heat of absorption is a quantification of the heat evolved when CO_2 reacts with the solvent in the absorber. This is the minimum amount of energy that has to be put into the reboiler in order to reverse the reaction in the stripper. On the other hand, a greater heat of absorption will reduce the stripping vapor rate with a greater temperature in the stripper.

The capacity of the solvent is a quantification of the amount of CO_2 a unit of solvent can absorb or desorb within a range of partial pressures. High capacity is a desirable characteristic of solvents because it reduces the sensible heat requirements with temperature swing desorption.

Solvents with fast rates of reaction with CO_2 are desirable because they yield richer solutions in the absorber, which are easily stripped thereby reducing the energy requirement for stripping. With a fixed solvent rate, the amount of packing used can be

significantly reduced if a fast reacting solvent is used in place of a slow reacting solvent. This will reduce the absorber size, thereby reducing the capital cost of the process.

2.2. 7m (30 wt %) Monoethanolamine (MEA)

The industrial state-of-the-art solvent for CO_2 capture is 7m (30 wt%) monoethanolamine. The current MEA system has been used for CO_2 removal from natural gas streams. To be applicable to CO_2 capture, some evolutional improvements are required.

The advantages of the MEA solvent technology are:

1. It is demonstrated technology with some semi-commercial plants around the world.
2. The solvent has reasonable rates of absorption/desorption but requires a significant amount of packing.
3. It possesses a high solution capacity and high alkalinity so it can readily react with acid components such as CO_2.
4. It can be reclaimed easily relative to other amines.

The disadvantages of this solvent technology are:

1. It has a high stripping energy requirement (Rochelle, Goff et al. 2002; Cullinane 2005). Since the steam used to run the reboiler is obtained from the power plant, this reduces the net output of the plant.

2. Significant solvent vapor losses are experienced because of the high vapor pressure of the amine. This can be overcome with a water wash section at the top of the column (Rochelle, Bishnoi et al. 2001).
3. The loaded amine causes carbon steel equipment corrosion and as such stainless steel will have to be used or corrosion inhibitors added to the solvent (Rochelle, Bishnoi et al. 2001).
4. The amine suffers from both oxidative and thermal degradation. This requires make-up solvent and introduces an additional cost component for solvent make-up (Rochelle, Bishnoi et al. 2001; Goff and Rochelle 2004; Sexton and Rochelle 2006).

Evolutional improvement of this technology should retain the advantages of the MEA and minimize or eliminate the disadvantages. This work is focused on reducing the energy requirements for the absorption/stripping and compression processes to minimize the parasitic losses to the power plant.

Before improvements can be made to this technology, an understanding of the current state of the technology is required. This is achieved by carrying out simulations to study the effect of different parameters on the capture process and identify areas of improvement.

2.3. Stripper Configurations

This section describes three stripper configurations; simple, vacuum and multipressure. The current industrial baseline configuration is a simple reboiled stripper

operating at 160 kPa with 7m MEA. Vacuum strippers could be attractive for some other solvent formulations and could help reduce the degradation of the amine and possible corrosion of equipment. The use of low-pressure steam could be advantageous in reducing energy requirements under vacuum operation. A third configuration, the multipressure stripper, integrates the stripping and compression operations and makes use of the latent heat of the water vapor stream at the rich end. There is a shift in energy from heat to work.

2.3.1. Simple Stripper. In the baseline configuration, the simple reboiled stripper is run at 160 kPa. Pressure drop across the stripper was neglected since it might not be critical for this configuration. The vapor leaving the top of the stripper is cooled and the condensed water is refluxed. The CO_2 is compressed in five stages (intercooled to 313K) to 1000 kPa. The reboiler runs at 110 to 120^{o}C in this configuration. Five compression stages were selected for all configurations. Stripping at 160 kPa has the following features:

1. Less steam should be required to strip the CO_2. The ratio of the equilibrium partial pressures of CO_2 and water vapor is proportional to temperature. Hence increasing the stripper temperature (and pressure) makes the CO_2 easier to strip.

$$\frac{P_{CO2}^*}{P_{H2O}^*} = f(T) \qquad (2\text{-}1)$$

2. The reactions with CO_2 are very fast, approaching the instantaneous regime.

3. Moderate pressure steam is used to run the reboiler. This steam has a high work value and constitutes a greater loss to the power plant than if low-pressure steam were used.

2.3.2. Vacuum Stripper. This configuration is identical to the simple stripper. The stripper is operated at 30 kPa and the reboiler runs at 60 to 80°C. The CO_2 is compressed in five intercooled stages to 1000 kPa.

Vacuum stripping has the following features:

1. Lower temperature (less valuable) steam is used to run the reboiler so more electricity

   can be extracted before the steam is used in the stripper. In some cases, waste heat may be used in the reboiler.
2. Additional compression is required for the CO_2.
3. The mass transfer is not as fast as that of the simple stripper because the lower temperature results in slower kinetics.
4. Lower stripper temperature will reduce amine degradation and corrosion.

2.3.3. Multipressure Stripper. In this configuration (Figure 2-1), the stripper is divided into three sections, each operating at a different pressure. The CO_2 compressor is integrated with the stripper. The vapor from a lower pressure stage is compressed and subsequently used as stripping vapor in a higher-pressure section. Water vapor condenses with the increased pressure and the latent heat of water is recovered. This leads to a lower

reboiler duty and the CO_2 is produced at a greater pressure than with the simple (isobaric) stripper. However the compression work is greater than that of the simple stripper because some water vapor is compressed with the CO_2. The pressure levels are 160 kPa, 212 kPa and 280 kPa from the bottom to the top of the stripper. The vapor exiting the stripper is cooled and water is refluxed. The CO_2 is further compressed in three stages (intercooled to 313K) to 1000 kPa. Therefore, the five compression stages include two integrated with the stripper and three downstream of the stripper.

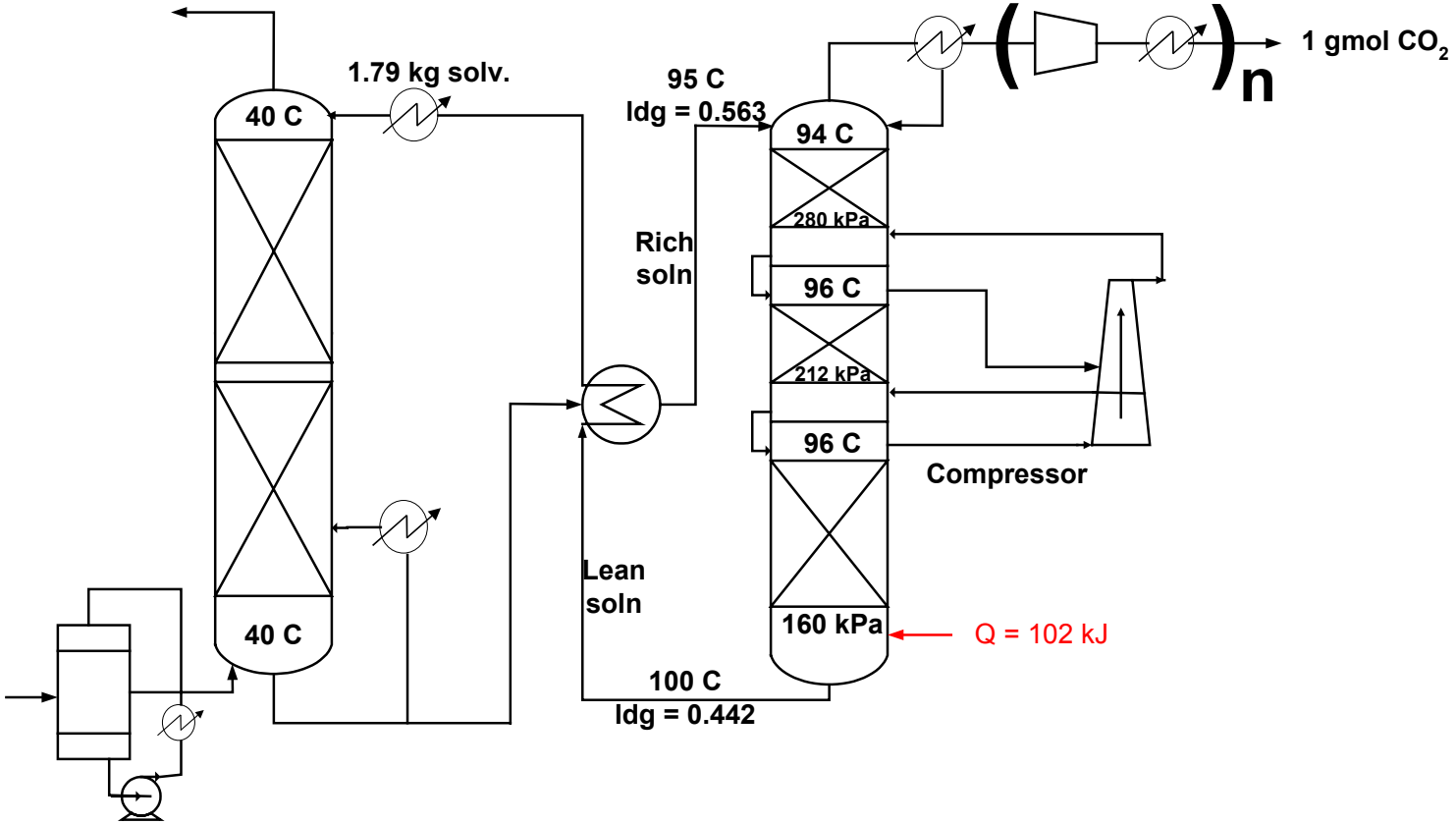

Figure 2-1: Multipressure Stripper for 7m MEA

Multipressure stripping has the following features:

1. The latent heat of water is recovered at the rich end.
2. It makes use of the high temperature preheat in the high pressure flash thereby rewarding a closer approach temperature in the cross exchanger.
3. CO_2 can be recovered at a greater concentration and pressure. This leads to less compression work downstream of the stripper.
4. This configuration should be best with high ΔH_{abs} solvents such as 7m MEA.

2.4. Model development

An equilibrium stripper model for aqueous solvents developed in Aspen Custom Modeler (ACM) was used to evaluate the different process configurations and solvents. The stripper consisted of a flash region, ten segments with 40% Murphree efficiency assigned to CO_2, and a reboiler with 100% CO_2 efficiency. The flash region in the column was quantified in terms of actual section performance. In the multipressure configuration, four sections are at 160 kPa, four at 212 kPa, and two at 280 kPa.

2.4.1. Modeling Assumptions.

(a) The sections are well mixed in the liquid and vapor phases.

(b) The reboiler is in vapor/liquid equilibrium.

(c) There is negligible vaporization of the amine.

(d) The pressure drop across the column is negligible.

The CO_2 vapor pressure under stripper conditions for 7m MEA is represented by the empirical expression in Table 2-1. The adjustable constants in Table 2-1 were obtained

by regressing points obtained from equilibrium flashes in AspenPlus using the Electrolyte Non Random Two Liquid (E-NRTL) model developed by Freguia (Freguia 2002) from data of Jou et al. (Jou, Mather et al. 1995). The heat of desorption was calculated by differentiating the VLE expression with respect to 1/T.

The equilibrium CO_2 loading (γ) in 7m MEA at 40^{o}C is shown in Table 2-2. The equilibrium CO_2 loading is defined as mol CO_2/ mol Alk.

The mol Alk is given by:

mol Alk = [mol K+ + 2* mol PZ + mol MEA + mol MDEA + mol KS-1] (2-2)

Thus for 7m MEA, mol Alk = mol MEA (2-3)

Table 2-1: VLE expression for 7m MEA

$$\ln P_{CO2}^{*} = a + b\gamma + \frac{c}{T} + d\frac{\gamma^2}{T^2} + e\frac{\gamma}{T^2} + f\frac{\gamma}{T}$$

$$-\frac{\Delta H}{R} = c + 2d\frac{\gamma^2}{T} + 2e\frac{\gamma}{T} + (f\,\gamma)$$

a	35.11
b	-45.04
c	-14281
d	-546277
e	-3400441
f	32670.01

Table 2-2: Equilibrium CO_2 loading (mol / mol Alk) at 40°C

P (kPa)	CO_2 loading (mol/mol Alk)	
	Regression	Freguia (2002)
0.125	0.373	0.400
0.5	0.442	0.455
0.75	0.463	0.466
5	0.563	0.545
7.5	0.586	0.565
10	0.602	0.590

The heat of vaporization of water, partial pressure of water, and the molar heat capacities for the CO_2, water were calculated with equations from the DIPPR database (American Institute of Chemical Engineers 2004). The molar heat capacities for the CO_2 and amine were assumed to be equal and set to that of one mole of water.

The partial pressure of CO_2 and water in each section was calculated by:

$$P_n = E_{mv}(P_n^* - P_{n-1}) + P_{n-1} \quad (2\text{-}4)$$

A Murphree efficiency (E_{mv}) of 40% and 100% was assigned to CO_2 and water. The model assumed that temperature equilibrium is achieved in each section.

The model inputs were the rich loading and liquid rate, the temperature approach on the hot side of the cross exchanger (difference between the temperature of the rich stripper feed and the lean solution leaving the bottom of the stripper), and column pressure. Initial

guesses of the lean loading, section temperatures, partial pressures, and loading were provided. The model solves equations for calculating VLE and for material and energy balances (Table 2-3). The constants in Table 2-3 and the detailed model equations are presented in Appendix A. It calculates temperature and composition profiles, reboiler duty, and equivalent work.

Table 2-3: Main equations in the equilibrium model

Material balance over a segment
$l_{ij-1} + (V_{ij+1} * y_{i,j+1}) = l_{ij} + (V_{ij} * y_{ij})$

Negligible vaporization of amine
$l_{ij-1} = l_{ij}$ i = amine, j = segment

Equilibrium expressions
CO_2:

$$P_{CO2} * = \exp\left(A + (B\gamma) + \frac{C}{T} + \left(\frac{D\gamma^2}{T^2}\right) + \left(\frac{E\gamma}{T^2}\right) + \left(f\frac{\gamma}{T}\right)\right)$$

H_2O:

$$P_{H2O} = \left[\exp\left(A + \frac{B}{T} + C\ln T + DT^E\right)\right] / 1000$$

The constants A,B,C,D and E in the P_{H2O} equation are obtained from the DIPPR database.

Summation Equations
$1.0 = \sum_i y_{ij}$ where i = component in vapor phase and j = segment

Enthalpy Equations (Energy balance)

$V_j + [y_{h2o,j+1} * (H_{vap} + (C_{pH2O,j+1} * T_{j+1} - T_{ref}))] + y_{co2,j+1} * ((\Delta H_{j+1}/1000) + (C_{pco2,j+1} * (T_{j+1} - T_{ref}))) + (L_{j-1} * C_{pL,j-1} * (T_{j-1} - T_{ref})) + Q_j + Q_{comp,j} = V_j + [y_{h2o,j} * (H_{vap} + (C_{pH2O,j} * T_j - T_{ref}))] + y_{co2,j} * ((\Delta H_j/1000) + (C_{pco2,j} * (T_j - T_{ref}))) + (L_j * C_{pL,j} * (T_j - T_{ref}))$

Total pressure on a segment

$P_{CO2} + P_{H2O} = P_T$

Internal work of compression

$$W_{comp,j} = \frac{G_{j+1}\ R\ T_{j+1}\ nn1\left[\left(\frac{P_{T,j}}{P_{T,j+1}}\right)^{\frac{1}{nn1}} - 1\right]}{polyeff}$$

$Q_{comp,j} = W_{comp,j}$ where j = segment

nn1 = (k/(k-1)) * polyeff

$k = c_p/c_v = 1.4$

polyeff = 0.75

The total energy required by the stripper is given as total equivalent work:

$$W_{eq} = 0.75Q\left[\frac{(T_{reb} + 10) - 313}{(T_{reb} + 10)}\right] + W_{comp} \qquad (2\text{-}5)$$

The work lost by extracting steam from a turbine is the first term on the right hand side of (2-5). The condensing temperature of the steam is assumed to be 10K higher than the reboiler fluid. The turbine assumes condensing steam at 313K and has been assigned an effective Carnot efficiency of 75%. This is the cooling water temperature assumed to be 303K with a 10^oC approach. The second term on the right hand side of (2.5) is the compressor work. W_{comp} constitutes the isentropic work of compression to 1000 kPa of the gas exiting the top of the stripper. An efficiency of 75% was assumed for the compressor. Five stages of compression were used with intercooling to 313K between

stages. The multipressure configuration has two internal, and three external stages of compression.

The capacity of the solution is given by:

$$\text{capacity}\left(\frac{\text{mol}\,CO_2}{\text{kg}\,H_2O}\right) = \left(\gamma_{\text{rich}} - \gamma_{\text{lean}}\right)\left(\frac{\text{mol}\,\text{Alk}}{\text{kg}\,H_2O}\right) \quad (2\text{-}6)$$

2.5. Results and Discussion

2.5.1. Predicted Stripper performance. The optimization of the lean loading in a simple stripper using 7m MEA with a rich loading of 0.563 mol CO_2/mol Alk and $\Delta T = 10^oC$ is shown in Figure 2-2. The minimum equivalent work (26.3 kJ/gmol CO_2) occurs at a CO_2 loading of 0.306 mol CO_2/mol Alk with a reboiler duty of 126.7 kJ/gmol CO_2. The reboiler temperature at the optimized lean loading is 110.3^{o}C. The lean loading required to minimize reboiler duty (0.288 mol CO_2/ mol Alk) does not coincide with that required to minimize equivalent work. The equilibrium partial pressure of CO_2 in the rich solution leaving the absorber at 40^{o}C was set at 5 kPa. The lean equilibrium partial pressure leaving the stripper bottom is 0.0308 kPa at 40^{o}C corresponding to 99.3% CO_2 removal. This implies that > 90% removal can be achieved with the equivalent work minimized. Even though the reboiler duty is changing, equivalent work is flat in the lean loading region of 0.3 –0.4 mol CO_2/mol Alk. This is because the temperature is also changing and the combined effects of the reboiler duty and the temperature affect the equivalent work.

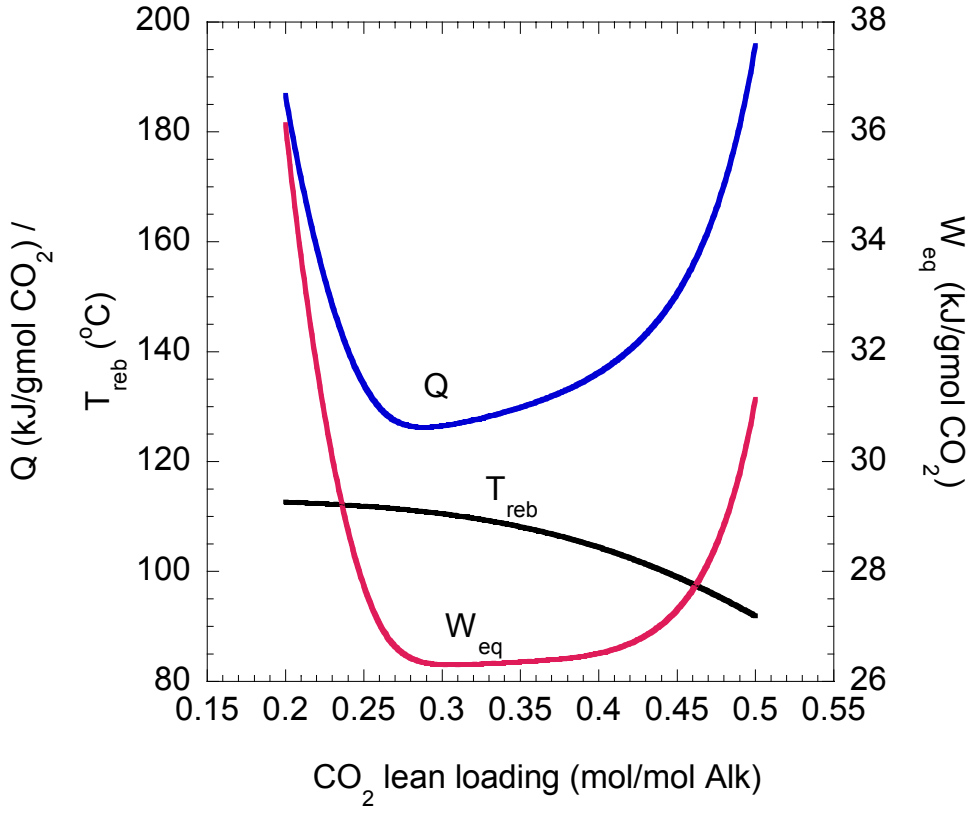

Figure 2-2: Optimization of the lean loading for minimum equivalent work with 7m MEA (rich ldg = 0.563 mol CO_2/mol Alk, 160 kPa stripper, $\Delta T = 10^oC$, P_{final} = 1000 kPa)

The optimization of the lean loading in a simple stripper using 7m MEA with a rich loading of 0.563 mol CO_2/mol Alk and $\Delta T = 5^oC$ is shown in Figure 2-3. The minimum equivalent work (23.6 kJ/gmol CO_2) occurs at a CO_2 loading of 0.459 mol CO_2/mol Alk with a reboiler duty of 125.3 kJ/gmol CO_2. The reboiler temperature at the optimized lean loading is 97.9°C. The lean loading required to minimize reboiler duty (0.351 mol CO_2/ mol Alk) does not coincide with that required to minimize equivalent

work. The equilibrium partial pressure of CO_2 in the rich solution leaving the absorber at 40°C was set at 5 kPa.

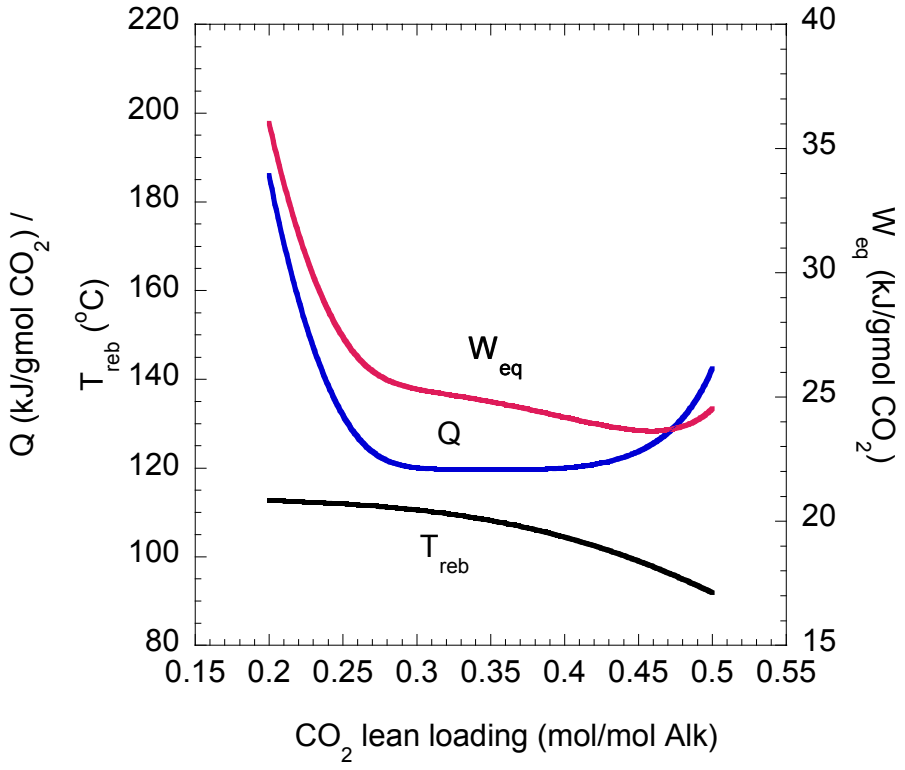

Figure 2-3: Optimization of the lean loading for minimum equivalent work with 7m MEA (rich ldg = 0.563 mol CO_2/mol Alk, 160 kPa stripper, $\Delta T = 5^oC$, P_{final} = 1000 kPa)

The lean equilibrium partial pressure leaving the stripper bottom is 0.683 kPa at 40°C corresponding to 86% CO_2 removal. This implies that 90% removal cannot be achieved with the equivalent work minimized.

The equivalent work in Figure 2-3 decreases in the region where the reboiler duty is flat. This is as a result of the decreasing reboiler temperature in that region.

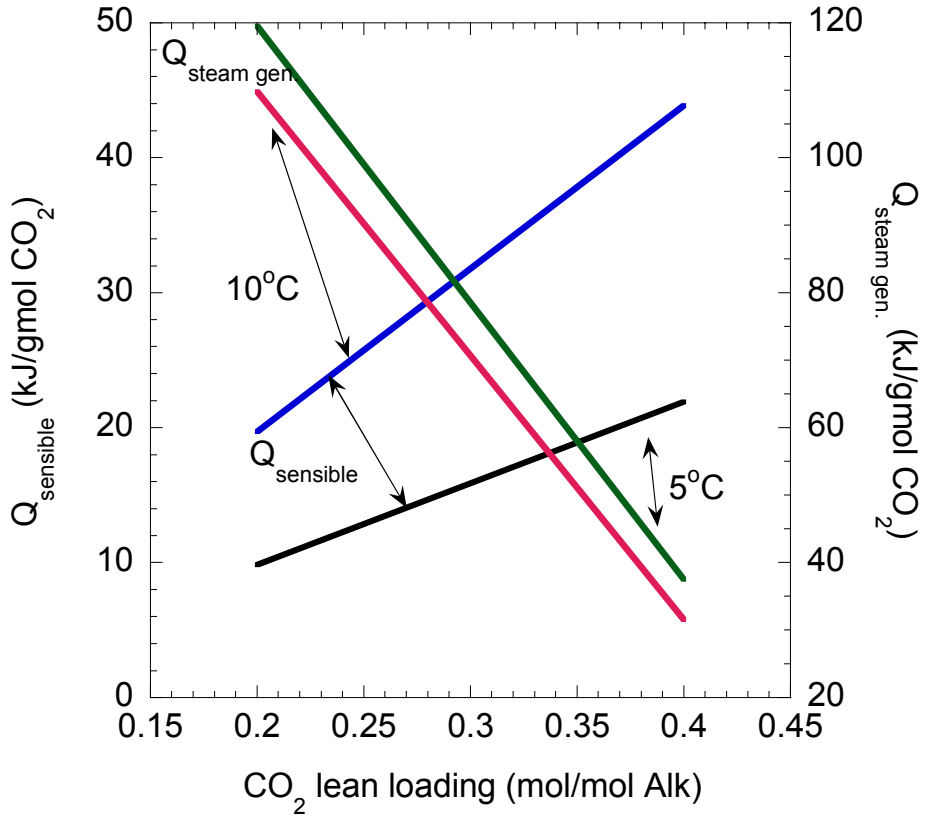

Figure 2-4: Optimization of the lean loading for minimum equivalent work with 7m MEA (rich ldg = 0.563 mol CO_2/mol Alk, 160 kPa stripper)

Figure 2-2 and Figure 2-3 show the lean loading that minimizes reboiler duty is different for the 160 kPa stripper operating 10°C and 5°C approach. The lean loading that minimizes reboiler duty shifts to the right with the 5°C approach. This is as a result of different sensible heat and steam generation requirements for the two cases. The loading at which the two heat contributions intersect minimizes reboiler duty (Figure 2-4).

Table 2-4 shows the predicted performance of a 160 kPa stripper for 7m MEA with a 5°C and 10°C approach on the hot side of the cross exchanger. The results for the

10°C approach cases correspond to lean loadings that minimize total equivalent work. The optimized cases for the 10°C cases are greater than 90% removal. This will increase the capacity of the solvent for absorption.

Table 2-4: Predicted performance of 160 kPa stripper to achieve ≥ 90% removal (P_{final} = 1000 kPa) using 7m MEA.

Rich P_{CO2}* @ 40°C	Lean P_{CO2}* @ 40°C	Rich loading	Lean loading	Operating Capacity	ΔT	Q	Total W_{eq}	CO_2 removal
kPa		mol CO_2/mol Alk		mol CO_2/kg H_2O	°C	kJ/gmol CO_2		%
1.25	0.027	0.489	0.300	1.323	10	156.9	31.0	97.8
2.5	0.028	0.526	0.302	1.568	10	139.4	28.3	98.9
5.0	0.031	0.563	0.306	1.799	10	126.7	26.3	99.3
7.5	0.220	0.584	0.401	1.281	10	127.6	25.3	97.1
10.0	0.416	0.602	0.433	1.183	10	126.6	24.5	95.8
1.25	0.115	0.489	0.369	0.84	5	151.1	29.2	90.8
2.5	0.25	0.526	0.407	0.833	5	135.0	26.2	90
5.0	0.5	0.563	0.442	0.847	5	122.6	23.7	90
7.5	0.75	0.584	0.463	0.847	5	116.3	22.3	90
10.0	1.00	0.602	0.478	0.868	5	112.6	21.5	90

The results for the 5°C approach cases correspond to lean loadings to achieve 90% change in equilibrium partial pressures from the rich to the lean ends. The lean loadings that minimize total equivalent work resulted in less than 90% change in equilibrium partial pressures (90% removal). The criterion for the optimization was to achieve 90% or greater change in the equilibrium partial pressure of CO_2 in the rich and lean streams.

The savings in total equivalent work are at the expense of operating capacity. The results predict a 56% capacity increase with a rich equilibrium partial pressure of 1.25 kPa at 40°C using a 10°C cross exchanger approach than with 5°C approach.

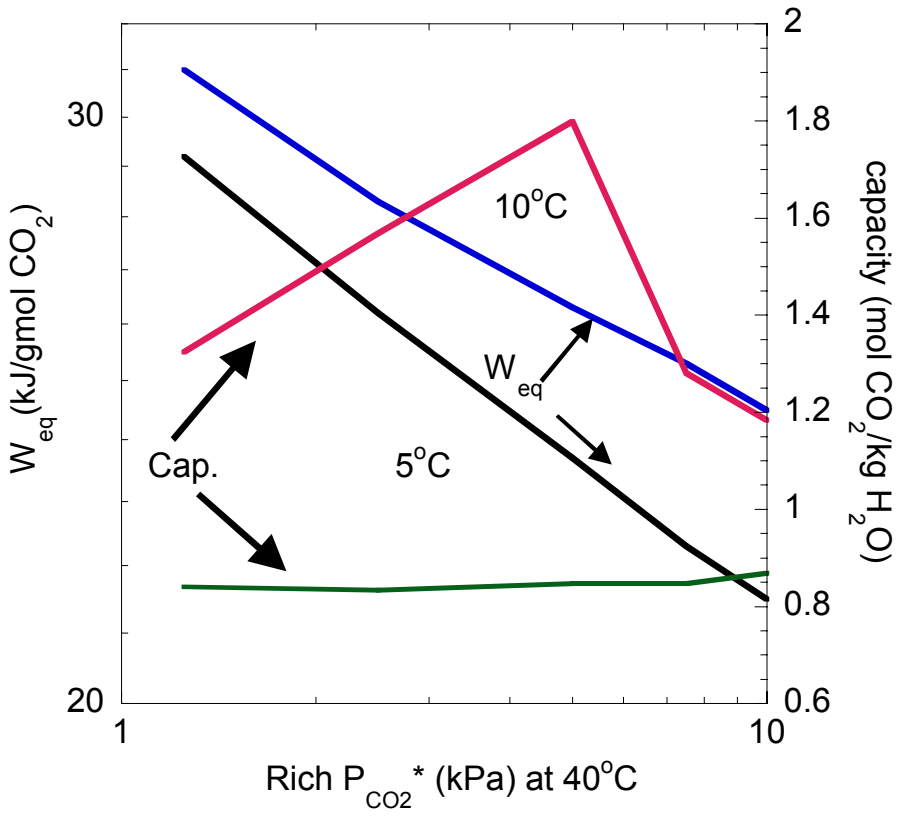

Figure 2-5: Total equivalent work with 7m MEA (160 kPa stripper, ΔT= 10°C, P_{final} = 1000 kPa)

At a rich equilibrium partial pressure of 5 kPa, the capacity increase with a 10°C approach in the cross exchanger is 112% greater than with a 5°C approach. This means that the solvent rate is about twice the amount with a 5°C approach than with a 10°C approach. This will affect the size of the cross exchanger and the pumps used for solvent

circulation and impact the cost of the process. The maximum capacity of the solvent seems to occur at about a rich partial pressure of 5 kPa at 40°C.

Table 2-5 shows the predicted performance of 7m MEA with the simple (160 kPa), vacuum (30 kPa) and multipressure (highest pressure = 280 kPa) strippers with a 5°C approach in the cross exchanger with a rich loading of 0.563 mol CO_2/ mol Alk and a lean loading of 0.442 mol CO_2/ mol Alk.

The reboiler duty for the 160 kPa stripper is 122 kJ/gmol CO_2 while that for the 30 kPa stripper is 152.5 kJ/gmol CO_2. Even though the reboiler duty increases with vacuum operation, the work value of the steam is significantly less because the steam temperature is reduced (65°C under vacuum and 100°C at 160 kPa). The work of compression downstream of the stripper operation is more with the vacuum stripper. If the multipressure configuration is employed, the reboiler duty is 101.8 kJ/gmol CO_2, a 17% reduction relative to the 160 kPa stripper.

Table 2-5: Predicted performance of stripper configurations (rich loading = 0.563 mol CO_2/ mol Alk, lean loading = 0.442 mol CO_2/ mol Alk ΔT= 5°C,Abs. rich T = 40°C,P_{final} = 1000 kPa)

Configuration	Q	W_{comp} (from P to 1000 kPa)	Total W_{eq}	T_{reb}	n_{CO2}/n_{H2O} in stripper overhead
	kJ/gmol CO_2			°C	
Simple (160 kPa)	122.6	6.9	23.7	100	1.361
Vacuum (30 kPa)	152.5	15.1	26.6	65	0.808
Multipressure (280/160)	101.8	8.3	22.2	100	2.459

Even though the work of compression downstream of the stripper is less, the internal work of compression is significant giving a greater total compression work. The multipressure configuration leads to a shift of heat to work relative to the 160 kPa stripper. The disruption to the power plant is less but the electrical work to run the compressors is more.

The total equivalent work to 1000 kPa for the different configurations shows that the multipressure configuration is the most attractive of the three configurations. The total equivalent work of the multipressure configuration is 6% less than the simple and 17% less than the vacuum configuration. This is because the multipressure configuration makes use of the latent heat of water vapor at the rich end of the stripper to perform more stripping of CO_2. As such there is more CO_2 in the stripper overhead stream in the multipressure configuration relative to the simple and vacuum strippers. The condition of the stripper feed determines the mechanism of stripping and affects column profiles. McCabe-Thiele diagrams for the three configurations were constructed to give insight into different phenomena.

Figure 2-6 shows the McCabe-Thiele plot for a simple stripper using 7m MEA. The rich feed is a superheated liquid with a CO_2 loading of 0.563 mol/mol Alk and a temperature of 95^{o}C. The liquid flashes to 89^{o}C at the stripper inlet. Its CO_2 loading decreases to 0.517 mol/mol Alk by the time it leaves the first section. The liquid temperature increases steadily to the reboiler.

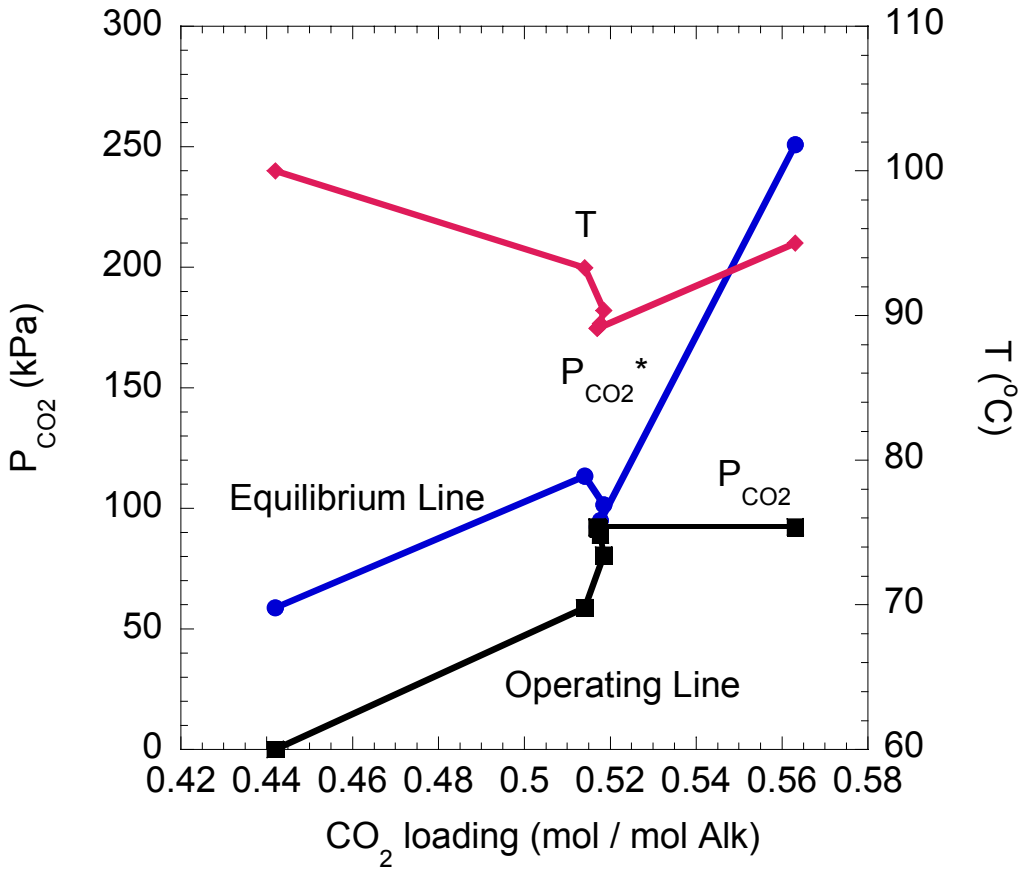

Figure 2-6:McCabe-Thiele plot for a simple stripper (rich loading = 0.563 mol CO_2/ mol Alk, lean loading = 0.442 mol CO_2/mol Alk, Q = 122.6 kJ/gmol CO_2, Total W_{eq} = 23.7 kJ/gmol CO_2, $\Delta T=5^oC$, abs rich T = 40^oC, P_{final} = 1000 kPa)

The driving force (P_{CO2}*-P_{CO2}) suggests a pinch at the rich end. The pinch experienced may be as a result of large contacting capability inherent in the model. Very little change in loading occurs over seven sections, so the column could provide almost

equivalent performance with three sections rather than ten. Desorption occurs mainly in the flash segment and in the reboiler.

The McCabe-Thiele plot for a vacuum stripper (30 kPa) using 7m MEA is shown in Figure 2-7.

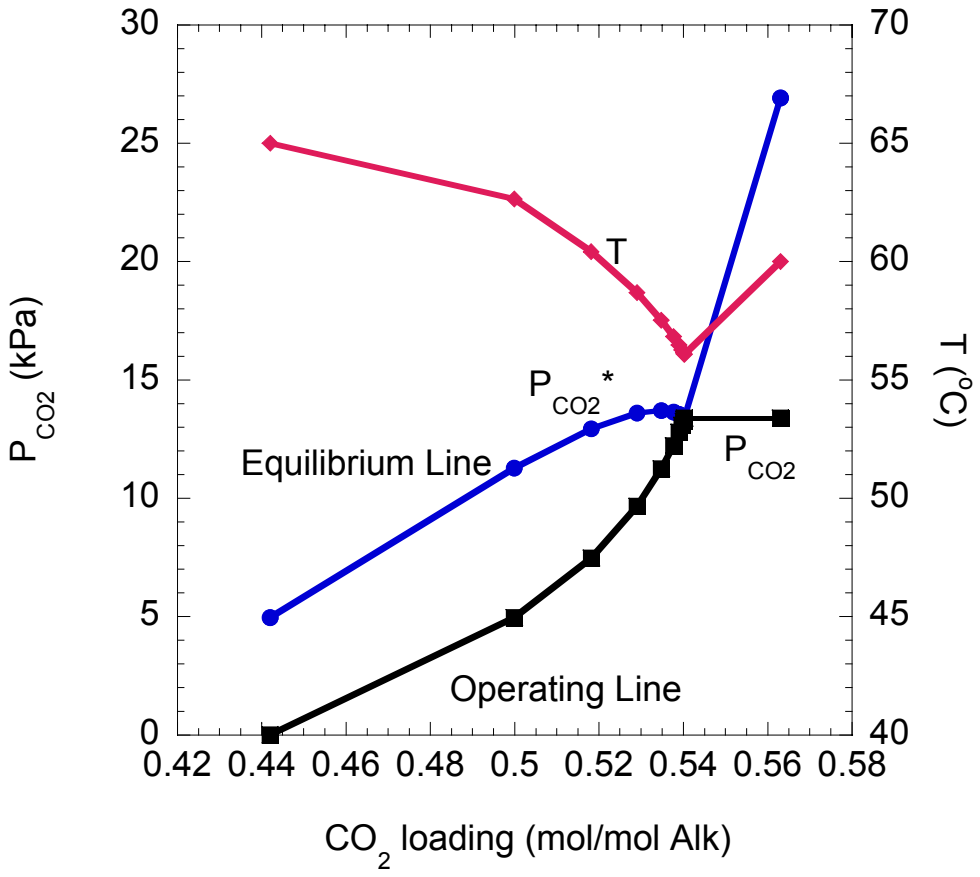

Figure 2-7:McCabe-Thiele plot for a vacuum stripper (rich loading = 0.563 mol CO_2/ mol Alk, lean loading = 0.442 mol CO_2/mol Alk, Q = 152.5 kJ/gmol CO_2, Total W_{eq} = 26.6 kJ/gmol CO_2, $\Delta T=5^oC$, abs rich T = 40^oC, P_{final} = 1000 kPa)

The rich feed is a superheated liquid with a CO_2 loading of 0.563 mol/mol Alk and a temperature of 60^{o}C. On entering the column, the liquid flashes to 56^{o}C and the CO_2 loading decreases to 0.540 mol/ mol Alk.

There is an apparent pinch at the rich end of the column over three sections and subsequently an evenly distributed driving force towards the lean end of the column. A significant amount of stripping occurs in the reboiler as a result of the 100% CO_2 efficiency assigned to the reboiler.

Figure 2-8 shows the McCabe-Thiele plot for a multipressure stripper (280/212/160 kPa) using 7m MEA. The pressure levels decrease from the top (rich end) to the bottom (lean end). The rich feed is a superheated liquid with a CO_2 loading of 0.563 mol/mol Alk and a temperature of 95^{o}C. After some CO_2 desorption in the 280 kPa section, the large flow of subcooled liquid condenses water at the rich end of the 212 kPa and 160 kPa sections and CO_2 absorption occurs at the top of the 212 kPa section.

The CO_2 loading increases to 0.562 mol/mol Alk at the top of the 212 kPa section from 0.553 mol/mol Alk at the bottom of the 280 kPa. The stripper is pinched at rich ends of the 212 kPa and 160 kPa sections. Within a given pressure section, the temperature increases down the column. The temperature drop between pressure sections is as a result of flashing that accompanies the drop in pressure. This baseline analysis show that for the 7m monoethanolamine (MEA), operating the cross exchanger with a 5^{o}C temperature approach on the hot side reduces the equivalent work by between 6 and 12% as the rich equilibrium partial pressure increases from 1.25 kPa to 10 kPa at 40^{o}C

when compared to a 10°C approach. Of the three configurations presented in this chapter, the multipressure configuration requires the least equivalent work. It provides 6.3% energy savings over the simple (160 kPa) stripper and 16.5% energy savings over the vacuum configuration when stripping from a rich loading of 0.563 mol CO_2/mol Alk to a lean loading of 0.442 mol CO_2/mol Alk with a 5°C approach on the hot side of the cross exchanger.

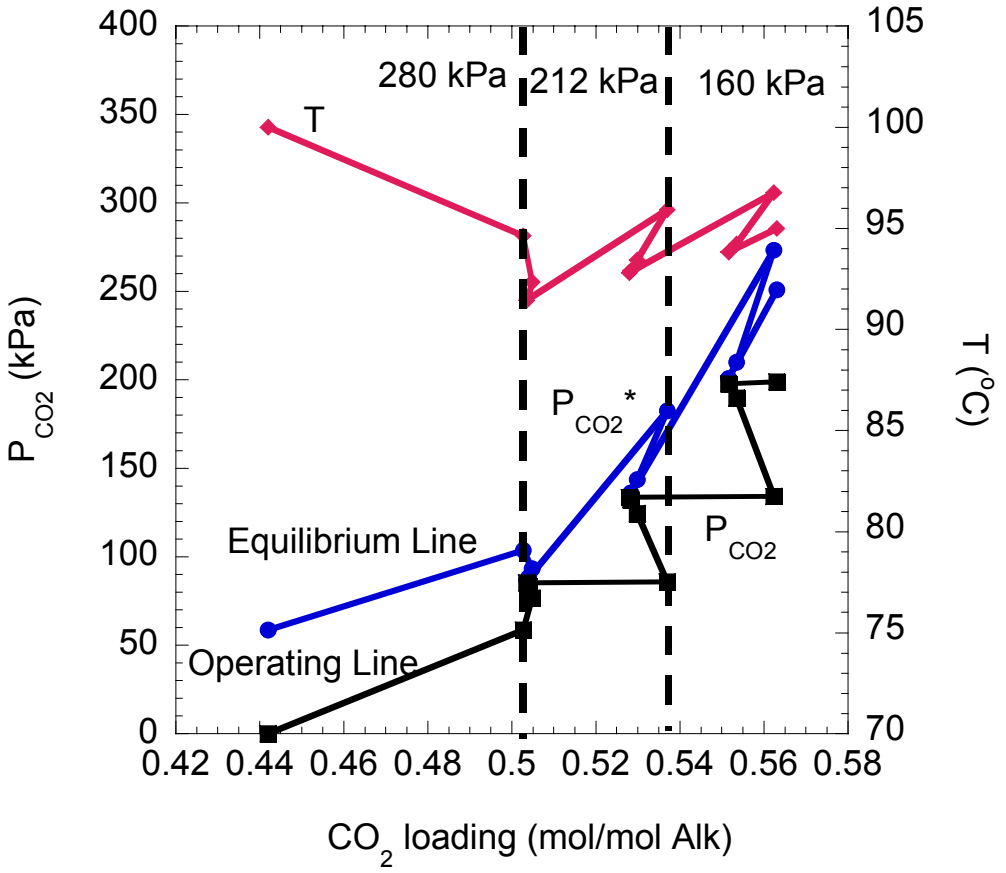

Figure 2-8:McCabe-Thiele plot for a multipressure (280/212/160 kPa) stripper (rich loading = 0.563 mol CO_2/ mol Alk, lean loading = 0.442 mol CO_2/mol Alk, Q = 101.8 kJ/gmol CO_2, Total W_{eq} = 22.2 kJ/gmol CO_2, ΔT=5°C, abs rich T = 40°C, P_{final} = 1000 kPa)

2.6. Generic Solvent Modeling

A three-parameter expression for the vapor-liquid equilibrium was used to model generic solvents:

$$\ln P = a + b * \text{ldg} -\frac{\Delta H}{RT} \qquad (2\text{-}7)$$

The constant, b, was set to 24.76 while the constant, a, was varied. The value of the constant, a , used in Equation (2-7) for the generic solvents is shown in Table 2-6.

Figure 2-9 shows the minimum total equivalent work for the generic solvents using at 160 kPa and 30 kPa with a 5^{o}C approach on the hot side of the cross exchanger.

The results show that at 160kPa, the optimum generic solvent is one with a heat of absorption of ~ 126 kJ/gmol CO_2 which is greater than 7m MEA (80-100 kJ/gmol CO_2).

Table 2-6: Constant in generic solvent VLE expression

ΔH_{abs} (kJ/gmol CO_2)	a
42	3.82
63	11.85
83	19.89
105	27.92
126	35.96
146	43.99
167	52.03

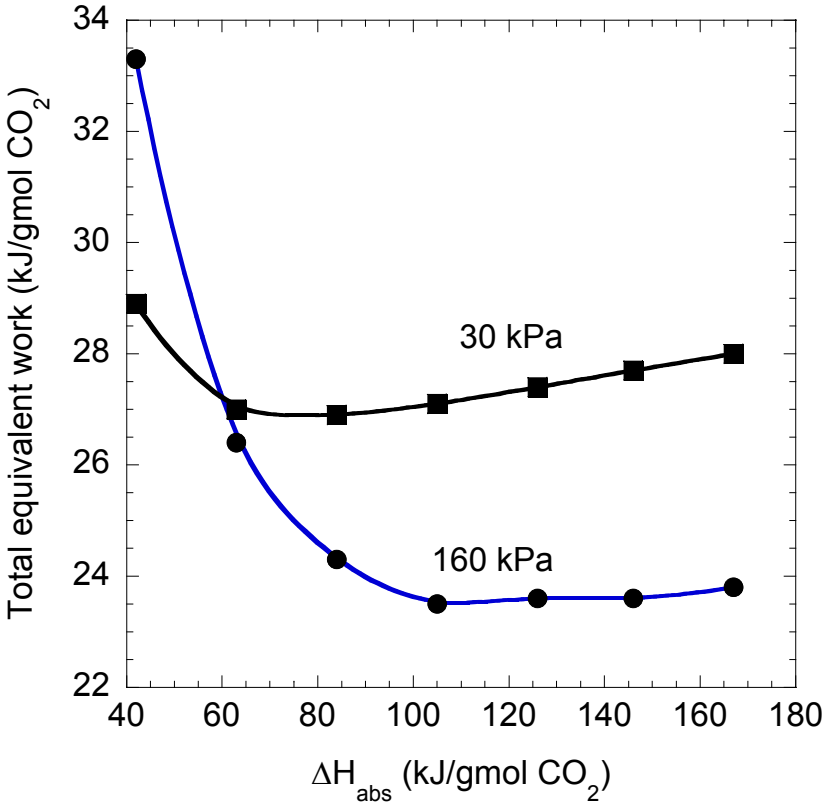

Figure 2-9: Total Equivalent Work for Generic Solvents (Rich P_{CO2}= 5 kPa at 40°C, $\Delta T = 5^{o}C$, 90% removal, P_{final} = 1000 kPa).

At 30 kPa, the optimum generic solvent is one with a heat of absorption ~ 80 kJ/gmol CO_2 (about that of 7m MEA). For solvents with ΔH_{abs} < 60 kJ/gmol CO_2, stripping at 30 kPa is more attractive than stripping at 160 kPa.

Figure 2-10 shows the reboiler duty for the generic solvents at 160 kPa and 30 kPa. The reboiler duty is minimized at ~ 80 kJ/gmol CO_2 at 160 kPa and ~ 63 kJ/gmol CO_2 at 30 kPa. Figure 2-10 suggests that for solvents with ΔH_{abs} < 40 kJ/gmol CO_2,

stripping at 30 kPa may be more attractive than stripping at 160 kPa in operations where energy use is not critical, for example in natural gas processing.

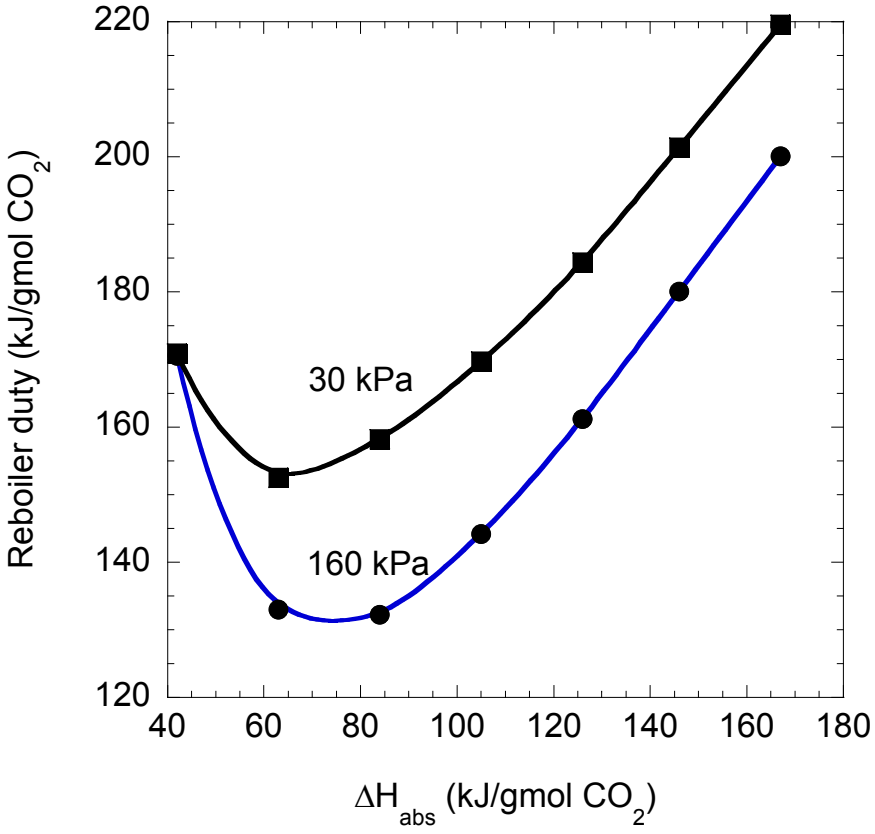

Figure 2-10: Reboiler duty for generic solvents (Rich P_{CO2}= 5 kPa at 40°C, ΔT = 5°C, 90% removal).

Chapter 3 : Alternative Stripper Flow Schemes for CO_2 Capture by Aqueous Amines

This chapter introduces four innovative stripper configurations (matrix, internal exchange, flashing feed, and multipressure with split feed). Equilibrium model results using these configurations and five different solvents: 7m (30 wt%) monoethanolamine (MEA), potassium carbonate promoted by piperazine (PZ), promoted MEA, methyldiethanolamine (MDEA) promoted by PZ, and hindered amines are presented.

3.1 Solvents and process configurations for CO_2 Capture

Current efforts to reduce the capital and operating cost of aqueous absorption/stripping technology include the development of alternative solvents to the industrial state-of-the-art, 7m (30 wt%) monoethanolamine (MEA), the use of innovative process configurations, flowsheet optimization, and energy integration with other sections of the power plant. Alternative solvents should provide equivalent or greater CO_2 absorption rates than MEA, adequate capacity for CO_2 and reduced cost of

regeneration. The important alternative solvents include promoted K_2CO_3 (Cullinane, Oyenekan et al.; Cullinane 2002; Cullinane and Rochelle 2004; Cullinane 2005), promoted MEA (Dang 2000; Okoye 2005), promoted tertiary amines (Bishnoi 2000; Aroonwilas and Veawab 2006; Idem, Wilson et al. 2006) and mildly hindered amines including the proprietary solvent KS-1 (Mimura, Simayoshi et al. 1997; Yagi, Mimura et al. 2006).

Alternative process configurations have also been proposed to reduce capital and operating costs of the CO_2 capture process. Some configurations, such as the use of multiple absorber feeds and split flow, have been proposed for the gas sweetening industry (Polasek, Bullin et al. 1982; Bullin, Polasek et al. 1983). The performance and cost structure of the split flow configuration has been evaluated by some authors (Aroonwilas 2004; Aroonwilas and Veawab 2006). Vacuum and multipressure configurations were evaluated in Chapter 2 while multipressure stripping with vapor recompression have been evaluated by Jassim and Rochelle (Jassim and Rochelle 2006). Other more complex configurations to reduce energy requirement for CO_2 removal have been proposed by some researchers (Leites, Sama et al. 2003).

In this work, an evaluation of four new stripper configurations (matrix, internal exchange, flashing feed, and multipressure with split feed) with seven representative solvent profiles is presented. The solvent properties are approximate and are not necessarily accurate representations of specific solvents, but can be viewed as generic

surrogates. The stripper model is equilibrium based and does not include absorber modeling and economics.

3.2 Analysis of the baseline configuration

Previous investigators (Draxler, Stevens et al. 2004; Oyenekan and Rochelle 2006) suggests the optimum generic solvent at 160 kPa (normal pressure) is one with a higher heat of desorption than 7m (30-wt%) MEA. Since PZ/K_2CO_3 solvents have heats of desorption lower than 7m MEA, they cannot be employed in a simple stripper with lower energy requirement than 7m MEA. The PZ/K_2CO_3 solvents possess some characteristics that may be exploited in optimized configurations. These include a lower heat of desorption which lends itself to better isothermal system operation and stripping at vacuum. The faster rates of reaction with CO_2 permit richer solutions than MEA. Since piperazine is not subject to the same chemistry of thermal degradation as MEA, it may be possible to operate the stripper at a much higher temperature and pressure than MEA. This will reduce the reboiler duty and total equivalent work because of the greater temperature swing giving an effect of a higher heat of desorption solvent.

3.2.1 Temperature approach in the cross exchanger. Chapter 2 showed that a 5^oC approach in the cross exchanger requires less total equivalent work for stripping than a 10^oC approach, at the expense of capacity. At a given reboiler pressure, operating at a 5^oC approach gives a higher temperature at the top of the column than a 10^oC approach. The temperature change across the stripper is also smaller and the reboiler duty is reduced. Achieving a 5^oC approach on the hot side of the cross exchanger may require a

small fraction of the rich solution from the absorber to bypass the cross exchanger, and be directly heated by exchange with the stripper overhead vapor because of differences in the heat capacities of the rich solution to the stripper and the lean solution from the stripper.

3.2.2 Rich end pinching. The stripper operation is frequently determined by a rich end pinch because of the larger L/G ratio at the top of the column relative to that at the bottom. With rich end pinches, the driving force at the lean end is excessively large with a loss of available work. There may be configurations that will result in an equally distributed driving force from the rich to the lean end and therefore reduce reboiler duty and total equivalent work.

3.2.3 Latent heat loss in stripper overhead. Typically, the stripper overhead includes 0.5 to 2 moles of water vapor / mole CO_2. If this stream is condensed with cooling water, the latent heat of water vapor in the stream is lost. It would be beneficial if this heat could be recovered. The simple and vacuum configurations do not recover this heat but the multipressure system does. The new configurations in this work also recover this heat.

3.3 Alternative Solvent Types

The solvents investigated are seven potential compositions best viewed as generic solvents. The generic solvents give specific heats of absorption (ΔH_{abs}), capacity and rates of reaction with CO_2. The vapor-liquid equilibrium (VLE) representation of the solvents was obtained from different sources. The heat of desorption was obtained by differentiating the VLE expression with respect to the inverse of temperature.

Moles of Alkalinity (mol Alk) is given by:

$$\text{mol Alk} = \text{mol MEA} + \text{mol } K^+ + 2 * \text{mol PZ} + \text{mol MDEA} + \text{mol KS-1} \quad (2\text{-}2)$$

3.3.1 Potassium carbonate/piperazine. This class of solvents proposed by Cullinane (Cullinane 2005) takes advantage of the fast reaction rates of CO_2 with piperazine (PZ) and the low heat of CO_2 desorption from potassium carbonate (K_2CO_3). The most studied formulation has been 5m K^+/2.5m PZ. This formulation and 6.4m K^+/1.6m PZ have been studied at the pilot scale (Chen, Rochelle et al. 2006). A third formulation, 4m K^+/4m PZ, is proposed because it will provide greater capacity for CO_2 absorption. The vapor-liquid equilibrium (VLE) representation of the solvents was obtained by fitting points calculated by the thermodynamic model of Cullinane (Cullinane 2005) to a six parameter expression.

3.3.2 Promoted MEA. The reaction rates of CO_2 with MEA can be enhanced by the addition of piperazine (Dang 2000; Dang and Rochelle 2003; Okoye 2005). In this work, the CO_2 solubility in 7m MEA/2m PZ has been represented by the surrogate solvent 11.4 m MEA.

3.3.3 Promoted tertiary amines. Tertiary amines such as methyldiethanolamine (MDEA) have been used in natural gas processing for decades. MDEA has a high capacity for CO_2 absorption and requires low regeneration energy. However it has slow rates of CO_2 absorption. To make MDEA attractive for CO_2 capture, it can be promoted by PZ (Appl 1982; Bishnoi 2000; Bishnoi and Rochelle 2002; Bishnoi and Rochelle

2002). In this work, the solubility of CO_2 in MDEA promoted by PZ is represented by the solubility of CO_2 in 4.28M (50-wt%) MDEA.

3.3.4 Hindered amines. This class of solvents has been found to possess adequate rates of reaction with CO_2, good CO_2 capacities, and low heat of regeneration and has been reported by some authors for CO_2 removal (Imai and Ishida; Sartori and Savage 1983; Sartori and Savage 1983; Sartori, Ho et al. 1987; Suzuki, Iwaki et al. 1999). In this work, KS-1 is used as a representative hindered amine solvent with limited equilibrium data extracted from Mitsubushi publications (Suzuki, Iwaki et al. 1999).

3.4. Alternative Configurations

Figure 3-1 to Figure 3-4 show four configurations that minimize energy requirement for stripping. The energy requirement is minimized at the expense of increased capital cost and process complexity. Each of these configurations assumes appropriate cross-exchange of the hot lean stream(s) with the cold rich stream(s) with an approach temperature of 5^{o}C on the hot side. Each box represents a countercurrent packing section of gas/liquid contacting.

3.4.1 Matrix Stripper. In this two-stage matrix (Figure 3-1), the temperature change across the stripper is reduced as in the multipressure configuration but without the inefficiencies associated with mechanical compression. The rich solution from the absorber is split into two streams. The first is sent to the first stripper at a higher pressure resulting in a slightly superheated feed. Heat is applied in the form of reboiler steam. The lean solution from the first column is the semi-rich feed to the middle of the

second column (which operates at a lower pressure). The other rich stream is fed to the top of the second stripper. The second column produces a semi-lean and a lean stream.

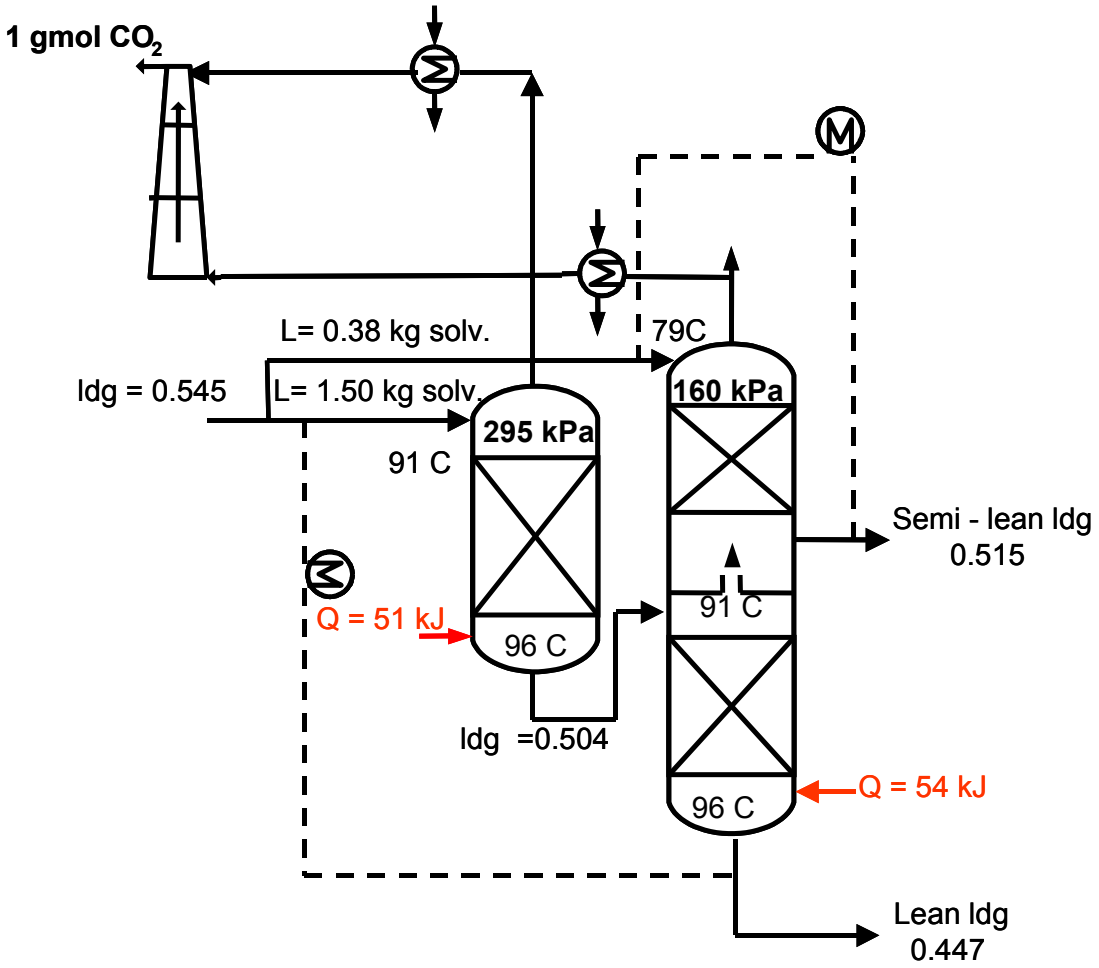

Figure 3-1: Double Matrix (295/160) Stripper for MEA/PZ (Liquid rate = 1.88 kg solvent, Rich ldg = 0.545 mol CO_2/mol Alk, Lean ldg = 0.447 mol CO_2/mol Alk, ΔT = 5^{o}C)

The semi-lean stream is cross-exchanged with the rich feed to the second column while the lean solution is cross-exchanged with the rich solution to the first stripper. The water vapor from the overhead of the second column is condensed and the CO_2 is sent to the first stage of the compression train. The water vapor in the overhead from the first column is condensed and the CO_2 is sent to the second stage in the compression train.

The compression work in this configuration is reduced because some of the CO_2 is recovered at a higher pressure, therefore requiring less compression downstream. The lower pressure column is set to 160 kPa for normal pressure operations and 30 kPa for vacuum operations. The pressure of the higher-pressure column and the flow into the flash section are optimized to minimize the total equivalent work of the system. Even though a two-stage matrix is described in this work, a three-stage matrix can also be used with reduced energy requirement but increased complexity. The equations in the double matrix stripper are shown in Appendix B.

3.4.2 Internal Exchange Stripper. This configuration Figure 3-2, integrates the stripping process with heat transfer. It serves to approach the theoretical limit of adding and removing material and energy streams along the entire column. This process has been described by Leites et al. (Leites, Sama et al. 2003) It is approximated in a configuration tested by Mitsubishi (Yagi, Mimura et al. 2006).

The configuration alleviates the temperature drop across the stripper by exchanging the hot lean solution with the solution in the stripper. One implementation

would place continuous heat exchange surface in the stripper so that there is countercurrent heat exchange of the hot lean solution with the solution coming down the stripper. A large overall heat transfer capability of 41.84 W/K-mol solvent per segment was used. This gave a typical ΔT of 1.2 K and 3K in the internal exchanger for the vacuum operation and for operation at normal pressure respectively.

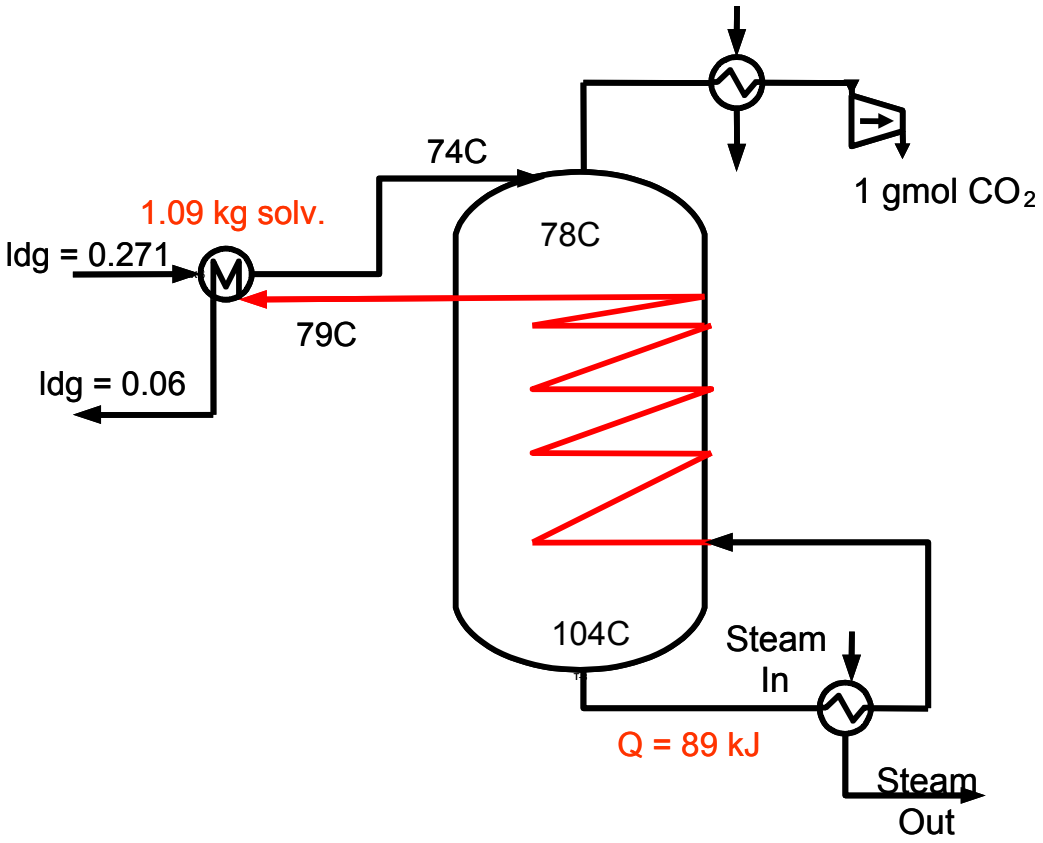

Figure 3-2: Internal Exchange Stripper at 160 kPa for MDEA/PZ (Liquid rate = 1.09 kg solvent, Rich ldg = 0.271 mol CO_2 / mol Alk, lean ldg = 0.06 mol CO_2 / mol Alk, ΔT = 5°C)

3.4.3 Multipressure with Split Feed. The multipressure configuration was described in Chapter 2 and by some authors (Jassim and Rochelle 2006). This advanced configuration (Figure 3-3) takes a 10% split feed from the liquid flowing from the middle to the lowest pressure level in a multipressure stripper and sends this stream to an appropriate point in the absorber. The temperatures at the bottom of the stripper pressure sections are equal and heat is added to each stripper pressure section. This configuration takes advantage of the favorable characteristics of the multipressure configuration and the split flow concepts. The top pressure has been optimized for all solvents and configurations. The middle pressure was taken as the geometric mean.

3.4.4 Flashing Feed Stripper. This configuration (Figure 3-4) is a special case of the split flow concept described by Leites et al. (Leites, Sama et al. 2003) and Aroonwilas (Aroonwilas 2004). A fraction of the rich stream is sent to the middle of the stripper where stripping occurs and a lean solution exits at the bottom. The rich solution is cross-exchanged with the lean solution exiting the stripper bottom. The vapor leaving the stripper is then contacted with the absorber rich flow in a five-staged upper section where the latent heat of water vapor is used to strip the CO_2 in the "cold feed" and a semi-lean stream is produced. The semi-lean product is cross-exchanged with the rich solution fed to the upper section. The reboiler duty remains unchanged and "free stripping" can be achieved in the upper section.

The split ratio of the rich streams into the middle and upper sections was optimized to minimize equivalent work.

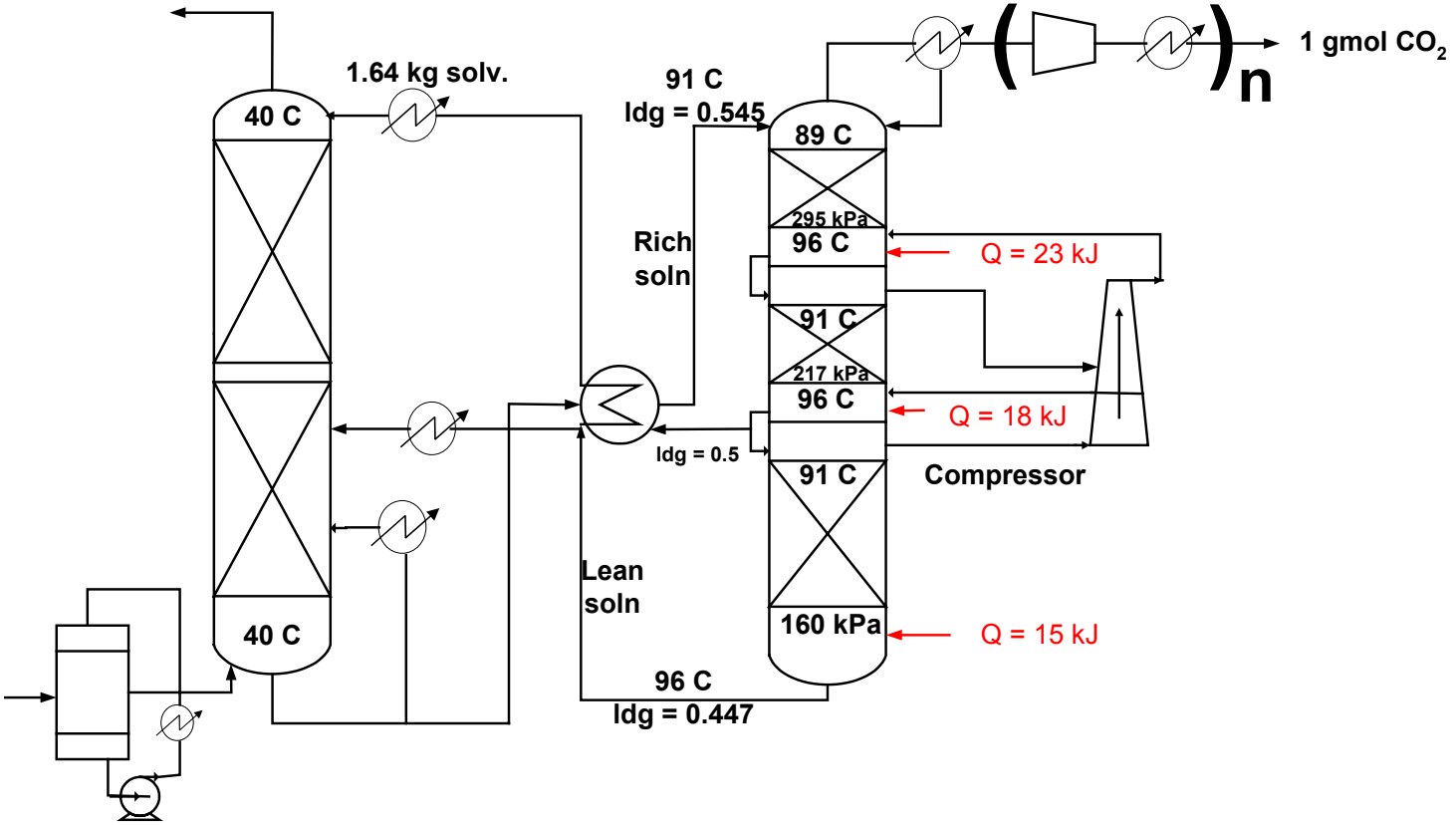

Figure 3-3: Multipressure with Split Feed Stripper (295/217/160 kPa) for MEA/PZ (Rich ldg = 0.545 mol CO_2 / mol Alk, lean ldg = 0.447 mol CO_2 / mol Alk, $\Delta T = 5^{o}C$)

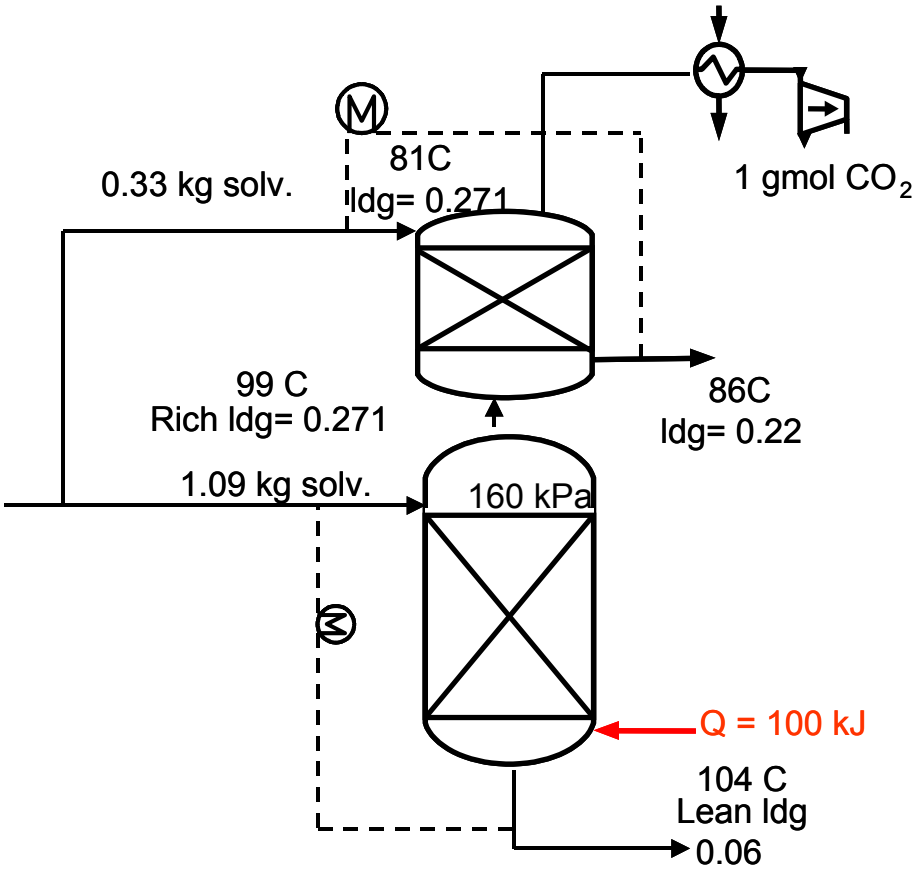

Figure 3-4: Flashing Feed Stripper at 160 kPa for MDEA/PZ (Rich ldg = 0.271 mol CO_2 / mol Alk, lean ldg = 0.06 mol CO_2 / mol Alk, $\Delta T = 5^oC$)

3.5. Model Development

An equilibrium stripper model for aqueous solvents developed in Aspen Custom Modeler (ACM) was used to evaluate the different process configurations and solvents. A rich end pinch is usually predicted because of the generous amount of contacting assumed in the model. The stripper consisted of a flash region, ten segments with 40%

Murphree efficiency assigned to CO_2, and a reboiler with 100% CO_2 efficiency. The flash region in the column was quantified in terms of actual section performance.

3.5.1 Modeling Assumptions.

a. The sections are well mixed in the liquid and vapor phases.

b. The reboiler is in vapor/liquid equilibrium.

c. There is negligible vaporization of the amine.

The CO_2 vapor pressure under stripper conditions for 7m MEA, promoted MEA and different PZ/K_2CO_3 blends is represented by the empirical expression in Table 3-1

Table 3-1: VLE expression for PZ/K_2CO_3, MEA, and promoted MEA.

$$\ln P_{CO2}^{*} = a + b\gamma + \frac{c}{T} + d\frac{\gamma^2}{T^2} + e\frac{\gamma}{T^2} + f\frac{\gamma}{T}$$

$$-\frac{\Delta H}{R} = \frac{\partial(\ln P_{CO2}^{*})}{\partial\left(\frac{1}{T}\right)} = c + 2d\frac{\gamma^2}{T} + 2e\frac{\gamma}{T} + f\gamma$$

	6.4m K^+/ 1.6m PZ	5m K^+/ 2.5m PZ	4m K^+/ 4m PZ	7m MEA	MEA/PZ (11.4m MEA)
a	-19.49	-4.59	12.088	35.11	30.27
b	24.46	34.21	42.39	-45.04	-38.87
c	3435.22	-3834.67	-7087.74	-14281	-11991
d	1464774	-1747284	-925155	-546277	1110073
e	-5514009	-1712091	1393782	-3400441	-4806203
f	12068.45	8186.474	-8552.74	32670.01	31355.6

The adjustable constants in Table 3-1 for the PZ/K_2CO_3 solutions were obtained by regressing points from the rigorous thermodynamic model by Cullinane (Cullinane 2005). The constants for the MEA solvents were regressed from points obtained from equilibrium flashes in AspenPlus using the Electrolyte Non Random Two Liquid (E-NRTL) model developed by Freguia (Freguia 2002) from data of Jou et al. (Jou, Mather et al. 1995).

The CO_2 vapor pressure over 4.28M MDEA and KS-1, based on the model by Posey et al. (Posey, Tapperson et al. 1996) is shown in Table 3-2. For 4.28M MDEA, the constants in Table 3-2 are taken from Posey et al. For KS-1 the constant, A, was set at 32.45 while constants, B-D, in the equilibrium constant expression were adjusted to fit available data (Suzuki, Iwaki et al. 1999). The amine mole fraction shown in Table 3-2 for KS-1 is set at the same value as 4.28M MDEA. The fit of the KS-1 data is shown in. Table 3-3. The CO_2 solubility in the different solvents at 40^{o}C is shown in Table 3-4.

Table 3-2: VLE expression for promoted MDEA and KS-1.

$$P_{CO2}^{*} = K_{CO2} \; X_{CO2} \left[\frac{\gamma}{1-\gamma}\right]$$

$$\ln K_{CO2} = A + \frac{B}{T} + C\,\gamma X^{o}_{amine} + D\,(\gamma X^{o}_{amine})^{0.5}$$

	MDEA/PZ (4.28 M MDEA) (8.39 m MDEA)	KS-1 (8.39 m amine)
A	32.45	32.45
B	-7440	-8870

C	33	52
D	-18.5	-15
X^{o}_{amine}	0.1313	0.1313

The heat of desorption for 4.28M MDEA and KS-1 was assumed to be constant at 62 and 73 kJ/gmol CO_2 respectively.

Table 3-3: Fit of KS-1 VLE data

		KS-1 data (Mitsubishi Heavy Industries)	Model
T (K)	CO_2 loading	P_{CO2}* (kPa)	
313.15	0.375	0.7	1.0
	0.45	1.8	2.0
	0.5	3.1	3.0
	0.575	7.6	5.9
393.15	0.05	3.8	3.3
	0.0625	5.5	4.9
	0.21	51.7	57.3
	0.325	248.2	189.1

Table 3-4: Equilibrium CO_2 loading (mol / mol Alk) at 40°C

P (kPa)	6.4m K^+/ 1.6m PZ	5m K^+/ 2.5m PZ	4m K^+/ 4m PZ	7m MEA	MEA/PZ (11.4m MEA)	MDEA/ PZ (8.39m MDEA)	KS-1 (8.39m amine)
0.125	0.468	0.416	0.322	0.373	0.363	0.019	0.177
0.5	0.532	0.467	0.384	0.442	0.428	0.046	0.303
0.75	0.549	0.482	0.402	0.463	0.447	0.060	0.345
5	0.627	0.560	0.493	0.563	0.528	0.213	0.556
7.5	0.643	0.578	0.514	0.586	0.545	0.2701	0.602
10	0.654	0.592	0.529	0.602	0.556	0.317	0.633

The heat of vaporization of water, partial pressure of water, and heat capacities of solvent (assumed to be water), steam, and CO_2 were calculated with equations from the DIPPR database (American Institute of Chemical Engineers 2004). The molar heat capacities for the CO_2, water and amine were assumed to be equal and set to that of one mole of water.

The partial pressure of CO_2 and water in each section was calculated by:

$$P_n = E_{mv}(P_n^* - P_{n-1}) + P_{n-1} \quad (2\text{-}4)$$

A Murphree efficiency (E_{mv}) of 40% and 100% was assigned to CO_2 and water. The model assumed that temperature equilibrium is achieved in each section.

The model inputs were the rich loading and liquid rate, the temperature approach on the hot side of the cross exchanger (difference between the temperature of the rich stripper feed and the lean solution leaving the bottom of the stripper), and column pressure. Initial guesses of the lean loading, section temperatures, partial pressures, and loading were provided. The model solves equations for calculating VLE and for material and energy balances. It calculates temperature and composition profiles, reboiler duty, and equivalent work.

The total energy required by the stripper is given as total equivalent work:

$$W_{eq} = 0.75\,Q\left[\frac{(T_{reb}+10)-313}{(T_{reb}+10)}\right] + W_{comp} \qquad (2\text{-}5)$$

The reboiler duty, Q, required for stripping can be approximated as the sum of three terms: the heat required to desorb the CO_2, that required to generate the water vapor at the top of the column, and the sensible heat requirement.

$$Q = Q_{des} + Q_{H2O\ gen.} + Q_{sens} \qquad (3\text{-}1)$$

$$= \Delta H_{des} + \left(\frac{n_{H2O}}{n_{CO2}}\,H_{vap}\right) + \left(\frac{L\ Cp\ \Delta T}{n_{CO2}}\right) \qquad (3\text{-}2)$$

W_{comp} constitutes the isentropic work of compression to 330 kPa of the gas exiting the top of the stripper. An efficiency of 75% was assumed for the compressor. For the vacuum operations, five compressor stages were used, while for the normal pressure cases, three compressor stages were used. Two stages of compression were used to get to the maximum pressure of the process and an additional stage to 330 kPa with intercooling to 313K between compressor stages.

The work lost by extracting steam from a turbine is the first term on the right hand side of (3-2), while the second is the compressor work. The condensing temperature of the steam is assumed to be 10K higher than the reboiler fluid. The turbine assumes condensing steam at 313K and has been assigned an effective Carnot efficiency of 75%.

3.6. Results and Discussion

Table 3-5 gives the performance (stripping and compression work to 330 kPa) of the stripper configurations investigated and the capacities of the solvents to achieve 90% CO_2 removal. The rich P_{CO2}* shown in the table are typical rich partial pressures expected for the solvents investigated. 4m K^+/4m PZ, MEA/PZ, and MDEA/PZ are assigned greater rich P_{CO2}* because they are solvents with faster rates of reaction with CO_2 which result in richer solutions. In this work, the lean loading for each configuration was optimized to minimize equivalent work. The optimum lean loading, the lean loading that minimized equivalent work, was quite flat and was approximately that for 90% change in equilibrium partial pressure of CO_2. The lean loading and results shown in Table 3-5 correspond to a 90% equilibrium partial pressure change in CO_2 at 40^{o}C. The 10^{o}C approach cases were optimized with respect to lean loading as these usually give more capacity for absorption.

The heat of absorption shown in Table 3-5 is that calculated at the lean loading and 40^{o}C.

The capacity of the solution is given by:

$$\text{capacity}\left(\frac{\text{mol}\,CO_2}{\text{kg}\,H_2O}\right) = \left(\gamma_{\text{rich}} - \gamma_{\text{lean}}\right) \quad \frac{\text{mol}\,\text{Alk}}{\text{kg}\,H_2O} \tag{2-6}$$

3.6.1 Effect of varying temperature approach. The baseline configuration is a stripper operating at 160 kPa with a 10^{o}C approach on the hot side of the cross exchanger. The lean loadings for the baseline in Table 3-5 were optimized and frequently resulted in overstripping to increase the capacity of the solvents for absorption. With a 5^{o}C approach on the hot side of the cross exchanger, 3% and 12% energy savings are obtained for the 6.4m K^{+}/1.6m PZ and 7m MEA, respectively. This savings in energy is at the expense of a larger investment in heat exchange surface.

The relative contributions of the components of the reboiler duty with a 5^{o}C and 10^{o}C approach are shown in Table 3-6.

Table 3-5: Predicted performance of seven solvents and various stripper configurations (90% removal, $\Delta T = 5^{o}C$, P_{final} = 330 kPa)

Solvent		6.4m K^+/ 1.6m PZ	5m K^+/ 2.5m PZ	4m K^+/ 4m PZ	7m MEA	MEA/PZ	MDEA/PZ	KS-1
ΔH_{abs} (kJ/gmol CO_2)		50	63	66	84	85	62	73
Rich P_{CO2}* (kPa) at 40°C		5	5	7.5	5	7.5	7.5	5
Capacity (mol CO_2/kg H_2O)		0.91	0.93	1.34	0.85	1.12	1.77	2.11
Configuration	Pressure (kPa)	Equivalent Work (kJ/gmol CO_2)						
Baseline	160 ($\Delta T=10^{o}C$)	28.1	24.9	21.4	22.3	20.0	18.3	19.1
Improved Baseline	160	27.4	22.6	19.0	19.7	17.5	17.2	17.9
Multipressure	x/160	27.0	20.5	17.8	18.2	16.2	16.3	17.0
	x	180	265	295	280	295	295	295
Matrix	x/160	24.3	21.7	15.6	18.0	15.7	15.1	16.1
	x	250	295	295	265	295	295	295
	Feed split (%)	120	40	20	25	25	30	30
Internal Exchange	160	25.3	19.5	17.3	17.5	16.0	15.7	16.5
Multi P with 10% split feed		29.7	20.7	17.5	18.1	15.9	15.7	16.6
Flashing feed	160	23.5	20.7	18.0	18.7	16.8	16.3	17.2
	Feed split (%)	85	35	20	25	20	30	35
Vacuum	30	23.7	23.1	21.1	22.6	21.1	19.8	21.2
Multipressure	x/30	23.7	22.5	20.2	21.6	19.9	19.2	20.7
	X	30	42	45	45	47	45	42
Matrix	x/30	22.5	21.8	18.1	21.2	19.4	18.2	19.8
	x	42	45	47	47	45	45	45
	Feed split (%)	90	55	40	50	35	40	70
Internal Exchange	30	22.5	21.6	19.8	21.0	19.8	19.0	20.4
Multi P with 10% split feed		31.3	22.6	20.2	21.6	19.7	19.9	20.7
Flashing feed	30	22.7	22.5	20.6	22.1	20.6	19.5	20.8
	Feed split (%)	55	35	35	35	30	35	45

x = highest pressure in configuration

Table 3-6: Relative contributions to reboiler duty for 7m MEA with varying temperature approach (Rich loading = 0.563 mol CO_2/molAlk, optimized lean loading, P = 160 kPa)

ΔT	5°C	10°C
Q_{des} (kJ/gmol CO_2)	65.7	65.0
$Q_{H2O\ gen.}$ (kJ/gmol CO_2)	32.2	27.0
Q_{sens} (kJ/gmol CO_2)	29.8	59.4

The differences in the contributions to the overall reboiler duty are in the heat required to generate water vapor at the top of the column and the sensible heat requirement. Operation at a 10°C approach requires twice the sensible heat requirement than a 5°C approach. The heat required to generate water vapor in the overhead gas stream is slightly higher with the 5°C approach. The net effect is that operation at a 5°C approach provides significant sensible heat savings.

3.6.2 Effect of operating pressure. Operating the stripper under vacuum (30 kPa) with a 5°C temperature approach in the cross exchanger offers a 14% reduction in equivalent work for 6.4m K^+/1.6m PZ and 4% and 20% more energy with 5m K^+/2.5m PZ and MEA/PZ respectively. Solvents with high heats of absorption take advantage of the temperature swing. The relative vapor pressure of CO_2 and water changes with temperature. This change is greater with solvents with high heats of absorption as shown in Table 3-7.

Table 3-7: Contributions to reboiler duty - effect of temperature swing on simple strippers

	6.4m K^+/ 1.6m PZ		MEA/PZ	
P (kPa)	30	160	30	160
$\left(\frac{P_{CO2}}{P_{H2O}}\right)$ at rich end	0.538	0.415	1.065	1.850
ΔH_{des} (kJ/gmol CO_2)	51	34	76	68
$\left(\frac{n_{H2O}}{n_{CO2}}\right) H_{vap}$ (kJ/gmol CO_2)	81	105	41	24
$\left(\frac{L\ Cp\ \Delta T}{n_{CO2}}\right)$ (kJ/gmol CO_2)	30	30	24	24
Q (kJ/gmol CO_2)	162	169	141	115

Table 3-7 shows the contributions to the reboiler duty for 6.4m K^+/1.6m PZ and MEA/PZ with ΔH_{abs} of 50 and 85 kJ/gmol CO_2 respectively. The major difference between the reboiler duties is the relative amount of the heat of desorption of CO_2 and the heat required to generate the water vapor at the top of the stripper. Vacuum operation for a fixed solvent and CO_2 removal generates a larger amount of water vapor at the top of the column relative to operation at normal pressure. The overall effect is a 30 kPa stripper is attractive with 6.4m K^+/1.6m PZ and normal pressure (160 kPa) favors solvents with high heats of desorption (e.g. MEA/PZ).

3.6.3 Predicted Performance of Alternative Configurations. Table 3-5 shows that the multipressure configuration with a 160 kPa reboiler is more attractive for the solvents with a high heat of absorption than solvents with a lower heat of absorption. The performance of the alternative configurations is matrix > internal exchange >

multipressure with split feed > flashing feed. The matrix and internal exchange configurations with a 160 kPa reboiler and 5°C approach with 7m MEA offer 9% and 11% energy savings respectively over the simple stripper operated at 160 kPa with a 5°C approach.

The characteristics of the matrix (265/160 kPa) and simple strippers for MEA are shown in Table 3-8. The matrix stripper recovers about 40% of the CO_2 at a higher pressure and does not have the inefficiencies associated with the multipressure stripper. The reboiler duty is also slightly less for the matrix than the vacuum stripper.

Table 3-8: Performance of matrix (265/160 kPa) stripper and normal pressure (160 kPa) for MEA (Rich loading = 0.563 mol CO_2/mol Alk, lean loading = 0.442 mol CO_2/ mol Alk, $\Delta T = 5^oC$, P_{final} = 330 kPa)

	P	Fraction of CO_2 removed	Q	W_{comp}	Total W_{eq}
	kPa		kJ/gmol CO_2		
Matrix	265	0.4	56		
	160	0.6	58	2.1	17.9
160 kPa	160	1	123	2.9	19.7

The characteristics of the vacuum and the vacuum internal exchange strippers are shown in Table 3-9. The major difference between the two configurations is the difference in the ratio of the water vapor to CO_2 in the overhead stream. The internal exchange stripper has a smaller ratio of water vapor to CO_2. Multipressure with split feed reduces the flow into the bottom section of the stripper and thus equivalent work. The flashing feed makes use of the latent heat of water vapor in the simple/vacuum

configuration to strip some CO_2 in the rich stream entering the stripper at the top of the column.

Table 3-9: Characteristics of the vacuum and vacuum internal exchange strippers for 7m MEA (Rich loading = 0.563 mol CO_2/mol Alk, lean loading = 0.442 mol CO_2/ mol Alk, $\Delta T = 5^oC$)

	Vacuum	Vacuum Internal Exchange
$\left(\frac{P_{CO2}}{P_{H2O}}\right)$ at rich end	0.81	1.31
ΔH_{des} (kJ/gmol CO_2)	73	72
$\left(\frac{n_{H2O}}{n_{CO2}}\right) H_{vap}$ (kJ/gmol CO_2)	54	34
$\left(\frac{L\ Cp\ \Delta T}{n_{CO2}}\right)$ (kJ/gmol CO_2)	30	30
Q (kJ/gmol CO_2)	157	135

3.6.4 Solvent Performance. Table 3-5 shows the performance of the different solvent types. The results show that at 160 kPa, MEA/PZ and MDEA/PZ require significantly less equivalent work than 7m MEA. MEA/PZ offers a 13% and 8% savings over 7m MEA with the matrix and internal exchange configurations at 160 kPa. MDEA/PZ was the most attractive solvent under vacuum conditions. MDEA/PZ offers a 14% and 10% savings over 7m MEA with the matrix and internal exchange configurations at 30 kPa. This shows that, at normal pressure, solvents with high heats of absorption and reasonable capacities are attractive. Under vacuum conditions, solvents with lower heats

of absorption and higher capacities are attractive. Capacity seems to play a more important role in determining energy requirements at vacuum conditions.

3.6.5 Effect of heat of absorption. From Table 3-5, solvents with similar capacities but different heats of absorption can be compared. The results show that at a fixed capacity, solvents with high heats of absorption require less energy for stripping. This is a consequence of the temperature swing. 5m K^+/2.5m PZ offers 18% savings over 6.4m K^+/1.6m PZ at 160 kPa with a 5^{o}C approach and savings of 3% and 4% with the matrix and internal exchange configurations at vacuum conditions.

The performance of 6.4m K^+/1.6m PZ and 5m K^+/2.5m PZ are compared in Table 3-10.

Table 3-10: Effect of ΔH_{abs} on stripper performance (90% removal, $\Delta T = 5^oC$, P_{final} = 330 kPa)

	6.4m K^+/1.6m PZ		5m K^+/2.5m PZ	
ΔH_{abs} (kJ/gmol CO_2)	50		63	
Capacity (mol CO_2/kg H_2O)	0.91		0.93	
P (kPa)	30	160	30	160
Q_{des} (kJ/gmol CO_2)	51.1	34.3	67.4	57.9
$Q_{H2O\ gen.}$ (kJ/gmol CO_2)	81.3	105.5	61.2	51.3
Q_{sens} (kJ/gmol CO_2)	29.4	29.7	28.2	29.4
Equivalent Work (kJ/gmol CO_2)	23.7	27.4	23.1	22.6

The two solvents in Table 3-10, 6.4m K^+/1.6m PZ and 5m K^+/2.5m PZ, have similar capacities. The major difference between the solvents is the heat of absorption. The relative contributions to the reboiler duty show that for 6.4m K^+/1.6m PZ, most of the heat supplied in the reboiler is used to generate water vapor at the top of the column. For 5m K^+/2.5m PZ, more heat is used to desorb CO_2 relative to generating water vapor at the top of the column. The sensible heat requirement is approximately equal because of the similar capacities and percent removal required. The difference in equivalent work is significant at 160 kPa. The savings experienced by using 5m K^+/2.5m PZ is because of the temperature swing desorption. At vacuum conditions, 30 kPa, the effect of the temperature swing disappears and the performance of the solvents are approximately equal.

3.6.6 Effect of capacity. The capacity of a solvent is defined as the amount of CO_2 a solvent can absorb over a given range of loading or partial pressure. This reflects the vapor-liquid equilibrium characteristics of a solvent. A high capacity solvent can absorb or desorb more CO_2 than one with a low capacity. In Table 3-5, 5m K^+/2.5m PZ and MDEA/PZ have similar heats of absorption. However MDEA/PZ has a greater capacity than 5m K^+/2.5m PZ. MDEA/PZ provides 30% and 19% energy savings over 5m K^+/2.5m PZ with the matrix and internal exchange configurations with the reboiler operating at 160 kPa and 17% and 12% savings with these configurations at 30 kPa.

The two MEA solvents also have similar heats of absorption. MEA/PZ represented by 11.4 m MEA has a higher capacity than 7m MEA. MEA/PZ offers 13%

energy savings over 7m MEA with the matrix stripper operated with a 160 kPa reboiler temperature. The effect of capacity on the 160 kPa stripper performance using 5m K^+/2.5m PZ and MDEA/PZ are compared in Table 3-11. The solvents have similar heats of absorption MDEA/PZ possessing about twice the capacity of 5m K^+/2.5m PZ. The results show that the increased capacity of MDEA/PZ provides both sensible heat and steam generation savings.

Table 3-11: Effect of capacity on 160 kPa stripper performance (90% removal, $\Delta T = 5^oC$, $P_{final} = 330$ kPa)

	5m K^+/2.5m PZ	MDEA/PZ
ΔH_{abs} (kJ/gmol CO_2)	63	62
Capacity (mol CO_2/kg H_2O)	0.93	1.77
Q_{des} (kJ/gmol CO_2)	57.9	61.9
$Q_{H2O\ gen.}$ (kJ/gmol CO_2)	51.3	29.2
Q_{sens} (kJ/gmol CO_2)	29.4	14.2
Equivalent Work (kJ/gmol CO_2)	22.6	15.1

3.6.7 Insight into stripper operation. McCabe-Thiele plots provide insight into stripping phenomena. Figure 3-5 shows the McCabe-Thiele plot for 6.4m K^+/1.6m PZ at 30 kPa comprising of a flash section, ten segments, and an equilibrium reboiler. The stripper operation approaches a lean end pinch. Since this column is not pinched, it could benefit significantly by using more contacting. This is shown in Figure 3-6 where the

number of contacting segments is doubled. Flashing of the rich solution occurs at the top of the column. A rich end pinch is observed. The total equivalent work to generate CO_2 at 330 kPa decreases from 23.7 kJ/gmol CO_2 with ten segments to 23.2 kJ/gmol CO_2 (a 2% reduction) when the number of segments is doubled. Increasing the number of segments implies increased capital cost.

The McCabe-Thiele plot for 7m MEA with the matrix (265/160kPa) configuration is shown in Figure 3-7.

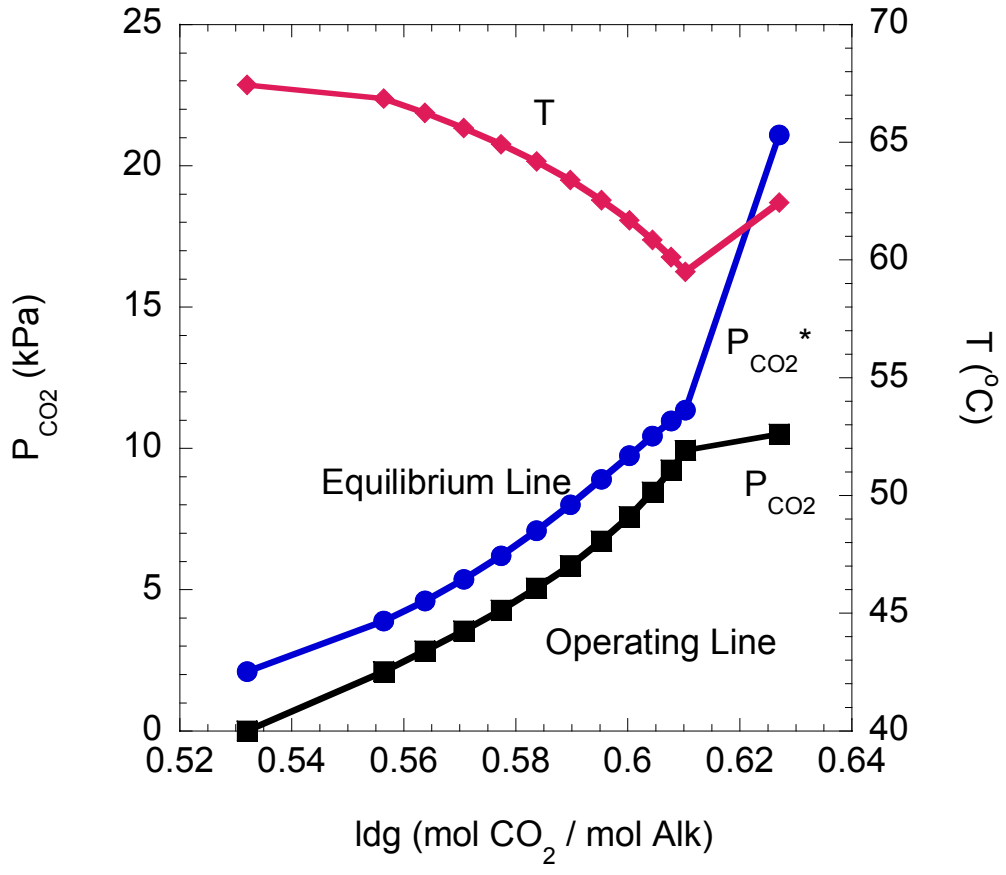

Figure 3-5: McCabe-Thiele plot for 30 kPa stripper using 6.4m K^+/1.6m PZ with 10 segments (rich ldg = 0.627 mol CO_2/mol Alk, lean ldg = 0.532 mol CO_2/ mol Alk, $\Delta T = 5^oC$)

It is observed that the high and low pressure columns are highly pinched. A significant amount of CO_2 desorption occurs due to flashing and under boiling conditions in the reboiler. The rich, semi-rich, and lean loadings are 0.563, 0.513, and 0.447 mol CO_2/ mol Alk. This implies that a significant amount of desorption occurs in both sections of the low-pressure column.

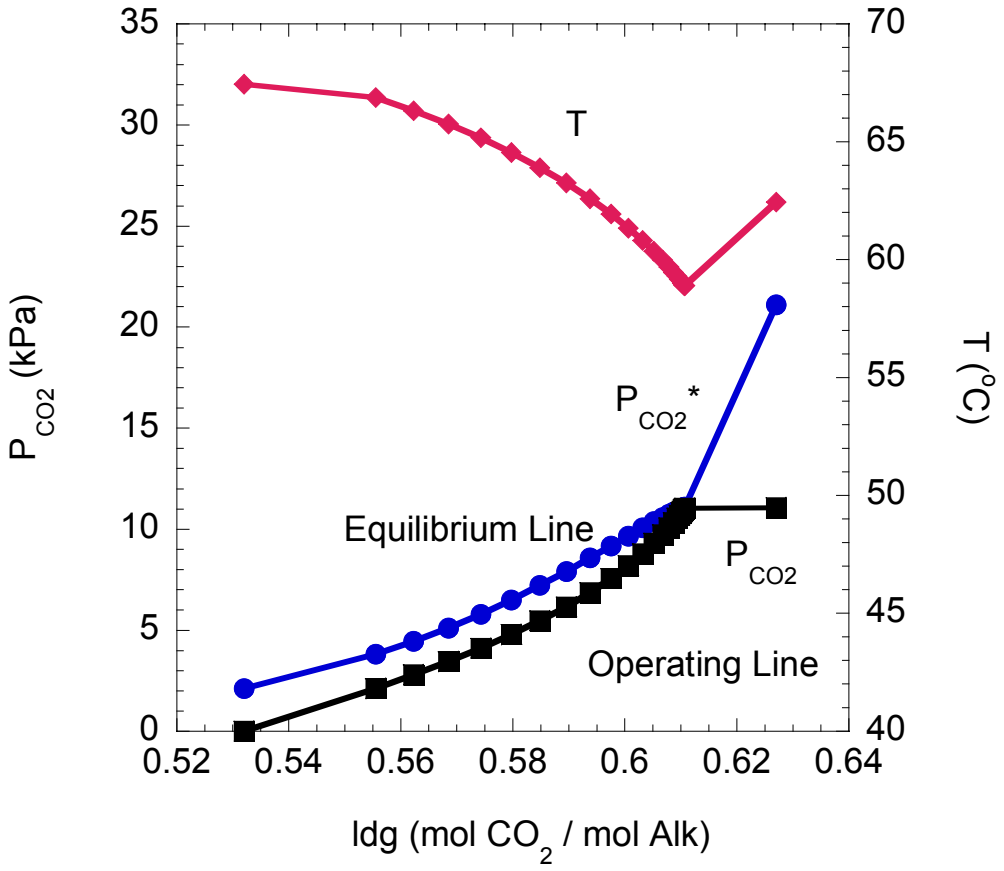

Figure 3-6: McCabe-Thiele plot for 30 kPa stripper using 6.4m K^+/1.6m PZ with 22 segments (rich ldg = 0.627mol CO_2/mol Alk, lean ldg = 0.532 mol CO_2/ mol Alk, $\Delta T = 5^oC$)

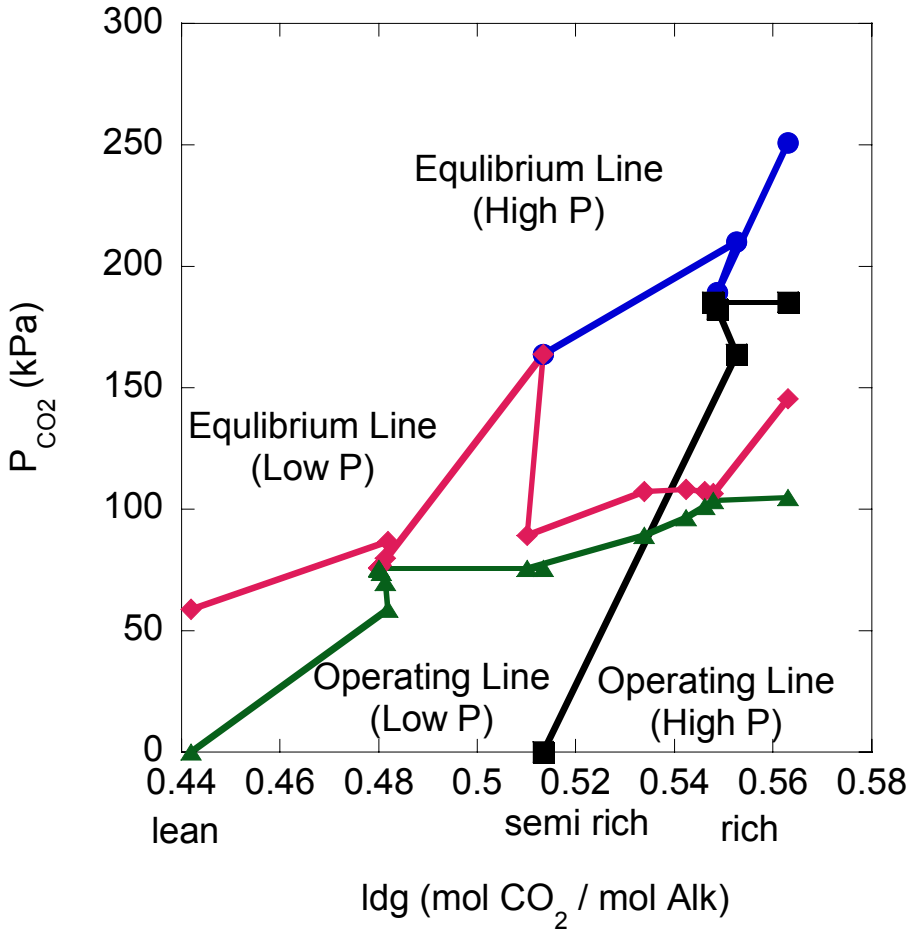

Figure 3-7: McCabe-Thiele plot for matrix (265/160 kPa) stripper using 7m MEA (rich ldg = 0.563 mol CO_2/ mol Alk, lean ldg = 0.442 mol CO_2/ mol Alk, $\Delta T = 5^oC$)

Figure 3-8 shows the McCabe-Thiele plot for the internal exchange stripper with 7m MEA at 160 kPa. The feed is subcooled with a loading of 0.563 mol CO_2/mol Alk. Some CO_2 absorption occurs at the stripper feed, increasing the loading to 0.583 mol CO_2/mol Alk in the first segment in the stripper before subsequent stripping. The stripper has a rich end pinch. A significant amount of stripping occurs in the reboiler because it is assumed to be an equilibrium stage.

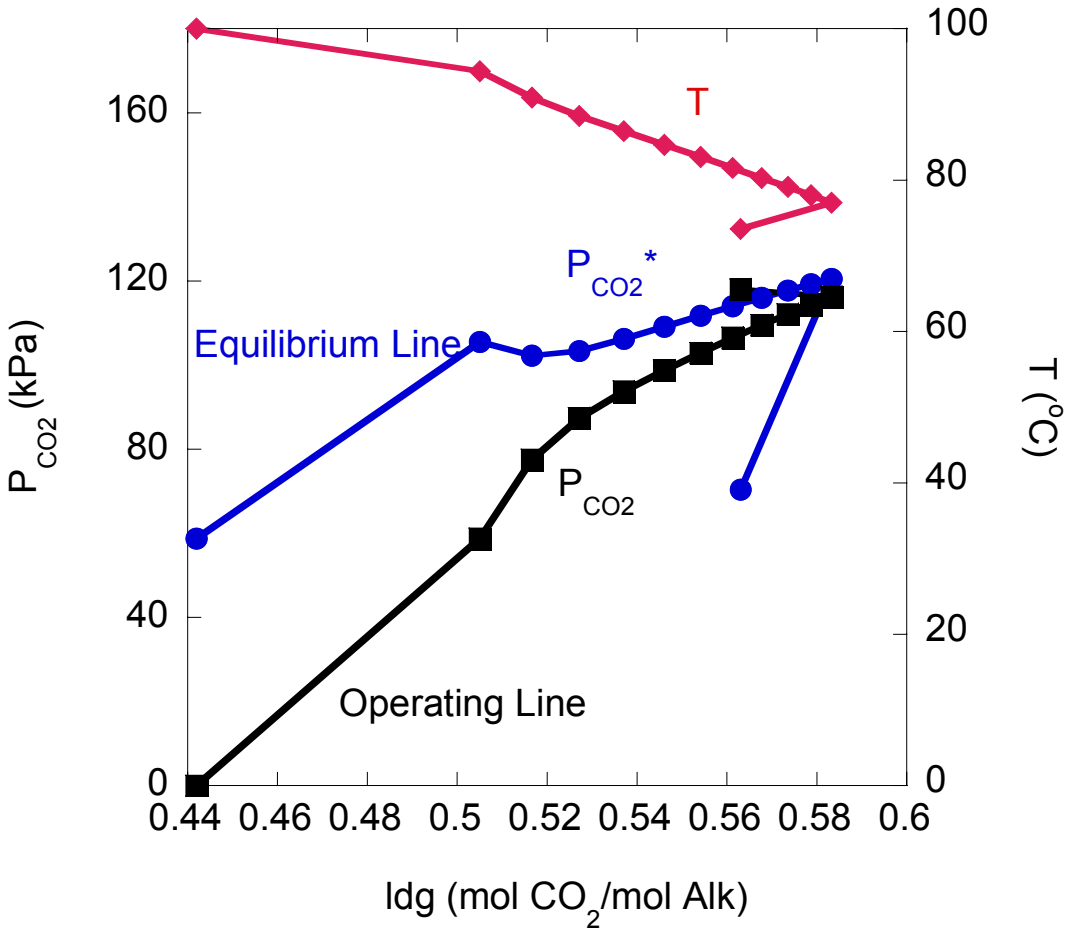

Figure 3-8: McCabe-Thiele plot for internal exchange stripper using 7m MEA at 160 kPa (rich ldg = 0.563 mol CO_2/ mol Alk, lean ldg = 0.442 mol CO_2/ mol Alk, $\Delta T = 5^oC$)

3.6.8 Effect on power plant output and process improvement. The addition of an absorption/stripping system to a power plant will reduce the plant efficiency by reducing the net power produced from the plant since steam is withdrawn from the plant to drive the reboiler and electrical power is used to operate compressors, blowers etc. Based on

process analysis and economic studies (Fisher, Beitler et al. 2005), the net power output of a 500 MW power plant is about 150 kJ/gmol CO_2 with 90% CO_2 removal. Different separation techniques are compared by separation and compression work in Table 3-12. The smaller energy requirements for fans and pumps have not been included in this analysis.

Table 3-12: Energy requirement for separation and compression to 10 MPa

Separation Method	W_{sep}	W_{comp} to 330 kPa	W_{sep} + W_{comp} to 330 kPa	W_{comp} (330 kPa to 10 MPa)	Total W_{eq}
	kJ/gmol CO_2				
Isothermal Sep. (40°C, 100 kPa), Ideal Comp.	7.3	3.1	10.4	7.7	18.1
Isothermal Sep. (40°C, 100 kPa), 75% adiabatic compression in 5 stages	7.3	5.7	13.0	11.1	24.1
Isothermal Sep. (40°C), 75% adiabatic compression in 5 stages (Membrane-like)	11.6	5.7	17.3	11.1	28.4
Baseline (7m MEA, $\Delta T = 10^oC$, 160 kPa)	19.4	2.9	22.3	11.1	33.5
Improved Baseline (7m MEA, $\Delta T = 5^oC$, 160 kPa)	16.8	2.9	19.7	11.1	30.9
Matrix 4m K^+/4m PZ (295/160)	15.1	0.5	15.6	11.1	26.7
Matrix MEA/PZ (295/160)	15.2	0.5	15.7	11.1	26.8
Matrix MDEA/PZ (295/160)	14.6	0.5	15.1	11.1	26.2
Matrix KS-1 (295/160)	15.6	0.5	16.1	11.1	27.2
Matrix 4m K^+/ 4m PZ (47/30)	9.6	8.5	18.1	11.1	29.1
Matrix MEA/PZ (45/30)	10.7	8.7	19.4	11.1	30.5
Matrix MDEA/PZ (45/30)	9.5	8.7	18.2	11.1	29.3
Matrix KS-1 (45/30)	11.1	8.7	19.8	11.1	30.9

The ideal separation work at 40°C and 100 kPa is calculated from the theoretical minimum thermodynamic work (Figure 3-9):

$$W_{min} = W_{min,flue\ gas} - (W_{min,CO2\ removed} + W_{min,product}) \quad (3\text{-}3)$$

where W_{min} is the theoretical minimum thermodynamic work

$W_{min,flue\ gas}$ is the work associated with the flue gas

$W_{min,CO2\ removed}$ is the work associated with the CO_2 rich stream

$W_{min,product}$ is the work associated with the N_2 rich stream.

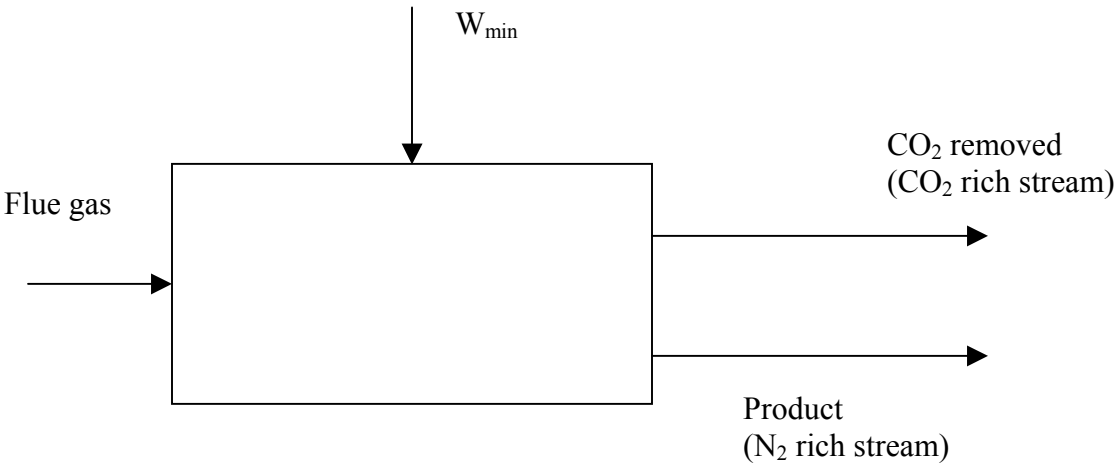

Figure 3-9: Minimum thermodynamic separation work

$$W_{min,flue\,gas} = -R\,T\left[\frac{n_{CO2}}{n_{CO2}+n_{N2}}\ln x_{CO2} + \frac{n_{N2}}{n_{CO2}+n_{N2}}\ln x_{N2}\right] \quad (3\text{-}4)$$

Assuming 1 gmol of flue gas containing 12% CO_2 and 88% N_2, the $W_{min,fluegas}$ is:

$W_{min,fluegas}$ = -(8.314) (313) (0.12 ln 0.12 + 0.88 ln 0.88)

= 0.953 kJ

$$W_{min,CO2\ removed} = -RT\left[\frac{n_{CO2\ removed}}{n_{CO2}+n_{N2}}\ln x_{CO2\ removed} + \frac{n_{N2\ removed}}{n_{CO2}+n_{N2}}\ln x_{N2\ removed}\right] \quad (3\text{-}5)$$

For a pure CO_2 stream, $x_{CO2} = 1$ and $W_{min,CO2\ removed} = 0$.

$$W_{min,product} = -RT\left[\frac{n_{CO2\ product}}{n_{CO2}+n_{N2}}\ln x_{CO2\ product} + \frac{n_{N2\ product}}{n_{CO2}+n_{N2}}\ln x_{N2\ product}\right] \quad (3\text{-}6)$$

$$= -(8.314)(313)(0.012 \ln 0.01345 + 0.88 \ln 0.98655)$$

$$= 0.167 \text{ kJ}$$

$W_{min} = 0.953 - 0.167 = 0.786$ kJ

Since 90% CO_2 removal is targeted, then $N_{CO2\ removed} = 0.9\ (0.12) = 0.108$ gmol.

$W_{min,normalized} = 0.786/0.108 = 7.3$ kJ/gmol CO_2.

The total equivalent work for isothermal separation at 100 kPa and 40°C, and subsequent compression to 10 MPa, is 18.1 kJ/gmol CO_2. This is the theoretical minimum work for separation and compression to 10 MPa. This constitutes about 12% of the power plant output.

The ideal compression work was calculated by:

$$W_{ideal} = RT\ln\left[\frac{P_2}{P_1}\right] \quad (3\text{-}7)$$

If five compressors with 75% adiabatic efficiency are used, the total equivalent work is 24.1 kJ/gmol CO_2 (16% of the power plant output). If isothermal separation at 40°C and 75% adiabatic compression in five stages is used to create the driving force for separation, the total equivalent work is 28.4 kJ/gmol CO_2. This can be likened to separation with a perfect membrane.

The best solvent and process configuration is the matrix (295/160 kPa) with MDEA/PZ. This consumes 26.2 kJ/gmol CO_2 (18% of the net output from a 500 MW power plant with 90% CO_2 capture). This best case offers 22% energy savings over the current industrial baseline (7m MEA, $\Delta T = 10^oC$, 160 kPa) and 15% savings over the improved baseline (7m MEA, $\Delta T = 5^oC$, 160 kPa). This best case requires 2.1 kJ/gmol CO_2 more work than the theoretical minimum with real compressors. Therefore, there is little room for improvement.

3.7. Improved stripper flow schemes

This section presents twelve clear flowsheets and simplified heat and material balances for improved stripper flow schemes.

The cases presented are:

1. Base case with 5^oC approach for MEA - This reduces the sensible heat requirement in heating the rich solution to the lean solution by using a larger cross exchanger area. It improves on the industrial base case cross exchanger approach of 10^oC.

2. Double matrix stripper for 4m K^+/ 4m PZ - This constitutes the best K_2CO_3/PZ solvent. This solvent possesses increased capacity advantages over the 5m K^+/2.5m PZ that have been studied at laboratory and pilot scales (Cullinane 2005; Chen, Rochelle et al. 2006).

3. Double matrix stripper for MEA/PZ - This is a proposed promoted MEA case with superior CO_2 reaction rates than 7m MEA. Limited data has been collected in our laboratories and simulation results show over 10% energy savings over the 7m MEA system.

4. Best vacuum case for 6.4m K^+/1.6m PZ (i.e. double matrix)- The effect of using a solvent with a low heat of absorption will be quantified with this solvent. Previous work suggests that vacuum stripping favors solvents with a low heat of absorption.

5. Vacuum for MEA/PZ - The effect of running strippers at vacuum for MEA/PZ to reduce degradation and corrosion and also reduce capital costs of the stripping column on energy requirements will be studied here.

6. Retrofit concepts to maximize shift of Q to W for 6.4m K^+/1.6m PZ e.g. (double matrix with vapor recompression).

7. Multipressure vacuum with MEA/PZ.

8. Multipressure vacuum with vapor recompression for MEA/PZ.

9. Multipressure vacuum with heat recovery for MEA/PZ (scheme1).

10. Multipressure vacuum with heat recovery for MEA/PZ (scheme2).

11. Multipressure vacuum with heat recovery for MEA/PZ (scheme3).

12. Multipressure vacuum with heat recovery for MEA/PZ (scheme 4).

3.7.1. Description of alternative stripper concepts with heat recovery

3.7.1.1 Double matrix with Vapor Recompression Stripper. In this configuration, the overhead stream from each of the two columns in the matrix stripper is compressed and the product is then cooled to the condensing temperature of the steam used in the reboiler after which the vapor is compressed in four stages with intercooling to the condensing temperature of the reboiler steam. The heat contained in the water condensed in the intercooling operation supplies part of the reboiler duty. This configuration reduces the

reboiler duty but increases the work requirement for the process. This configuration maximizes the shift of heat to work and is best with low ΔH solvents such as 6.4m K^+/1.6m PZ.

3.7.1.2 Multipressure Vacuum Stripper with Vapor Recompression. In this configuration, the overhead stream from the multipressure stripper is compressed and the product is then cooled to the condensing temperature of the steam used in the reboiler after which the vapor is compressed in four stages with intercooling to the condensing temperature of the reboiler steam. The heat contained in the water condensed in the intercooling operation supplies part of the reboiler duty. This configuration reduces the reboiler duty but increases the work requirement for the process.

3.7.1.3 Multipressure Vacuum Stripper with Heat Recovery (Scheme 1). In this configuration, the overhead stream from the multipressure vacuum stripper is cooled with cooling water, compressed and then cooled to the condensing temperature of the steam used in the reboiler. The exiting stream is then cooled to 40^{o}C with cooling water and the process is repeated from the compression operation until the final pressure of 10 MPa is reached.

3.7.1.4 Multipressure Vacuum Stripper with Heat Recovery (Scheme 2). In this configuration, the overhead stream from the multipressure vacuum stripper is compressed and then cooled to the condensing temperature of the steam used in the reboiler. The exiting stream is then cooled to 40^{o}C with cooling water and the process is repeated until the final pressure of 10 MPa is reached.

3.7.1.5 Multipressure Vacuum Stripper with Heat Recovery (Scheme 3). In this configuration, the overhead stream from the multipressure vacuum stripper is compressed and then cooled to the condensing temperature of the steam used in the reboiler. The exiting stream is compressed, cooled to the condensing steam temperature in the reboiler and then with cooling water to 40^{o}C and the process is repeated from the second compression operation until the final pressure of 10 MPa is reached.

Detailed flowsheets for the twelve concepts in this section are shown in Figure 3-10 to Figure 3-21 and a summary of the results is shown in Table 3-13.

Table 3-13: Heat and material balance summary for improved stripper flowsheets

Basis: 1 gmol of CO_2 removed

Case	L	Rich loading	Lean loading	Q	W_{comp} to 10 MPa	Total W_{eq}
	kg solvent	mol CO_2/mol Alk		KJ		
Base case	1.11	0.563	0.442	123	14.1	30.9
DM – 4m K^+/4m PZ	1.57	0.514	0.402	59/49	11.8	26.7
DM – MEA PZ	1.88	0.545	0.447	51/54	11.6	26.8
DM – 6.4m K^+/1.6m PZ	3.34	0.627	0.532	30/110	12.3	35.5
DM –MEA/PZ (vacuum)	1.92	0.545	0.447	59/73	19.5	30.5
DMVR 6.4m K^+/1.6m PZ	3.34	0.627	0.532	27/58*	23.2	36.2
MPV - MEA/PZ	1.61	0.545	0.447	118	23.6	32.2
MPVVR-MEA/PZ	1.61	0.545	0.447	35*/83**	26.9	32.9
MPVHR1 – MEA/PZ	1.61	0.545	0.447	9*/109**	22.9	30.8
MPVHR2 – MEA/PZ	1.61	0.545	0.447	23*/95**	24.7	31.6

MPVHR3 – MEA/PZ	1.61	0.545	0.447	32*/86**	26.3	32.6
MPVHR4 – MEA/PZ	1.61	0.545	0.447	18*/100**	24.2	31.5

DM- double matrix, DMVR- double matrix vapor recompression
MPV – multipressure vacuum, MPVVR – multipressure with vapor recompression
MPVHR - multipressure vacuum with heat recovery, * Heat supplied by vapor recompression / heat recovery, **Net heat required by stripper

The results show that only the double matrix with 4m K^+/4m PZ and the double matrix with MEA/PZ provide significantly less equivalent work compared to base case. The savings with these two configurations is about 10%. The other stripper configurations can only recover a small percentage of the heat in the overhead stream. Since these configurations have a greater compression work requirement the overall effect is that the total equivalent work increases by about 3% over the base case configuration.

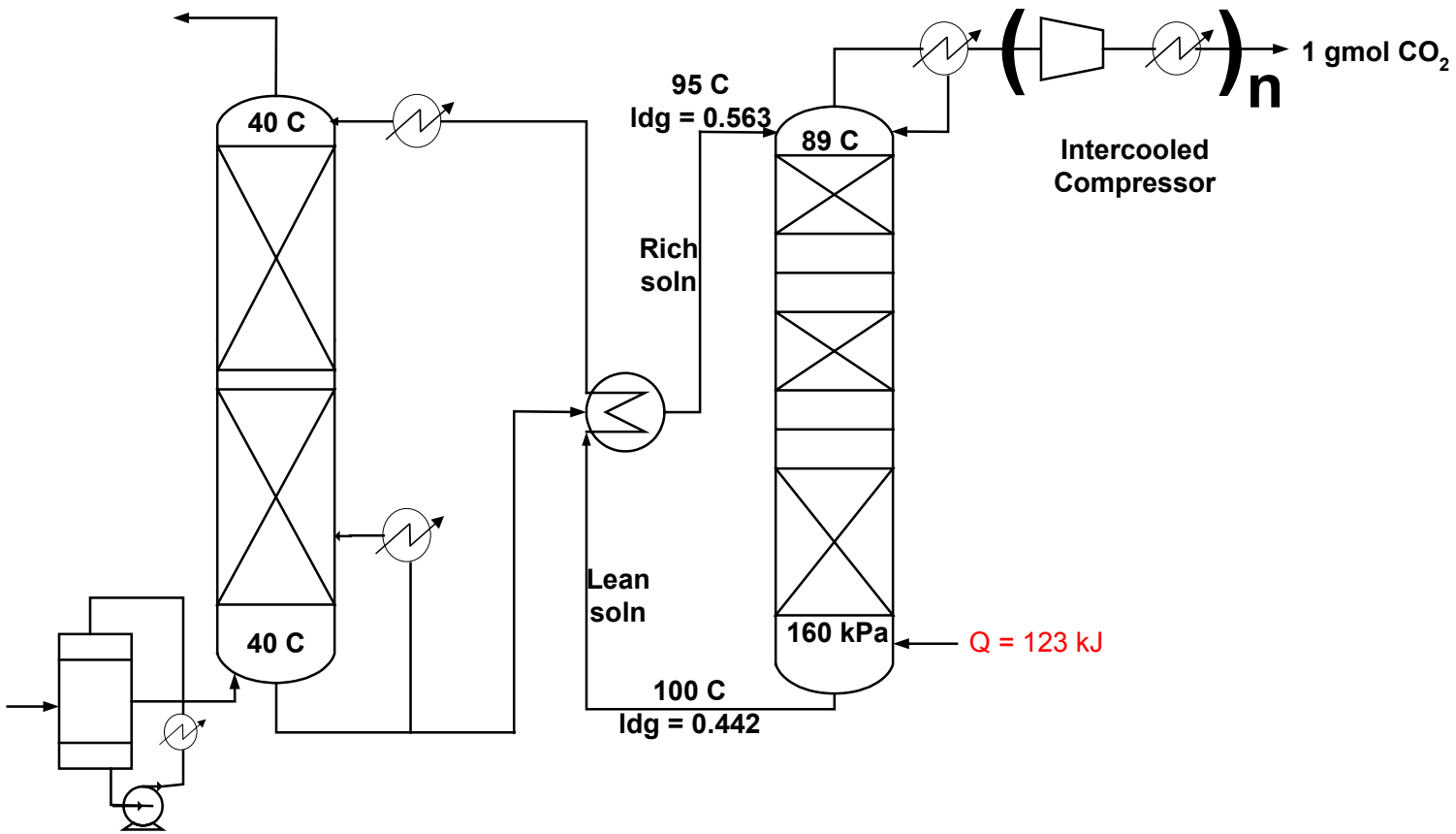

Figure 3-10: Base case Stripper for 7m MEA (Liquid = 1.11 kg solvent, Rich ldg = 0.563 mol CO_2/mol Alk, Lean ldg = 0.442 mol CO_2/mol Alk, $\Delta T = 5^oC$)

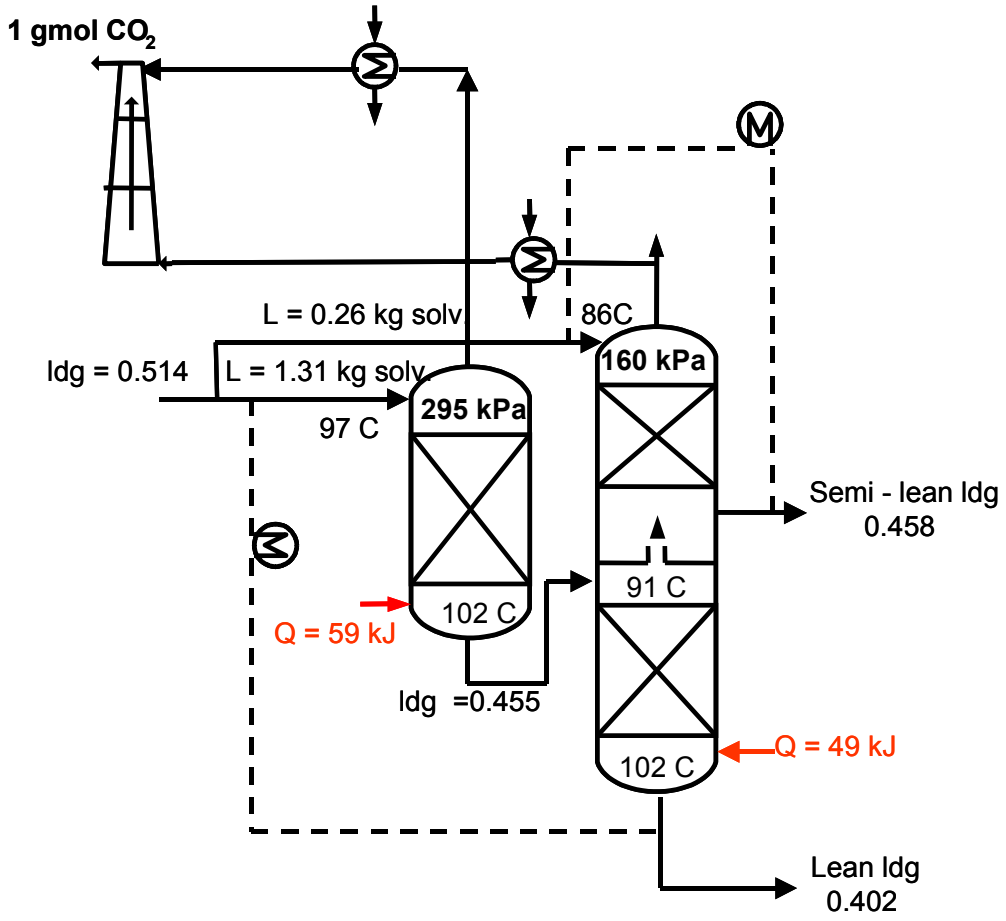

Figure 3-11:Double Matrix (295/160) Stripper for 4m K^+/4m PZ (Liquid rate = 1.57 kg solvent, Rich ldg = 0.514 mol CO_2/mol Alk, Lean ldg = 0.402 mol CO_2/mol Alk, $\Delta T = 5^oC$)

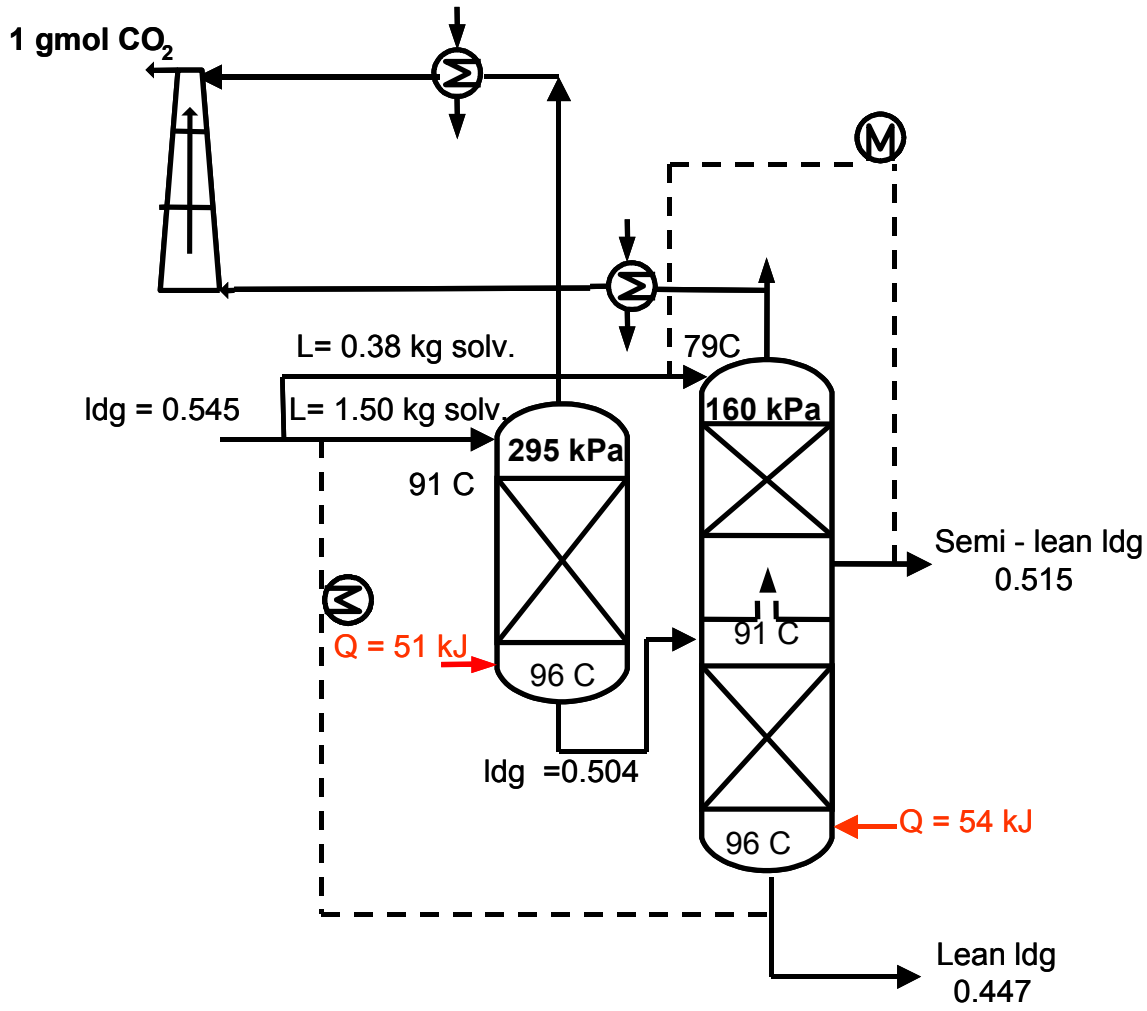

Figure 3-12:Double Matrix (295/160) Stripper for MEA/PZ (Liquid rate = 1.88 kg solvent, Rich ldg = 0.545 mol CO_2/mol Alk, Lean ldg = 0.447 mol CO_2/mol Alk, $\Delta T = 5^oC$)

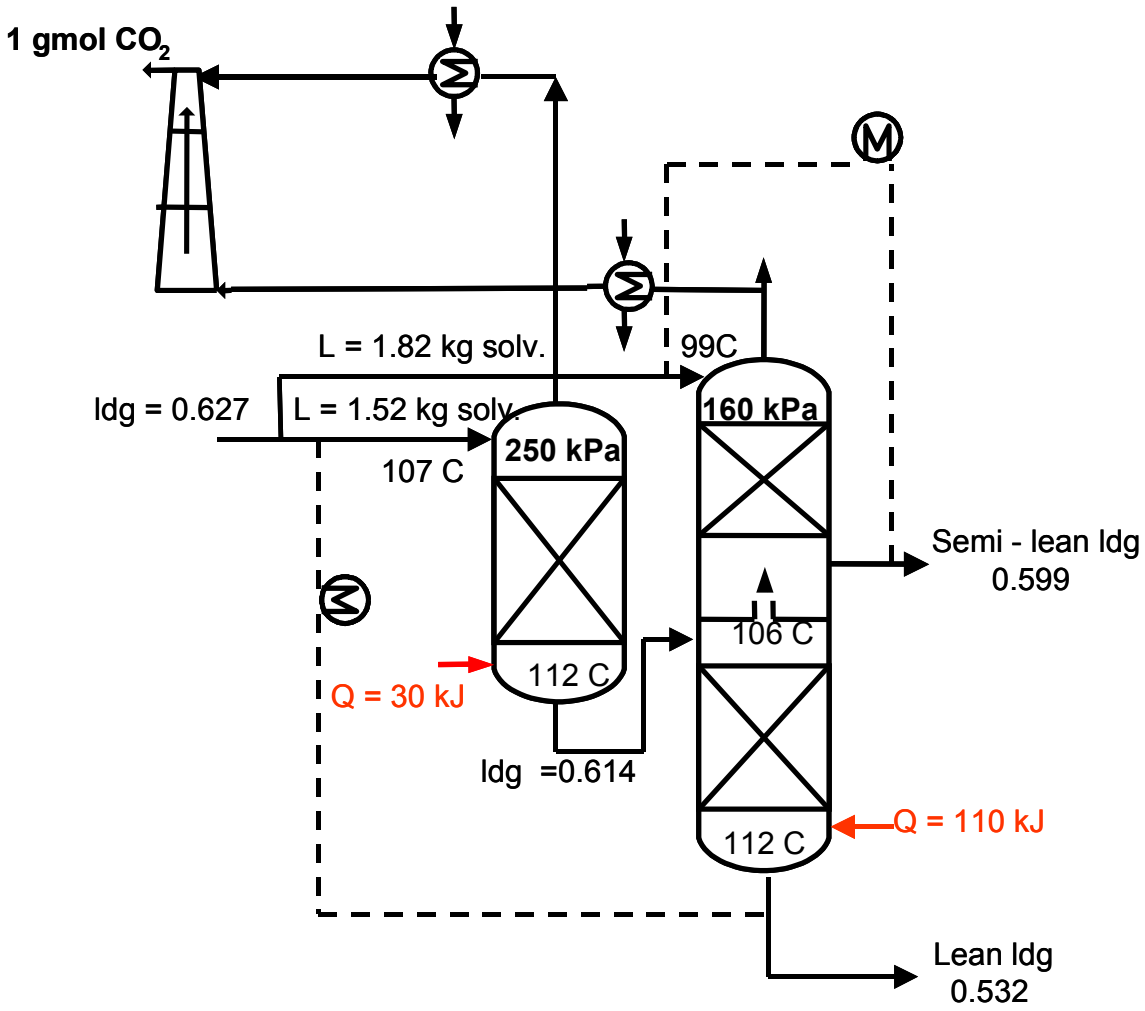

Figure 3-13: Double Matrix (250/160) Stripper for 6.4m K^+/1.6m PZ (Liquid rate = 3.34 kg solvent, Rich ldg = 0.627 mol CO_2/mol Alk, Lean ldg = 0.532 mol CO_2/mol Alk, $\Delta T = 5^oC$)

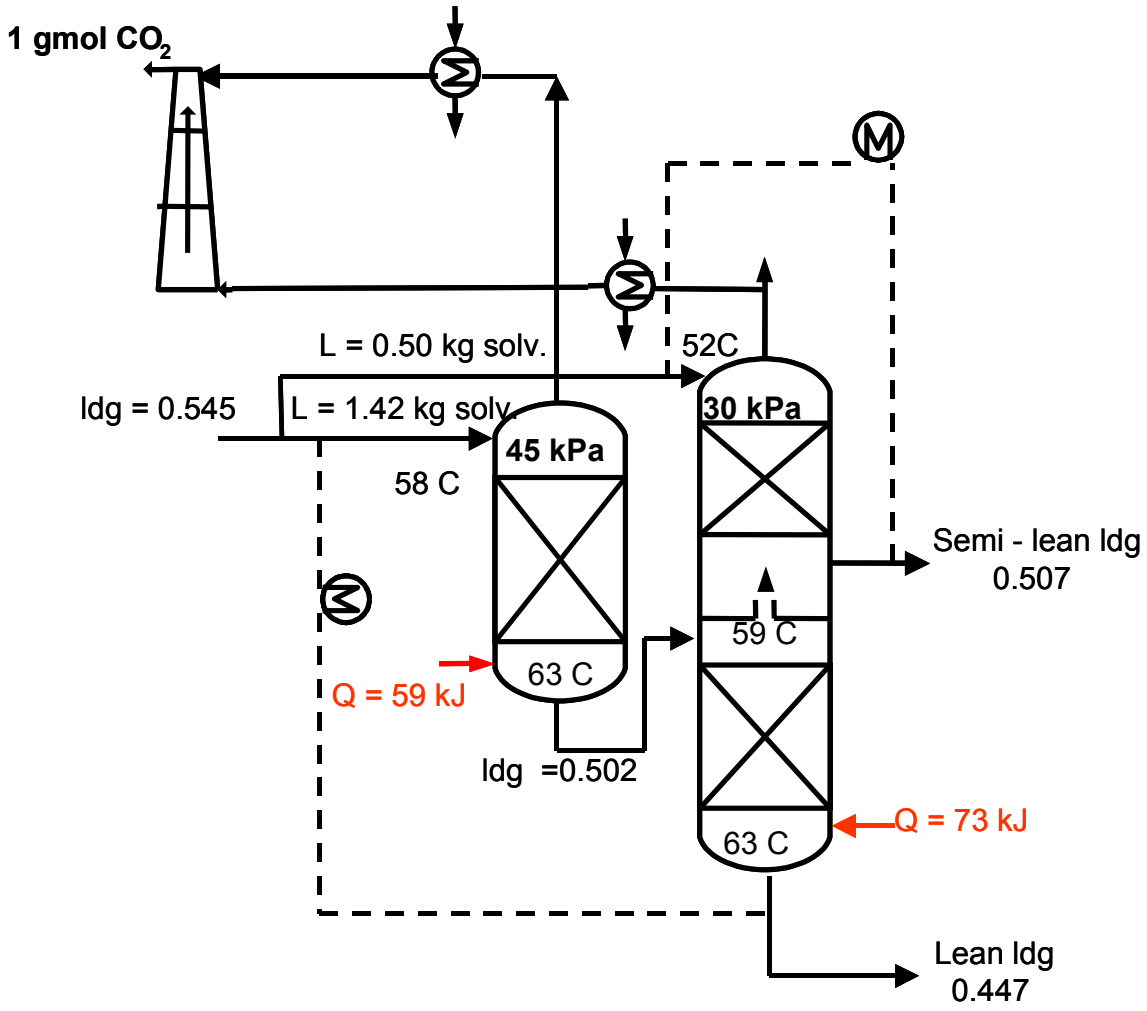

Figure 3-14: Double Matrix (45/30) Stripper for MEA/PZ (Liquid rate = 1.92 kg solvent, Rich ldg = 0.545 mol CO_2/mol Alk, Lean ldg = 0.447 mol CO_2/mol Alk, $\Delta T = 5^oC$)

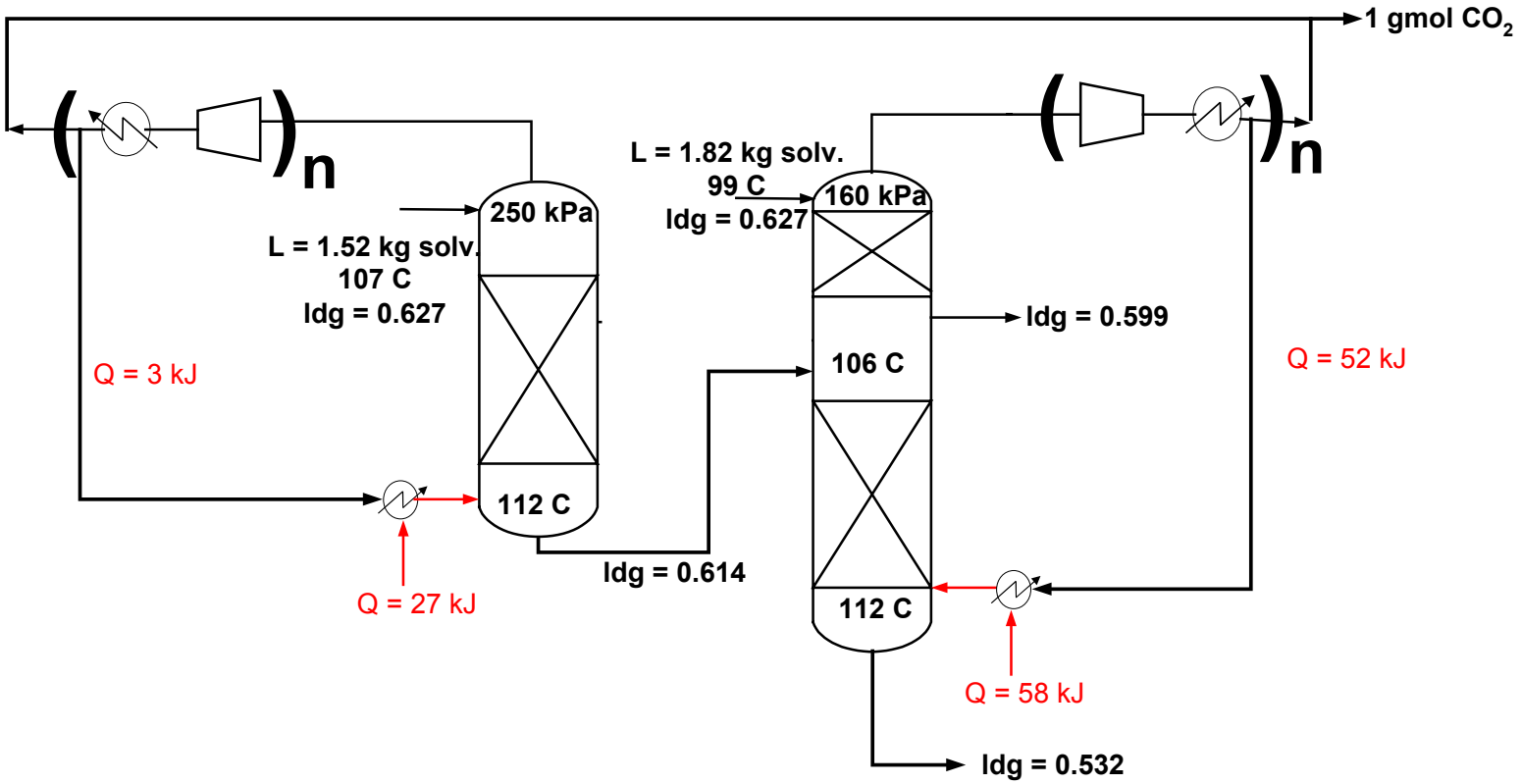

Figure 3-15: Double Matrix (250/160) with Vapor Recompression Stripper for 6.4m K^+/1.6m PZ (Liquid rate = 3.34 kg solvent, Rich ldg = 0.627 mol CO_2/mol Alk, Lean ldg = 0.532 mol CO_2/mol Alk, $\Delta T = 5^oC$)

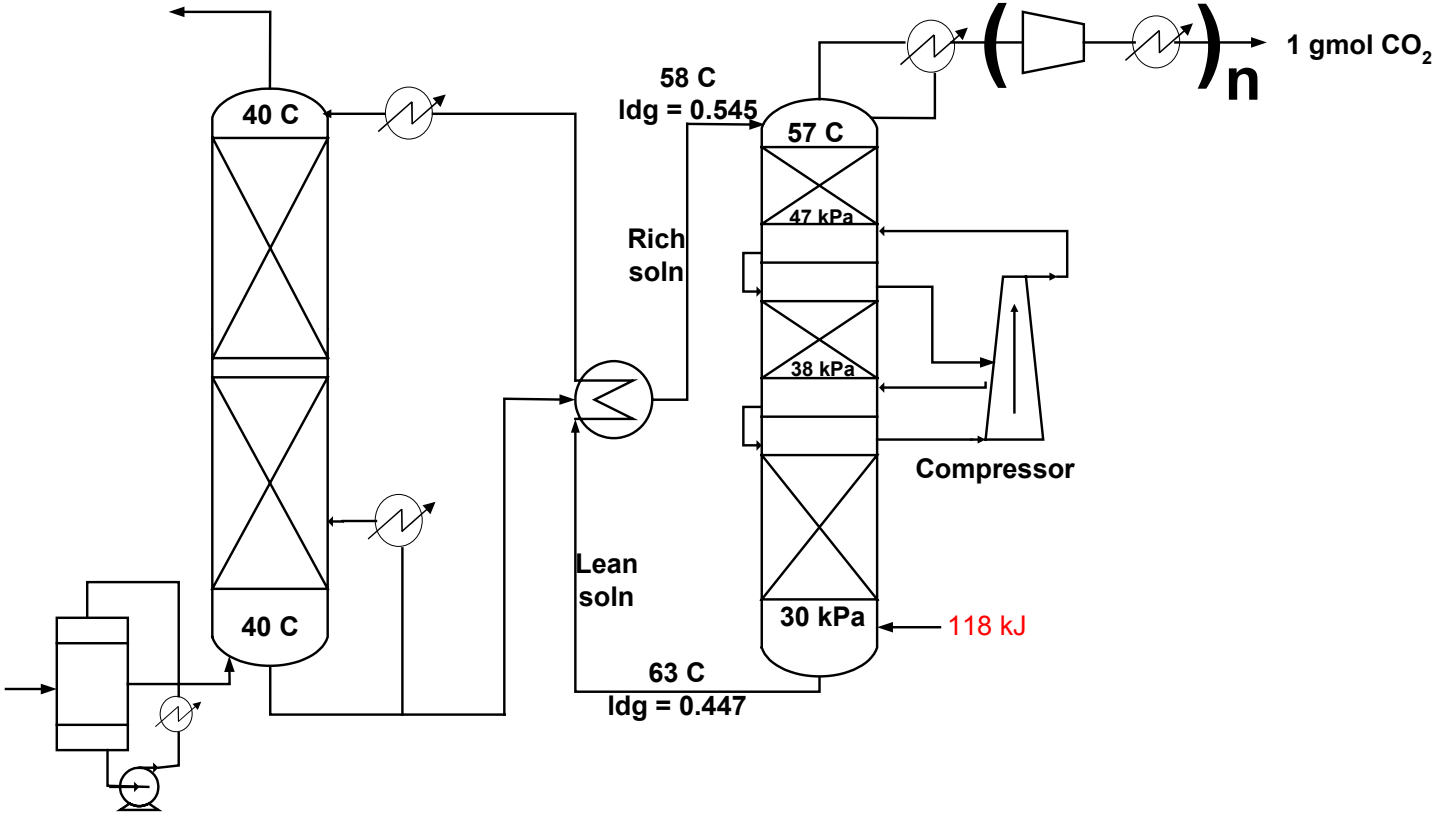

Figure 3-16: Multipressure vacuum (47/30) with Vapor Recompression Stripper for MEA/PZ (Liquid rate = 1.61 kg solvent, Rich ldg = 0.545 mol CO_2/mol Alk, Lean ldg = 0.447 mol CO_2/mol Alk, $\Delta T = 5^oC$)

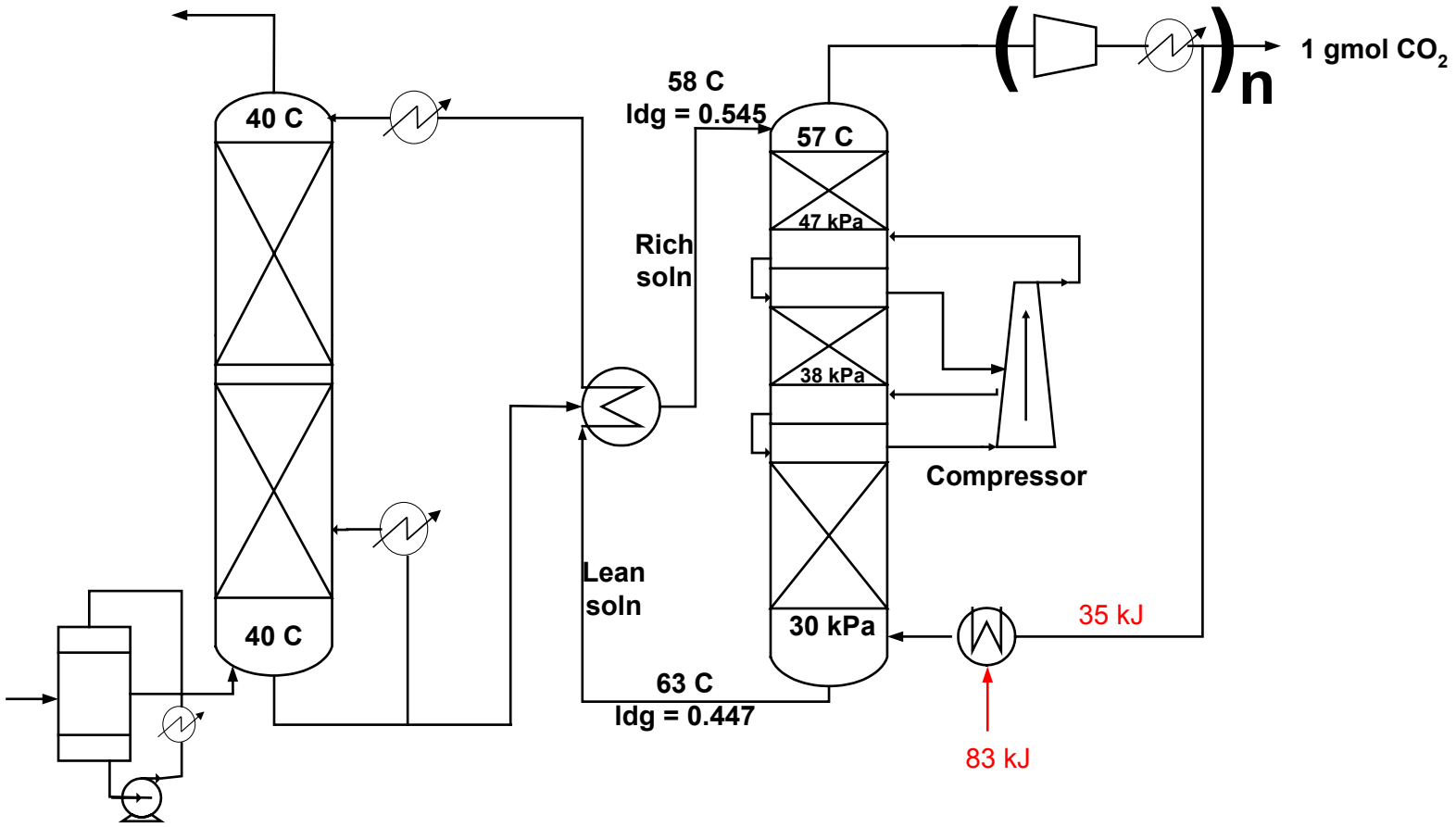

Figure 3-17: Multipressure vacuum (47/30) with Vapor Recompression Stripper for MEA/PZ (Liquid rate = 1.61 kg solvent, Rich ldg = 0.545 mol CO_2/mol Alk, Lean ldg = 0.447 mol CO_2/mol Alk, $\Delta T = 5^oC$)

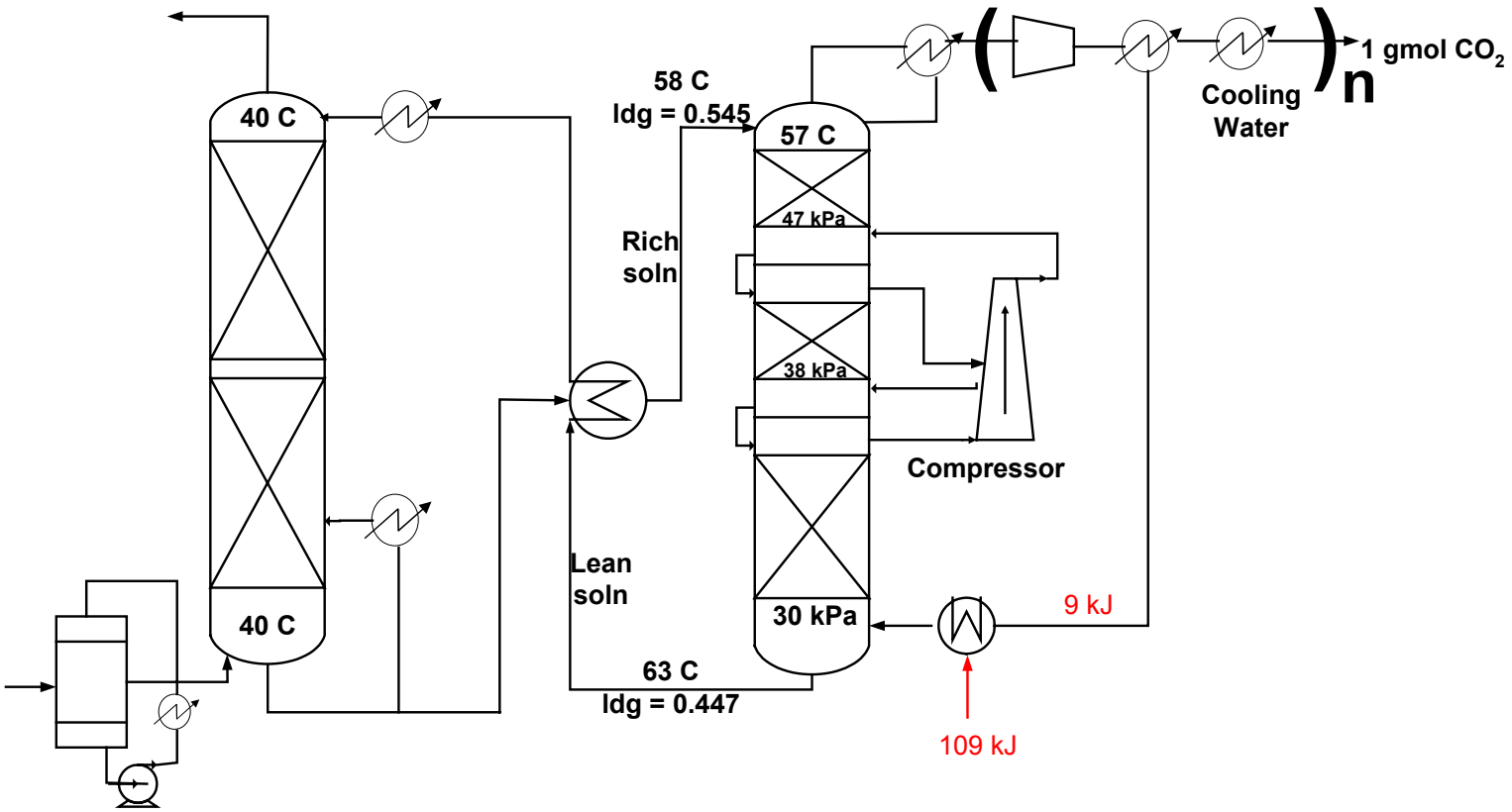

Figure 3-18: Multipressure vacuum (47/30) with Heat Recovery Stripper (Scheme 1) for MEA/PZ (Liquid rate = 1.61 kg solvent, Rich ldg = 0.545 mol CO_2/mol Alk, Lean ldg = 0.447 mol CO_2/mol Alk, $\Delta T = 5^oC$)

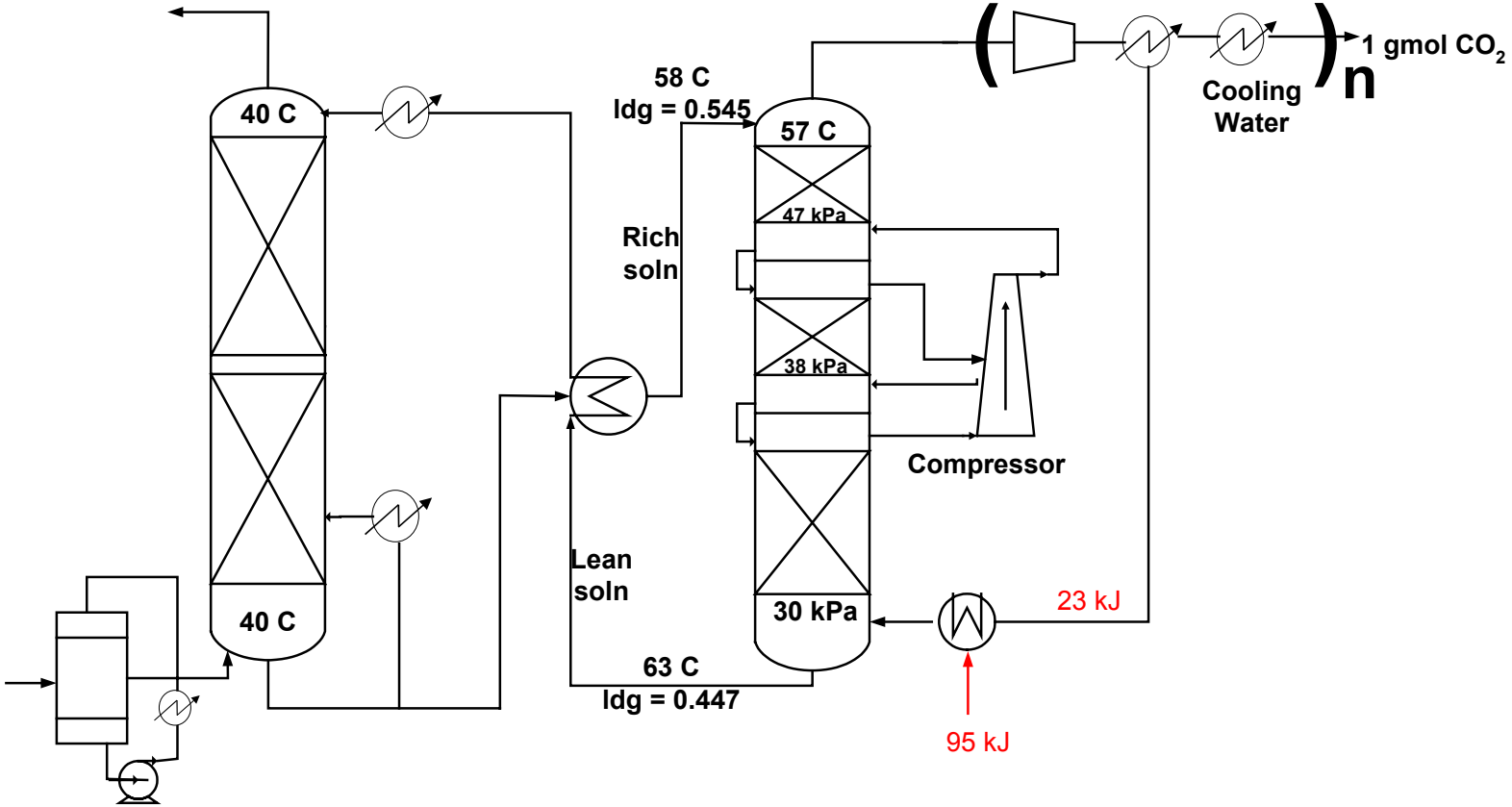

Figure 3-19: Multipressure vacuum (47/30) with Heat Recovery Stripper (Scheme 2) for MEA/PZ (Liquid rate = 1.61 kg solvent, Rich ldg = 0.545 mol CO_2/mol Alk, Lean ldg = 0.447 mol CO_2/mol Alk, $\Delta T = 5^oC$)

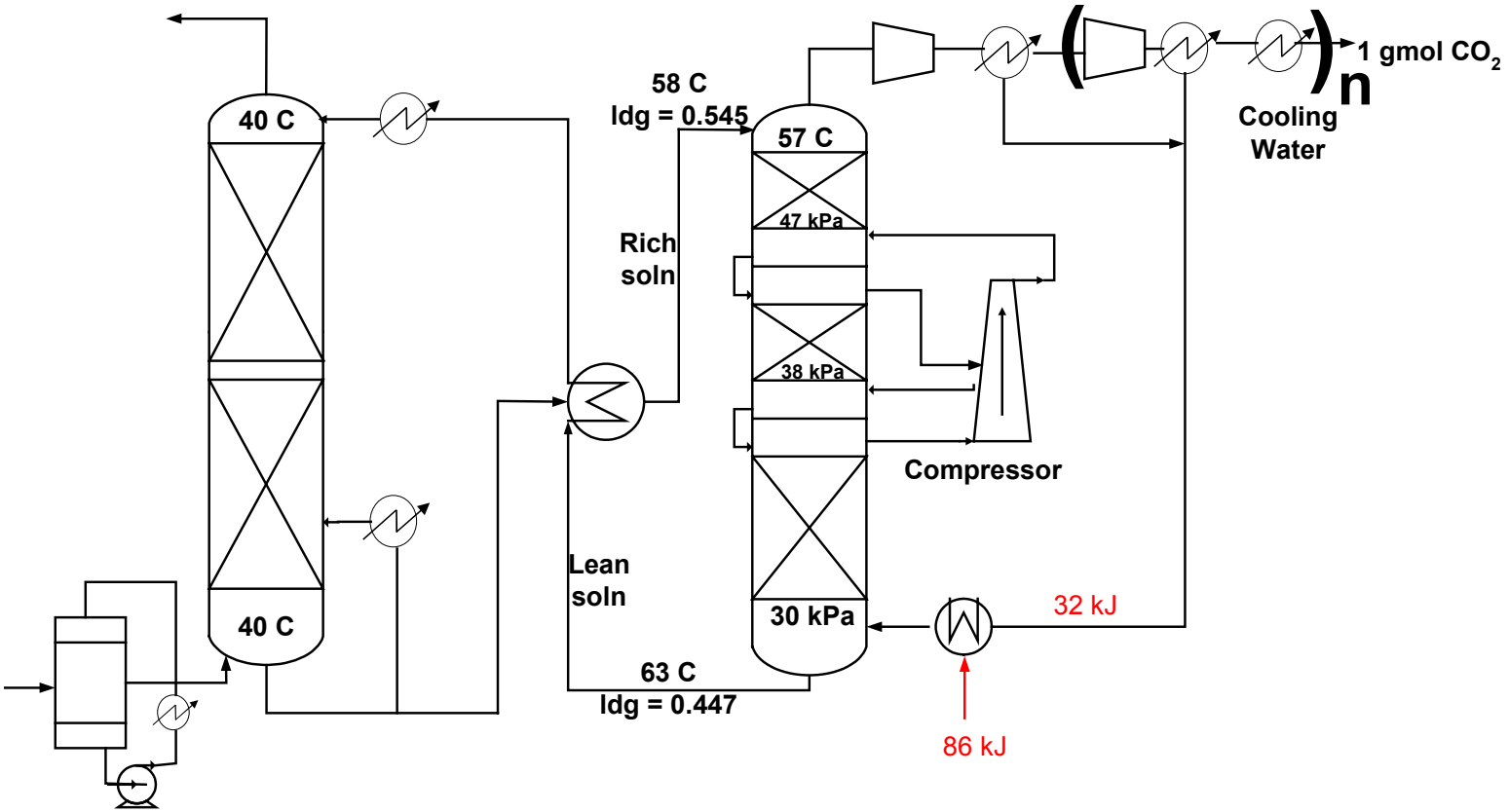

Figure 3-20:Multipressure vacuum (47/30) with Heat Recovery Stripper (Scheme 3) for MEA/PZ (Liquid rate = 1.61 kg solvent, Rich ldg = 0.545 mol CO_2/mol Alk, Lean ldg = 0.447 mol CO_2/mol Alk, $\Delta T = 5^oC$)

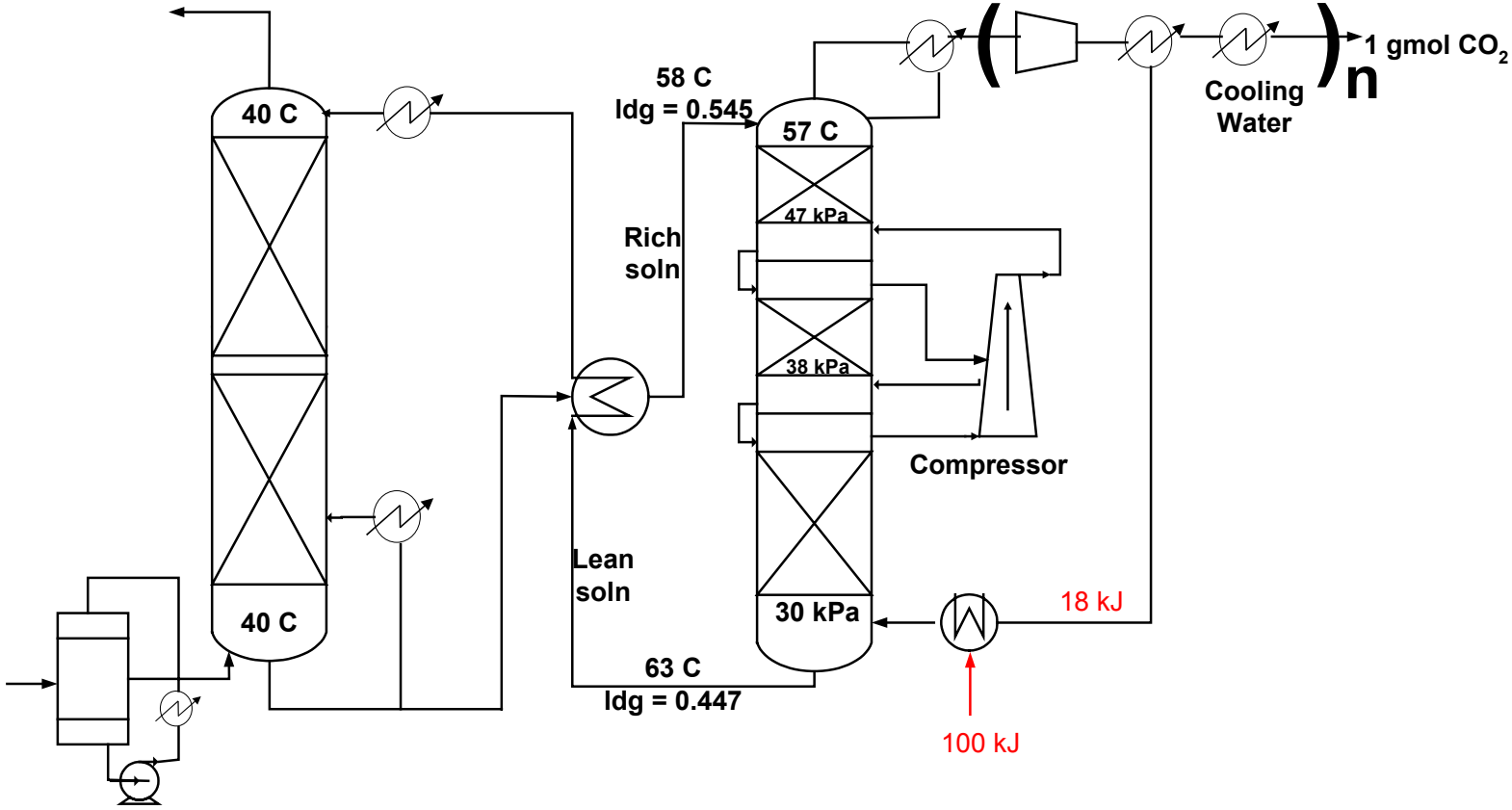

Figure 3-21: Multipressure vacuum (47/30) with Heat Recovery Stripper (Scheme 4) for MEA/PZ (Liquid rate = 1.61 kg solvent, Rich ldg = 0.545 mol CO_2/mol Alk, Lean ldg = 0.447 mol CO_2/mol Alk, $\Delta T = 5^oC$)

3.8. Conclusions

1. Operating the cross exchanger at a 5°C approach instead of a 10°C approach can reduce the equivalent work of the baseline configuration by 12%.
2. Stripping at 30 kPa is more attractive for 6.4m K^+/1.6m PZ than stripping at 160 kPa. Stripping at normal pressure (160 kPa) favors solvents with high heats of desorption. This is because solvents with a high heat of desorption take advantage of the temperature swing.
3. MEA/PZ and MDEA/PZ are alternatives to 7m MEA that can reduce total equivalent work by at least 10% for all configurations and operating conditions studied.
4. The performance of the alternative configurations is matrix > internal exchange > multipressure with split feed > flashing feed. The matrix, internal exchange, multipressure with split feed and flashing feed offer 15%, 13%, 13% and 11% energy savings over the improved baseline with stripping and compression to 10 MPa.
5. At a fixed capacity, solvents with high heats of absorption require less energy for stripping. 5m K^+/2.5m PZ offers 18% over 6.4m K^+/1.6m PZ at 160 kPa with a 5°C approach and savings of 3% and 4% with the matrix and internal exchange configurations at stripper conditions. The savings experienced with 5m K^+/2.5m PZ at 160 kPa is because of the temperature swing desorption. At

vacuum conditions this effect disappears and the performance of the solvents are equal.

6. Less energy is required with high capacity solvents with equivalent heat of absorption. 5m K^+/2.5m PZ and MDEA/PZ have similar heats of absorption. MDEA/PZ has about twice the capacity for CO_2 as 5m K^+/2.5m PZ. MDEA/PZ provides 30% and 19% energy savings over 5m K^+/2.5m PZ with the matrix and internal exchange configurations with the reboiler operating at 160 kPa and 17% and 12% savings with these configurations at 30 kPa.
7. The typical predicted energy requirement for stripping and compression to 10 MPa (30 kJ/gmol CO_2) is about 20% of the power output from a 500 MW power plant with 90% CO_2 removal. This does not include power for pumping, the flue gas fan and other auxiliaries.
8. The best solvent and process configuration in this study, matrix (295/160) using MDEA/PZ, offers 22% energy savings over the baseline and 15% savings over the improved baseline with stripping and compression to 10 MPa.
9. The best solvent and process configuration requires 26 kJ/gmol CO_2 compared to 24.1 kJ/gmol CO_2 for isothermal separation and real compression to 10 MPa. This means that there is little room for improvement. MDEA/PZ with the matrix configuration is 67% efficient when compared with the minimum thermodynamic work requirement of 18.1 kJ/gmol CO_2.

Chapter 4 : Rate Modeling of CO_2 desorption from K_2CO_3/PZ

This chapter describes the rate model for CO_2 desorption from 5m K^+/2.5m PZ and presents results from the model with a temperature approach of 5 and 10^oC on the hot side of the cross exchanger. The stripper is equipped with IMTP #40 random packing. The effect of stripper diameter and effective volume of packing (volume of packing divided by liquid rate) on energy requirement was investigated. The mass transfer phenomenon in 30 kPa and 160 kPa strippers is also investigated.

4.1. Rate Modeling of Strippers

Absorption / stripping with aqueous amines is an important technological option for CO_2 capture from combustion gas. Quantitative models based on our understanding of the vapor-liquid equilibrium and mass transfer rates can provide optimal design of economic processes. In aqueous absorption/stripping (Figure 4-1) CO_2 is absorbed into the solvent in a countercurrent contactor. The rich solution leaving the absorber is cross-exchanged with the lean solution from the stripper. CO_2 desorption occurs in the stripper.

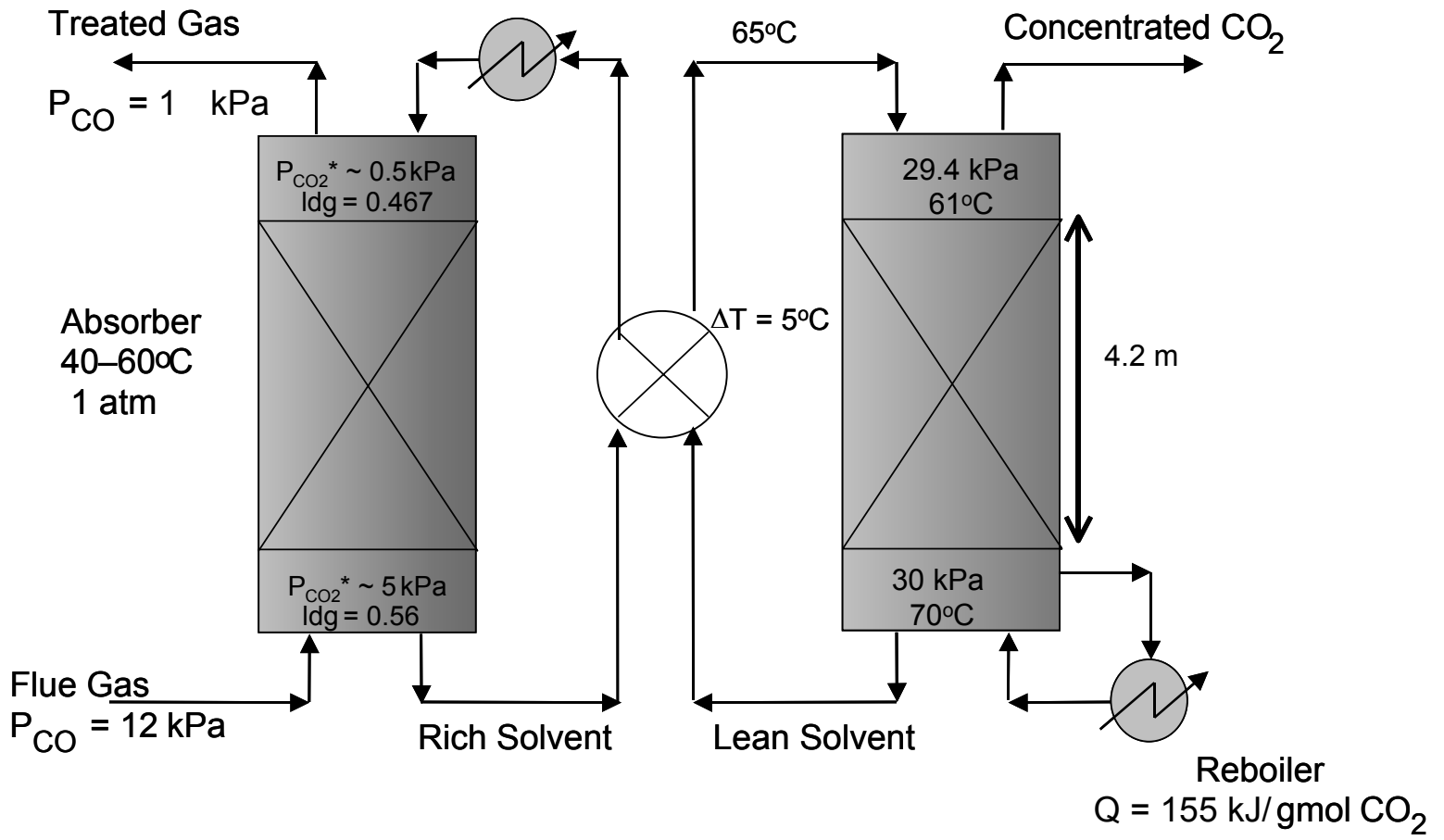

Figure 4-1: Typical absorber / stripper configuration for 5m K^+/ 2.5m PZ (τ = 461 s^{-1}, 30% flood, rich ldg = 0.56 mol CO_2/mol Alk, lean ldg = 0.467 mol CO_2/ mol Alk, $\Delta T = 5^oC$)

Stripping occurs in three regions (Figure 4-2): (a) at the stripper inlet where flashing can occur if the sum of the equilibrium partial pressures of CO_2 and water is greater than the operating pressure of the stripper, (b) within a section of trays or packing due to normal mass transfer and (c) in the reboiler under boiling conditions.

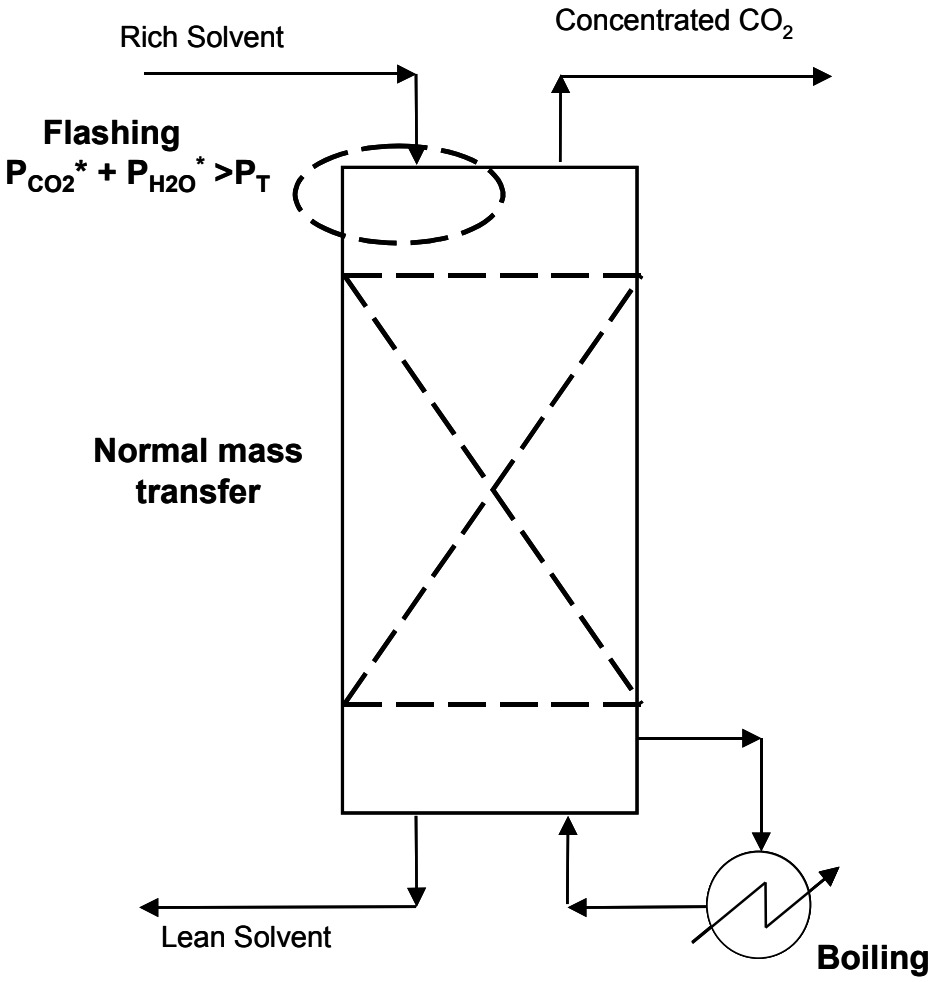

Figure 4-2: Mass transfer regions in Stripper

Optimal stripper design is critical because the stripping energy requirement accounts for 80% of the operating cost of an absorption/stripping system. Modeling will provide a detailed understanding of the stripper operation and mass transfer with chemical reaction at stripper conditions.

Table 1-1 summarizes previous studies that involve stripper modeling for both gas purification and CO_2 capture. A number of studies include absorption/stripping (Suenson, Georgakis et al. 1985; Escobillana, Saez et al. 1991; Alatiqi, Sabri et al. 1994; Desideri and Paolucci 1999; Freguia and Rochelle 2003; Aroonwilas 2004; Alie, Backham et al. 2005; Jassim and Rochelle 2006), others include only the stripper (Tobiesen, Svendsen et al. 2005). There are three approaches used in addressing mass transfer in strippers - the equilibrium approach such as that employed in Chapters 2 and 3, mass transfer with equilibrium reaction, (Weiland, Rawal et al. 1982; Freguia and Rochelle 2003; Tobiesen, Svendsen et al. 2005; Tobiesen and Svendsen 2006) and mass transfer with reaction in the liquid boundary layer and diffusion of reactants and products as used in this work.

At a high approach to flood for which most stripping columns are designed, operating under vacuum results in high pressure drop and increased reboiler duty and equivalent work. Modeling of stripping systems will provide insight into the stripping phenomenon and result in optimal designs.

4.2. Modeling Approaches

There are two main approaches to modeling strippers: the equilibrium and rate-based approaches. The rate-based approach is used in this chapter.

4.2.1 Equilibrium Modeling. In this approach, the stripping column is divided into a user-defined number of segments (section of packing) assumed to be well mixed in the liquid and vapor phases as in the Chapters 2 and 3. The reboiler is assumed to be an equilibrium segment. Murphree efficiencies are assigned to CO_2, water and temperature to account for the departure from equilibrium. This approach is useful in carrying out quick evaluations of process concepts but does not allow for quantitative predictions of Murphree efficiencies and packing height. Only the material, equilibrium, summation and enthalpy (MESH) equations are solved using this approach.

4.2.2 Rate-based (non-equilibrium) modeling. In this approach, the rate of desorption is finite. In addition to the conventional MESH equations, the mass and heat transfer rate equations are solved. Since these equations require physical properties, reaction rate parameters and contactor specific information, this approach better describes a real process. Vacuum stripping could be attractive for low heat of desorption solvents such as 5m K^+/2.5m PZ. Since vacuum strippers suffer a greater pressure drop penalty, designing a larger diameter column while maintaining the same volume of packing will reduce the height of the stripper and as such reduce pressure drop and energy requirements. Rate-based modeling helps in optimum contactor (trays, random or structured packing) selection. It provides insight into the fundamental mechanisms of mass transfer and could help predict the operation of a constant diameter column as well as aid in the design of columns with variable diameter at constant percent flood.

4.2.2.1 Mass Transfer with equilibrium reaction. This approach assumes that the reaction film is very close to the gas-liquid interface. The mass transfer process can be described in terms of diffusion alone with no consideration of the kinetics of the reactions. This approach has been used by some authors (Weiland, Rawal et al. 1982; Escobillana, Saez et al. 1991; Desideri and Paolucci 1999; Freguia 2002; Freguia and Rochelle 2003; Alie, Backham et al. 2004; Aroonwilas 2004; Tobiesen and Svendsen 2004; Tobiesen, Svendsen et al. 2005; Jassim and Rochelle 2006; Tobiesen, Mejdell et al. 2006; Tobiesen and Svendsen 2006).

4.2.2.2 Mass Transfer with reaction in the liquid boundary layer and diffusion of reactants and products. This rigorous approach is the method used in this chapter. It assumes that the CO_2 diffuses from the bulk liquid through the liquid film to the reaction film, where it reacts with the amine, and subsequently diffuses through the gas film into the bulk gas. The reaction film is close to the gas-liquid interface. It is postulated that CO_2 absorption/desorption in amines, potassium carbonate and PZ/K_2CO_3 follow this mechanism.

4.3. Rate Model Development

A stripper model for aqueous solutions of 5m K^+/ 2.5m PZ was developed in Aspen Custom Modeler. This model divides the stripper into a "flash" region at the top with a height equal to that of a normal mass transfer segment (this was done to quantify the effect of the flash in terms of segment performance), ten segments, and an

equilibrium reboiler. The main equations solved in the model are shown in Table 4-1. Detailed equations in the rate model are presented in Appendix C.

Table 4-1: Main equations used in the rate-based model.

Material balance over a segment

$l_{ij-1} + (V_{ij+1} * y_{i,j+1}) = l_{ij} + (V_{ij} * y_{ij})$

Negligible vaporization of amine

$l_{ij-1} = l_{ij}$ i = amine, j = segment

Equilibrium expressions

CO_2: $P_{CO2} * = \exp\left(A + (B\gamma) + \frac{C}{T} + \left(\frac{D\gamma^2}{T^2}\right) + \left(\frac{E\gamma}{T^2}\right) + \left(f\frac{\gamma}{T}\right)\right)$

H_2O: $P_{H2O} = \left[act * \exp\left(A + \frac{B}{T} + C\ln T + DT^E\right)\right] / 1000$

Activity of water

act = act1 + (act2 *γ) + (act3/T)

The activity coefficients were obtained by regressing points obtained from Hillard (Hilliard 2005)

With act1, act2 and act3 given by 0.978, -0.05 and, -31.56 respectively.

Summation Equation

$1.0 = \sum_i y_{ij}$ where i = component and j = segment

Enthalpy Equations (Energy balance)

$V_j + [y_{h2o,j+1} * (H_{vap} + (C_{pH2O,j+1} * T_{j+1} - T_{ref}))] + y_{co2,j+1} * ((\Delta H_{j+1}/1000) + (C_{pco2,j+1} * (T_{j+1} - T_{ref}))) + (L_{j-1} * C_{pL,j-1} * (T_{j-1} - T_{ref})) + Q_j + Q_{comp,j} = V_j + [y_{h2o,j} * (H_{vap} + (C_{pH2O,j} * T_j - T_{ref}))] + y_{co2,j} * ((\Delta H_j/1000) + (C_{pco2,j} * (T_j - T_{ref}))) + (L_j * C_{pL,j} * (T_j - T_{ref}))$

Total pressure on a segment

$P_{CO2,i} + P_{H2O,i} = P_T$

$P_{CO2} + P_{H2O} = P_T$

Note that the bubble point relationship is not satisfied:

$P_{CO2}^* + P_{H2O}^* \neq P_T$

CO_2 flux based on the liquid phase

$N_{CO2} = k_g' * 1000 * (P_{CO2}^* - P_{CO2,i})$

CO_2 flux expression in the gas phase

$$N_{CO2} = k_g * 1000 * \left(P_{CO2,i} - P_{CO2}\right) + \left[\left(N_{CO2} + N_{H2O}\right)\frac{P_{CO2,i} - P_{CO2}}{P_T \ln\left(\frac{P_{CO2i}}{P_{CO2}}\right)}\right]$$

Pump Work

$$W_{pump} = \frac{L\ H_p\ \rho_l\ g}{\eta_p\ g_{co2}}$$

The compressor work was calculated in Aspen Plus using a 75% adiabatic efficiency for the compressor.

An empirical expression with six adjustable constants (Table 3-1) was used to represent the vapor-liquid equilibrium (VLE) and heat of desorption for 5m K^+/2.5m PZ. Strippers with reboiler pressures of 30 kPa and 160 kPa were modeled. The rich and lean loadings and cross exchanger temperature approach were fixed. The mass transfer coefficients, loadings and temperature on each segment, reboiler duty, and equivalent work consumed by the process are calculated.

4.3.1 Modeling Assumptions.

(i) The sections are well mixed in the liquid and vapor phases.

(ii) The reaction takes place in the liquid phase.

(iii) The reboiler is in vapor/liquid equilibrium.

(iv) There is negligible vaporization of the amine.

The model accounts for mass transfer resistances in the gas and liquid phases and the simultaneous and unequal flux of CO_2 and water across the interface.

4.3.2 Thermodynamics.

The CO_2 vapor pressure (kPa) under stripper conditions and heat of desorption (ΔH) are represented by the empirical expressions:

$$\ln P_{CO2}^{*}[\text{kPa}] = a + b\gamma + \frac{c}{T} + d\frac{\gamma^2}{T^2} + e\frac{\gamma}{T^2} + f\frac{\gamma}{T} \tag{4-1}$$

$$-\frac{\Delta H}{R} = \frac{\partial(\ln P_{CO2}^{*})}{\partial\left(\frac{1}{T}\right)} = c + 2d\frac{\gamma^2}{T} + 2e\frac{\gamma}{T} + f\gamma \tag{4-2}$$

The empirical constants, a through f, are given in Table 3-1.

4.3.3 Mass Transfer Calculations.

The flux of CO_2, N_{CO2}, from the bulk liquid to the bulk gas is given by the expression

$$N_{CO2} = K_G (P_{CO2}^{*} - P_{CO2}) \tag{4-3}$$

The overall mass transfer coefficient, K_G, can be expressed as a sum of series resistances comprised of gas phase, ($1/k_g$), and liquid phase, ($1/k_g'$), components.

$$\frac{1}{K_G} = \frac{1}{k_g} + \frac{1}{k_g'} \tag{4-4}$$

Desorption is gas film controlled if k_g controls the desorption rate and is liquid film controlled if kinetics and diffusion of reactants and products control the desorption rate.

The mass transfer model used was that developed by Bishnoi (Bishnoi 2000) for PZ/MDEA solutions and modified for PZ/K_2CO_3 solutions by Cullinane (Cullinane 2005). The model is a rigorous rate model based on eddy diffusivity theory (King 1966). It integrates a series of differential equations for the thermodynamics in the bulk liquid using the Electrolyte Non-Random Two Liquid (E-NRTL) (Chen, Britt et al. 1982; Chen

and Evans 1986; Mock, Evans et al. 1986), diffusion across the liquid film, and reaction in the boundary layer, and calculates the liquid-phase mass transfer coefficient with a partial pressure driving force, k_g'. Points generated from running the model developed by Cullinane (Cullinane 2005) were regressed and fit to the expression in Table 4-2.

Table 4-2: k_g' expression for 5m K^+/ 2.5m PZ

$$k_g'\,[\text{kmol/Pa-m}^2\text{-s}] = \exp\left[\begin{array}{l} A + (B\gamma) + \left(\frac{C}{T}\right) + (D\,k_l) + (E\;P_{CO2,i}) + \left(F\frac{\gamma}{T}\right) + \left(G\;\frac{k_l}{T}\right) + \\ \left(H\frac{P_{CO2,i}}{T}\right) + \left(I\;\frac{\gamma^2}{T}\right) + \left(J\;\frac{\gamma}{T^2}\right) + \left(K\frac{\gamma^2}{T^2}\right) \end{array}\right]$$

A= -46.6868 G= -3182533

B= -11.5447 H= -6.06135

C= 8197.802 I= -87538.9

D= 10050.46 J= -2E-7

E= 0.012346 K= 26254990

F= 69294.95

The liquid-phase mass transfer coefficient with a partial pressure driving force, k_g', can be separated into contributions from kinetics ($1/k_g$'') and diffusion of reactants and products ($m/k_{l,prod}$) given by:

$$\frac{1}{k_g'} = \frac{1}{k_g''} + \frac{m}{k_{l,prod}} \qquad (4\text{-}5)$$

where m is the slope of the equilibrium line obtained from Cullinane (Cullinane 2005).

The kinetic resistance is given by:

$$\frac{k_g'}{k_g''} = \frac{k_{l,prod}}{k_{l,prod} + m k_g''} \tag{4-6}$$

The resistance due to the diffusion of reactants and products is:

$$\frac{k_g'}{k_g''} = \frac{m k_g''}{k_{l,prod} + m k_g''} \tag{4-7}$$

The contribution of the kinetic and diffusion components to the liquid phase mass transfer was determined by a sensitivity analysis on k_l. This was done by setting up two equations for k_g'. The first equation (4.8) had the k_l at the point being considered and the second (4.9) had its k_l equal to 1.03 times k_l in (4.8). For each k_l value, k_g' can be calculated.

$$\frac{1}{k_{g1}'} = \frac{1}{k_g''} + \frac{m}{k_{l,prod}} \tag{4-8}$$

$$\frac{1}{k_{g2}'} = \frac{1}{k_g''} + \frac{m}{1.03\ k_{l,prod}} \tag{4-9}$$

Solving (4-8) and (4-9) simultaneously gives values for k_g'' and m.

The gas, kinetic and diffusion of reactants and products resistances can be calculated from (4-10) to (4-12).

$$\text{gas resistance}(\%) = \left(\frac{K_G}{k_g}\right) 100 \tag{4-10}$$

$$\text{kinetic resistance}(\%) = \left(\frac{K_G}{k_g''}\right) 100 \tag{4-11}$$

$$\text{diffusion resistance}(\%) = \left(\frac{K_G\, m}{k_{l,prod}} \right) 100 \tag{4-12}$$

If the reaction occurs very fast the approximate expression for K_G for mass transfer with equilibrium reaction given by:

$$\frac{1}{K_G} = \frac{1}{k_g} + \frac{m}{k_{l,prod}} \tag{4-13}$$

The hydraulic parameters (k_g, k_l, a_w) for the IMTP #40 packing were obtained from Onda (Onda, Takeuchi et al. 1968) and Wilson (Wilson 2004). The characteristics of this packing are shown in Table 4-3.

Table 4-3: Characteristics of IMTP #40 random packing

Property	Value
Total dry packing area	145 m^2/m^3
Packing factor	24 m^{-1}
Packing diameter	0.04 m
Critical surface tension	0.075 m^{-1}

The mass transfer coefficient in the gas and liquid phases used in the model was obtained by:

$k_g = k_g\, a_w$ (Onda, Takeuchi et al. 1968) / a_w (Wilson 2004) (4-14)

$k_l = k_l\, a_w$ (Onda, Takeuchi et al. 1968) / a_w (Wilson 2004) (4-15)

The Onda expressions for the hydraulic parameters are:

$$k_g = 5.23\, (a_T D_G) \left(\frac{G_o}{a_w\, \mu_G} \right)^{0.7} \left(\frac{\mu_G}{\rho_G D_G} \right)^{0.33} (a_T d_p)^{-2} \tag{4-16}$$

$$k_l = 0.0051 \ (a_T d_p)^{0.4} \left(\frac{L_o}{a_w \ \mu_L}\right)^{0.667} \left(\frac{\mu_L}{\rho_L D_L}\right)^{-0.5} \left(\frac{\rho_L}{\mu_L g}\right)^{-0.333} \quad (4\text{-}17)$$

$$a_w = a_T \left\{1 - \exp\left[-1.45\left(\frac{\sigma_c}{\sigma_L}\right)^{0.75} \left(\frac{L_o}{a_T \mu_L}\right)^{0.1} \left(\frac{a_T L_o^{\ 2}}{\rho_L^{\ 2} g}\right)^{-0.05} \left(\frac{L_o^{\ 2}}{a_T \rho_L \sigma_L}\right)^{0.2}\right]\right\} \quad (4\text{-}18)$$

Wilson (Wilson 2004) measured the effective area, a_w, on a wide variety of packings and correlations were developed for the packings studied.

The correlation for the wetted area of IMTP #40 based on Wilson (Wilson 2004) data is:

$$a_w = \exp(4.73) \ \ u_g^{\ 0.061} \ \ \left(\frac{L \ M_l}{1000 \ A}\right)^{0.148} \quad (4\text{-}19)$$

The pressure drop in the column is calculated by:

$$\Delta P = f^2 \ \Delta P_{flood} \ \ h_{seg} \quad (4\text{-}20)$$

The pressure drop at flood ΔP_{flood} was set at 1.63 kPa/m.

The model inputs were the liquid rate, rich and lean loading, the temperature approach in the cross exchanger (difference between the temperature of the rich stripper feed and the lean solution leaving the bottom of the stripper), the fractional approach to flood (ratio of gas velocity to gas velocity at flood) and reboiler pressure. Initial guesses of the segment temperatures, partial pressures, and loadings were provided. The model solves the MESH equations, the mass and energy transfer rate equations and calculates temperature and composition profiles, reboiler duty, and equivalent work.

The total energy required by the stripper is given as total equivalent work:

$$W_{eq} = W_{pump} + 0.75Q\left[\frac{(T_{reb} + 10) - 313}{(T_{reb} + 10)}\right] + W_{comp} \quad (4\text{-}21)$$

W_{pump} is the work required by the pumps to raise the rich solution to the pressure at the stripper feed, overcome the feed point elevation. An efficiency of 65% was assumed for the pumps. W_{comp} constitutes the isentropic work of compression of the gas exiting the top of the stripper to 1000 kPa carried out in five stages with intercooling to 313K. An adiabatic efficiency of 75% was assumed for the compressor.

The second term in equation (4-21) accounts for the electricity generation lost by extracting steam from a turbine. The condensing temperature of the steam is assumed to be 10K higher than the reboiler fluid. The turbine assumes condensing steam at 313K and has been assigned an effective efficiency of 75% relative to a Carnot cycle.

4.4. Results and Discussion

Table 4-4 gives the performance (reboiler duty and total equivalent work to 1000 kPa) for strippers with reboiler pressures of 30 kPa and 160 kPa using 5m K^+/2.5m PZ with 5°C and 10°C approaches on the hot side of the cross exchanger. The rich loading is always 0.56 mol CO_2/mol Alk, corresponding to an equilibrium partial pressure (P_{CO2}*) of 5 kPa at 40°C , typical of the rich end of the absorber. The lean loading is always 0.467 mol CO_2/ mol Alk giving an equilibrium partial pressure of 0.5 kPa at 40°C and corresponds to a 90% change in equilibrium partial pressure of the rich solution. The effective packing volume, τ, is the ratio of the volume of packing to the liquid rate. The approach to flood at the bottom of the column is the ratio of the actual superficial gas velocity to the superficial gas velocity at flood.

Table 4-4: Stripper design orientation – 'short and fat' vs 'tall and skinny' Column (5m K^+/2.5m PZ, τ = 461 s, rich ldg = 0.56 mol CO_2/mol Alk, lean ldg = 0.467 mol CO_2/ mol Alk)

Reboiler P	ΔT	Flood	v_L ($x10^3$)	H	ΔP	ΔP/P	$T_{reb} - T_{top}$	Q	W_{comp}	Total W_{eq}
kPa	°C	%	m/s	m	kPa	-	°C	kJ/gmol CO_2		
30	10	80	21.2	9.8	10.2	0.34	15.9	192.6	18.1	35.7
		30	8.7	4.0	0.6	0.02	11.6	165.3	15.3	30.4
160		80	54.9	25.3	26.4	0.16	17.6	153.1	7.7	33.2
		30	20.4	9.4	1.4	0.01	15.4	146.3	6.9	30.9
30	5	80	21.8	10.1	10.5	0.35	14.4	187.4	18.1	35.2
		30	9.2	4.2	0.6	0.02	8.8	154.9	15.3	29.5
160		80	59.4	27.4	28.6	0.18	15.3	137.1	7.6	30.8
		30	22.5	10.4	1.5	0.01	12.5	127.9	6.9	28.1

4.4.1 Effect of Approach to Flood and column design orientation. Table 4-4 shows the effect of varying the approach to flood at the bottom of the stripper with 5m K^+/2.5m PZ for a constant effective packing volume, τ, of 461 s and ΔT of 5°C and 10°C. Since the volume of packing is constant, varying the liquid velocity, v_L, or approach to flood (essentially the column cross sectional area) changes the height of packing required. At a given approach to flood, the reboiler duty is greater at vacuum than at 160 kPa. This is because the volumetric mass transfer coefficients $k_l a_w$ and $k_g a_w$ are reduced at low liquid velocity. The work value of the steam used to drive the reboiler is of greater value at the higher pressure than the lower one. The work of compression to 1000 kPa is less at 160 kPa than at 30 kPa.

Operating the strippers at 80% flood leads to a "tall and skinny" column and operating at 30% flood leads to a "short and fat" column. The "tall and skinny" column leads to a

greater pressure drop in the column, greater compression work downstream and a larger temperature drop across the column. Greater pressure drop means greater loss of irreversible work in the column. A larger temperature drop across the column leads to a greater sensible heat requirement to heat the stripper feed to the bottoms temperature.

At 30 kPa, a "short and fat" column (lower approach to flood) offers 15% energy savings over a "tall and skinny" column. At 160 kPa, a "short and fat" column (lower approach to flood) offers 7% energy savings over a "tall and skinny" column.

Although the "short and fat" column uses the same volume of packing, its capital cost may be greater because it requires a larger diameter.

4.4.2 Effect of temperature approach in cross exchanger on stripper performance. The effect of varying the cross exchanger temperature approach from 10^{o}C to 5^{o}C is also shown in Table 4-4. The results show that at 30 kPa, operating the cross exchanger with a 5^{o}C approach offers 1.4% and 3% energy savings at 80% and 30% approach to flood. The pressure and temperature drops across the column are not significantly different.

At 160 kPa, the energy savings in operating the cross exchanger with a 5^{o}C approach is 7-9% when compared to a 10^{o}C approach. The increased savings can be attributed to a lower temperature drop across the column which results in reduced sensible heat requirements.

4.4.3 Effect of volume of packing. Varying the effective packing volume, τ, gives different energy requirements and column design specifications. In simple systems we expect the performance to increase with packing volume. In columns with no pressure

drop and an infinite packing volume, the minimum work requirement for 90% removal of CO_2 from a rich loading of 0.56 mol CO_2 / mol Alk to a lean loading of 0.467 mol CO_2 / mol Alk with subsequent compression to 1000 kPa is 29.0 kJ/gmol CO_2 and 28.0 kJ/gmol CO_2, respectively at 30 kPa and 160 kPa.

4.4.3.1 Stripper performance at 30 kPa.

Table 4-5 shows the performance of the 30 kPa stripper and column design specifications with varying effective packing volume for 5m K^+/2.5m PZ with a 5^oC approach on the hot side of the cross exchanger.

Figure 4-3 shows the relative equivalent work (equivalent work divided by the minimum equivalent work) as a function of effective packing volume. when the stripper is operated at 30 kPa under different flood conditions. The results include the effect of pressure drop. A useful design point for strippers will be to operate at a point with somewhat more than the minimum equivalent work. Figure 4-3 shows an equivalent work within 4% of the minimum total equivalent work can be achieved with only 7 m of packing at 50% approach to flood.

With low effective packing volume, the effect of pressure drop is unimportant and operation at a higher approach to flood is attractive. The mass transfer coefficients in the gas (k_g) and liquid (k_l) phases are greater at higher flood. At τ = 461 s, the gas phase mass transfer coefficient is 3.41×10^{-8} kmol/Pa-m^2-s and 1.96×10^{-8} kmol/Pa-m^2-s at 80% and 30% approach to flood, respectively. The liquid phase mass transfer coefficient is

$3.33x10^{-4}$ m/s and 2.26 $x10^{-4}$ m/s at 80% and 30% approach to flood, respectively. The increased rates of mass transfer reduce the reboiler duty and equivalent work.

Table 4-5: 30 kPa stripper performance and design specification with varying effective packing volume (5m K^+/2.5m PZ, rich ldg = 0.56 mol CO_2/mol Alk, lean ldg = 0.467 mol CO_2/ mol Alk, $\Delta T = 5^oC$, P_{reb} = 30 kPa, P_{final} = 1000 kPa)

Flood	τ	v_L ($x10^3$)	H	ΔP	$\frac{\Delta P}{P}$	$T_{bottom} - T_{top}$	Q	Total W_{eq}
%	s	m/s	m	kPa	-	^oC	kJ/gmol CO_2	
80	921	19.3	17.8	18.5	0.62	23.2	229.0	43.4
	461	21.8	10.1	10.5	0.35	14.4	187.4	35.2
	230	22.6	5.2	5.4	0.18	10.5	174.9	32.1
	115	20.9	2.4	2.5	0.08	6.8	191.3	32.9
	58	17.8	1.0	1.1	0.04	3.5	237.4	36.3
50	921	15.1	13.9	5.7	0.19	11.7	164.5	31.4
	461	15.1	7.0	2.8	0.09	9.9	160.1	30.4
	230	14.6	3.4	1.4	0.05	8.2	164.7	30.3
	115	12.8	1.5	0.6	0.02	5.1	194.7	32.8
	58	10.8	0.6	0.3	0.01	2.6	247.0	37.0
30	921	9.5	8.7	1.3	0.04	9.7	152.3	29.4
	461	9.2	4.2	0.6	0.02	8.8	154.9	29.5
	230	8.7	2.0	0.3	0.01	7.3	166.1	30.2
	115	7.4	0.9	0.1	0.00	4.2	204.9	33.4
	58	6.3	0.4	0.1	0.00	2.1	258.7	37.4

At high effective packing volume, the effect of pressure drop on column performance is important. A higher approach to flood leads to increased pressure drop. The loss of work due to increased pressure drop leads to higher reboiler duties and equivalent work.

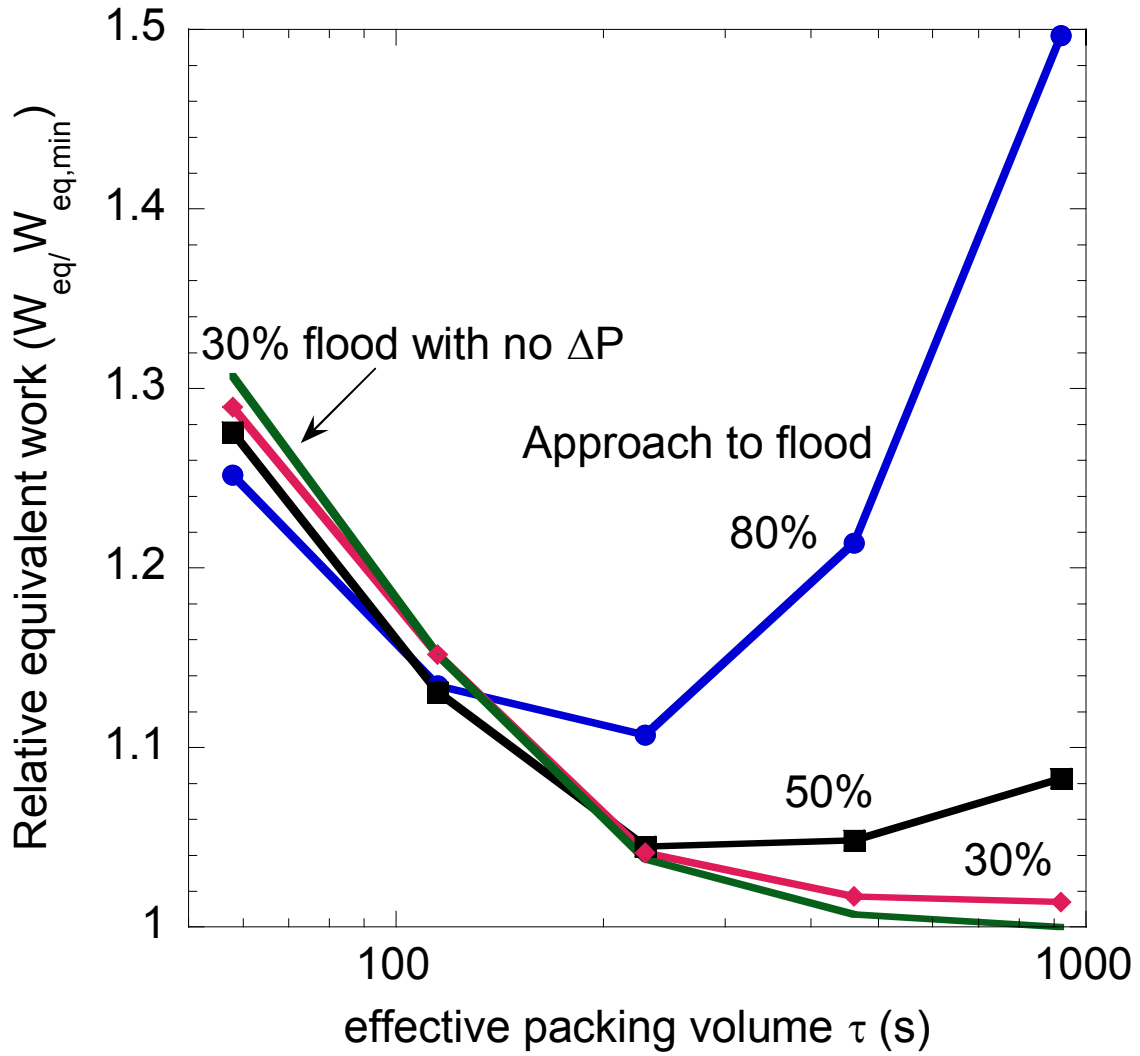

Figure 4-3: Performance of 30 kPa Stripper (rich ldg = 0.56 mol CO_2/mol Alk, lean ldg = 0.467 mol CO_2/mol Alk, $\Delta T = 5^oC$, $W_{eq,min} = 29.0$ kJ/gmol CO_2), accounting for pressure drop

At a fixed approach to flood, a high effective volume of packing leads to a tall column with a significant pressure drop across the stripper. An optimum effective packing volume is apparent at τ = 230 s. An optimum operating point for the 30 kPa

stripper could be at τ = 230 s and 50% approach to flood. This may be a compromise between the competing effects of mass transfer rates and pressure drop considerations.

4.4.3.2 Stripper performance at 160 kPa. . Table 4-6 shows the performance of the 160 kPa stripper and column design specifications with varying effective packing volumes for 5m K^+/2.5m PZ with a 5^oC approach on the hot side of the cross exchanger.

Figure 4-4 shows the relative equivalent work as a function of effective packing volume. An equivalent work within 4% of the minimum total equivalent work can be achieved with only 6.5 m of packing at 80% approach to flood.

With low effective packing volume, the effect of pressure drop is unimportant and operation at a higher approach to flood is attractive. The mass transfer coefficients in the gas (k_g) and liquid (k_l) phases are greater at higher flood. At τ = 461 s, the gas phase mass transfer coefficient is $6.89x10^{-9}$ kmol/Pa-m^2-s and $3.78x10^{-9}$ kmol/Pa-m^2-s at 80% and 30% approach the flood respectively. The liquid phase mass transfer coefficient is $9.34x10^{-4}$ m/s and $5.94x10^{-4}$ m/s at 80% and 30% approach to flood respectively. The increased mass transfer coefficients lead to enhanced mass transfer rates at higher packing volumes, the effect of pressure drop on column performance is important. A higher approach to flood leads to increased pressure drop. The loss of work due to approach to flood reduced the reboiler duty and equivalent work.

At high effective packing volumes, increased pressure drop leads to higher reboiler duties and equivalent work. For τ = 230 s, 461 s, and 921 s, the optimum operating condition appears to be at a low approach to flood. At τ = 115 s, the optimum

operating condition is about 50% flood with a total equivalent work of 28.7 kJ/gmol CO_2 while at lower τ values, higher than 50% flood is required to minimize total equivalent work. An economic analysis is required to determine the optimum design specification that will minimize overall costs.

Table 4-6: 160 kPa stripper performance and design specification with varying effective packing volume (5m K^+/2.5m PZ, rich ldg = 0.56 mol CO_2/mol Alk, lean ldg = 0.467 mol CO_2/ mol Alk, $\Delta T = 5^oC$, $P_{reb} = 160$ kPa, $P_{final} = 1000$ kPa)

Flood	τ	v_L ($x10^3$)	H	ΔP	$\frac{\Delta P}{P}$	$T_{bottom} - T_{top}$	Q	Total W_{eq}
%	s	m/s	m	kPa	-	^oC	kJ/gmol CO_2	
80	921	57.1	52.6	54.9	0.34	18.9	150.7	35.1
	461	59.4	27.4	28.6	0.18	15.3	137.1	30.8
	230	58.7	13.5	14.1	0.09	13.5	132.9	29.2
	115	56.0	6.5	6.7	0.04	12.1	133.2	29.0
	58	52.1	3.0	3.1	0.02	10.9	136.3	29.2
50	921	38.7	35.7	14.5	0.09	14.2	129.9	29.4
	461	38.0	17.5	7.1	0.04	13.2	128.8	28.7
	230	36.4	8.4	3.4	0.02	12.3	130.0	28.4
	115	34.0	3.9	1.6	0.01	11.3	133.2	28.7
	58	31.3	1.8	0.7	0.01	10.2	137.7	29.4
30	921	23.3	21.5	3.2	0.02	13.1	126.9	28.2
	461	22.5	10.4	1.5	0.01	12.5	127.9	28.1
	230	21.2	4.9	0.7	0.00	11.7	130.7	28.4
	115	19.6	2.3	0.3	0.00	10.7	134.9	28.9
	58	18.0	1.0	0.2	0.00	9.7	140.0	29.7

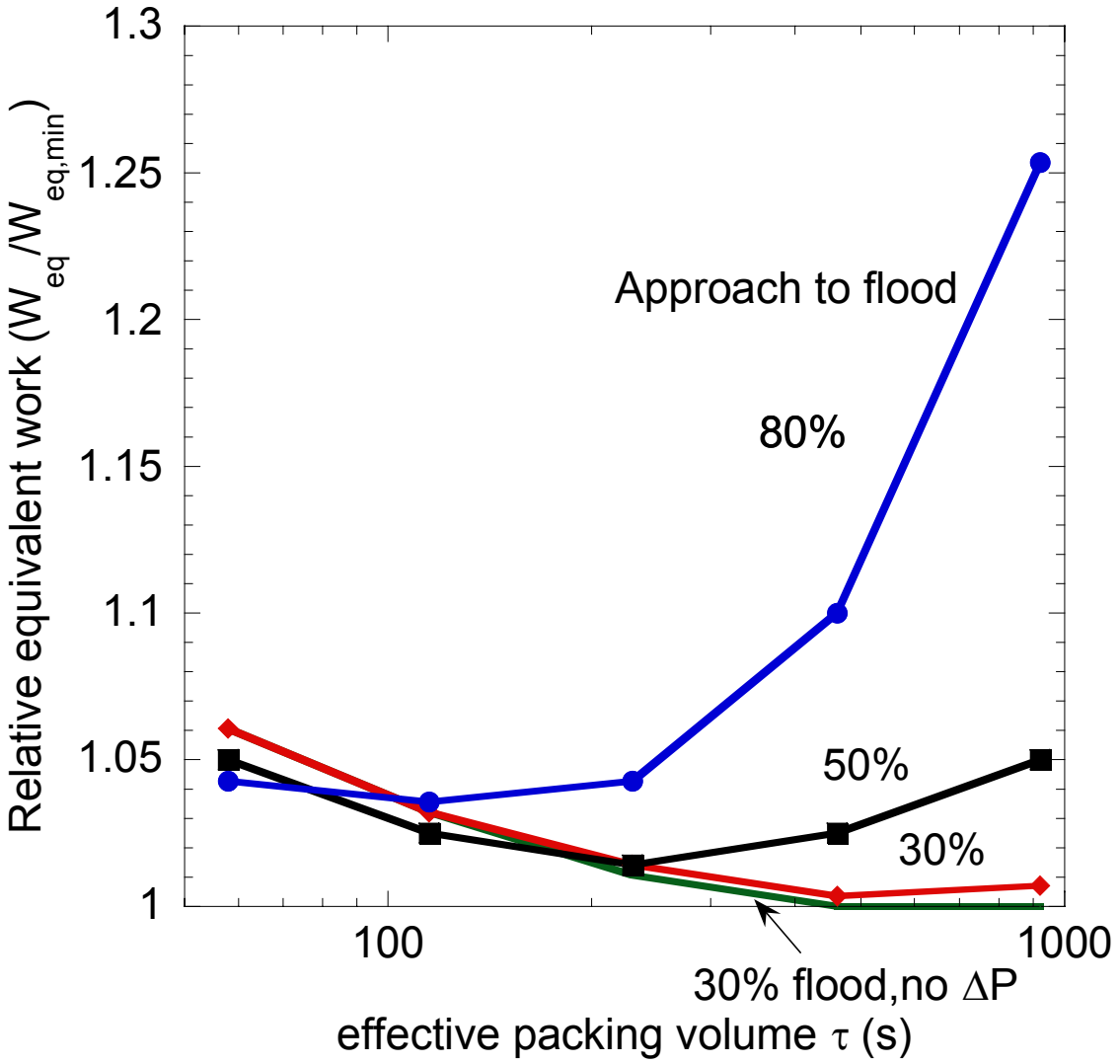

Figure 4-4: Performance of 160 kPa Stripper (rich ldg = 0.56 mol CO_2/mol Alk, lean ldg = 0.467 mol CO_2/mol Alk, $\Delta T = 5^oC$, $W_{eq,min} = 28.0$ kJ/gmol CO_2), accounting for pressure drop

4.4.4 Relative contributions to total equivalent work for stripping and compression to 10 MPa. The contributions to the total equivalent work, the reboiler work, pump work, and compression work to 10 MPa (a typical pressure for CO_2 sequestration) for 5m

K^+/2.5m PZ at 80% approach to flood for the 30 kPa and 160 kPa strippers are shown in Table 4-7. The typical predicted energy requirement is about 37 kJ/gmol CO_2 which is 25% of the net power output of a 500 MW power plant with 90% CO_2 removal. The relative contribution to equivalent work for the 30 kPa stripper is 37% reboiler work, 3% pump work and 60% compression work. The relative contribution to total equivalent work for the 160 kPa stripper is 56% reboiler work, 5% pump work and 39% compression work. The pump work is not as significant as the reboiler and compression work components.

Table 4-7: Relative contributions to total equivalent work for CO_2 sequestration at 10 MPa (5m K^+/2.5m PZ, τ = 461 s, 80% approach to flood, $\Delta T = 5^oC$, rich ldg = 0.56 mol CO_2/mol Alk, lean ldg = 0.467 mol CO_2/ mol Alk)

Reboiler Pressure	$W_{reboiler}$	W_{pump}	W_{comp}	Total W_{eq} to 10 MPa
kPa	kJ/gmol CO_2			
30	15.8	1.4	25.3	42.5
160	21.2	1.9	14.9	38.0

4.4.5 Mass Transfer Mechanisms. The liquid phase mass transfer coefficient based on the gas phase driving force expressed in mole fraction units, k_y', and the overall mass transfer coefficient, K_y, expressed in mole fraction units are shown in Table 4-8 and defined as:

$$k_y' = k_g' P_T \quad (4\text{-}22)$$

$$K_y = K_G P_T \quad (4\text{-}23)$$

where P_T is the total pressure of the segment.

In the 30 kPa stripper, k_y', increases from 1.5 x 10^{-5} kmol/m^2-s at the rich end to 3.7 x 10^{-5} kmol/m^2-s at the lean end. At 160 kPa, K_y at the rich and lean ends of the stripper was 22.8 x 10^{-5} kmol/m^2-s and 37.7 x 10^{-5} kmol/m^2-s respectively. The increase in K_y from the rich to the lean end is due to the presence of more free amine in the liquid available for reaction. It also reflects a change in the slope of the equilibrium relationship.

Table 4-8: Mass transfer mechanisms in stripper (5m K^+/2.5m PZ, rich ldg = 0.56 mol CO_2/mol Alk, lean ldg = 0.467 mol CO_2/ mol Alk, τ = 461 s, 80% flood, ΔT = 5^{o}C)

Mole fraction units (x 10^5) kmol/m^2-s	P = 30 kPa		P = 160 kPa	
	Rich End	Lean End	Rich End	Lean End
k_y'	1.5	3.7	22.8	37.7
K_y	1.5	3.5	19.8	28.0
Gas resistance (%)	2	3	14	26
Kinetic resistance (%)	88	71	3	-
Diffusion resistance (%)	10	25	84	74

The mass transfer process in the stripper can be separated into its component mechanisms. The gas resistance is negligible accounting for about 2% and 4% at the rich and lean ends of the vacuum stripper. The gas resistance is 14% at the rich end and 26% at the lean end of the stripper at 160 kPa.

For the vacuum stripper, the kinetic resistance accounts for 88% (at the rich end) and 71% (at the lean end) of the total resistance. This shows the importance of kinetics at lower temperature in a vacuum stripper. The resistance associated with diffusion of reactants and products dominates the stripper operation at 160 kPa. There are still appreciable contributions by the gas phase resistance. Most studies on stripping operations have assumed the stripping operation (typically at 160 kPa) to be controlled by diffusion of reactants and products with the influence of kinetics usually neglected. This work shows that the stripping operation mass transfer mechanism is kinetic controlled at vacuum conditions and mostly diffusion controlled at 160 kPa. Diffusion resistance controls the stripping operation at 160 kPa because of the increased reaction rates at high temperature.

4.4.6 Insight into Stripper Operation. Figure 4-5 shows the McCabe-Thiele plot for the 30 kPa stripper with τ = 461 s at 50% flood. At the stripper feed inlet, flashing of the rich solution is accompanied by a drop of 5^{o}C. There is some degree of pinching occurring at the rich end but going from the rich end (top of column) to the lean end (bottom of column), there is a well-defined driving force. The bulk of the stripping is observed in the reboiler. The partial pressure of CO_2 in the gas phase increases in the first three segments from the rich end because of the constraint that the total pressure on a segment is the sum of the partial pressures of CO_2 and H_2O. In order to satisfy the constraint, there is movement of water from the liquid phase to the vapor. The reboiler

duty is 160.1 kJ/gmol CO_2 while the total equivalent work to 1000 kPa is 30.4 kJ/gmol CO_2.

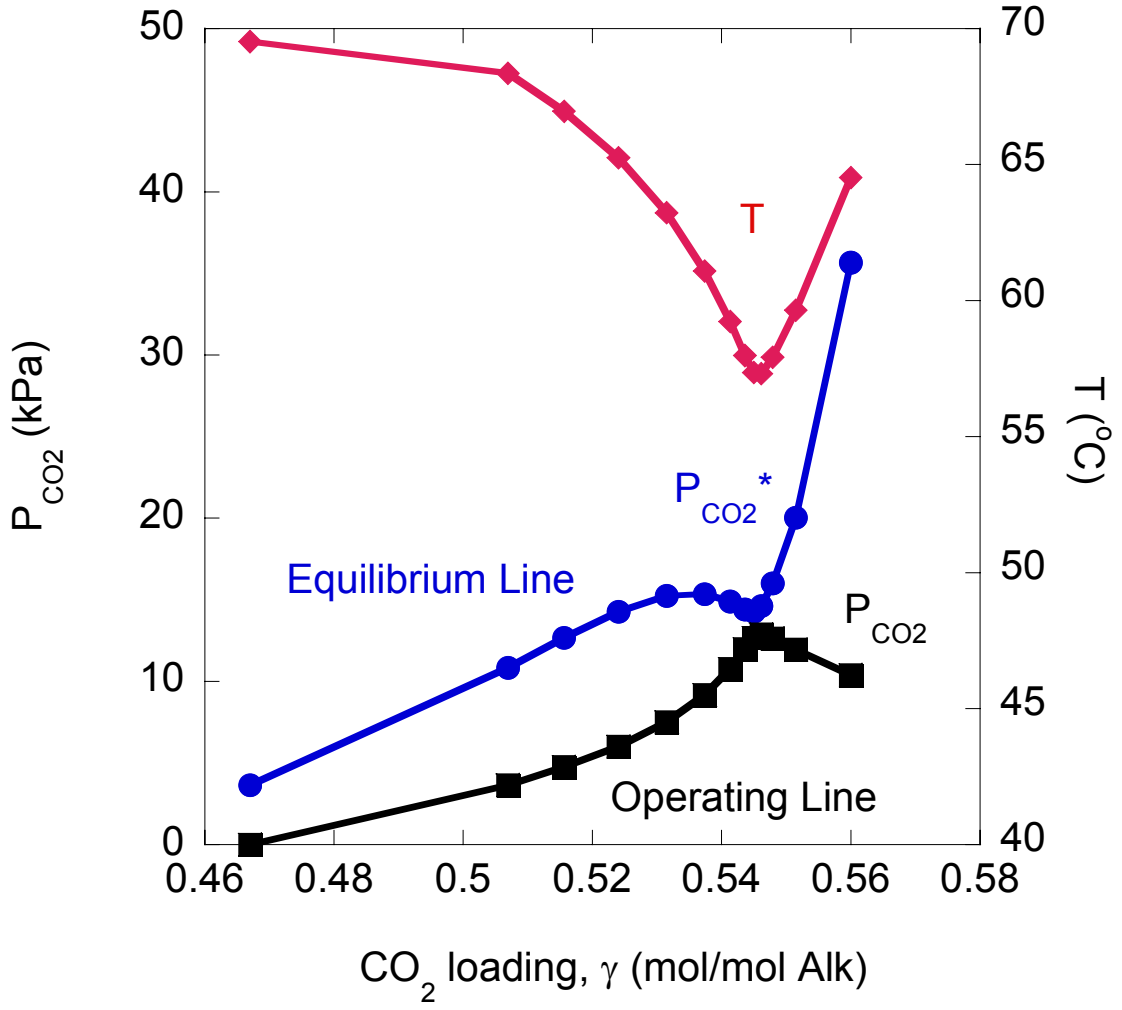

Figure 4-5: McCabe-Thiele Plot for 30 kPa Stripper (τ = 461 s, 50% flood, rich ldg = 0.56 mol CO_2/mol Alk, lean ldg = 0.467 mol CO_2/mol Alk, ΔT = 5°C)

Figure 4-6 shows the McCabe-Thiele plot for the 160 kPa stripper with τ = 461 s at 50% flood. The rich solution flashes to a greater extent than in the vacuum stripper with 8°C drop at the inlet. This is because the equilibrium partial pressure of CO_2 increases with increasing temperature. The stripping operation is seen to occur mostly due to flashing and in the reboiler. The reboiler duty is 128.8 kJ/gmol CO_2 and the total equivalent work to 1000 kPa is 28.7 kJ/gmol CO_2.

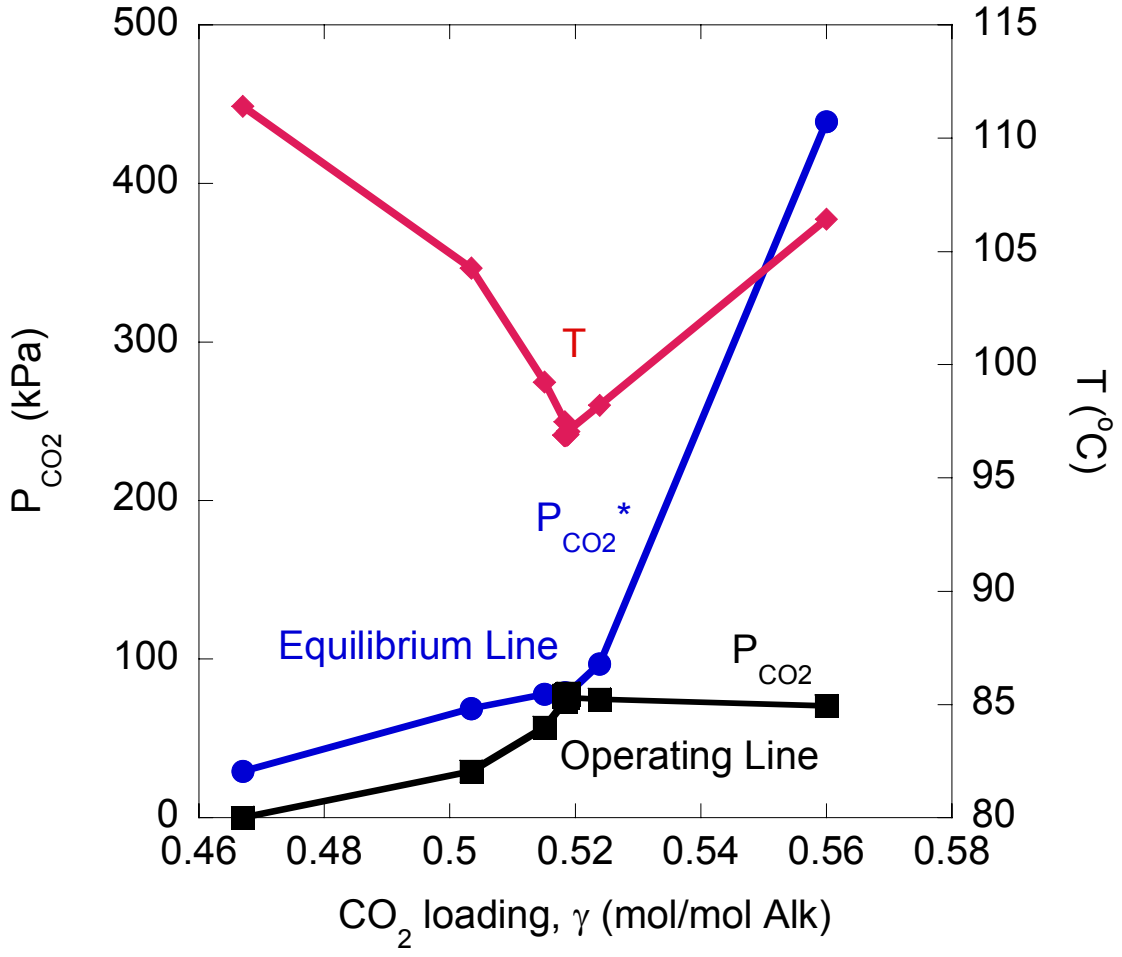

Figure 4-6: McCabe-Thiele Plot for 160 kPa Stripper (τ = 461 s, 50% flood, rich ldg = 0.56 mol CO_2/mol Alk, lean ldg = 0.467 mol CO_2/mol Alk, ΔT = 5°C)

4.4.7. Comparison of equilibrium and rate model results.

The equilibrium and rate model results for 5m K^+/2.5m PZ are compared in

Table 4-9. The table includes results from the equilibrium model without the activity of water included in the partial pressure of water in the gas calculation, the equilibrium model with the activity of water included in the calculation of the partial pressure of water, the rate model with the pressure drop neglected and the rate model with the influence of pressure drop considered. The results show that the equilibrium model without the activity of water correction gives a reboiler duty of 131 kJ/gmol CO_2 while that with the activity of water correction gives a reboiler duty of 126.8 kJ/gmol CO_2 (a 3% deviation). A 3^oC deviation in temperatures is also observed.

The rate model with pressure drop neglected gives a reboiler duty of 130.4 kJ/gmol CO_2, which is comparable to that from the equilibrium calculation. When the influence of pressure drop is considered, the reboiler duty is 133.2 kJ/gmol CO_2. The equivalent work for the different simulations is also presented. The equivalent work with the two equilibrium simulations is approximately equal at 33.7 kJ/gmol CO_2. The rate simulations have slightly higher values. The equivalent work with the rate model and no pressure drop is 35.6 kJ/gmol CO_2 while that with pressure drop is 36.2 kJ/gmol CO_2. The increased equivalent work with the latter due to the pressure drop and slightly greater temperature drop across the column.

Table 4-9: Comparison of equilibrium and rate model results for 5m K^+/2.5m PZ (rich loading =0.56 mol CO_2/mol Alk, lean loading =0.467 mol CO_2/mol Alk, ΔT = 5°C, P_{reb}=160 kPa, P_{final} =10MPa)

Property	Equilibrium Model 1	Equilibrium Model 2	Rate Model 1	Rate Model 2
Activity of water included in P_{H2O} calculation	NO	YES	YES	YES
Flood (%)	-	-	80	80
Height (m)	-	-	6.5	6.5
ΔP (kPa)	-	-	-	6.7
$\Delta P/P$	-	-	-	0.04
Q (kJ/gmol CO_2)	131	126.8	130.4	133.2
Total Weq (kJ/gmol CO_2)	33.7	33.7	35.6	36.2
T_{reb} (°C)	108.2	111.6	111.4	111.4
ΔT (°C)	12.6	12.9	11.7	12.2

4.5. Conclusions

1. A 'short and fat' column requires 7 to 15% less equivalent work than a 'tall and skinny' one because it has a lower pressure drop and less temperature change. This is especially evident in the vacuum stripper.
2. The optimum stripper design could be one that operates between 50% and 80% flood at the bottom. This optimal design will have to be determined by an economic analysis of the attractive options.

3. The vacuum stripper requires 230 s of effective packing volume to get an equivalent work 4% greater than the minimum work. This is a packing height of 7 meters with 50% flood. Because kinetics do not limit stripping at 160 kPa, only 115 s is required to get within 4% of the equivalent work giving a packing height of 6.5m.
4. The stripping operation is liquid phase controlled. Kinetics is the dominant mechanism for mass transfer in the vacuum stripper while diffusion of reactants and products is the controlling mechanism at 160 kPa.
5. The typical predicted energy requirement for stripping and compression to 10 MPa to achieve 90% removal from 5m K^+/2.5m PZ with a rich loading of 0.56 mol CO_2/ mol Alk is about 37 kJ/gmol CO_2. This is about 25% of the net power output of a typical power plant with 90% CO_2 removal. This includes pumping power but not the flue gas fan and other auxiliaries. This is 3.3 kJ/gmol CO_2 greater than the corresponding equilibrium work prediction. The total equivalent work for the rate prediction is 10% more than the equilibrium prediction.
6. At 30 kPa, operating the cross exchanger with a 5^oC approach rather than 10^oC offers 1.4% and 3% energy savings at 80% and 30% approach to flood. The pressure and temperature drops across the column are not significantly different.
7. At 160 kPa, the energy savings in operating the cross exchanger with a 5^oC approach is 7-9% compared to a 10^oC approach. The increased savings can be

attributed to a lower temperature drop across the column which results in reduced sensible heat requirements.

Chapter 5 : Pilot Plant Description and Results

This chapter outlines a detailed description of the pilot plant for aqueous absorption/stripping of CO_2 from 5m K^+/2.5m PZ and 6.4m K^+/1.6m PZ with focus on the stripping conditions. Detailed experimental results are presented and compared to those obtained from the rate-based stripper model. This model is different from that in Chapter 4 because it incorporates structured packing and includes both 5m K^+/2.5m PZ and 6.4m K^+/1.6m PZ. In order to fit the data, the wetted area in the model had to be adjusted.

5.1. Pilot Plant for CO_2 Capture

The closed loop pilot plant for CO_2 capture (Figure 5-1) situated at the Pickle Research Campus of The University of Texas at Austin was used to test K_2CO_3/PZ and validate model predictions. A simplified diagram of the stripper section of the pilot plant is shown in Figure 5.2. The set up was modified from an original set up that has been used in the past for distillation and liquid-liquid extraction experiments.

The absorber and stripper were carbon steel columns with 0.427m internal diameter. 6.1m of Flexipac AQ Style 20 packing with a specific area of 213 m^2/m^3 divided into two equal sections. The total column height was 10.7 m. There was a chimney tray with a redistributor between the beds. There were six resistance temperature detectors (RTDs) (T20710, T2078, T2076, T2075, T2073 and T2071 in Figure 5-2) at different points in the stripper. There were observation windows at different points in the column. The pressure drop between the top and the middle and the middle and the top of the stripper was measured. The reboiler duty was calculated by performing an energy balance with a program developed at the University of Texas Separations Research Program (UTSRP).

The pilot plant is controlled by the Delta V control system from Fisher Rosemount. Temperatures, flowrates and pressures are measured in real time. Appendix D-1 shows a detailed process flow diagram for the pilot plant.

A liquid distributor was situated at the stripper inlet and in the middle of the column. The top and side elevations of the liquid distributors are shown in Figure 5-3. Detailed drawings of the distributor are shown in Appendix D-2.

Table 5-1 summarizes the specifications for the 304 stainless steel reboiler. Detailed drawings of the reboiler and tubes are shown in Appendix D-3.

The cross exchanger is a plate heat exchanger made of 316 stainless steel. Table 5-2 shows the specifications for the cross exchanger. A detailed drawing of the cross exchanger is shown in Appendix D-4.

The specification of the condenser, made of 316L carbon steel, is shown in Table 5-3. Detailed drawings of the condenser are in Appendix D-5.

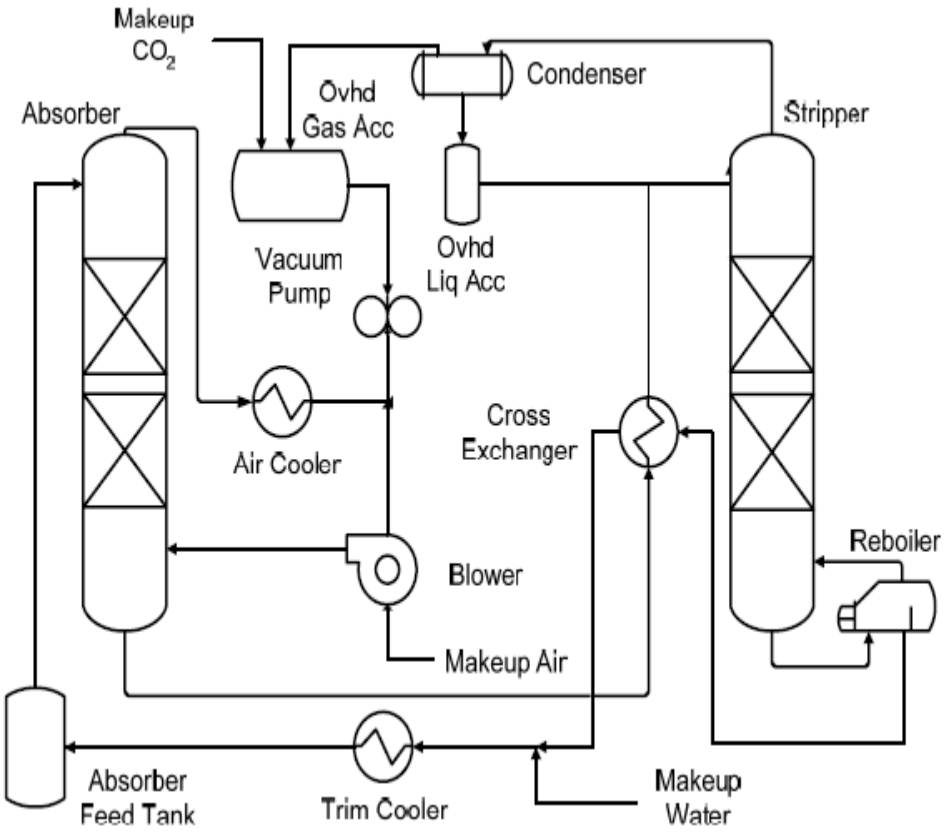

Figure 5-1: Schematic of pilot plant for CO_2 capture.

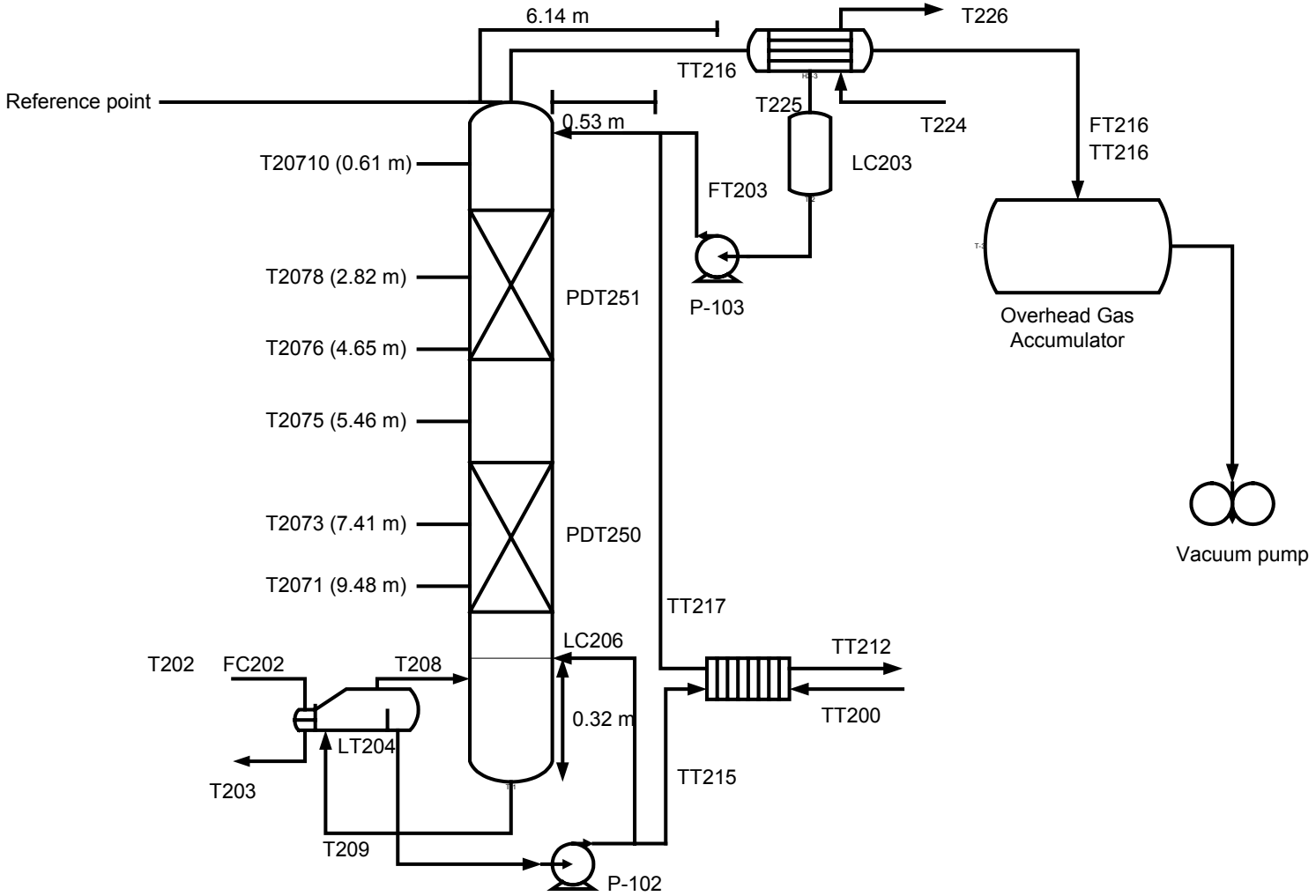
6.14 m
T226
TT216
Reference point
T225
T224
0.53 m
FT216
TT216
T20710 (0.61 m)
LC203
FT203
T2078 (2.82 m)
PDT251
P-103
Overhead Gas
Accumulator
T2076 (4.65 m)
T2075 (5.46 m)
Vacuum pump
T2073 (7.41 m)
PDT250
T2071 (9.48 m)
TT217
LC206
TT212
T202
FC202
T208
0.32 m
TT200
LT204
TT215
T203
T209
P-102

Figure 5-2: Stripper section of pilot plant.

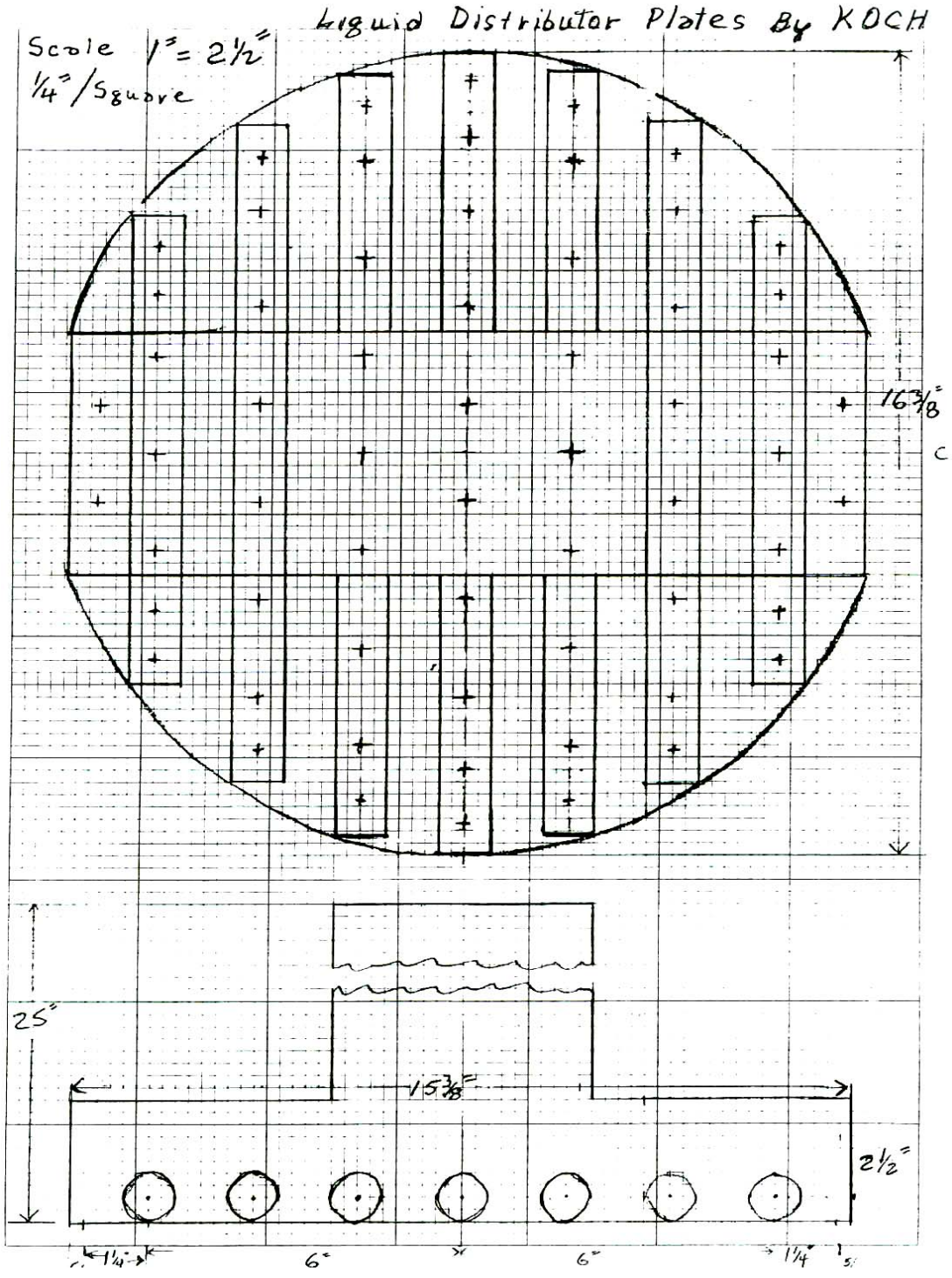

Figure 5-3: Top and side elevations of the liquid distributors

Table 5-1: Reboiler specifications

Property	Specification
MAWP psi @ ^{o}F (Shell)	100 & FV @ 400
MAWP psi @ ^{o}F (Tubes)	175 @ 400
MDMT ^{o}F @ psi (Shell)	20 @ 100 & FV
MDMT ^{o}F @ psi (Tubes)	20 @ 175
Test pressure, psig (Shell)	138
Test pressure, psig (Tubes)	241
Design fluid (Shell)	Methanol
Design fluid (Tubes)	Saturated steam
Tube type	U-tube
Number of tube holes	138
Weir height, in	25.375

Table 5-2: Specifications for the cross exchanger

Property	Specification
MAWP psi @ ^{o}F (Shell)	150 @ 257
MDMT ^{o}F @ psi	- 20 @ 150
Pressure drop, psi (hot side)	14.3
Pressure drop, psi (cold side)	14.5
Heat exchanged, kBtu/h	1070
L.M.T.D., ^{o}F	18
Service U value, Btu/ft^2-h-^{o}F	379.2
Overall length x width x height	27 x 13 x 36
Heat transfer area, ft^2	159.8
Relative direction of fluids	Countercurent
Number of plates	99
Number of hot and cold side passes	5

Table 5-3: Condenser specifications

Property	Specification
MAWP psi @ ^{o}F (Shell)	355 @ 350
MAWP psi @ ^{o}F (Tubes)	180 @ 250
MDMT ^{o}F @ psi (Shell)	-7 @ 355
MDMT ^{o}F @ psi (Tubes)	-7 @ 180
Number of tubes	105
Size of tubes, in	0.625

5.2. Experimental Conditions and Analytical Methods

Simulated flue gas was used in the tests. The desired solvent loadings were achieved by injecting CO_2 from gas cylinders. A summary of the experimental conditions for the pilot plant tests is shown in Table 5-4. The CO_2 gas concentrations were measured at the inlet, middle and outlet of the absorber. In situ Vaisala CO_2 analyzers measured the inlet and the outlet of the absorber. A Horiba CO_2 analyzer, which was an extractive system, was used to measure the middle concentration. A Fourier Transform Infra Red (FTIR) analyzer also was used to measure the inlet and outlet concentration of CO_2, water, and test for piperazine volatility. An online pH meter was used to help maintain a constant loading and the density was monitored to maintain the water balance.

Table 5-4: Summary of Pilot Plant Operations

	5m K^+/2.5m PZ	6.4m K^+/1.6m PZ
K_2CO_3 Concentration (wt%)	22	28
K^+/PZ mole ratio	2	4
Inlet CO_2 (%)	8.3 – 17.2	9.9 – 12.9
CO_2 Removal (%)	56 – 92	40 – 81
Lean Loading (mol CO_2/K+2*PZ)	0.39 – 0.45	0.45 – 0.51
Gas Rate (kg/m^2-s)	1.2 – 2.0	1.2 – 2.0
L/G Ratio (kg/kg)	3.9 – 10.8	8.3 – 14.5
Top $P_{Stripper}$ (kPa)	160	35 – 76

Liquid samples were taken at the inlet, middle, and outlet of the absorber as well at the middle and outlet of the stripper. The liquid samples were extracted using sample bombs to minimize any flashing that may occur. The samples were analyzed for CO_2 loading using an inorganic carbon analyzer. Piperazine and potassium concentration was measured using ion chromatography.

5.3. Energy balance of pilot plant data

In order to calculate the normalized reboiler duty in kJ/gmol CO_2, an energy balance was performed over the stripper. The boundary for the energy balance is shown in Figure 5-4. The CO_2 production rate was converted from standard cubic foot per minute (scfm) to gmol/hr. The actual rich solution flow rate is the sum of the absorber rich flow rate (FT200) and the stripper return feed (FT203).

The enthalpy of the rich feed is calculated by:

$\Delta H_{rich} = L_{rich} * C_{p,rich} * (T_{rich} - T_{lean})$.

A material and energy balance across the mixing point of the absorber rich stream and the stripper water reflux stream calculates the rich stream temperature.

The enthalpy of the lean stream is calculated by:

$\Delta H_{lean} = L_{lean} * C_{p,lean} * (T_{lean} - T_{lean})$.

The heat capacity of the liquid is set at 4.186 kJ/kg K.

Note: The reference temperature for the energy balance is the stripper lean temperature. This makes the enthalpy of the lean stream equal to zero.

The sensible heat contribution to the reboiler duty is given as:

$Q_{sensible} = \Delta H_{rich} - \Delta H_{lean}$

The heat consumed in the overhead condenser is calculated from an energy balance around the condenser.

$Q_{cond} = Q_{overhead} - Q_{CO2,overhead} - Q_{H2O\ reflux}$

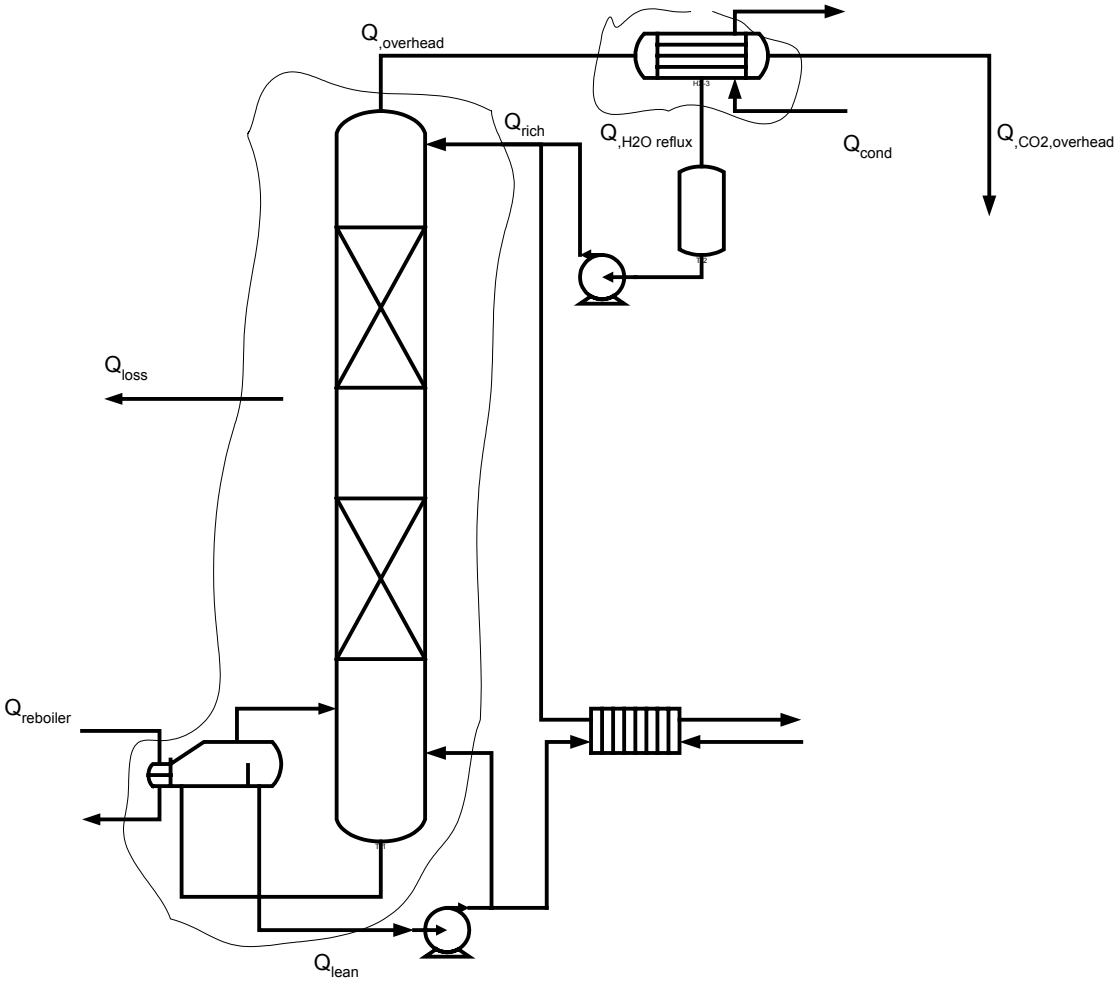

Figure 5-4: Boundary for energy balance over the stripper

The steam rate $Q_{steam\ rate}$ is given by:

$Q_{steam\ rate} = Q_{sensible} + Q_{cond} + Q_{CO2,overhead} + Q_{loss}$

From where the heat loss can be calculated as:

$Q_{loss} = Q_{reboiler} - Q_{sensible} - Q_{cond} - Q_{CO2,overhead}$

The CO_2 production rate in the overhead stream in gmol/hr was calculated by:

CO_2 rate (gmol/hr) = CO_2 flow (scfm) * 6.32/0.0022

The actual steam rate (kJ/hr) is obtained by:

$Q_{actual\ steam\ rate} = Q_{sensible} + Q_{cond} + Q_{CO2,overhead}$

The actual reboiler duty (kJ/gmol) is given as:

$Q_{actual\ reb\ duty} = Q_{actual\ steam\ rate} / CO_2$ rate

A sample calculation of the actual reboiler duty is shown in Appendix D-6.

5.3.1. Observations from pilot plant tests

In the pilot tests severe foaming was observed in the stripper during the first four and last three tests with 5m K^+/2.5m PZ. Foaming was observed in most tests but the tests in the middle seemed to be more controllable than the aforementioned. Q2-3183A anti-foam was added at various times during the tests. This helped to reduce the foaming but only for a short while in most cases. The foaming could have been due to the presence of residual hexane from prior tests in the stripping column as observed in some analysis by McLees (McLees 2006). The presence of possible degradation products from prior tests could have been responsible for some foaming. Foaming in the upper half of the stripper

probably resulted in very poor gas/liquid contact, poor liquid distribution and very high pressure drop. A possible flow path for the liquid is shown in Figure 5-5. The liquid is hypothesized to flow down the walls of the column instead of flowing through the packing.

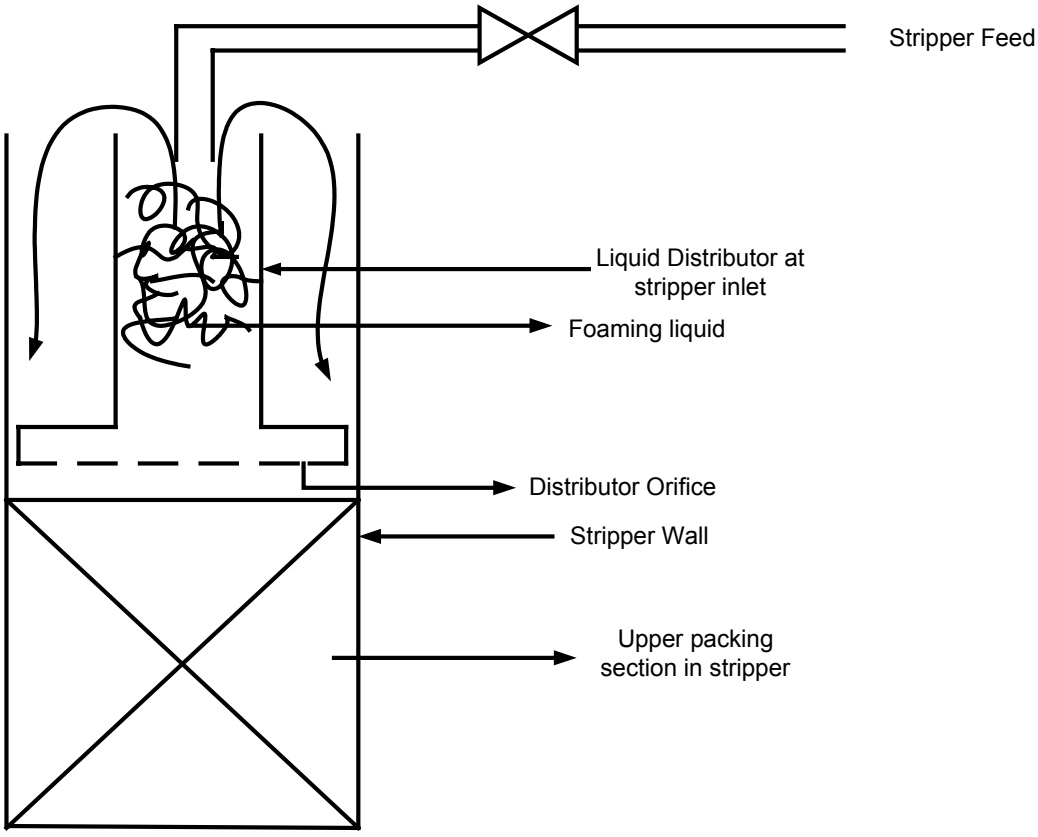

Figure 5-5:Possible flow path for liquid in upper half of stripper

5.4. Rate Model using structured packing

The rate model for structured packing is similar to that described in Chapter 4. The vapor/liquid equilibrium representation used was that presented in Table 3-1. The k_g' expression and constants for 5m K^+/2.5m PZ are presented in Table 4-2.

k_g' for 6.4m K^+/1.6m PZ is represented by:

$$k_g'\,[\text{kmol/Pa-m}^2\text{-s}] = \exp\left[\begin{array}{l} A + (B\gamma) + \left(\frac{C}{T}\right) + (D\,k_l) + (E\;P_{CO2,i}) + \left(F\,\frac{\gamma}{T}\right) + \left(G\;\frac{k_l}{T}\right) + \\ \left(H\,\frac{P_{CO2,i}}{T}\right) + \left(I\;\frac{\gamma^2}{T}\right) + \left(J\;\frac{\gamma}{T^2}\right) + \left(K\,\frac{\gamma^2}{T^2}\right) \end{array}\right] \quad (5\text{-}1)$$

A= -25.6343 G= -8347649

B= -11.0774 H= 1.459463

C= 2339.198 I= -39167.8

D= 22155.44 J= -7345645

E= -0.00538 K= 11627720

F= 26925.35

The main difference with structured packing involves the calculation of the mass transfer coefficients and the wetted area of contact between the gas and the liquid.

The hydraulic parameters (k_g, k_l, a_w) for Flexipac AQ Style 20 were obtained from the Rocha- Bravo-Fair (Rocha, Bravo et al. 1996) models for structured packing and packing

performance tests at The University of Texas Separations Research program (UTSRP). The characteristics of this packing needed with the Rocha-Bravo-Fair model were not readily available but since the packing is very similar to Intalox 2T packing (with known characteristics), Flexipac AQ Style 20 was assumed to have the same characteristics as Intalox 2T. The characteristics of Intalox 2T packing are shown in Table 5-5.

Table 5-5: Characteristics of Intalox 2T Packing

Property	Value
Specific dry packing area	213 m^2/m^3
Packing factor	17 m^{-1}
Crimp height, b	0.0388 m
Crimp depth, s	0.022352 m
Void fraction	0.97
Theta	45

The mass transfer coefficient in the gas and liquid phases used in the model was obtained by:

$k_g = k_g a_w$ (Rocha, Bravo et al. 1996) / a_w (SRP) (5-2)

$k_l = k_l a_w$ (Rocha, Bravo et al. 1996)/ a_w (SRP) (5-3)

The actual Rocha-Bravo-Fair expressions for the hydraulic parameters are:

$$k_g = 0.054 \left(\frac{\rho_G (U_{Ge} + U_{Le}) s}{\mu_G}\right)^{0.8} \left(\frac{\mu_G}{\rho_G D_G}\right)^{0.33} \left(\frac{D_G}{s}\right) \quad (5\text{-}4)$$

$$k_l = 2\sqrt{\frac{D_L U_{Le}}{0.9 \pi s}} \quad (5\text{-}5)$$

$$a_w = a_T \; F_{se} \; F_t \quad (5\text{-}6)$$

The correlation for the wetted area of Flexipac AQ Style 20 was obtained from tests at the University of Texas Separations Research Program shown in Figure 5-6.

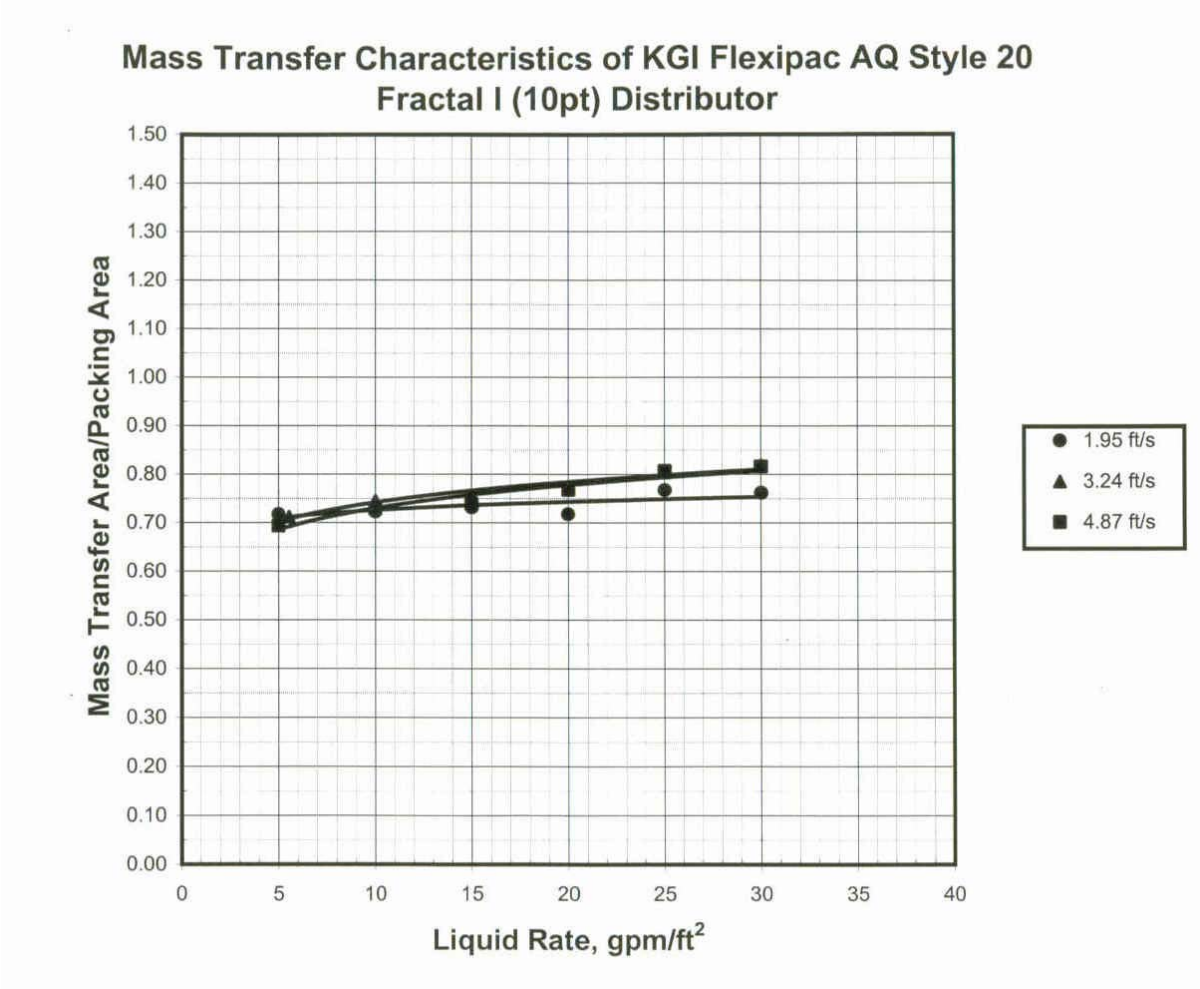

Figure 5-6:Wetted area data for Flexipac AQ Style 20 packing (Source: UTSRP)

The wetted area is calculated from the expression:

$$a_w = 0.7\ a_T \qquad (5\text{-}7)$$

where a_T is the specific packing area of the packing.

The top half of the stripper was assumed to have an effective area that is a tenth of the specific packing area while the bottom half was assumed to behave as expected based on (5-7). As a consequence of foaming the liquid in the distributor at the inlet tends to fill the receiver box. The liquid that actually wets the top half of the packing is significantly reduced.

The detailed equations for the rate based structured packing model are outlined in Appendix D-7. The model inputs were the liquid rate, the rich and lean stream temperatures, the top stripper pressure, packing height, and the overhead CO_2 rate. Initial guesses of the segment temperatures, partial pressures, and loadings were provided. The model solves the MESH equations, the mass and energy transfer rate equations and calculates the rich and lean loadings, temperature and composition profiles, and reboiler duty.

5.5. Results and discussion – pilot plant data for 5m K^+/2.5m PZ

Detailed pilot plant test results are presented in Table 5-6. The measured and predicted liquid rate, rich and lean loadings, overhead CO_2 rate, pressures, temperatures, reboiler duty and packing height for 5m K^+/2.5m PZ are presented in Table 5-7. Recent data from Hilliard shown in Figure 5-7 suggest that the equilibrium partial pressure of CO_2 in 5m K^+/2.5m PZ was overpredicted by Cullinane (Cullinane 2005). Hence, the equilibrium partial pressure of CO_2 was set at half that predicted by Cullinane (Cullinane 2005). There is some uncertainty as to what the equilibrium partial pressure of CO_2 in 5m

K^+/2.5m PZ is at high temperatures. More experiments will need to be performed and models refined to reduce this uncertainty. The following variables were fixed in the ACM Model:

a. Liquid rate (sum of absorber liquid flow rate and water reflux rate).
b. Overhead CO_2 production rate.
c. Height of packing (6.1m).
d. Stripper feed and lean temperature. The stripper feed temperature was calculated from an energy balance based on mixing the absorber rich liquid exiting the cross exchanger and the water reflux stream.
e. The pressure at the top of the stripper.

The above variables were chosen because they were identified as variables with a high confidence level amongst measured variables.

Table 5-6: Pilot plant stripper results for 5m K^+/2.5m PZ

Run Number	STRIPPER FEED			STRIPPER BOTTOMS			STRIPPER REFLUX						STRIPPER BED TEMPERATURES		
	STR Return FT200	STR Return FT200	STR Return FT200	STR Return FT201	STR Return FT201	STR Return FT201	STR Return FT203	STR Return FT203	STR Return FT203	STR Return FT204	STR Return FT204	STR Return FT204	Top Temp T20710	Top Mid Temp T2078	Top Bot Temp T2076
	(gpm)	(F)	(lb/ft^3)	(gpm)	(F)	(lb/ft^3)	(gpm)	(F)	(lb/ft^3)	(gpm)	(F)	(lb/ft^3)	(F)	(F)	(F)
5.1	14.00	119.51	76.89	13.57	104.35	76.22	2.74	129.00	61.07	0.16	126.45	61.81	239.38	240.4	242.88
5.2	12.89	118.35	77.56	12.32	103.74	76.57	2.36	127.63	61.77	0.14	122.32	62.56	236.54	237.7	242.87
5.3	13.35	122.27	77.33	12.98	110.98	76.49	0.67	102.20	61.60	0.15	101.39	62.03	222.61	232.0	239.88
5.4	14.86	122.50	77.43	14.39	113.70	76.49	0.72	103.59	61.56	0.17	102.44	62.02	223.42	234.9	241.17
5.5	14.83	115.89	77.64	14.29	110.33	76.72	0.52	97.30	61.72	0.23	96.69	62.12	222.03	233.8	240.20
5.6	12.30	123.47	76.74	11.85	114.89	75.70	1.59	113.96	61.52	0.11	110.19	62.15	235.76	235.2	242.10
5.7	14.84	123.26	76.68	14.37	116.13	75.72	2.06	122.83	61.28	0.09	120.18	61.97	237.26	237.4	242.26
5.8	13.33	123.14	76.59	12.90	111.35	75.78	0.46	100.59	61.68	0.09	98.89	62.13	221.08	229.4	237.66
5.9	14.85	119.55	76.63	14.40	108.01	75.92	0.40	94.35	61.82	0.13	92.48	62.21	220.51	229.4	236.84
5.10	14.81	115.26	76.69	14.36	105.21	76.07	0.33	94.68	61.82	0.19	94.12	62.19	221.78	229.9	235.88
5.11	29.28	118.83	76.23	28.65	108.44	75.85	0.77	103.96	61.62	0.15	102.94	62.08	222.36	230.8	237.02
5.12	30.54	118.29	76.28	29.88	109.68	75.95	0.67	96.81	61.77	0.15	96.11	62.15	222.04	231.2	235.93
5.13	23.86	113.54	76.41	23.37	104.23	76.07	0.46	100.24	61.68	0.08	99.06	62.10	218.88	227.0	233.11
5.14	25.55	118.50	76.31	24.80	107.69	75.97	0.78	99.79	61.74	0.19	98.55	62.18	222.91	230.1	237.80
5.15	25.74	122.44	76.27	24.93	105.14	75.89	1.89	117.03	61.40	0.21	114.75	62.03	235.06	238.3	240.99
5.16	20.66	124.13	76.66	20.06	105.23	76.23	2.56	128.77	61.12	0.14	127.21	61.83	238.25	240.6	242.44
5.17	20.57	125.59	76.65	19.94	104.97	76.20	2.39	132.08	61.02	0.14	130.49	61.77	236.92	239.3	241.12
5.18	14.00	119.51	76.89	13.57	104.35	76.22	2.74	129.00	61.07	0.16	126.45	61.81	239.38	240.4	242.88

Table 5-6: Pilot plant stripper results for 5m K^+/2.5m PZ (Contd.)

Run Number	STRIPPER BED TEMPERATURE			STRIPPER PRESSURE			STRIPPER LEVELS			COOLING WATER				
	Bot Top Temp T2075	Bot Mid Temp T2073	Bot Temp T2071	Column P PC215	PrsDrp (low) PDT250	PrsDrp (high) PDT251	Column Level LT206	Acc Level LT203	Reboiler Level LT204	OHD Vapor TT216	Cond Liq T225	CW Inlet T224	CW Outlet T226	CW Flow FT205
	(F)	(F)	(F)	(psia)	(in H_2O)	(in H_2O)	(in)	(in)	(in)	(F)	(F)	(F)	(F)	(gpm)
5.1	243.4	240.99	244.64	23.49	5.96	14.85	11.95	10.13	11.90	236.2	123.8	57.2	73.1	221
5.2	243.3	241.22	245.05	23.51	5.96	14.90	11.99	10.31	12.79	235.5	128.1	54.8	68.1	221
5.3	240.1	241.22	244.09	23.50	4.28	4.39	13.50	10.02	11.90	226.8	68.0	48.4	52.6	242
5.4	241.3	242.61	244.38	23.50	5.96	7.00	12.36	9.91	13.35	226.1	81.3	49.1	53.8	242
5.5	241.0	242.44	244.36	23.50	5.96	7.21	12.50	9.94	14.20	224.0	63.6	48.3	52.3	242
5.6	242.7	241.34	244.41	23.49	5.96	14.31	12.49	9.06	12.69	233.1	101.1	51.7	60.3	244
5.7	242.5	239.81	244.42	23.50	5.96	13.99	12.59	6.90	12.69	233.9	114.7	53.6	64.7	244
5.8	238.9	238.96	243.18	23.50	5.54	5.72	12.50	6.99	10.19	222.5	57.2	47.3	50.5	242
5.9	238.0	240.22	243.40	23.50	5.96	7.43	12.51	7.04	11.05	221.9	54.4	46.5	49.6	241
5.10	236.9	240.19	243.40	23.50	5.96	8.07	12.50	7.07	11.34	222.8	54.2	46.8	49.8	241
5.11	238.3	240.87	243.41	23.51	5.96	10.42	12.05	7.08	5.68	224.3	88.6	49.7	55.3	210
5.12	236.9	239.98	243.46	23.50	5.96	14.01	11.99	6.82	5.80	222.8	83.0	49.4	54.0	213
5.13	233.8	238.31	242.81	23.50	5.96	8.91	12.00	6.92	7.02	221.3	59.8	48.4	51.7	213
5.14	238.9	240.70	243.73	23.50	5.96	10.84	12.00	6.95	6.78	225.3	87.1	49.7	55.3	213
5.15	241.7	241.60	244.29	23.50	5.96	11.67	11.98	6.94	6.09	230.8	126.7	54.5	66.3	214
5.16	242.9	241.14	244.64	23.51	5.96	12.60	14.03	6.79	10.25	234.1	137.4	55.8	71.0	214
5.17	241.8	240.34	243.73	23.28	5.35	13.39	13.96	6.39	10.17	233.3	136.7	56.4	70.1	214
5.18	243.4	240.99	244.64	23.49	5.96	14.85	11.95	10.13	11.90	236.2	123.8	57.2	73.1	221

Table 5-6: Pilot plant stripper results for 5m K^+/2.5m PZ (Contd.)

Run Number	STEAM FLOW							CROSS EXCHANGER AND STRIPPER FEED						
	Reboiler duty QIC202	Steam Flow FC202	Steam Temp T202	Cond Ret T203	Steam Annubar Pressure	Bot Liq to Reb T209	Vapor Inlet T208	Bot Prod TT 215	Bot Prod TT 212	Feed Inlet TT200	Feed Outlet TT217	Trim Temp TT210	Str feed TT211	CO_2 flow
	(MMBTU/hr)	(lb/hr)	(F)	(F)	(psia)	(F)	(F)	(F)	(F)	(F)	(F)	(F)	(F)	(scfm)
5.1	2.1389	2224.2	334.1	261.3	117.3	244.9	245.5	245.7	128.5	119.5	232.0	230.9	228.2	26.72
5.2	1.8687	1949.3	335.7	265.3	119.8	245.3	246.6	246.1	127.2	118.4	232.0	231.1	229.1	42.48
5.3	0.8283	855.0	342.0	258.9	127.6	243.7	244.1	243.5	131.3	122.3	230.9	229.3	226.4	25.90
5.4	0.9428	974.3	341.6	259.9	127.3	244.1	242.3	243.9	131.6	122.5	230.7	229.1	226.5	35.19
5.5	0.8698	897.4	342.9	259.0	129.5	244.1	243.7	243.9	125.6	115.9	229.7	228.2	225.6	36.37
5.6	1.4102	1465.9	338.3	263.4	122.4	244.3	245.3	244.4	131.8	123.5	231.5	229.8	226.0	30.98
5.7	1.7408	1816.1	336.3	265.7	119.7	244.1	242.6	244.6	132.2	123.3	231.0	229.8	226.7	35.62
5.8	0.6822	701.6	343.1	256.1	130.3	242.5	243.1	242.4	132.3	123.1	229.9	228.4	225.7	24.88
5.9	0.7402	760.4	343.6	255.4	131.4	242.7	242.9	242.4	129.1	119.6	229.0	226.9	223.5	28.76
5.10	0.6997	719.0	343.7	255.6	132.0	242.7	242.8	242.6	125.3	115.3	228.5	227.1	224.1	28.05
5.11	1.2014	1245.3	339.8	261.5	124.6	242.1	240.6	242.0	132.1	118.8	226.3	226.0	224.7	50.76
5.12	1.1470	1189.4	339.1	261.5	123.8	242.2	240.1	241.8	131.9	118.3	225.8	225.5	224.0	39.89
5.13	0.8687	895.5	341.8	257.6	127.9	241.1	244.0	240.5	126.4	113.5	225.0	224.5	222.7	28.05
5.14	1.2123	1258.1	338.7	262.1	123.5	242.5	240.2	242.0	131.0	118.5	226.2	225.6	224.1	43.34
5.15	1.8610	1960.9	334.8	274.2	118.7	243.3	245.9	243.7	134.7	122.4	228.0	227.8	226.7	59.68
5.16	2.1676	2259.4	333.6	263.4	116.4	244.0	244.9	244.2	135.2	124.1	229.4	229.0	227.0	43.44
5.17	1.8574	1938.0	327.8	261.2	106.8	243.6	245.0	244.0	136.5	125.6	229.3	229.1	227.5	38.26
5.18	2.1389	2224.2	334.1	261.3	117.3	244.9	245.5	245.7	128.5	119.5	232.0	230.9	228.2	26.72

Table 5-7: Measured and predicted variables for 5m K^+/2.5m PZ

Run Number	Liquid rate*	CO_2 rate*	Temperature*		Top Pressure*	Rich loading		Lean loading		Reboiler Duty		Pressure Drop	
	($x10^4$) m^3/s	gmol/s	°C		kPa	mol CO_2/mol Alk				kJ/gmol CO_2		kPa	
			Feed	Lean		Meas.	Model	Meas.	Model	Meas.	Model	Meas.	Model
5.1	10.56	0.5338	97.81	118.25	161.81	0.498	0.470	0.398	0.393	1007	1423	35.7	4.3
5.2	9.62	0.8486	98.16	118.50	161.98	0.549	0.530	0.403	0.392	597	1067	35.8	5.4
5.3	8.85	0.5175	105.12	117.63	161.93	0.549	0.496	0.457	0.405	406	787	14.9	1.5
5.4	9.83	0.7029	105.12	117.81	161.91	0.534	0.513	0.458	0.403	337	749	22.2	2.4
5.5	9.68	0.7266	105.82	117.81	161.92	0.553	0.517	0.429	0.402	312	725	22.6	2.4
5.6	8.76	0.6190	99.60	117.96	161.87	0.549	0.506	0.418	0.397	636	998	34.8	2.9
5.7	10.67	0.7115	99.60	117.81	161.93	0.500	0.507	0.376	0.404	686	736	34.2	2.4
5.8	10.63	0.9235	99.07	117.71	161.94	0.512	0.542	0.402	0.408	570	523	30.2	2.1
5.9	8.70	0.4970	106.11	116.95	161.88	0.521	0.515	0.446	0.427	335	336	19.3	0.4
5.10	9.62	0.5746	106.11	117.03	161.90	0.546	0.519	0.434	0.425	302	340	23.0	0.5
5.11	9.55	0.5603	106.50	117.04	161.93	0.540	0.517	0.432	0.425	301	346	24.1	0.5
5.12	18.95	1.0141	105.14	116.70	161.99	0.484	0.521	0.434	0.439	309	236	28.1	1.1
5.13	19.69	0.7970	105.14	116.76	161.93	0.508	0.500	0.432	0.437	359	301	34.3	1.1
5.14	15.34	0.5603	105.14	116.14	161.93	0.514	0.503	0.443	0.448	357	264	25.5	0.5
5.15	16.61	0.8659	104.48	116.92	161.92	0.545	0.513	0.445	0.433	355	286	28.8	1.0
5.16	17.43	1.1923	102.35	117.41	161.92	0.499	0.527	0.400	0.422	412	323	30.3	2.0
5.17	14.65	0.8678	100.56	117.75	161.97	0.499	0.501	0.393	0.411	641	565	31.9	2.6
5.18	14.49	0.7643	101.38	117.57	160.40	0.510	0.489	0.413	0.407	679	701	32.2	2.9
* set at measured values													

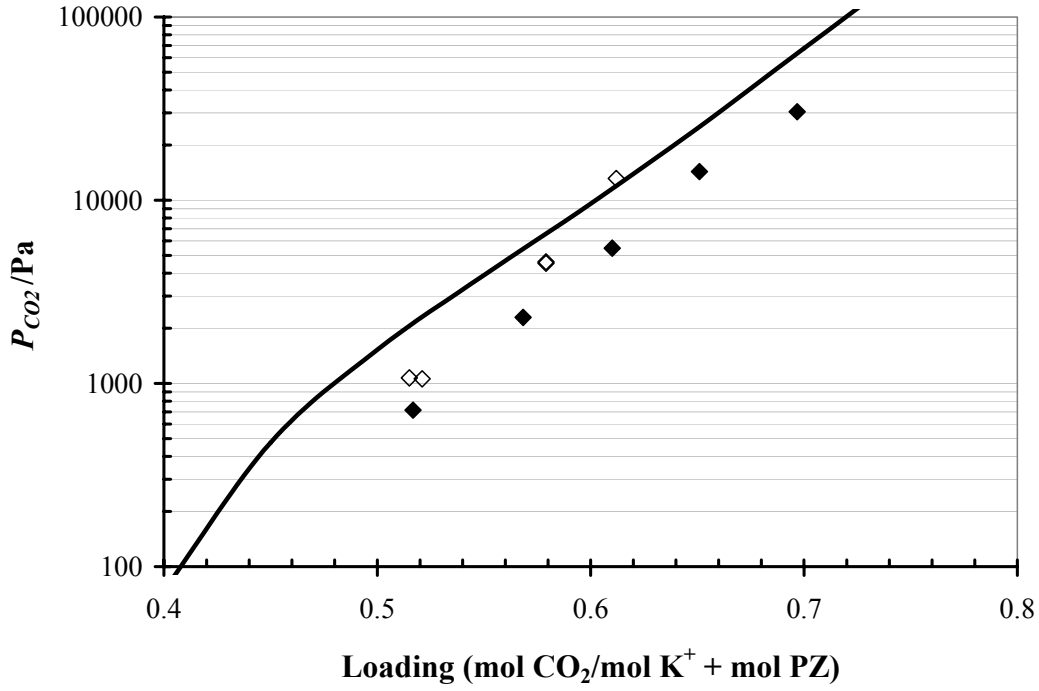

Figure 5-7: Comparison of the solubility of CO_2 in 5 m K^+/2.5 m PZ system at 100 ^oC: ♦, experimental data; ◊, Cullinane and Rochelle (Cullinane and Rochelle 2004); line, Hilliard (Hilliard 2005).

5.5.1. Capacity for 5m K^+/2.5m PZ. Figure 5-8 shows the parity plot for the measured capacity and that obtained from the ACM model. The operating capacity is defined as

$$\text{capacity}\left(\frac{\text{mol}\,CO_2}{\text{mol}\,\text{Alk}}\right) = \left(\gamma_{\text{rich}} - \gamma_{\text{lean}}\right) \tag{5-8}$$

Figure 5-8 shows the ACM capacity is slightly lower than the measured capacities. The differences in the capacity could be as a result of errors associated with the sample analyses. During analysis, the sample concentrations measured changed even between five minutes intervals on a given sample.

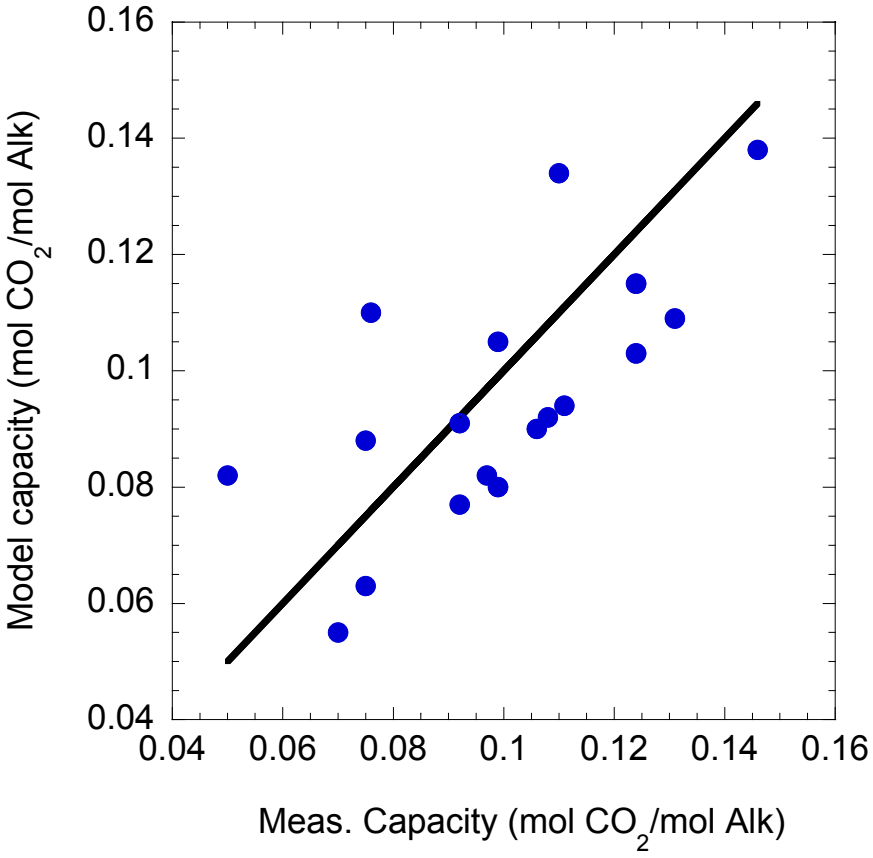

Figure 5-8:Material balance parity plot for 5m K^+/2.5m PZ pilot plant runs

5.5.2. Reboiler duty for 5m K^+/2.5m PZ. Figure 5-9 shows the parity plot for the measured and predicted reboiler duty. Figure 5-9 shows the ACM model predicts the general trend of the pilot plant data.

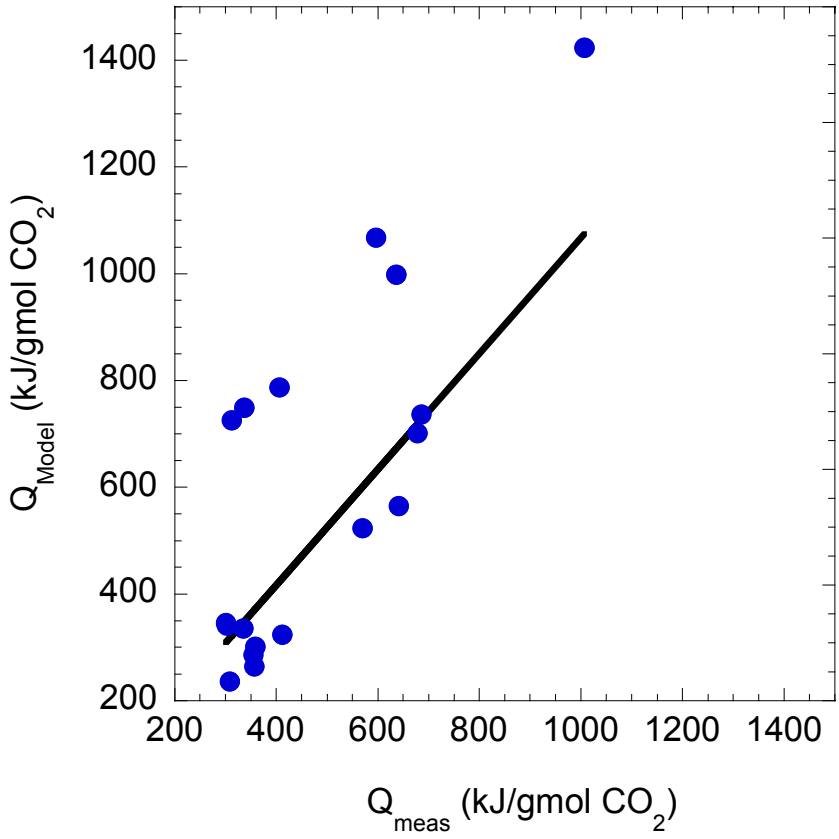

Figure 5-9: Comparison of reboiler duty for 5m K^+/2.5m PZ

5.5.3. Effect of liquid rate on reboiler duty for 5m K^+/2.5m PZ. Figure 5-10 shows the effect of liquid rate on the reboiler duty. The measured reboiler duty is systematically greater than the predicted duty.

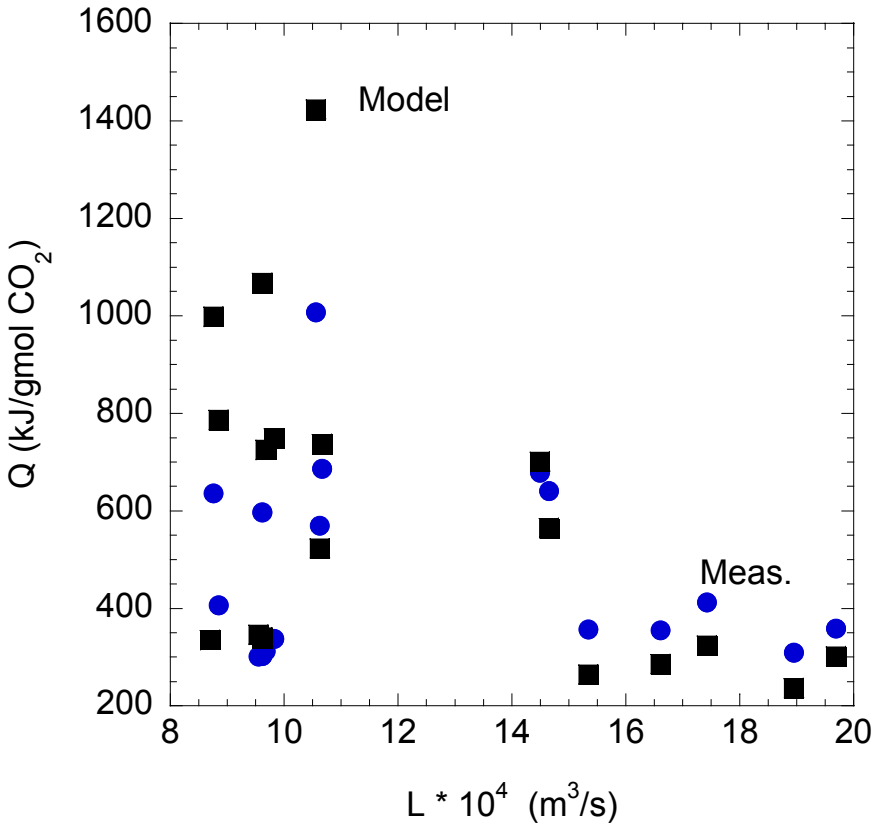

Figure 5-10: Effect of liquid rate on reboiler duty for 5m K^+/2.5m PZ

5.5.4. Effect of lean loading on reboiler duty for 5m K^+/2.5m PZ. Figure 5-11 shows the effect of the measured lean loading on the measured reboiler duty at a liquid rate of 9.62 x 10^{-4} m^3/s and a rich loading of 0.546 mol CO_2/mol Alk. The result shows that lowering the lean loading increases the reboiler duty. This is expected because in order to achieve a lower lean loading (more CO_2 in overhead stream), more heat will have to be supplied to the column.

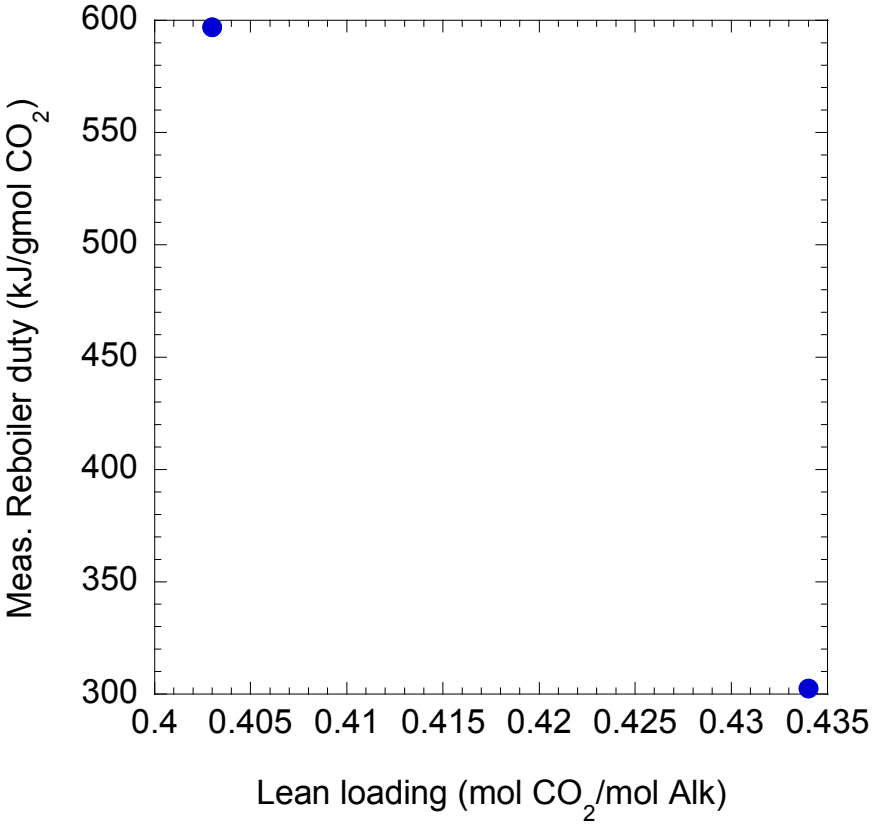

Figure 5-11: Effect of lean loading on reboiler duty on 5m K^+/2.5m PZ (Liquid rate = 9.62 x 10^{-4} m^3/s, rich loading of 0.546 mol CO_2/mol Alk)

5.5.5. Effect of pressure drop for 5m K^+/2.5m PZ. Figure 5-12 shows relative pressure drop as a function of the measured pressure drop for 5m K^+/2.5m PZ. The pressure drop calculated by the model ranges from 2-16% of that measured. The high pressure drop experienced during the tests could be as a result of severe foaming.

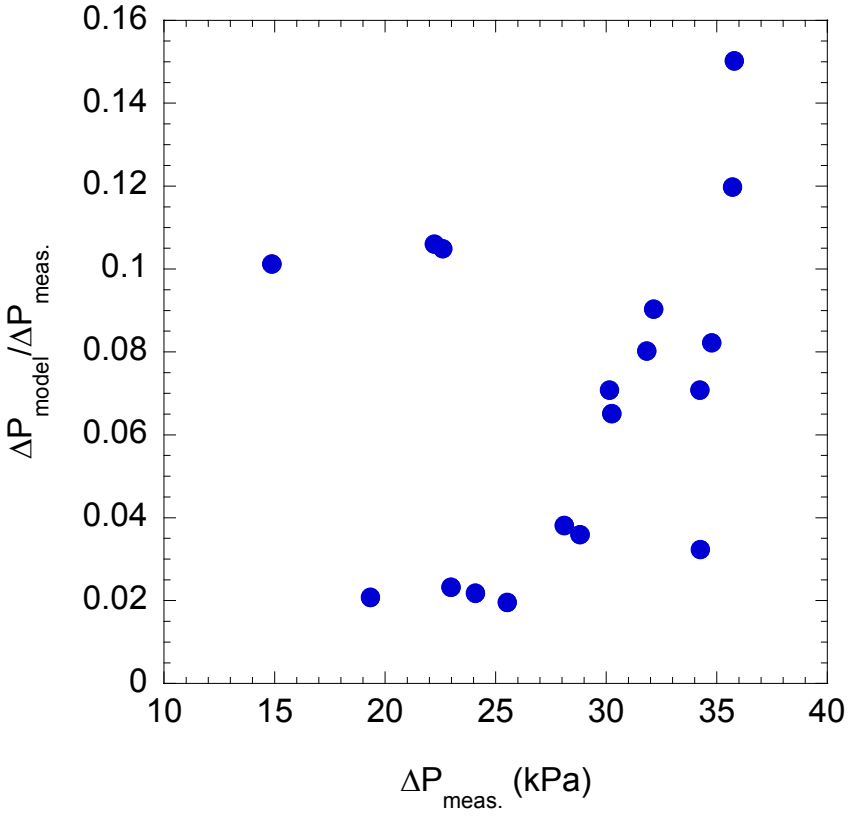

Figure 5-12: Effect of pressure drop for 5m K^+/2.5m PZ

5.5.6. Insight into stripper operation for 5m K^+/2.5m PZ. McCabe-Thiele plots are useful in understanding stripper operation. Figure 5-13 shows the stripper operation for run 5.13. The results show that the feed is subcooled. A well-defined driving force is observed along the stripper. Most of the CO_2 desorption occurs in the reboiler and in the top half of the column. The loadings for the five sections at the bottom of the column are close because in this region, there is very little change in the temperature over the five sections. The optimum condition in terms of energy from Chapter 2 was one with a rich

end pinch. Based on the model results, the stripper was operated far from its optimum condition in terms of energy requirement.

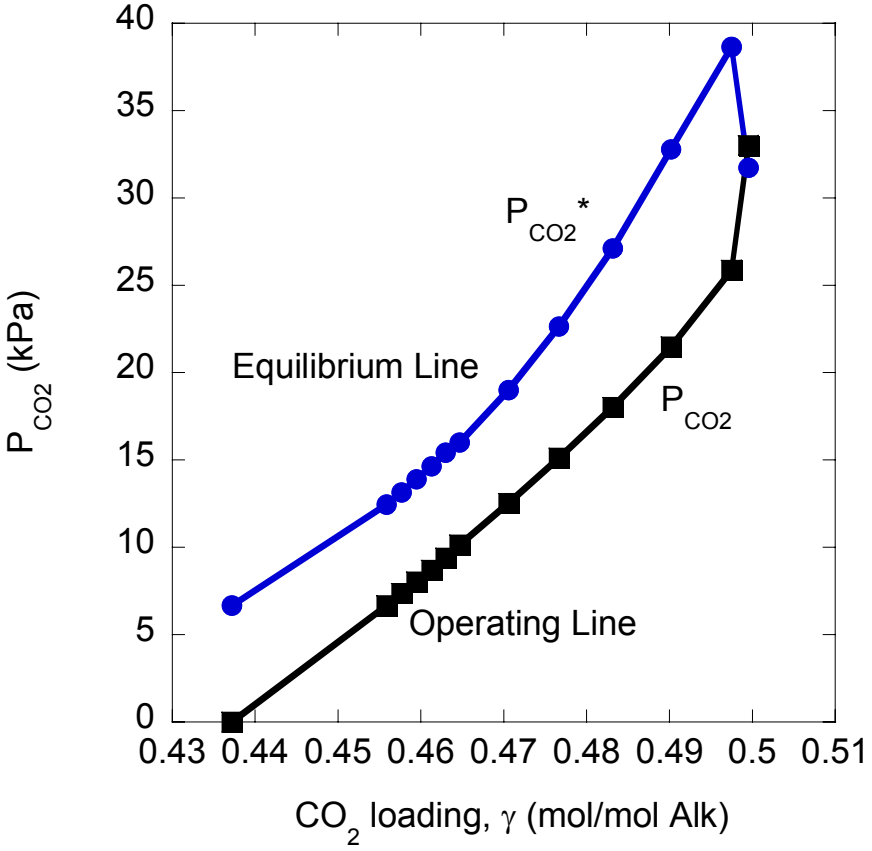

Figure 5-13: McCabe-Thiele plot for run 5-13 (Liquid rate = 19.69 x 10^{-4} m^3/s, rich loading = 0.500 mol CO_2/mol Alk, lean loading = 0.437 mol CO_2/mol Alk, ΔT= 11.62°C)

5.5.7. Temperature profile in stripper for 5m K^+/2.5m PZ. Figure 5-14 compares the measured and predicted temperature profiles in the column for run 5.13. The stripper feed and lean temperatures are fixed. The result shows that a large temperature difference is observed in the upper half of the column. This may be due to the model assumption that

the flash segment (near the stripper feed) operates just as any other segment in the column.

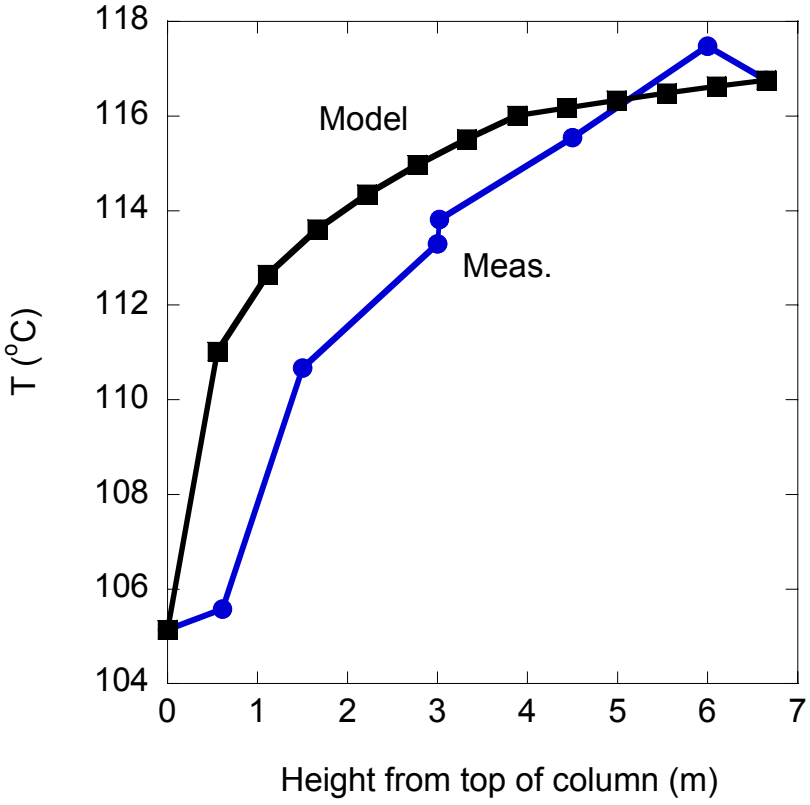

Figure 5-14: Temperature profile for run 5-13 (Liquid rate = 19.69 x 10^{-4} m^3/s, rich loading = 0.500 mol CO_2/mol Alk, lean loading = 0.437 mol CO_2/mol Alk, ΔT= 11.62°C)

5.5.8. Average stripper height for 5m K^+/2.5m PZ. In sections 5.5.1 through 5.5.7, the packing height is fixed and the reboiler duty is calculated. In this section, the reboiler duty is fixed at the measured value and the packing height is calculated. If the liquid rate, pressure at the top of the column, rich and lean solution temperatures, measured reboiler duty and CO_2 flow are fixed; rich and lean loadings and a packing height can be

calculated. Table 5-8 shows the effective packing height for runs 5-1 to 5-18. The actual packing height was 6.1m. For 5m K^+/2.5m PZ, the average packing height was calculated from the predicted heights for run 5-7 and runs 5-9 to 5-18. Runs 5-1 through 5-6 and 5-8 were neglected because they experienced severe foaming and were at the beginning of the campaigns when stable operation was yet to be achieved. The average effective packing height is 5.09m.

Table 5-8:Effective packing height for 5m K^+/2.5m PZ runs

Run Number	Effective packing height (m)
5-1	10.7
5-2	15.4
5-3	21.2
5-4	24.8
5-5	29.0
5-6	12.7
5-7	6.84
5-8	13.0
5-9	6.14
5-10	8.17
5-11	8.55
5-12	2.66
5-13	3.24

5-14	1.69
5-15	3.42
5-16	3.88
5-17	4.92
5-18	6.46

5.6. Results and discussion – pilot plant data for 6.4m K^+/1.6m PZ

Detailed pilot plant results for 6.4m K^+/1.6m PZ are shown in Table 5-9. The pilot plant and predicted model variables for 6.4m K^+/1.6m PZ are shown in Table 5-10. The 6.4m K^+/1.6m PZ runs were carried out under vacuum. At low temperature (vacuum conditions), the equilibrium data of Cullinane (Cullinane 2005) and Hilliard (Hilliard 2005) agree reasonably well. As such in running the ACM model, the equilibrium partial pressure for 6.4m K^+/1.6m PZ was not adjusted as 5m K^+/2.5m PZ cases.

5.6.1. Capacity for 6.4m K^+/1.6m PZ. Figure 5-15 shows the parity plot for the measured capacity and that obtained from the ACM model. Figure 5-15 shows the ACM capacity is slightly higher than the measured capacities. The differences in the capacity could be as a result of errors associated with the liquid sample analyses.

Table 5-9: Pilot plant stripper results for 6.4m K^+/1.6m PZ

Run Number	STRIPPER FEED			STRIPPER BOTTOMS			STRIPPER REFLUX						STRIPPER BED TEMPERATURES		
	STR Return FT200	STR Return FT200	STR Return FT200	STR Return FT201	STR Return FT201	STR Return FT201	STR Return FT203	STR Return FT203	STR Return FT203	STR Return FT204	STR Return FT204	STR Return FT204	Top Temp T20710	Top Mid Temp T2078	Top Bot Temp T2076
	(gpm)	(F)	(lb/ft^3)	(gpm)	(F)	(lb/ft^3)	(gpm)	(F)	(lb/ft^3)	(gpm)	(F)	(lb/ft^3)	(F)	(F)	(F)
5.19	23.43	110.25	79.57	22.91	100.87	79.50	1.25	92.43	62.67	0.06	90.97	63.07	160.82	163.34	165.48
5.20	26.61	112.72	78.95	26.00	103.85	78.99	1.65	95.94	63.88	0.10	93.53	64.39	164.32	168.08	170.16
5.21	15.56	110.91	79.39	14.69	97.96	79.39	0.63	95.09	61.68	0.09	94.98	62.06	161.53	162.74	166.74
5.22	15.54	113.53	79.51	15.08	100.79	79.51	1.43	97.28	61.66	0.05	95.29	62.11	165.77	167.46	168.47
5.23	22.10	113.22	79.46	21.91	103.65	79.36	1.78	98.34	63.34	0.05	95.81	63.63	166.62	171.23	173.24
5.24	17.66	111.96	79.02	17.08	106.48	79.03	2.28	102.53	65.16	0.07	99.23	65.77	165.34	170.10	171.36
5.25	21.56	113.52	78.99	21.12	101.93	78.91	1.92	108.42	61.62	0.05	107.04	62.14	181.87	185.54	187.03
5.26	18.64	113.76	79.10	18.20	103.89	79.00	1.67	104.57	61.61	0.07	102.18	62.14	181.82	184.27	185.50
5.27	15.56	112.29	78.90	15.13	101.45	78.81	1.24	101.11	61.63	0.08	97.73	62.14	180.97	182.24	184.49
5.28	15.57	115.50	79.22	15.22	104.28	79.13	2.08	107.63	62.27	0.08	104.35	62.85	181.33	185.37	186.61
5.29	18.57	115.17	79.07	18.06	105.70	78.97	2.21	111.95	61.46	0.08	106.86	62.12	200.37	202.93	204.76
5.30	21.78	116.58	78.95	21.03	107.80	78.88	1.90	107.80	61.53	0.14	105.66	62.08	199.30	201.90	204.10
5.31	18.68	118.18	79.12	18.16	111.94	78.99	1.47	103.10	61.60	0.18	100.89	62.12	198.55	201.11	203.23

Table 5-9: Pilot plant stripper results for 6.4m K^+/1.6m PZ (Contd.)

Run Number	STRIPPER BED TEMPERATURE			STRIPPER PRESSURE			STRIPPER LEVELS			COOLING WATER				
	Bot Top Temp T2075	Bot Mid Temp T2073	Bot Temp T2071	Column P PC215	PrsDrp (low) PDT250	PrsDrp (high) PDT251	Column Level LT206	Acc Level LT203	Reboiler Level LT204	OHD Vapor TT216	Cond Liq T225	CW Inlet T224	CW Outlet T226	CW Flow FT205
	(F)	(F)	(F)	(psia)	(in H_2O)	(in H_2O)	(in)	(in)	(in)	(F)	(F)	(F)	(F)	(gpm)
5.19	166.15	169.40	171.73	5.16	5.76	6.43	12.03	6.08	8.21	158.09	84.90	48.57	56.05	217.29
5.20	170.22	172.61	174.82	5.07	5.96	20.96	17.01	5.60	13.63	162.18	96.63	52.31	61.83	215.83
5.21	166.62	165.73	169.38	5.09	3.32	3.34	16.91	5.86	12.15	157.07	57.55	48.41	52.61	215.05
5.22	168.87	167.30	171.16	5.13	5.96	6.48	16.98	6.23	13.48	161.95	87.72	50.91	59.70	216.00
5.23	173.38	175.84	178.04	5.42	5.96	23.16	16.82	6.34	15.13	164.86	98.87	51.89	61.77	216.06
5.24	171.11	170.32	174.99	5.20	5.96	18.35	16.00	5.89	14.20	163.62	104.94	53.08	64.36	220.23
5.25	187.25	188.08	190.29	7.50	5.96	19.54	16.00	5.42	13.49	179.34	104.83	53.68	65.23	215.41
5.26	186.06	184.46	188.32	7.50	5.96	10.96	16.01	6.08	12.93	178.72	97.16	51.95	61.75	218.03
5.27	184.82	183.57	186.89	7.49	5.96	6.50	16.00	6.00	12.87	176.78	89.11	50.13	57.66	217.38
5.28	186.72	184.56	189.06	7.50	5.96	15.30	16.01	5.99	14.05	179.59	106.85	53.45	65.39	218.16
5.29	204.86	203.67	207.03	10.99	5.96	16.18	15.99	5.80	13.84	197.11	115.99	54.47	67.43	218.49
5.30	204.43	203.89	206.94	11.00	5.96	17.67	16.00	6.25	13.62	195.72	112.36	53.85	65.50	218.07
5.31	203.74	200.95	205.76	11.00	5.96	9.30	16.05	6.09	13.55	194.48	102.59	51.76	61.03	219.86

Table 5-9: Pilot plant stripper results for 6.4m K^+/1.6m PZ (Contd.)

Run Number	STEAM FLOW							CROSS EXCHANGER AND STRIPPER FEED						
	Reboiler duty QIC202	Steam Flow FC202	Steam Temp T202	Cond Ret T203	Steam Annubar Pressure	Bot Liq to Reb T209	Vapor Inlet T208	Bot Prod TT 215	Bot Prod TT 212	Feed Inlet TT200	Feed Outlet TT217	Trim Temp TT210	Str feed TT211	CO_2 flow
	(MMBTU/hr)	(lb/hr)	(F)	(F)	(psia)	(F)	(F)	(F)	(F)	(F)	(F)	(F)	(F)	(scfm)
5.19	1.07	1015.8	343.25	172.81	131.43	170.16	171.63	170.59	116.19	110.25	162.79	163.07	162.46	33.34
5.20	1.39	1307.2	338.63	165.99	123.38	173.06	175.53	173.86	118.96	112.72	165.48	165.47	164.61	35.49
5.21	0.64	600.56	342.23	168.99	127.91	167.82	168.66	168.09	115.00	110.91	160.94	161.00	160.00	20.30
5.22	1.17	1103.3	343.84	166.78	131.29	170.06	172.20	171.08	118.30	113.53	164.34	164.28	163.33	31.65
5.23	1.40	1320.8	342.50	172.31	129.35	176.53	178.87	177.54	119.67	113.22	168.50	168.49	167.49	39.94
5.24	1.58	1493.8	338.07	167.69	122.66	173.08	175.75	174.45	117.06	111.96	166.47	165.93	164.31	34.23
5.25	1.53	1481.3	338.42	191.76	122.43	188.93	191.17	189.60	121.04	113.52	179.96	180.11	179.29	36.81
5.26	1.35	1306.0	339.16	195.01	123.75	186.86	189.02	187.46	120.79	113.76	178.37	178.37	177.60	33.08
5.27	1.07	1026.8	342.24	184.51	128.48	185.43	187.25	185.85	118.62	112.29	177.06	176.85	175.84	28.46
5.28	1.57	1520.6	336.82	191.27	120.75	187.64	190.01	188.81	122.01	115.50	180.20	179.83	178.62	34.29
5.29	1.80	1785.6	336.66	216.69	120.73	205.31	207.64	206.16	123.72	115.17	194.82	194.38	192.92	36.91
5.30	1.68	1665.4	336.60	214.74	119.98	205.20	207.07	205.89	125.31	116.58	194.20	193.93	192.69	41.81
5.31	1.39	1374.0	336.90	215.00	120.89	204.25	206.32	204.82	126.27	118.18	193.82	193.36	192.14	40.54

Table 5-10: Measured and predicted variables for 6.4m K^+/1.6m PZ

Run Number	Liquid rate*	CO_2 rate*	Temperature*		Top Pressure*	Rich loading		Lean loading		Reboiler Duty		Pressure Drop	
	($x10^4$) m^3/s	gmol/s	°C		kPa	mol CO_2/mol Alk				kJ/gmol CO_2		kPa	
			Feed	Lean		Meas.	Model	Meas.	Model	Meas.	Model	Meas.	Model
5.19	15.52	0.6450	69.42	76.75	35.6	0.550	0.592	0.520	0.530	431	398	20.94	2.90
5.20	17.79	0.6626	70.52	78.37	34.96	0.550	0.575	0.500	0.519	522	575	46.22	5.39
5.21	17.03	0.4432	70.25	75.45	35.08	0.620	0.573	0.560	0.534	388	389	11.44	1.74
5.22	10.60	0.6145	68.59	76.70	35.34	0.560	0.608	0.500	0.520	480	428	21.36	2.52
5.23	10.98	0.7631	69.62	80.30	37.35	0.570	0.612	0.470	0.507	496	622	49.99	5.81
5.24	11.36	0.6734	67.87	78.38	35.84	0.540	0.602	0.510	0.512	671	554	41.75	4.27
5.25	15.14	0.6975	77.34	87.19	51.7	0.560	0.581	0.490	0.511	559	644	43.79	5.04
5.26	12.11	0.6683	75.75	86.03	51.68	0.560	0.599	0.490	0.515	554	501	29.06	2.99
5.27	14.38	0.5817	76.87	85.24	51.66	0.570	0.586	0.490	0.525	486	429	21.39	2.11
5.28	14.76	0.6577	76.87	86.46	51.68	0.550	0.583	0.470	0.515	617	572	36.51	3.86
5.29	13.25	0.7032	83.03	96.28	75.79	0.550	0.587	0.460	0.506	647	656	38.02	3.89
5.30	12.87	0.8285	83.26	96.22	75.82	0.570	0.608	0.470	0.509	540	563	40.58	3.90
5.31	10.60	0.8030	83.26	95.70	75.86	0.570	0.629	0.480	0.512	459	440	26.20	2.37
* set at measured values													

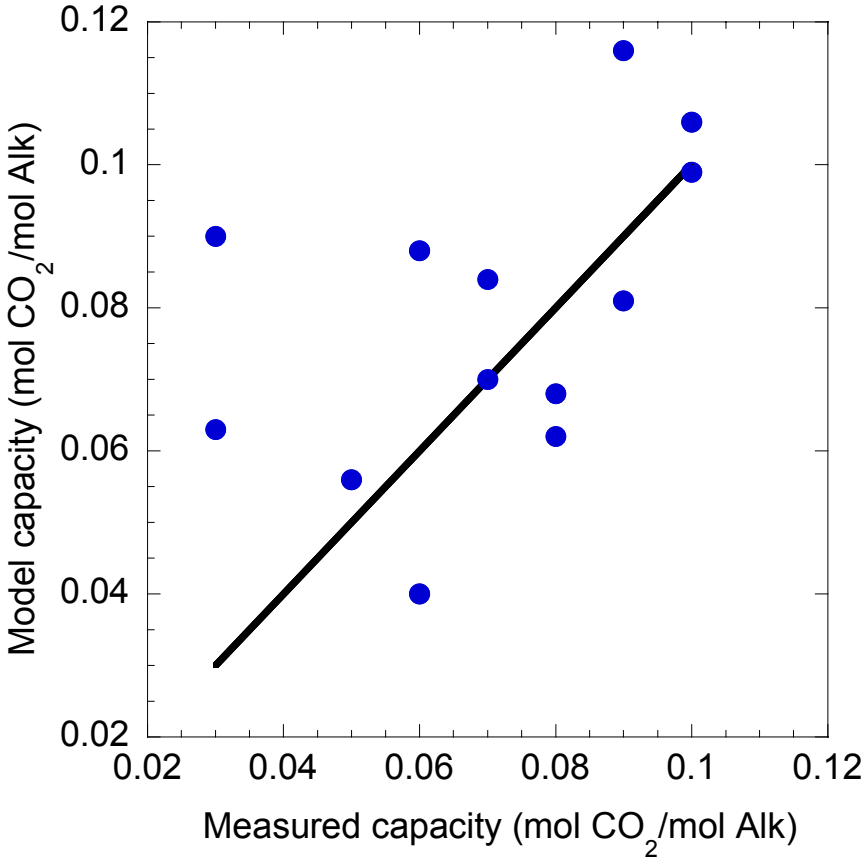

Figure 5-15 Material balance parity plot for 6.4m K^+/1.6m PZ pilot plant runs

5.6.2. Reboiler duty for 6.4m K^+/1.6m PZ. Figure 5-16 shows the parity plot for the measured and predicted reboiler duty. Figure 5-16 shows the ACM model predicts the general trend of the pilot plant data.

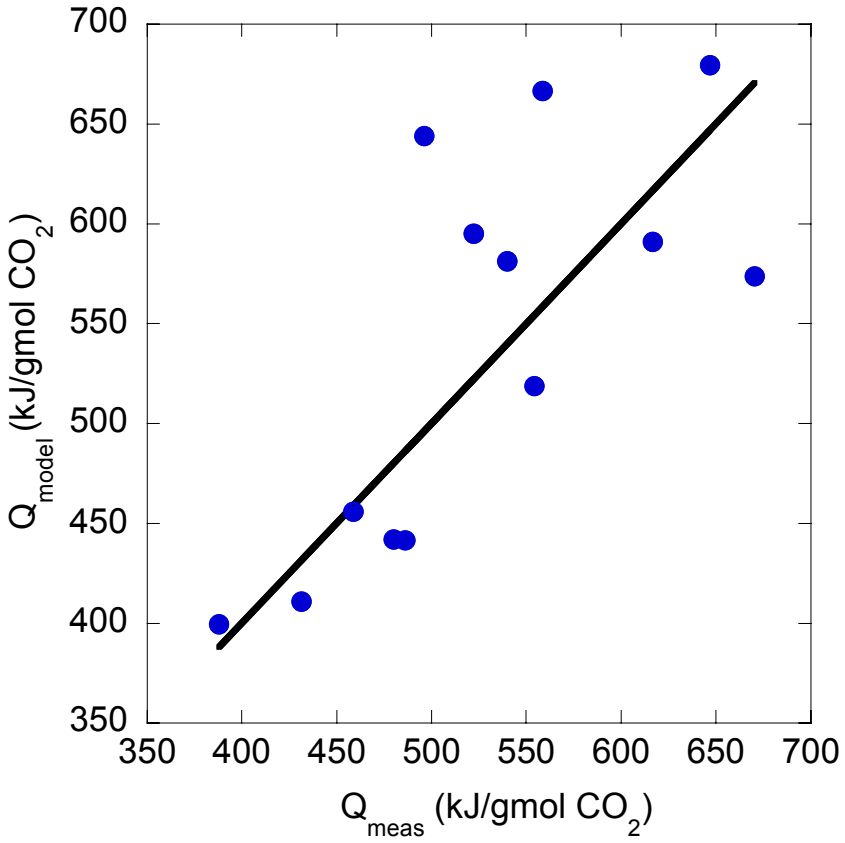

Figure 5-16: Comparison of reboiler duty for 6.4m K^+/1.6m PZ

5.6.3. Effect of liquid rate on reboiler duty for 6.4m K^+/1.6m PZ. Figure 5-17 shows the effect of liquid rate on the reboiler duty. The measured reboiler duty is systematically greater than the predicted duty.

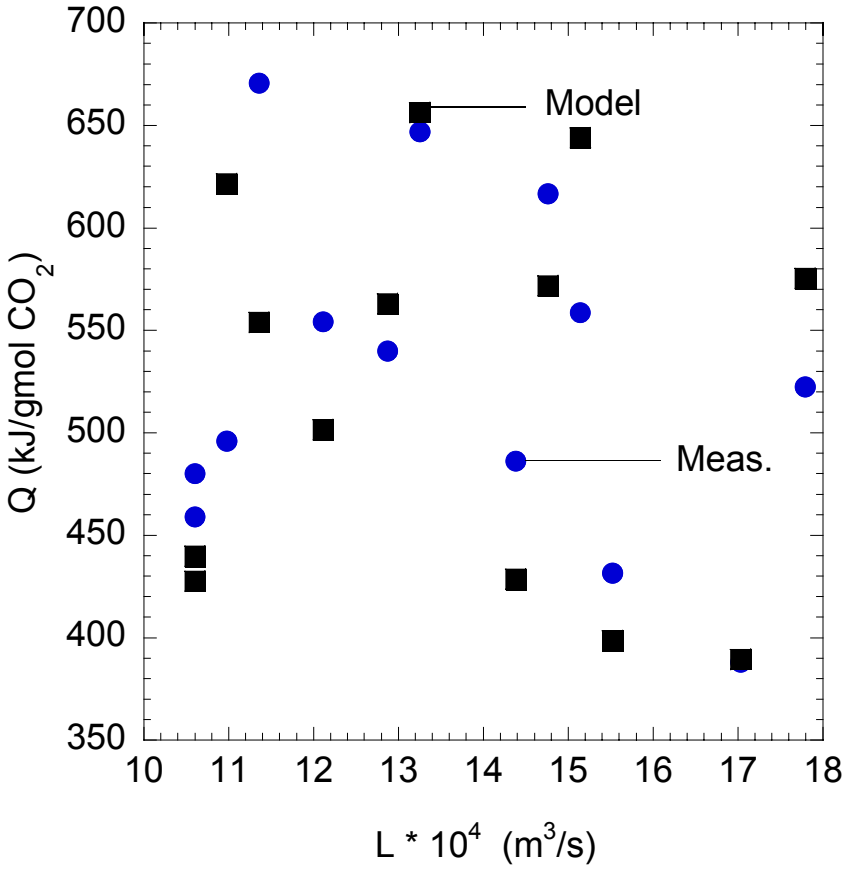

Figure 5-17: Effect of liquid rate on reboiler duty for 6.4m K^+/1.6m PZ

5.6.4. Effect of pressure drop for 6.4m K^+/1.6m PZ. Figure 5-18 shows relative pressure drop as a function of the top pressure of the column. The pressure drop is correlated with the operating pressure of the column. Greater operating pressure leads to lower percent drop in pressure across the column. This emphasizes the importance of pressure drop in vacuum operations.

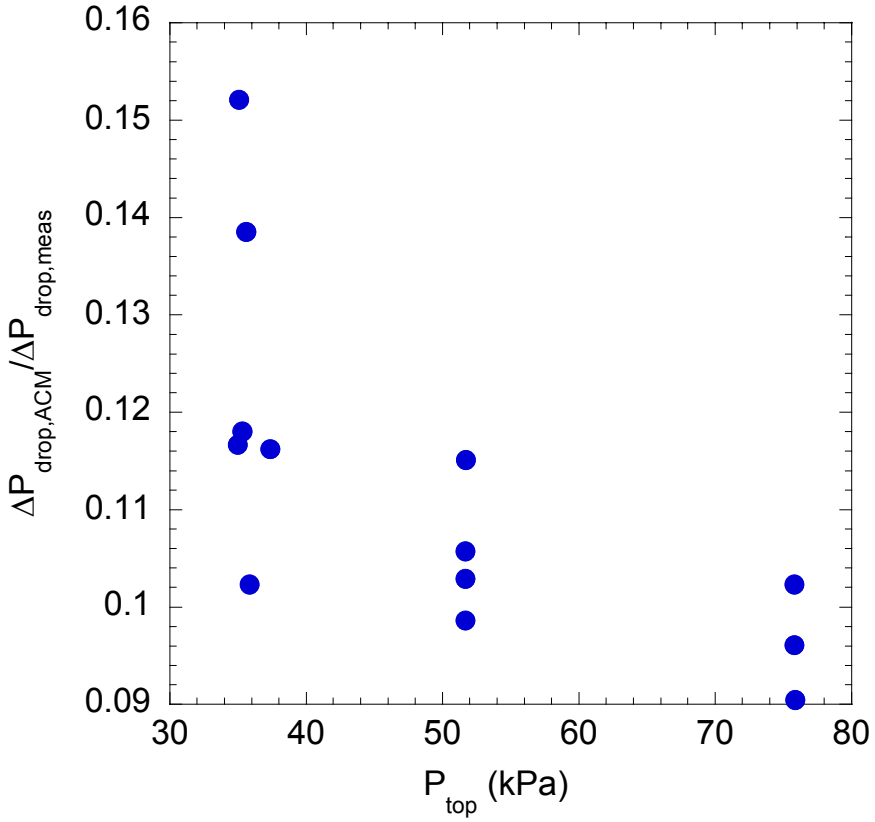

Figure 5-18: Effect of pressure drop for 6.4m K^+/1.6m PZ

5.6.5. Insight into stripper operation for 6.4m K^+/1.6m PZ. McCabe-Thiele plots are useful in understanding stripper operation. Figure 5-19 shows the stripper operation for run 5.25. The results show that the feed is subcooled. A well-defined driving force is observed along the stripper. Most of the CO_2 desorption occurs in the reboiler. The loadings for the five sections in the upper half of the column are close because in this region, there is very little wetted area and corresponding mass transfer taking place. The optimum condition in terms of energy from Chapter 2 was one with a rich end pinch.

Based on the model results, the stripper was operated far from its optimum condition in terms of energy requirement.

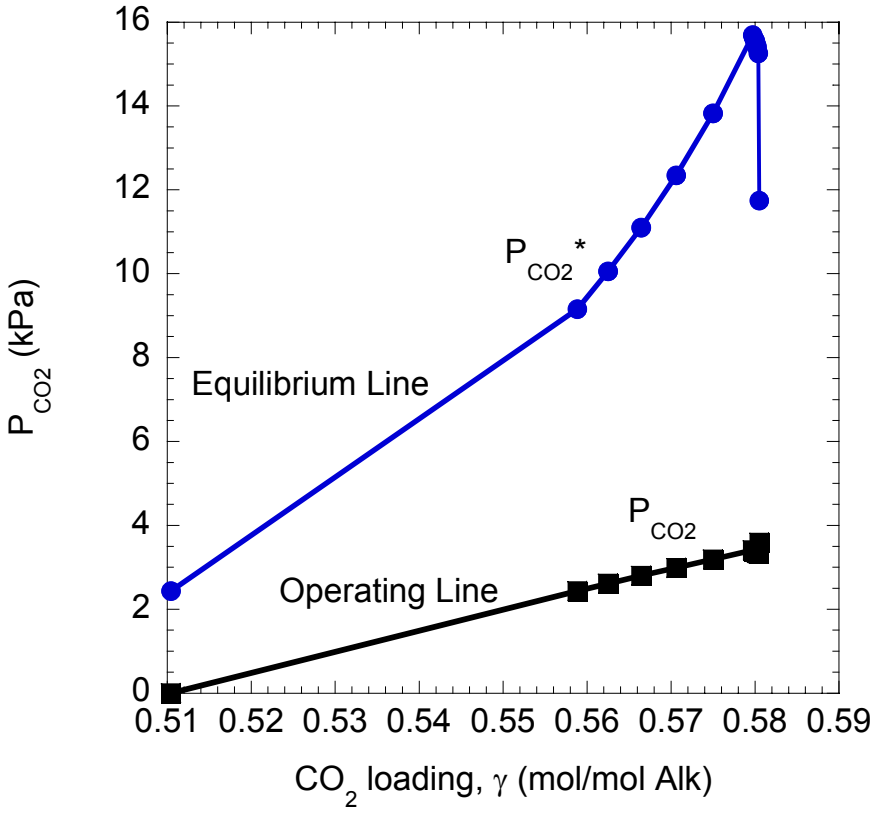

Figure 5-19: McCabe-Thiele plot for run 5-25 (Liquid rate = 15.14 x 10^{-4} m^3/s, rich loading = 0.581 mol CO_2/mol Alk, lean loading = 0.511 mol CO_2/mol Alk, ΔT= 9.8°C)

5.6.6. Temperature profile in stripper for 6.4m K^+/1.6m PZ. Figure 5-20 compares the measured and predicted temperature profiles in the column for run 5.25. The stripper feed and lean temperatures are fixed. The result shows that a difference of 1°C is observed

between the predicted and measured temperatures. The model predicts the trend of the temperature profile fairly well.

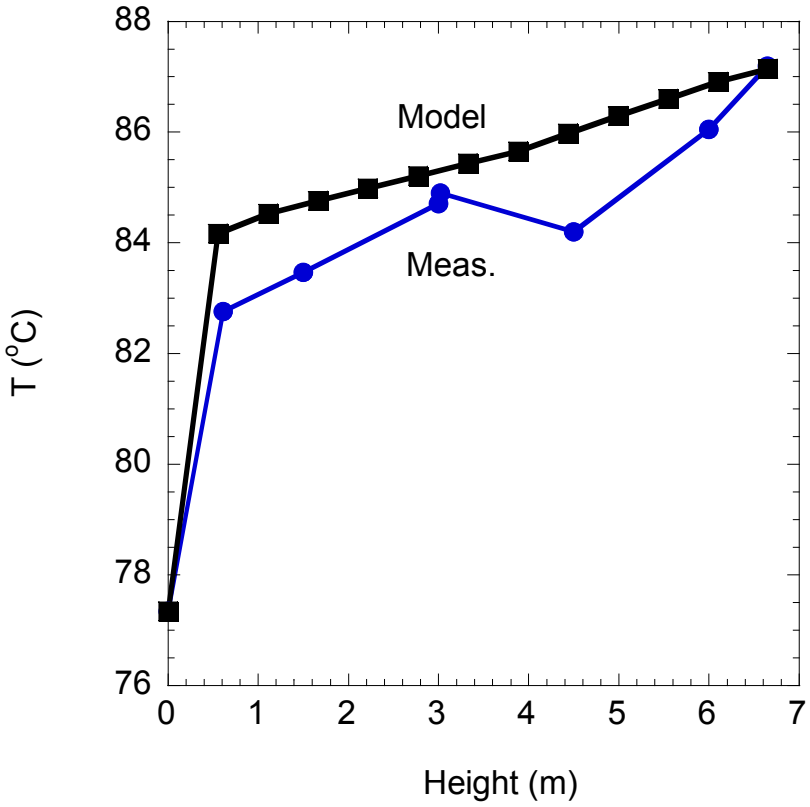

Figure 5-20: Temperature profile for run 5-25 (Liquid rate = 15.14 x 10^{-4} m^3/s, rich loading = 0.581 mol CO_2/mol Alk, lean loading = 0.511 mol CO_2/mol Alk, ΔT= 9.8°C)

5.6.7. Average stripper height for 6.4m K^+/1.6m PZ. If the liquid rate, pressure at the top of the column, rich and lean solution temperatures, measured reboiler duty and CO_2 flow are fixed; rich and lean loadings and a packing height can be calculated. shows the effective packing height for runs 5-19 to 5-31. The actual packing height was fixed at 6.1m. For 6.4m K^+/1.6m PZ, all the packing heights calculated with runs 5-19 through 5-

31 were included in the average packing height calculation. The average effective packing height is 6.47m.

Table 5-11: Effective packing height for 6.4m K^+/1.6m PZ

Run Number	Effective packing height (m)
5-19	5.53
5-20	7.67
5-21	6.10
5-22	5.24
5-23	9.41
5-24	4.64
5-25	8.27
5-26	5.34
5-27	3.76
5-28	8.62
5-29	6.64
5-30	6.91
5-31	6.03

5.7. Conclusions

1. In order to match the model to the measured data, the wetted area in the top half of the column was adjusted to 10% of the dry specific packing area while the lower half was set at 70% of the dry specific packing area. The effective packing height was 5.09m for 5m K^+/2.5m PZ and 6.47m for 6.4m K^+/1.6m PZ.
2. Foaming was experienced in the stripper during these tests. The high pressure drop experienced was an indication of foaming. This foaming could be due to the presence of residual hexane from other tests in the stripping column prior to the CO_2 capture (McLees 2006).
3. The heavily adjusted ACM Model predicts the general trend of the pilot plant data. Even though differences existed between the absolute rich and lean loadings, the measured and predicted capacities seemed to close to a reasonable extent.
4. The pilot plant test conditions were far from the optimum.

Chapter 6 : Conclusions and recommendations

This chapter summarizes the conclusions from this work and presents recommendations for future work.

6.1. Equilibrium modeling conclusions

1. Operating the cross exchanger at a 5^{o}C approach instead of a 10^{o}C approach can reduce the equivalent work of the baseline configuration by 12%.
2. At a fixed capacity, solvents with high heats of absorption require less energy for stripping. 5m K^{+}/2.5m PZ offers 18% over 6.4m K^{+}/1.6m PZ at 160 kPa with a 5^{o}C approach and savings of 3% and 4% with the matrix and internal exchange configurations at stripper conditions. The savings experienced with 5m K^{+}/2.5m PZ at 160 kPa are because of the temperature swing desorption. At vacuum conditions this effect disappears and the performance of the solvents are equal.

3. Vacuum operation favors solvents with heats of desorption approximately equal to the heat of vaporization of water while operation at normal pressure favors solvents with high heats of desorption. This is because solvents with a high heat of desorption take advantage of the temperature swing.
4. MEA/PZ and MDEA/PZ are alternatives to 7m MEA that can reduce total equivalent work by at least 10% for all configurations and operating conditions studied.
5. The performance of the alternative configurations is matrix > internal exchange > multipressure with split feed > flashing feed. The matrix, internal exchange, multipressure with split feed and flashing feed offer 15%, 13%, 13% and 11% energy savings over the improved baseline with stripping and compression to 10 MPa.
6. Less energy is required with high capacity solvents with equivalent heat of absorption. 5m K^+/2.5m PZ and MDEA/PZ have similar heats of absorption. MDEA/PZ has about twice the capacity for CO_2 as 5m K^+/2.5m PZ. MDEA/PZ provides 30% and 19% energy savings over 5m K^+/2.5m PZ with the matrix and internal exchange configurations with the reboiler operating at 160 kPa and 17% and 12% savings with these configurations at 30 kPa.
7. The typical predicted energy requirement for stripping and compression to 10 MPa (30 kJ/gmol CO_2) is about 20% of the power output from a 500 MW

power plant with 90% CO_2 removal. This does not include power for pumping, the flue gas fan and other auxiliaries.

8. The best solvent and process configuration in this study, matrix (295/160) using MDEA/PZ, offers 22% energy savings over the baseline and 15% savings over the improved baseline with stripping and compression to 10 MPa.
9. The best solvent and process configuration requires 26 kJ/gmol CO_2 compared to 24.1 kJ/gmol CO_2 for isothermal separation and real compression to 10 MPa. This means that there is little room for improvement. MDEA/PZ with the matrix configuration is 67% efficient when compared with the minimum thermodynamic work requirement of 18.1 kJ/gmol CO_2.

6.2. Rate modeling conclusions

1. A 'short and fat' column requires 7 to 15% less equivalent work than a 'tall and skinny' one because it has a lower pressure drop and less temperature change. This is especially evident in the vacuum stripper.
2. The optimum stripper design could be one that operates between 50% and 80% flood at the bottom. This optimal design will have to be determined by an economic analysis of the attractive options.
3. The vacuum stripper requires 230 s of effective packing volume to get an equivalent work 4% greater than the minimum work. This is a packing height of 7 meters with 50% flood. Because kinetics do not limit stripping at 160 kPa, only

115 s is required to get within 4% of the equivalent work, giving a packing height of 6.5m.

4. The stripping operation is liquid phase controlled. Kinetics is the dominant mechanism for mass transfer in the vacuum stripper while diffusion of reactants and products is the controlling mechanism at 160 kPa.
5. The typical predicted energy requirement for stripping and compression to 10 MPa to achieve 90% removal from 5m K^+/2.5m PZ with a rich loading of 0.56 mol CO_2/ mol Alk is about 37 kJ/gmol CO_2. This is about 25% of the net power output of a typical power plant with 90% CO_2 removal. This includes pumping power but not the flue gas fan and other auxiliaries. This is 3.3 kJ/gmol CO_2 greater than the corresponding equilibrium work prediction. The total equivalent work for the rate prediction is 10% more than the equilibrium prediction.
6. At 30 kPa, operating the cross exchanger with a 5^oC approach rather than 10^oC offers 1.4% and 3% energy savings at 80% and 30% approach to flood. The pressure and temperature drops across the column are not significantly different.
7. At 160 kPa, the energy savings in operating the cross exchanger with a 5^oC approach is 7-9% compared to a 10^oC approach. The increased savings can be attributed to a lower temperature drop across the column which results in reduced sensible heat requirements.

6.3. Pilot plant test conclusions

1. In order to match the model to the measured data, the wetted area in the top half of the column was adjusted to 10% of the dry specific packing area while the lower half was set at 70% of the dry specific packing area. The effective packing height was 5.09m for 5m K^+/2.5m PZ and 6.47m for 6.4m K^+/1.6m PZ.
2. Foaming was experienced in the stripper during these tests. The high pressure drop experienced was an indication of foaming. This foaming could be due to the presence of residual hexane from other tests in the stripping column prior to the CO_2 capture.
3. The ACM model predicts the general trend of the pilot plant data. Even though differences existed between the absolute rich and lean loadings, the measured and predicted capacities seemed to close to a reasonable extent.
4. The pilot plant test conditions were far from the optimum.

6.4. Recommendations for future work

1. More thermodynamic and rate data should be collected on the bench and pilot scales with MEA/PZ and 4m K^+/4m PZ at stripper conditions. This will provide enough data for more comprehensive process models.
2. Tests should be performed to understand the flashing and reboiler operation to better understand these processes. The results will relax the assumptions in this work concerning flashing and reboiler mass transfer and improve model predictability.

3. Foaming should be significantly reduced or eliminated. Possible causes of foaming in the pilot tests could be the presence of residual hexane and/or degradation products from prior tests. This may have impacted the stripper performance adversely. Adequate cleaning of the column and removal of possible degradation products from the process loop could help reduce foaming.
4. If foaming occurs and antifoam is added, sufficient time should be allowed for steady state to be reached before samples are withdrawn for analysis. This will ensure agreement between duplicate experimental conditions.
5. Better liquid distributor designs that can accommodate two-phase flow in the receiver should be developed. The presence of flashing liquid in the distributor receiver may have lead to entrainment problems. A mist eliminator could be incorporated in the design of the distributor at the top of the stripper.
6. More accurate/consistent methods of quantitative analysis of solution loadings should be developed. This will improve data integrity and aid better model predictability.
7. Temperature and pressure measurements could be used as on-line indicators of liquid composition.
8. Heat loss experiments could be performed so that a reliable heat loss model could be incorporated into the process model.
9. Rate models based on 4m K^+/4m PZ solvents with the double matrix configurations should be carried out.

10. The ACM model should be converted to an Aspen Plus block so that it can be used in the Aspen Plus environment with other unit operations.

6.5. Contributions of this work

This research provides the following contributions to scientific knowledge:

1. Comparison of seven generic solvents for CO_2 absorption/stripping.
2. New stripper configurations (e.g. matrix, internal exchange, flashing feed, multipressure with split feed, and multipressure stripper) and the advantages of this over the conventional design were developed.
3. Rate models have been developed for K_2CO_3/PZ. This provides insight into mass transfer with chemical reaction at stripper conditions.
4. The stripper model developed has been used to verify pilot plant data for 5m K^+/2.5m PZ and 6.4m K^+/1.6m PZ using two packings IMTP #40 and Flexipac AQ Style 20. The model has the ability to model other packings (CMR #2, CMR #2A, Pall rings, IMTP #25, Montz B1-250, Montz B1-350).

Appendix A: Detailed equilibrium model

This appendix contains the detailed equilibrium model used for 7m MEA, MEA/PZ and K_2CO_3/PZ using the simple, vacuum and multipressure configurations. The model for the internal exchange, multipressure with split feed, and flashing feed are available from Dr. Gary Rochelle at the University of Texas at Austin.

```
Model Equilibrium model

// This is the equilibrium model for MEA, MEA/PZ and K PZ solvents
// This model can be used for the simple, vacuum and multipressure configurations

//declaration of variables

// Solvent refers to the different solvent types
Solvent as SolventType;

// ns is the number of segments into which the stripper is divided
// The last segment is the reboiler. The reboiler is assumed to be
// an equilibrium segment
ns as integerparameter(12);
// nsf refers to the segment from which the side stream is introduced
nsf as integerparameter(2);
```

```
// L is the liquid rate, mol/s
L([0:2*ns]) as realvariable;
// lco2,lh2o,lamine are the molar  rates in the liquid of
// co2,water and amine respectively, mol/s
lco2([0:2*ns]) as realvariable;
lh2o([0:2*ns]) as realvariable;
lamine([0:2*ns]) as realvariable;

// S is the liquid rate in the side stream, mol/s
S([0:ns-1]) as realvariable;
// lco2,lh2o,lamine are the molar  rates in the side liquid stream of
// co2,water and amine respectively, mol/s
sco2([0:ns-1]) as realvariable;
sh2o([0:ns-1]) as realvariable;
samine([0:ns-1]) as realvariable;


// ldg is the CO2 loading in the liquid
ldg([0:2*ns]) as realvariable;
// ldgin is the rich loading, mol CO2/mol Alk
ldgin as realvariable;
//ldgout is the lean loading, mol CO2/mol Alk
ldgout as realvariable;


// CpL  and CpS are the heat capacities of the liquid and side liquid streams, kcal/gmol-K
CpL([0:2*ns]) as realvariable;
CpS([0:ns-1]) as realvariable;


// G is the gas rate, mol/s
G([1:ns+1]) as realvariable;

// yco2 is the mole fraction of CO2 in the gas phase
yco2([1:ns+1]) as realvariable;
// yh2o is the mole fraction of CO2 in the gas phase
yh2o([1:ns+1]) as realvariable;

// Pco2e is the equilibrium partial pressure of CO2 in the liquid,kPa
Pco2e([0:2*ns]) as realvariable;
// Pco2 is the partial pressure of CO2 in the gas phase,kPa
```

```
Pco2([1:ns+1]) as realvariable;
// Ph2o is the partial pressure of CO2 in the gas phase,kPa
Ph2o([1:ns]) as realvariable;
// Total pressure on a segment, kPa
Pt([1:ns]) as realvariable(160,fixed);

//Murphree efficiency for CO2
// This is assumed to be 40% for all segments
// but 100% for the reboiler
meff([1:ns]) as realvariable(fixed);

// Heat of desorption of CO2, kcal/gmol CO2
dH([1:ns+1]) as realvariable;


// Tref is the reference temperature, K
Tref as realvariable(298.15,fixed);
// T and Ts are the temperatures of the liquid and side liquid stream temperatures, Kelvin
T([0:2*ns]) as realvariable;
Ts([0:ns-1]) as realvariable;
// Treb is the reboiler temperature, K
Treb as realvariable;
// Tcond is the condensing steam temperature, K
// In this model this is set at 10K higher than the reboiler temperature
Tcond as realvariable;
// Tcool is the temperature of cooling water with a 10K driving force,K
Tcool as realvariable(313.15,fixed);

// Qkcal is the reboiler duty, kcal/gmol CO2
Qkcal as realvariable;

// Work of compression, kcal
Wcomp([1:ns]) as realvariable;

// Weq1 is the equivalent work, kcal
Weq1 as realvariable;
// Weq2 is the equivalent work, kcal/gmol CO2
Weq2 as realvariable;


// heat associated with compression on a segment, kcal
Qcomp([1:ns]) as realvariable;
```

```
// Heat input and rejection from any segment, kcal
Q([1:ns]) as realvariable;
// This is the reboiler duty, kcal/gmol CO2
Qreboiler as realvariable;

// This is the Universal gas constant
R as realvariable(0.08206,fixed);
// This is the ratio of heat capacity at constant pressure
// to that at constant volume i.e. k = cp/cv
k as realvariable(1.3,fixed);
// nn1 = n/(n-1)
// n/(n-1) = k/(k-1)  *  polyeff
nn1 as realvariable;

// polyeff is the polytropic efficiency set to 75%
polyeff as realvariable(0.75,fixed);

//heat capacity coefficients for co2
cpco2([1:ns+1]) as realvariable;
// The constants from the DIPPR database
cpc([1:5]) as realvariable;
cpc(1) : 29370,fixed;
cpc(2):34540,fixed;
cpc(3):1428,fixed;
cpc(4):26400,fixed;
cpc(5): 588,fixed;

//heat capacity coefficients for h2o
cph2o([1:ns+1]) as realvariable;
// The constants from the DIPPR database
cph([1:5]) as realvariable;
cph(1) : 33363.0,fixed;
cph(2):26790,fixed;
cph(3):2610.5,fixed;
cph(4):8896.0,fixed;
cph(5): 1169.0,fixed;

// Heat of vaporisation of water for a stage,kcal/gmol
Hvap as realvariable(10.47,fixed);
//Constants for water vapor pressure
AA as realvariable(73.649,fixed);
BB as realvariable(-7258.2,fixed);
```

```
CC as realvariable(-7.3037,fixed);
DD as realvariable(4.1653e-6,fixed);
EE as realvariable(2.0,fixed);

// Heat of desorption constants
aeq as realvariable;
beq as realvariable;
ceq as realvariable;
deq as realvariable;
eeq as realvariable;
feq as realvariable;

// Temperature approach in cross exchanger, K
Tapp as realvariable;
// Temperature of the gas
// aqssumed to be equal to that of the liquid
Tg([1:ns+1]) as realvariable;

// heat capacity constants for solvent
// assumes molar heat capacities of co2,amine and water
// are equal to those of one mole of water
cp([1:5]) as realvariable;
cp(1) : 276370.0,fixed;
cp(2):-2090.1,fixed;
cp(3):8.125,fixed;
cp(4):-0.014116,fixed;
cp(5): 9.3701e-006,fixed;

// molalK is the molality of K in the solvent
// molalPZ is the molality of PZ in the solvent
// molalMEA is the molality of MEA in the solvent
// molaltotal is the sum of the molality of K,PZ and MEA in the solvent
molalK as realvariable;
molalPZ as realvariable;
molalMEA as realvariable;
molaltotalk as realvariable;

// co2moles is the mole of co2 in the solvent
// h2omoles is the mole of h2o in the solvent
// totalmoles is the mole of co2,water and amine in the solvent
co2moles as realvariable;
h2omoles as realvariable;
```

```
Basis as realvariable;
factor as realvariable(fixed);

totalmoles as realvariable;

molaltotalk = molalK + molalPZ + molalMEA;

co2moles = ldgin * molaltotalk;

h2omoles = 1000/18.02;

totalmoles = co2moles + h2omoles + molaltotalk;

lamine(0) = molaltotalk * (L(0)/totalmoles);

// Fixed variables
//
Tg(ns+1) : 0,fixed;
Pco2(ns+1):0,fixed;
G(ns+1):0,fixed;

for i in [0:ns-1] do
Q(i):0,fixed;
endfor

in_r as input RichPort;
out_l as output LeanPort;
out_p as output VapPort;


//Rich stream
in_r.ldg = ldg(0);
//in_r.CpL = CpL(0);
//in_r.Pco2e = Pco2e(0);
in_r.T = T(0);
in_r.L = L(0);

//Lean stream
out_l.ldg = ldg(2*ns);
//out_l.CpL = CpL(0);
//out_l.Pco2e = Pco2e(0);
out_l.T = T(2*ns);
```

```
out_l.L = L(2*ns);

//vapor stream

out_p.G = G(1);
out_p.yco2 = yco2(1);
out_p.yh2o = yh2o(1);
out_p.Pco2 = Pco2(1);
out_p.Ph2o = Ph2o(1);
out_p.T = T(1);
out_p.Pt = Pt(1);


// VLE constants for solvents
if Solvent == "7m MEA"  then
aeq=35.1159;
beq=-45.04;
ceq=-14281;
deq=-546277;
eeq=-3400441;
feq=32670.01;
molalK =0;
molalPZ =0;
molalMEA = 7;
else

if Solvent == "7m MEA 2m PZ"  then
aeq=30.27305877;
beq=-38.86877528;
ceq=-11990.95019;
deq=1110072.577;
eeq=-4806202.584;
feq=31355.59731;
molalK =0;
molalPZ =0;
molalMEA = 11.85;
else

if Solvent == "5m K 2.5m PZ"  then
aeq=-4.59244;
beq=34.21513;
ceq=-3834.67;
```

```
deq=-1747284;
eeq=-1712091;
feq=8186.474;
molalK =5;
molalPZ =5;
molalMEA =0;
else

if Solvent == "6.4m K 1.6m PZ"  then
aeq=-19.4886;
beq=24.46361;
ceq=3435.22;
deq=1464774;
eeq=-5514009;
feq=12068.45;
molalK = 6.4;
molalPZ = 3.2;
molalMEA = 0;
else

if Solvent == "3.6m K 3.6m PZ"  then
aeq=14.70682;
beq=29.00715;
ceq=-7850.54;
deq=-779330;
eeq=427433;
feq=-1670.44;
molalK = 3.6;
molalPZ = 7.2;
molalMEA =0;
else

if Solvent == "4m K 4m PZ"  then
aeq=12.08799725;
beq=42.39442658;
ceq=-7087.741422;
deq=-925154.8763;
eeq=1393781.73;
feq=-8552.737971;
molalK = 4;
molalPZ = 8;
molalMEA = 0;
```

```
else

endif
endif
endif
endif
endif
endif


nn1 = (k/(k-1))*polyeff;

for i in [0:2*ns] do

L(i) = lco2(i) + lh2o(i) + lamine(i);

ldg(i) = lco2(i)/lamine(i);

endfor

for i in [0:ns-1] do
S(i) = sco2(i) + sh2o(i) + samine(i);
endfor


for i in [0:ns-1] do
lco2((2*i)+1) = lco2(2*i) + sco2(i);
lh2o((2*i)+1) = lh2o(2*i) + sh2o(i);
lamine((2*i)+1) = lamine(2*i) + samine(i);
endfor


for i in [0:2*ns] do

CpL(i) = (cp(1) + (cp(2)*T(i)) + (cp(3) * (T(i)^2))+ (cp(4)*(T(i)^3))+
(cp(5)*(T(i)^4)))*(0.000000239);

endfor

for i in [0:ns-1] do
CpS(i) = (cp(1) + (cp(2)*Ts(i)) + (cp(3) * (Ts(i)^2))+ (cp(4)*(Ts(i)^3))+
(cp(5)*(Ts(i)^4)))*(0.000000239);
endfor
```

```
//Mixing operation

 for i in [0:ns-1] do
(L(2*i) * CpL(2*i) * (T(2*i)-Tref)) + (S(i)*CpS(i)*(Ts(i)-Tref)) = L(2*i+1) * CpL(2*i+1) * (T(2*i+1)-Tref);
endfor

// heat capacity calculation for the gas phase

for i in [1:ns] do
cpco2(i)=(cpc(1) + (cpc(2)*(((cpc(3)/Tg(i)) /sinh(cpc(3)/Tg(i)))^2))+(cpc(4)*(((cpc(5)/Tg(i)) /cosh(cpc(5)/Tg(i)))^2)))*0.000000239;
cph2o(i)=(cph(1) + (cph(2)*(((cph(3)/Tg(i)) /sinh(cph(3)/Tg(i)))^2))+(cph(4)*(((cph(5)/Tg(i)) /cosh(cph(5)/Tg(i)))^2)))*0.000000239;
endfor


cpco2(ns+1):0,fixed;
cph2o(ns+1):0,fixed;

for i in [1:ns] do
Tg(i) = T(2*i);
endfor


// Material balance

for i in [1:ns] do
lco2(2*i-1) + (G(i+1)*yco2(i+1)) = lco2(2*i) + (G(i) * yco2(i));

lh2o(2*i-1) + (G(i+1)*yh2o(i+1)) = lh2o(2*i) + (G(i) * yh2o(i));

lamine(2*i-1) = lamine(2*i) ;

endfor


yco2(ns+1):0,fixed;
yh2o(ns+1):0,fixed;
```

```
dH(ns+1):0,fixed;


// energy balance
for i in [1:ns] do
(G(i+1)*((yh2o(i+1)*(Hvap+(cph2o(i+1)*(Tg(i+1)-
Tref))))+(yco2(i+1)*((dH(i+1)/1000)+(cpco2(i+1)*(Tg(i+1)-Tref))))))+(L(2*i-
1)*cpL(2*i-1)*(T(2*i-1)-Tref))+ Q(i)+ Qcomp(i) =(L(2*i)*cpL(2*i)*(T(2*i)-
Tref))+G(i)*(((yh2o(i))*(Hvap+(cph2o(i)*(Tg(i)-
Tref))))+((yco2(i))*((dH(i)/1000)+(cpco2(i)*(Tg(i)-Tref)))));
endfor


for i in [1:ns] do

Pco2(i)= Pco2(i+1) + (meff(i)*(Pco2e(2*i) - Pco2(i+1)));


Ph2O(i)= (exp(AA+(BB/Tg(i))+(CC*loge(Tg(i)))+ (DD*(Tg(i)^EE))))/1000;
endfor


for i in [1:ns-1] do
meff(i):0.2;
endfor

Tg(ns+1) : 0,fixed;
Pco2(ns+1):0,fixed;

for i in [1:ns] do

dH(i) = (ceq+(2*deq*ldg(2*i)*ldg(2*i)/T(2*i)) + (2*eeq*ldg(2*i)/T(2*i)) +
(feq*ldg(2*i)) )* -1.987;

endfor

// Total pressure on a section
for i in [1:ns] do
Pt(i) = Pco2(i) + Ph2o(i);
endfor

// vapor mole fractions
```

```
for i in [1:ns] do

yco2(i) = Pco2(i)/Pt(i);

yh2o(i) = Ph2o(i)/ Pt(i);

endfor


T(0) + Tapp = T(2*ns);

G(ns+1):0,fixed;

// equilibrium expression

for i in [0:2*ns] do

Pco2e(i) = exp(aeq + (beq*ldg(i)) + (ceq/T(i)) + (deq*ldg(i)*ldg(i)/T(i)/T(i)) +
(eeq*ldg(i)/T(i)/T(i)) + (feq*ldg(i)/T(i)));

endfor



Qreboiler = Q(ns)/G(1)/yco2(1);

//compression work

for i in [1:ns-1] do
Wcomp(i) = (G(i+1)*1.987*Tg(i+1)*nn1*(((Pt(i)/Pt(i+1))^(1/nn1))-1.0))/(1000*polyeff);
Qcomp(i)= Wcomp(i);
endfor

Wcomp(ns):0,fixed;
Qcomp(ns):0,fixed;

for i in [1:ns-1] do
Q(i):0,fixed;
endfor
```

```
for i in [0:ns-1] do
Ts(i):0,fixed;
S(i):0,fixed;
sco2(i):0,fixed;
samine(i):0,fixed;
endfor



ldg(2*ns):fixed;

meff(ns):1,fixed;


for i in [1:ns-1] do
Q(i) : 0,fixed;
endfor

Treb = T(2*ns);

Qkcal = Q(ns);

ldgin = ldg(0);

ldgout = ldg(2*ns);

Tcond = Treb +10;

//Equivalent work , kcal

Weq1 = (0.75*(Q(ns)*((Tcond - Tcool)/Tcond)))   + sigma(Qcomp([1:ns]));

//Equivalent work, kcal/gmol CO2

Weq2 = Weq1 / (G(1)*yco2(1));

end
```

Appendix B: Double Matrix Stripper Model

This appendix contains the detailed matrix stripper model used for MDEA/PZ and KS-1. The matrix model for 7m MEA, MEA/PZ and K_2CO_3/PZ are available from Dr. Gary Rochelle at the University of Texas at Austin.

```
Model Matrix model for MDEA and KS-1
// This is the matrix stripper model for 50 wt% MDEA and KS-1
// This section is for the first stripper in the matrix stripper

//declaration of variables

Solvent as SolventType;
// ns is the number of segments into which the stripper is divided
// The last segment is the reboiler. The reboiler is assumed to be
// an equilibrium segment
ns as integerparameter(12);
nns as integerparameter;

// L is the liquid rate, mol/s
L([0:2*ns]) as realvariable;
// lco2,lh2o,lamine are the molar  rates in the liquid of
// co2,water and amine respectively, mol/s
lco2([0:2*ns]) as realvariable;
lh2o([0:2*ns]) as realvariable;
```

```
lamine([0:2*ns]) as realvariable;

// S is the liquid rate in the side stream, mol/s
S([0:ns-1]) as realvariable;
// sco2,sh2o,samine are the molar  rates in the side liquid stream of
// co2,water and amine respectively, mol/s
sco2([0:ns-1]) as realvariable;
sh2o([0:ns-1]) as realvariable;
samine([0:ns-1]) as realvariable;

// ldg is the CO2 loading in the liquid
ldg([0:2*ns]) as realvariable;
// ldgin is the rich loading, mol CO2/mol Alk
ldgin as realvariable;
//ldgout is the lean loading, mol CO2/mol Alk
ldgout as realvariable;

// CpL  and CpS are the heat capacities of the liquid and side liquid streams, kcal/gmol-K
CpL([0:2*ns]) as realvariable;
CpS([0:ns-1]) as realvariable;

// G is the gas rate, mol/s
G([1:ns+1]) as realvariable;

// yco2 is the mole fraction of CO2 in the gas phase
// yh2o is the mole fraction of CO2 in the gas phase
yco2([1:ns+1]) as realvariable;
yh2o([1:ns+1]) as realvariable;

// Pco2e is the equilibrium partial pressure of CO2 in the liquid,kPa
Pco2e([0:2*ns]) as realvariable;
// Pco2 is the partial pressure of CO2 in the gas phase,kPa
Pco2([1:ns+1]) as realvariable;
// Ph2o is the partial pressure of CO2 in the gas phase,kPa
Ph2o([1:ns]) as realvariable;
// Total pressure on a segment, kPa
Pt([1:ns]) as realvariable(160,fixed);

//Murphree efficiency for CO2
// This is assumed to be 40% for all segments
// but 100% for the reboiler
meff([1:ns]) as realvariable(fixed);
```

```
// Heat of desorption of CO2, kcal/gmol CO2
dH([1:ns+1]) as realvariable;

// Tref is the reference temperature, K
Tref as realvariable(298.15,fixed);
// T and Ts are the temperatures of the liquid and side liquid stream temperatures, Kelvin
T([0:2*ns]) as realvariable;
Ts([0:ns-1]) as realvariable;
// Treb is the reboiler temperature, K
Treb as realvariable;
// Tcond is the condensing steam temperature, K
// In this model this is set at 10K higher than the reboiler temperature
Tcond as realvariable;
// Tcool is the temperature of cooling water with a 10K driving force,K
Tcool as realvariable(313.15,fixed);

// Qkcal is the reboiler duty, kcal/gmol CO2
Qkcal as realvariable;

// Work of compression, kcal
Wcomp([1:ns]) as realvariable;
// Weq1 is the equivalent work, kcal
Weq1 as realvariable;
// Weq2 is the equivalent work, kcal/gmol CO2
Weq2 as realvariable;

// heat associated with compression on a segment, kcal
Qcomp([1:ns]) as realvariable;
// Heat input and rejection from any segment, kcal
Q([1:ns]) as realvariable;
// This is the reboiler duty, kcal/gmol CO2
Qreboiler as realvariable;


// This is the Universal gas constant
R as realvariable(0.08206,fixed);
// This is the ratio of heat capacity at constant pressure
// to that at constant volume i.e. k = cp/cv
k as realvariable(1.3,fixed);
// nn1 = n/(n-1)
// n/(n-1) = k/(k-1)  *  polyeff
```

```
nn1 as realvariable;

// polyeff is the polytropic efficiency set to 75%
polyeff as realvariable(0.75,fixed);

//heat capacity coefficients for co2
cpco2([0:ns+1]) as realvariable;
// The constants from the DIPPR database
cpc([1:5]) as realvariable;
cpc(1) : 29370,fixed;
cpc(2):34540,fixed;
cpc(3):1428,fixed;
cpc(4):26400,fixed;
cpc(5): 588,fixed;

//heat capacity coefficients for h20
cph2o([0:ns+1]) as realvariable;
// The constants from the DIPPR database
cph([1:5]) as realvariable;
cph(1) : 33363.0,fixed;
cph(2):26790,fixed;
cph(3):2610.5,fixed;
cph(4):8896.0,fixed;
cph(5): 1169.0,fixed;

// Heat of vaporisation of water for a stage,kcal/gmol
Hvap as realvariable(10.47,fixed);

//Constants for water vapor pressure
AA as realvariable(73.649,fixed);
BB as realvariable(-7258.2,fixed);
CC as realvariable(-7.3037,fixed);
DD as realvariable(4.1653e-6,fixed);
EE as realvariable(2.0,fixed);

// Temperature approach in cross exchanger, K
Tapp as realvariable(fixed);

// Temperature of the gas
// assumed to be equal to that of the liquid
Tg([1:ns+1]) as realvariable;
```

```
// heat capacity constants for solvent
// assumes molar heat capacities of co2,amine and water
// are equal to those of one mole of water
cp([1:5]) as realvariable;
// The constants were taken from the DIPPR database
cp(1) : 276370.0,fixed;
cp(2):-2090.1,fixed;
cp(3):8.125,fixed;
cp(4):-0.014116,fixed;
cp(5): 9.3701e-006,fixed;

//gas free amine mole fraction from Posey et al (1996)
Xamine as realvariable ;

//acid gas liquid mole fraction
Xco2([0:2*ns]) as realvariable;

// Equilibrium constant

Kco2([0:2*ns]) as realvariable;

//constants for equilibrium constant expression

KA as realvariable ;

KB as realvariable ;

KC as realvariable ;

KD as realvariable;



molalK as realvariable;
molalPZ as realvariable;
molalMEA as realvariable;
molalAmine as realvariable;
molaltotalk as realvariable;
co2moles as realvariable;
h2omoles as realvariable;
```

```
totalmoles as realvariable;

molaltotalk = molalK + molalPZ + molalMEA + molalAmine;


co2moles = ldgin * molaltotalk;

h2omoles = 1000/18.02;


totalmoles = co2moles + h2omoles + molaltotalk;


lamine(0) = molaltotalk * (L(0)/totalmoles);


if Solvent == "KS-1"  then
molalK = 0;
molalPZ = 0;
molalMEA = 0;
molalAmine = 8.39;
KA = 32.45;
KB = -8807;
KC = 52;
KD =-15;
Xamine = 0.1313;
else
if Solvent == "50 wt% MDEA"  then
molalK = 0;
molalPZ = 0;
molalMEA = 0;
molalAmine = 8.39;
KA = 32.45;
KB = -7440;
KC = 33;
KD =-18.5;
Xamine = 0.1313;
endif
endif

// Specified variables
Tg(ns+1) : 0,fixed;
```

```
Pco2(ns+1):0,fixed;
G(ns+1):0,fixed;

for i in [1:ns-1] do
Q(i):0,fixed;
endfor

in_r as input RichPort;
out_l as output LeanPort;
out_p as output VapPort;


//Rich stream
in_r.ldg = ldg(0);
//in_r.CpL = CpL(0);
//in_r.Pco2e = Pco2e(0);
in_r.T = T(0);
in_r.L = L(0);

//Lean stream
out_l.ldg = ldg(2*ns);
//out_l.CpL = CpL(0);
//out_l.Pco2e = Pco2e(0);
out_l.T = T(2*ns);
out_l.L = L(2*ns);

//vapor stream

out_p.G = G(1);
out_p.yco2 = yco2(1);
out_p.yh2o = yh2o(1);
out_p.Pco2 = Pco2(1);
out_p.Ph2o = Ph2o(1);
out_p.T = T(1);
out_p.Pt = Pt(1);




nn1 = (k/(k-1))*polyeff;

for i in [0:2*ns] do
```

```
L(i) = lco2(i) + lh2o(i) + lamine(i);

ldg(i) = lco2(i)/lamine(i);

endfor

for i in [0:ns-1] do
S(i) = sco2(i) + sh2o(i) + samine(i);
endfor

for i in [0:ns-1] do
lco2((2*i)+1) = lco2(2*i) + sco2(i);
lh2o((2*i)+1) = lh2o(2*i) + sh2o(i);
lamine((2*i)+1) = lamine(2*i) + samine(i);
endfor


for i in [0:2*ns] do

CpL(i) = (cp(1) + (cp(2)*T(i))  + (cp(3) * (T(i)^2))+ (cp(4)*(T(i)^3))+
(cp(5)*(T(i)^4)))*(0.000000239);

endfor

for i in [0:ns-1] do
CpS(i) = (cp(1) + (cp(2)*Ts(i))  + (cp(3) * (Ts(i)^2))+ (cp(4)*(Ts(i)^3))+
(cp(5)*(Ts(i)^4)))*(0.000000239);
endfor


//Mixing operation

 for i in [0:ns-1] do
(L(2*i) * CpL(2*i) * (T(2*i)-Tref)) + (S(i)*CpS(i)*(Ts(i)-Tref)) = L(2*i+1) *
CpL(2*i+1) * (T(2*i+1)-Tref);
endfor

// heat capacity calculation for the gas phase

for i in [1:ns] do
```

```
cpco2(i)=(cpc(1) + (cpc(2)*(((cpc(3)/Tg(i))
/sinh(cpc(3)/Tg(i)))^2))+(cpc(4)*(((cpc(5)/Tg(i)) /cosh(cpc(5)/Tg(i)))^2)))*0.000000239;
cph2o(i)=(cph(1) + (cph(2)*(((cph(3)/Tg(i))
/sinh(cph(3)/Tg(i)))^2))+(cph(4)*(((cph(5)/Tg(i))
/cosh(cph(5)/Tg(i)))^2)))*0.000000239;
endfor


cpco2(ns+1):0,fixed;
cph2o(ns+1):0,fixed;

for i in [1:ns] do
Tg(i) = T(2*i);
endfor


// Material balance

for i in [1:ns] do
lco2(2*i-1) + (G(i+1)*yco2(i+1)) = lco2(2*i) + (G(i) * yco2(i));

lh2o(2*i-1) + (G(i+1)*yh2o(i+1)) = lh2o(2*i) + (G(i) * yh2o(i));

lamine(2*i-1) = lamine(2*i) ;

endfor


yco2(ns+1):0,fixed;
yh2o(ns+1):0,fixed;
dH(ns+1):0,fixed;


// energy balance
for i in [1:ns] do
(G(i+1)*((yh2o(i+1)*(Hvap+(cph2o(i+1)*(Tg(i+1)-
Tref))))+(yco2(i+1)*((dH(i+1)/1000)+(cpco2(i+1)*(Tg(i+1)-Tref))))))+(L(2*i-
1)*cpL(2*i-1)*(T(2*i-1)-Tref))+ Q(i)+ Qcomp(i) =(L(2*i)*cpL(2*i)*(T(2*i)-
Tref))+G(i)*(((yh2o(i))*(Hvap+(cph2o(i)*(Tg(i)-
Tref))))+((yco2(i))*((dH(i)/1000)+(cpco2(i)*(Tg(i)-Tref)))));
endfor
```

```
for i in [1:ns] do

Pco2(i)= Pco2(i+1) + (meff(i)*(Pco2e(2*i) - Pco2(i+1)));


Ph2O(i)= (exp(AA+(BB/Tg(i))+(CC*loge(Tg(i)))+ (DD*(Tg(i)^EE))))/1000;
endfor


for i in [1:ns-1] do
meff(i):0.4;
endfor

Tg(ns+1) : 0,fixed;
Pco2(ns+1):0,fixed;

for i in [1:ns] do
dH(i) = KB * -1.987;
endfor

// Total pressure on a section
for i in [1:ns] do
Pt(i) = Pco2(i) + Ph2o(i);
endfor

// vapor mole fractions

for i in [1:ns] do

yco2(i) = Pco2(i)/Pt(i);

yh2o(i) = Ph2o(i)/ Pt(i);

endfor


T(0) + Tapp = T(2*ns);

G(ns+1):0,fixed;

// equilibrium expression
```

```
for i in [0:2*ns] do

loge(Kco2(i)) = KA + (KB/T(i)) + (KC * ldg(i) * Xamine) + (KD*
((ldg(i)*Xamine)^0.5));


if Solvent == "50 wt% MDEA"  then
Xco2(i) = (ldg(i) * 0.4195) / ( (ldg(i)*0.4195) + 0.4195 + 2.7747);
else
if Solvent == "KS-1"  then
Xco2(i) = ldg(i) / ( (ldg(i)) + 1 +((1/Xamine)-1));
endif
endif

Pco2e(i) = Kco2(i) * Xco2(i) * (ldg(i)/ (1-ldg(i)));

endfor
Qreboiler = Q(ns)/G(1)/yco2(1);

//compression work

for i in [1:ns-1] do
Wcomp(i) = (G(i)*1.987*Tg(i+1)*nn1*(((Pt(i)/Pt(i+1))^(1/nn1))-1.0))/(1000*polyeff);
Qcomp(i)= Wcomp(i);
endfor

Wcomp(ns):0,fixed;
Qcomp(ns):0,fixed;

for i in [1:ns-1] do
Q(i):0,fixed;
endfor



for i in [0:ns-1] do
Ts(i):0,fixed;
S(i):0,fixed;
sco2(i):0,fixed;
samine(i):0,fixed;
endfor
```

```
ldg(2*ns):fixed;

meff(ns):1,fixed;


for i in [1:ns-1] do
Q(i) : 0,fixed;
endfor

//Ts(nns) = (T(2*ns))-5 ;

//Ts(nns)= T(0);

Treb = T(2*ns);

Qkcal = Q(ns);

ldgin = ldg(0);

ldgout = ldg(2*ns);

Tcond = Treb +10;

//Equivalent work , kcal

Weq1 = (0.75*(Q(ns)*((Tcond - Tcool)/Tcond)))   + sigma(Qcomp([1:ns]));

//Equivalent work, kcal/gmol CO2

Weq2 = Weq1 / (G(1)*yco2(1));

end



// This is the end of the first column equations
```

```
Model test10
// This is the matrix stripper model for 50 wt% MDEA and KS-1
// This section is for the second stripper in the matrix stripper

//declaration of variables
Solvent as SolventType;
// ns is the number of segments into which the stripper is divided
// The last segment is the reboiler. The reboiler is assumed to be
// an equilibrium segment
ns as integerparameter(12);
nns as integerparameter;
//nsf refers to the number of stages in the upper part of the second
//column
nsf as integerparameter(5);


//DECLARATION OF UPPER SECTION OF SECOND STRIPPER STAGE
VARIABLES
// Lcf is the liquid rate of the feed to the upper part of the second column, mol/s
Lcf([0:nsf]) as realvariable;
// Lwp is the liquid rate of the semi-lean stream, mol/s
Lwp as realvariable;
// lco2cf,lh2ocf,laminecf are the molar  rates in the liquid to the second column for
// co2,water and amine respectively, mol/s
lco2cf([0:nsf]) as realvariable;
lh2ocf([0:nsf]) as realvariable;
laminecf([0:nsf]) as realvariable;

// lco2wp,lh2owp,laminewp are the molar rates in the semi-lean stream for
// co2,water and amine respectively, mol/s
lco2wp as realvariable;
lh2owp as realvariable;
laminewp as realvariable;

//ldgcf is the loading of the solution in the upper part of the second column,mol/mol Alk
//ldgwp is the semi-lean loading, mol/mol Alk
ldgcf([0:nsf]) as realvariable;
ldgwp as realvariable;

// GCF is the gas rate in the upper part of the second column,mol/s
GCF([1:nsf+1]) as realvariable;
```

```
//yco2cf and yh2ocf are the mole fractions in the gas phase in the
//upper part of the second column
yco2cf([1:nsf+1]) as realvariable;
yh2ocf([1:nsf+1]) as realvariable;

//CpLcf is the liquid heat capacity in the upper part of the second column, kcal/mol-K
//CpLwp is the semi-lean liquid heat capacity, kcal/mol-K
CpLcf([0:nsf]) as realvariable;
CpLwp as realvariable;

//Tcf is the liquid temperature in the upper part of the second column,K
//Twp is the semi-lean temperature,K
Tcf([0:nsf]) as realvariable;
Twp as realvariable;

//Pco2ecf is the equilibrium partial pressure of co2 in the liquid in the upper part of the
second column,kPa
//Pco2ewp is the equilibrium partial pressure of co2 in the semi-lean stream,kPa
Pco2ecf([0:nsf]) as realvariable;
Pco2ewp as realvariable;

//Pco2cf is the partial pressure of co2 in gas phase in the upper part of the second
column,kPa
//Ph2ocf is the partial pressure of co2 in the gas phase,kPa
//Ptcf is the total pressure on a segment in the upper part of the second column,kPa
Ptcf([1:nsf+1]) as realvariable(160,fixed);
Ph2ocf([1:nsf+1]) as realvariable;
Pco2cf([1:nsf+1]) as realvariable;

//meffcf is the Murphree efficiency of co2 in the upper part of the second column,-
meffcf([1:nsf]) as realvariable(fixed);

//dHcf is the heat of desorption co2 in the upper part of the second column,kcal/gmol
CO2
dHcf([1:nsf+1]) as realvariable;

// cpco2cf is the heat capacity of co2 in the gas phase in the upper part of the second
column, kcal/gmol-K
// cph2ocf is the heat capacity of co2 in the gas phase in the upper part of the second
column, kcal/gmol-K
cpco2cf([1:nsf+1]) as realvariable;
```

```
cph2ocf([1:nsf+1]) as realvariable;

// This is the heat rate for each segment in the upper part of the second column,kcal
Qcf([1:nsf]) as realvariable;

//Gas phase temperature in the upper part of the second column,K
Tgcf([1:nsf+1]) as realvariable;

//END OF FLASH SEGMENTS VARIABLE DECLARATION



// The equations for the lower part of the second column start here

// L is the liquid rate, mol/s
L([0:2*ns]) as realvariable;
// lco2,lh2o,lamine are the molar  rates in the liquid of
// co2,water and amine respectively, mol/s
lco2([0:2*ns]) as realvariable;
lh2o([0:2*ns]) as realvariable;
lamine([0:2*ns]) as realvariable;

// S is the liquid rate in the side stream, mol/s
// sco2,sh2o,samine are the molar  rates in the side liquid stream of
// co2,water and amine respectively, mol/s
S([0:ns-1]) as realvariable;
sco2([0:ns-1]) as realvariable;
sh2o([0:ns-1]) as realvariable;
samine([0:ns-1]) as realvariable;

// ldg is the CO2 loading in the liquid
ldg([0:2*ns]) as realvariable;
// ldgin is the rich loading, mol CO2/mol Alk
ldgin as realvariable;
//ldgout is the lean loading, mol CO2/mol Alk
ldgout as realvariable;

// CpL  and CpS are the heat capacities of the liquid and side liquid streams, kcal/gmol-K
CpL([0:2*ns]) as realvariable;
CpS([0:ns-1]) as realvariable;

// G is the gas rate, mol/s
```

```
G([1:ns+1]) as realvariable;


// yco2 is the mole fraction of CO2 in the gas phase
// yh2o is the mole fraction of CO2 in the gas phase

yco2([1:ns+1]) as realvariable;
yh2o([1:ns+1]) as realvariable;

// Pco2e is the equilibrium partial pressure of CO2 in the liquid,kPa
Pco2e([0:2*ns]) as realvariable;
// Pco2 is the partial pressure of CO2 in the gas phase,kPa
Pco2([1:ns+1]) as realvariable;
// Ph2o is the partial pressure of CO2 in the gas phase,kPa
Ph2o([1:ns]) as realvariable;
// Total pressure on a segment, kPa
Pt([1:ns]) as realvariable(160,fixed);

//Murphree efficiency for CO2
// This is assumed to be 40% for all segments
// but 100% for the reboiler
meff([1:ns]) as realvariable(fixed);

// Heat of desorption of CO2, kcal/gmol CO2
dH([1:ns+1]) as realvariable;

// Tref is the reference temperature, K
Tref as realvariable(298.15,fixed);
// T and Ts are the temperatures of the liquid and side liquid stream temperatures, Kelvin
T([0:2*ns]) as realvariable;
Ts([0:ns-1]) as realvariable;
// Treb is the reboiler temperature, K
Treb as realvariable;
// Tcond is the condensing steam temperature, K
// In this model this is set at 10K higher than the reboiler temperature
Tcond as realvariable;
// Tcool is the temperature of cooling water with a 10K driving force,K
Tcool as realvariable(313.15,fixed);

// Qkcal is the reboiler duty, kcal/gmol CO2
Qkcal as realvariable;
```

```
// Work of compression, kcal
Wcomp([1:ns]) as realvariable;

// Weq1 is the equivalent work, kcal
Weq1 as realvariable;
// Weq2 is the equivalent work, kcal/gmol CO2
Weq2 as realvariable;
// heat associated with compression on a segment, kcal
Qcomp([1:ns]) as realvariable;

// Heat input and rejection from any segment, kcal
Q([1:ns]) as realvariable;
// This is the reboiler duty, kcal/gmol CO2
Qreboiler as realvariable;

// This is the Universal gas constant
R as realvariable(0.08206,fixed);

// This is the ratio of heat capacity at constant pressure
// to that at constant volume i.e. k = cp/cv
k as realvariable(1.3,fixed);
// nn1 = n/(n-1)
// n/(n-1) = k/(k-1)  *  polyeff
nn1 as realvariable;

// polyeff is the polytropic efficiency set to 75%
polyeff as realvariable(0.75,fixed);

//heat capacity coefficients for co2
cpco2([1:ns+1]) as realvariable;
// The constants from the DIPPR database
cpc([1:5]) as realvariable;
cpc(1) : 29370,fixed;
cpc(2):34540,fixed;
cpc(3):1428,fixed;
cpc(4):26400,fixed;
cpc(5): 588,fixed;

//heat capacity coefficients for h20
cph2o([1:ns+1]) as realvariable;
// The constants from the DIPPR database
```

```
cph([1:5]) as realvariable;
cph(1) : 33363.0,fixed;
cph(2):26790,fixed;
cph(3):2610.5,fixed;
cph(4):8896.0,fixed;
cph(5): 1169.0,fixed;

// Heat of vaporisation of water for a stage,kcal/gmol
Hvap as realvariable(10.47,fixed);

//Constants for water vapor pressure
AA as realvariable(73.649,fixed);
BB as realvariable(-7258.2,fixed);
CC as realvariable(-7.3037,fixed);
DD as realvariable(4.1653e-6,fixed);
EE as realvariable(2.0,fixed);



// Temperature approach in cross exchanger, K
Tapp as realvariable;
// Temperature of the gas
// assumed to be equal to that of the liquid
Tg([1:ns+1]) as realvariable;

// heat capacity constants for solvent
// assumes molar heat capacities of co2,amine and water
// are equal to those of one mole of water
cp([1:5]) as realvariable;
cp(1) : 276370.0,fixed;
cp(2):-2090.1,fixed;
cp(3):8.125,fixed;
cp(4):-0.014116,fixed;
cp(5): 9.3701e-006,fixed;


//gas free amine mole fraction from Posey et al (1996)
Xamine as realvariable ;

//acid gas liquid mole fraction
Xco2([0:2*ns]) as realvariable;
```

```
// Equilibrium constant
Kco2([0:2*ns]) as realvariable;

//constants for equilibrium constant expression

KA as realvariable ;

KB as realvariable ;

KC as realvariable ;

KD as realvariable;



molalK as realvariable;
molalPZ as realvariable;
molalMEA as realvariable;
molalAmine as realvariable;
molaltotalk as realvariable;
co2moles as realvariable;
h2omoles as realvariable;
factor as realvariable(fixed);

totalmoles as realvariable;

molaltotalk = molalK + molalPZ + molalMEA + molalAmine;


co2moles = ldgin * molaltotalk;

h2omoles = 1000/18.02;


totalmoles = co2moles + h2omoles + molaltotalk;


lamine(0) = molaltotalk * (L(0)/totalmoles);


if Solvent == "KS-1"  then
molalK = 0;
```

```
molalPZ = 0;
molalMEA = 0;
molalAmine = 8.39;
KA = 32.45;
KB = -8807;
KC = 52;
KD =-15;
Xamine = 0.1313;
else
if Solvent == "50 wt% MDEA"  then
molalK = 0;
molalPZ = 0;
molalMEA = 0;
molalAmine = 8.39;
KA = 32.45;
KB = -7440;
KC = 33;
KD =-18.5;
Xamine = 0.1313;
endif
endif


// Specified variables
Tg(ns+1) : 0,fixed;
Pco2(ns+1):0,fixed;
G(ns+1):0,fixed;


for i in [0:ns-1] do
Q(i):0,fixed;
endfor


in_r as input RichPort;
out_l as output LeanPort;
out_p as output VapPort;


//Rich stream
in_r.ldg = ldg(0);
//in_r.CpL = CpL(0);
```

```
//in_r.Pco2e = Pco2e(0);
in_r.T = T(0);
in_r.L = L(0);

//Lean stream
out_l.ldg = ldg(2*ns);
//out_l.CpL = CpL(0);
//out_l.Pco2e = Pco2e(0);
out_l.T = T(2*ns);
out_l.L = L(2*ns);

//vapor stream

out_p.G = G(1);
out_p.yco2 = yco2(1);
out_p.yh2o = yh2o(1);
out_p.Pco2 = Pco2(1);
out_p.Ph2o = Ph2o(1);
out_p.T = T(1);
out_p.Pt = Pt(1);



nn1 = (k/(k-1))*polyeff;

for i in [0:2*ns] do

L(i) = lco2(i) + lh2o(i) + lamine(i);

ldg(i) = lco2(i)/lamine(i);

endfor

for i in [0:ns-1] do
S(i) = sco2(i) + sh2o(i) + samine(i);
endfor

for i in [0:ns-1] do
lco2((2*i)+1) = lco2(2*i) + sco2(i);
lh2o((2*i)+1) = lh2o(2*i) + sh2o(i);
lamine((2*i)+1) = lamine(2*i) + samine(i);
endfor
```

```
for i in [0:2*ns] do

CpL(i) = (cp(1) + (cp(2)*T(i))  + (cp(3) * (T(i)^2))+ (cp(4)*(T(i)^3))+
(cp(5)*(T(i)^4)))*(0.000000239);

endfor

for i in [0:ns-1] do
CpS(i) = (cp(1) + (cp(2)*Ts(i))  + (cp(3) * (Ts(i)^2))+ (cp(4)*(Ts(i)^3))+
(cp(5)*(Ts(i)^4)))*(0.000000239);
endfor


//Mixing operation

 for i in [0:ns-1] do
(L(2*i) * CpL(2*i) * (T(2*i)-Tref)) + (S(i)*CpS(i)*(Ts(i)-Tref)) = L(2*i+1) *
CpL(2*i+1) * (T(2*i+1)-Tref);
endfor

// heat capacity calculation for the gas phase

for i in [1:ns] do
cpco2(i)=(cpc(1) + (cpc(2)*(((cpc(3)/Tg(i))
/sinh(cpc(3)/Tg(i)))^2))+(cpc(4)*(((cpc(5)/Tg(i)) /cosh(cpc(5)/Tg(i)))^2)))*0.000000239;
cph2o(i)=(cph(1) + (cph(2)*(((cph(3)/Tg(i))
/sinh(cph(3)/Tg(i)))^2))+(cph(4)*(((cph(5)/Tg(i))
/cosh(cph(5)/Tg(i)))^2)))*0.000000239;
endfor


cpco2(ns+1):0,fixed;
cph2o(ns+1):0,fixed;

for i in [1:ns] do
Tg(i) = T(2*i);
endfor


// Material balance
```

```
for i in [1:ns] do
lco2(2*i-1) + (G(i+1)*yco2(i+1)) = lco2(2*i) + (G(i) * yco2(i));

lh2o(2*i-1) + (G(i+1)*yh2o(i+1)) = lh2o(2*i) + (G(i) * yh2o(i));

lamine(2*i-1) = lamine(2*i) ;

endfor


yco2(ns+1):0,fixed;
yh2o(ns+1):0,fixed;
dH(ns+1):0,fixed;


// energy balance
for i in [1:ns] do
(G(i+1)*((yh2o(i+1)*(Hvap+(cph2o(i+1)*(Tg(i+1)-
Tref))))+(yco2(i+1)*((dH(i+1)/1000)+(cpco2(i+1)*(Tg(i+1)-Tref))))))+(L(2*i-
1)*cpL(2*i-1)*(T(2*i-1)-Tref))+ Q(i)+ Qcomp(i) =(L(2*i)*cpL(2*i)*(T(2*i)-
Tref))+G(i)*(((yh2o(i))*(Hvap+(cph2o(i)*(Tg(i)-
Tref))))+((yco2(i))*((dH(i)/1000)+(cpco2(i)*(Tg(i)-Tref)))));
endfor


for i in [1:ns] do

Pco2(i)= Pco2(i+1) + (meff(i)*(Pco2e(2*i) - Pco2(i+1)));


Ph2O(i)= (exp(AA+(BB/Tg(i))+(CC*loge(Tg(i)))+ (DD*(Tg(i)^EE))))/1000;
endfor


for i in [1:ns-1] do
meff(i):0.2;
endfor

Tg(ns+1) : 0,fixed;
Pco2(ns+1):0,fixed;
```

```
for i in [1:ns] do
dH(i) = KB * -1.987;
endfor

// Total pressure on a section
for i in [1:ns] do
Pt(i) = Pco2(i) + Ph2o(i);
endfor

// vapor mole fractions

for i in [1:ns] do

yco2(i) = Pco2(i)/Pt(i);

yh2o(i) = Ph2o(i)/ Pt(i);

endfor


T(0) + Tapp = T(2*ns);

G(ns+1):0,fixed;

// equilibrium expression

for i in [0:2*ns] do

loge(Kco2(i)) = KA + (KB/T(i)) + (KC * ldg(i) * Xamine) + (KD*
((ldg(i)*Xamine)^0.5));


if Solvent == "50 wt% MDEA"  then
Xco2(i) = (ldg(i) * 0.4195) / ( (ldg(i)*0.4195) + 0.4195 + 2.7747);
else
if Solvent == "KS-1"  then
Xco2(i) = ldg(i) / ( (ldg(i)) + 1 +((1/Xamine)-1));
endif
endif

Pco2e(i) = Kco2(i) * Xco2(i) * (ldg(i)/ (1-ldg(i)));
```

```
endfor



Qreboiler = Q(ns)/G(1)/yco2(1);

//compression work

for i in [1:ns-1] do
Wcomp(i) = (G(i)*1.987*Tg(i+1)*nn1*(((Pt(i)/Pt(i+1))^(1/nn1))-1.0))/(1000*polyeff);
Qcomp(i)= Wcomp(i);
endfor

Wcomp(ns):0,fixed;
Qcomp(ns):0,fixed;

for i in [1:ns-1] do
Q(i):0,fixed;
endfor



for i in [0:ns-1] do
Ts(i):0,fixed;
S(i):0,fixed;
sco2(i):0,fixed;
samine(i):0,fixed;
endfor



ldg(2*ns):fixed;

meff(ns):1,fixed;


for i in [1:ns-1] do
Q(i) : 0,fixed;
endfor

//Ts(nns) = (T(2*ns))-5 ;
```

```
//Ts(nns)= T(0);

Treb = T(2*ns);

Qkcal = Q(ns);

ldgin = ldg(0);

ldgout = ldg(2*ns);

Tcond = Treb +10;

//Equivalent work , kcal

Weq1 = (0.75*(Q(ns)*((Tcond - Tcool)/Tcond)))   + sigma(Qcomp([1:ns]));

//Equivalent work, kcal/gmol CO2

Weq2 = Weq1 / (Gcf(1)*yco2cf(1));

//UPPER PART OF SECOND COLUMN EQUATIONS

for i in [0:nsf] do

Lcf(i) = lco2cf(i) + lh2ocf(i) + laminecf(i);

ldgcf(i) = lco2cf(i)/laminecf(i);

endfor


for i in [0:nsf] do

CpLcf(i) = (cp(1) + (cp(2)*Tcf(i))  + (cp(3) * (Tcf(i)^2))+ (cp(4)*(Tcf(i)^3))+
(cp(5)*(Tcf(i)^4)))*(0.000000239);

endfor
```

```
// heat capacity calculation for the gas phase

for i in [1:nsf] do
cpco2cf(i)=(cpc(1) + (cpc(2)*(((cpc(3)/Tgcf(i))
/sinh(cpc(3)/Tgcf(i)))^2))+(cpc(4)*(((cpc(5)/Tgcf(i))
/cosh(cpc(5)/Tgcf(i)))^2)))*0.000000239;
cph2ocf(i)=(cph(1) + (cph(2)*(((cph(3)/Tgcf(i))
/sinh(cph(3)/Tgcf(i)))^2))+(cph(4)*(((cph(5)/Tgcf(i))
/cosh(cph(5)/Tgcf(i)))^2)))*0.000000239;
endfor


for i in [1:nsf] do
Tgcf(i) = Tcf(i);
endfor


// Material balance

for i in [1:nsf] do
lco2cf(i-1) + (Gcf(i+1)*yco2cf(i+1)) = lco2cf(i) + (Gcf(i) * yco2cf(i));

lh2ocf(i-1) + (Gcf(i+1)*yh2ocf(i+1)) = lh2ocf(i) + (Gcf(i) * yh2ocf(i));

lamineCf(i-1) = lamineCf(i) ;

endfor



// energy balance
for i in [1:nsf] do
(Gcf(i+1)*((yh2ocf(i+1)*(Hvap+(cph2ocf(i+1)*(Tgcf(i+1)-
Tref))))+(yco2cf(i+1)*((dHcf(i+1)/1000)+(cpco2cf(i+1)*(Tgcf(i+1)-Tref))))))+(Lcf(i-
1)*cpLcf(i-1)*(Tcf(i-1)-Tref))+ Qcf(i)=(Lcf(i)*cpLcf(i)*(Tcf(i)-
Tref))+Gcf(i)*(((yh2ocf(i))*(Hvap+(cph2ocf(i)*(Tgcf(i)-
Tref))))+((yco2cf(i))*((dHcf(i)/1000)+(cpco2cf(i)*(Tgcf(i)-Tref)))));
endfor


for i in [1:nsf] do
```

```
Pco2cf(i)= Pco2cf(i+1) + (meffcf(i)*(Pco2ecf(i) - Pco2cf(i+1)));


Ph2Ocf(i)= (exp(AA+(BB/Tgcf(i))+(CC*loge(Tgcf(i)))+ (DD*(Tgcf(i)^EE))))/1000;
endfor


for i in [1:nsf-1] do
meffcf(i):0.4;
endfor


for i in [1:nsf] do

dHcf(i) = KB * -1.987;

endfor

// Total pressure on a section
for i in [1:nsf] do
Ptcf(i) = Pco2cf(i) + Ph2ocf(i);
endfor

// vapor mole fractions

for i in [1:nsf] do

yco2cf(i) = Pco2cf(i)/Ptcf(i);

yh2ocf(i) = Ph2ocf(i)/ Ptcf(i);

endfor


Tcf(0) + Tapp = Tcf(nsf);



// equilibrium expression
Kco2cf([0:nsf]) as realvariable;
Xco2cf([0:nsf]) as realvariable;
```

```
for i in [0:nsf] do

loge(Kco2cf(i)) = KA + (KB/Tcf(i)) + (KC * ldgcf(i) * Xamine) + (KD*
((ldgcf(i)*Xamine)^0.5));

if Solvent == "50 wt% MDEA"  then
Xco2cf(i) = (ldgcf(i) * 0.4195) / ( (ldgcf(i)*0.4195) + 0.4195 + 2.7747);
else
if Solvent == "KS-1"  then
Xco2cf(i) = ldgcf(i) / ( (ldgcf(i)) + 1 +((1/Xamine)-1));
endif
endif

Pco2ecf(i) = Kco2cf(i) * Xco2cf(i) * (ldgcf(i)/ (1-ldgcf(i)));

endfor

for i in [1:nsf-1] do
Qcf(i):0,fixed;
endfor
Ptcf(nsf+1):free;
Ptcf(nsf+1)= Pt(1);
Ph2ocf(nsf+1)= Ph2o(1);
Tgcf(nsf+1) = Tg(1);
Pco2cf(nsf+1)=Pco2(1);
Gcf(nsf+1)=G(1);
yco2cf(nsf+1)=yco2(1);
yh2ocf(nsf+1)=yh2o(1);
dHcf(nsf+1)=dH(1);
cpco2cf(nsf+1)=cpco2(1);
cph2ocf(nsf+1) = cph2o(1);

ldgcf(0):fixed;
LCF(0): 1000,fixed;
Laminecf(0)= molaltotalk * (Lcf(0)/totalmoles);
meffcf(nsf):1,fixed;
Qcf(nsf):0,fixed;
ldgwp = ldgcf(nsf);

//END OF UPPER PART OF SECOND COLUMN EQUATIONS
end
```

Appendix C: Rate Model Using Random Packing

This appendix contains the rate model for 5m K^+/2.5m PZ. The model can be used for a wide variety of random packings including 1" pall rings, 2" pall rings, CMR #2, CMR #2A, IMTP #25 and IMTP #40. The model is available from Dr. Gary Rochelle at the University of Texas at Austin.

Model Rate model with random packing

```
//declaration of variables
Contactor as ContactorType;
ns as integerparameter(12);
nns as integerparameter;

L([0:2*ns]) as realvariable;
lco2([0:2*ns]) as realvariable;
lh2o([0:2*ns]) as realvariable;
lamine([0:2*ns]) as realvariable;

ldg([0:2*ns]) as realvariable;

S([0:ns-1]) as realvariable;
sco2([0:ns-1]) as realvariable;
sh2o([0:ns-1]) as realvariable;
```

samine([0:ns-1]) as realvariable;

CpL([0:2*ns]) as realvariable;

CpS([0:ns-1]) as realvariable;

Tref as realvariable(298.15,fixed);

T([0:2*ns]) as realvariable;

Ts([0:ns-1]) as realvariable;

Treb as realvariable;

Tcond as realvariable;

Tcool as realvariable(313.15,fixed);

Qkcal as realvariable;

ldgin as realvariable;

ldgout as realvariable(fixed);

Weq1 as realvariable;

Weq2 as realvariable;

G([1:ns+1]) as realvariable;

yco2([1:ns+1]) as realvariable;

yh2o([1:ns+1]) as realvariable;

Pco2e([0:2*ns]) as realvariable;

Pco2([1:ns+1]) as realvariable;

meff([1:ns]) as realvariable(fixed);

dH([1:ns+1]) as realvariable;

```
Pt([1:ns]) as realvariable(30);

Ph2o([1:ns]) as realvariable;

Q([1:ns]) as realvariable;

Qreboiler as realvariable;


Qx([1:ns]) as realvariable;

Wcomp([1:ns]) as realvariable;

Qcomp([1:ns]) as realvariable;

R as realvariable(0.08206,fixed);

k as realvariable(1.3,fixed);

nn1 as realvariable;

compeff as realvariable(0.75,fixed);

polyeff as realvariable(0.75,fixed);

cpco2([1:ns+1]) as realvariable;

UA as realvariable(1,fixed);

Tx([1:ns]) as realvariable;

Txdiff([1:ns]) as realvariable;


//heat capacity coefficients for co2
cpc([1:5]) as realvariable;
cpc(1) : 29370,fixed;
cpc(2):34540,fixed;
cpc(3):1428,fixed;
cpc(4):26400,fixed;
cpc(5): 588,fixed;
```

```
cph2o([1:ns+1]) as realvariable;
//heat capacity coefficients for h20
cph([1:5]) as realvariable;
cph(1) : 33363.0,fixed;
cph(2):26790,fixed;
cph(3):2610.5,fixed;
cph(4):8896.0,fixed;
cph(5): 1169.0,fixed;

// Heat of vaporisation of water for a stage,kcal/gmol
Hvap as realvariable(10.47,fixed);

//Constants for water vapor pressure
AA as realvariable(73.649,fixed);
BB as realvariable(-7258.2,fixed);
CC as realvariable(-7.3037,fixed);
DD as realvariable(4.1653e-6,fixed);
EE as realvariable(2.0,fixed);

// Heat of desorption constants
aeq as realvariable(-4.59244,fixed);
beq as realvariable (34.21513,fixed);
ceq as realvariable (-3834.67,fixed);
deq as realvariable (-1747284,fixed);
eeq as realvariable (-1712091,fixed);
feq as realvariable (8186.474,fixed);

Tapp as realvariable(10,fixed);

Tg([1:ns+1]) as realvariable;

// heat capacity constants for solvent

cp([1:5]) as realvariable;

cp(1) : 276370.0,fixed;
cp(2):-2090.1,fixed;
cp(3):8.125,fixed;
cp(4):-0.014116,fixed;
cp(5): 9.3701e-006,fixed;
```

```
molalK as realvariable (5,fixed);
molalPZ as realvariable(5,fixed);
molalMEA as realvariable(0,fixed);
molaltotalk as realvariable;
co2moles as realvariable;
h2omoles as realvariable;


totalmoles as realvariable;

molaltotalk = molalK + molalPZ + molalMEA;


co2moles = ldgin * molaltotalk;

h2omoles = 1000/18.02;


totalmoles = co2moles + h2omoles + molaltotalk;


lamine(0) = molaltotalk * (L(0)/totalmoles);




//


//rate equations added here

// Constants for calculation of gas phase viscosity
// the constants are from the DIPPR database

//muco2 is the gas phase viscosity of co2, Pa-s
muco2([1:nS]) as realvariable;
amuco2 as realvariable(fixed,2.148e-6);
bmuco2 as realvariable(fixed,4.6e-1);
cmuco2 as realvariable(fixed,2.9e2);
dmuco2 as realvariable(fixed,0);
```

```
//muh2o is the gas phase viscosity of h2o - steam, Pa-s
muh2o([1:nS]) as realvariable;
amuh2o as realvariable(fixed,1.7096e-8);
bmuh2o as realvariable(fixed,1.1146);
cmuh2o as realvariable(fixed,0);
dmuh2o as realvariable(fixed,0);

// binary mixture gas viscosity
mugas([1:nS]) as realvariable;
//constants needed to calculate the viscosity of the binary gas mixture
phi12([1:nS]) as realvariable;
phi21([1:nS]) as realvariable;

// Molecular weights of gases
Mco2 as realvariable(fixed,44.1);
Mh2o as realvariable(fixed,18.02);
//Mgas is the molecular weight of the gas stream
Mgas([1:nS]) as realvariable;
//Pressure of the gas phase expressed in atm
Pgas([1:nS]) as realvariable;

//Universal Gas constant expressed as L atm K-1 mol -1
RR as realvariable(0.08206,fixed);

// Density of the gas phase kg/m3
rhog([1:nS]) as realvariable;

//Diffusivity of gas m2/s
Dv([1:nS]) as realvariable;

//Schmidt Number for the gas

Scg([1:nS]) as realvariable;


//critical constants for co2 and water

Pcco2 as pressure(72.9,fixed);
Pch2o as pressure(220,fixed);
Tcco2 as temperature(304.2,fixed);
Tch2o as temperature(647,fixed);
```

```
//density of the  liquid
rhol([0:2*nS]) as realvariable;

//equivalent weight of PZK expressed as a percent

we as realvariable(22.14,fixed);

//mul is the liquid phase viscosity , Pa-s
mul([0:2*nS]) as realvariable;
amul as realvariable;
bmul as realvariable;
cmul as realvariable;

//viscosity of liquid water Pa-s
muliqh2o([0:2*nS]) as realvariable;
amuliqh2o as realvariable (-5.2843e1,fixed);
bmuliqh2o as realvariable (3.7036e3,fixed);
cmuliqh2o as realvariable (5.8660,fixed);
dmuliqh2o as realvariable (-5.8790e-29,fixed);
emuliqh2o as realvariable (10,fixed);

// Diffusivity of co2 in pure water m2/s
Dco2pureh2o([0:2*nS]) as realvariable;

// Diffusivity of the liquid m2/s
Dl([0:2*nS]) as realvariable;

// Packing factor Fp
Fp as realvariable;

// Pressure drop at flooding in H2o per ft of packing
deltaPflood as realvariable;

//Total surface area of packing m2/m3
ap as realvariable;

// gas phase mass transfer coefficient from the Onda correlation (1968)
//the unit of kg is kmol/m2.s.Pa

ONDAkg([1:nS]) as realvariable;
```

```
//kg for the contactor kmol/m2.s.Pa
kg([1:nS]) as realvariable;

//liquid phase mass tranfer coefficient from the ONDA correlation (1968)
//the unit of ONDAkl is m/s

ONDAkl([1:nS]) as realvariable;

//kl of contactor m/s
kl([1:nS]) as realvariable;


//column area m2
AREA as realvariable(0.143,fixed);

//constant for kg calculation
CO as realvariable;

// wetted area based on Wilson (2004) experiments

awet([1:nS]) as realvariable;

// nominal diameter of random packing, m

dn as realvariable;

//wetted area from the Onda correlation (1968)
// the unit of ONDAaw is m2/m3

ONDAaw([1:nS]) as realvariable;

//critical surface tension N/m
surftenc as realvariable;

//surface tension of the liquid
surftenl as realvariable(0.04,fixed);

//superficial velocity of the liquid
sul([0:2*nS]) as realvariable;


//correction factor for liq density
```

```
corrrhol([0:2*nS]) as realvariable;

//correction factor for liq viscosity
corrmul([0:2*nS]) as realvariable;

//liquid to gas kinetic energy ratio

FLG as realvariable;

//density of liquid water
rholiqh2o ([0:2*nS]) as realvariable;

//constants in water density equation obtained from the DIPPR database

arh2o as realvariable(1.7863e1,fixed);
brh2o as realvariable(5.8606e1,fixed);
crh2o as realvariable(-9.5396e1,fixed);
drh2o as realvariable(2.1389e2,fixed);
erh2o as realvariable(-1.4126e2,fixed);


// Y axis of Leva GPDC plot

Ygeneral as realvariable;

//Superficial gas velocity m/s
sug([1:nS]) as realvariable;

//Flooding fraction
f as fraction(free,0.8);

//superficial gas velocity at flooding

uo as realvariable;

//Diameter of Tower m

DT as realvariable;
Factor as realvariable(fixed);
height([1:ns]) as realvariable;

//acceleration due to gravity m/s2
```

```
gg as realvariable(9.81,fixed);
//New variables
Nco2([1:ns]) as realvariable;
kgprime([1:ns]) as realvariable;
Pco2i([1:ns]) as realvariable;
KGbig([1:ns]) as realvariable;
Nh2o([1:ns]) as realvariable;
Ph2oi([1:ns]) as realvariable;
volseg([1:ns]) as realvariable;
awetted([1:ns]) as realvariable(10);
heightseg([1:ns]) as realvariable(1.5);
kla([1:ns]) as realvariable;
kga([1:ns]) as realvariable;

// heat tranfer coefficient in the gas phase
hg([1:ns]) as realvariable;
// heat capacity of the gas
cpgas([1:ns]) as realvariable;
//Prandtl number of the gas
Prgas([1:ns]) as realvariable;
//thermal conductivity
thermalk as realvariable (0.02,fixed);
//heat transfer at the interface
Qint([1:ns]) as realvariable;

gasvelflood as realvariable;//ft/s
sugflood as realvariable;

Flowrate as realvariable(fixed);//gallons per sec

// definition of rate equation variables end here

// rate equations start

//calculation of gas phase viscosities

for i in[1:nS] do
muco2(i)= (amuco2*(Tg(i)^bmuco2))/(1+(cmuco2/Tg(i))+(dmuco2/Tg(i)/Tg(i)));
muh2o(i)= (amuh2o*(Tg(i)^bmuh2o))/(1+(cmuh2o/Tg(i))+(dmuh2o/Tg(i)/Tg(i)));
mugas(i)=
(muco2(i)/(1+((yh2o(i)/yco2(i))*phi12(i))))+(muh2o(i)/(1+((yco2(i)/yh2o(i))*phi21(i))));
```

```
//calculation of constants in binary gas mixture viscosity equation
phi12(i) = ((1+(((muco2(i)/muh2o(i))^0.5)*
((Mh2o/Mco2)^0.25)))^2)/(2*sqrt(2.0)*((1+(Mco2/Mh2o))^0.5));
phi21(i) = ((1+(((muh2o(i)/muco2(i))^0.5)*
((Mco2/Mh2o)^0.25)))^2)/(2*sqrt(2.0)*((1+(Mh2o/Mco2))^0.5));

// calculation of gas density in kg/m3

Mgas(i)= (yco2(i)*Mco2)  + (yh2o(i)*Mh2o);
Pgas(i) = Pt(i)*0.009869;//This converts the pressure from kPa to atm//
rhog(i)= Pgas(i)*Mgas(i)/RR/Tg(i);



//Calculation of diffusivity of the gas m2/s from BSL
Dv(i)=(((3.64e-
4*((Tg(i)/sqrt(Tcco2*Tch2o))^2.334))*((Pcco2*Pch2o)^(1/3))*((Tcco2*Tch2o)^(5/12))*
sqrt((1/Mco2)+(1/Mh2o)))/Pgas(i))/10000;

//calculation of Schmidt number for the gas
Scg(i)= mugas(i)/rhog(i)/Dv(i);

endfor

amul = (2.79e-7 *we*we)-(2.04e-6*we) + 9.65e-5;
bmul = (-2e-4 *we*we)+(1.37e-3*we) - 7.23e-2;
cmul = (3.63e-2 *we*we)-(0.225*we) + 13.86;


for i in [0:2*ns] do

// density of the liquid kg/m3
rhol(i)= ((((-1.93e-6*we)-(4.74e-4))*T(i))+(9.787e-3*we)+1.147)*1000;

// viscosity of the liquid Pa-s
// 0.001 is the conversion factor from cP to Pa-s

mul(i)= ((amul*T(i)*T(i))+(bmul*T(i))+cmul)*0.001;

//viscosity of pure liquid water Pa-s
```

```
muliqh2o(i) = exp(amuliqh2o+(bmuliqh2o/T(i))+ (cmuliqh2o*loge(T(i))) +
(dmuliqh2o*(T(i)^emuliqh2o)));

//Diffusivity of co2 in pure water
//This is given by Versteeg and van Swaaij(1998)

Dco2pureh2o(i) = (0.0240 * exp(-2122/T(i)))*0.0001;

// calculation of the density of liquid water

rholiqh2o(i) = (arh2o + (brh2o*((1-(T(i)/Tch2o))^0.35)) + (crh2o*((1-
(T(i)/Tch2o))^0.67)) + (drh2o*((1-(T(i)/Tch2o))^1.0))+ (erh2o*((1-
(T(i)/Tch2o))^1.33)))*Mh2o;

// calculation of correction factor for liquid density

corrrhol(i) = (1.7995*(rholiqh2o(i)/rhol(i)))-0.6469;

// calculation of correction factor for liquid viscosity

corrmul(i) = (0.1119*(mul(i)/0.001))+0.6664;

// Diffusivity of co2 in the liquid m2/s
// This is based on the Ratcliff and Holdcroft correlation (1963)
// factor 0.82 proposed by Joosten and Danckwerts (1972)

Dl(i) = Dco2pureh2o(i) / ((mul(i)/ muliqh2o(i))^0.82);

//calculation of the superficial velocity of the liquid
sul(i)=flowrate * 0.00378/AREA;
endfor

//for i in [1:ns] do
// calculation of liquid to gas kinetic energy ratio

FLG^2 = (L(2*0)*25.5/G(ns)/Mgas(ns))^2*(rhog(ns)/rhol(2*0));

deltaPpacking as realvariable;
gasvel as realvariable;

/*
// calculation of the superficial velocity of the gas m/s
```

```
Ygeneral = (-0.3148 * loge(FLG)) + 0.7936  ;
//deltaP as realvariable;

f = sug(ns)/sugflood;

//deltaPpacking = f * deltaPflood;

//f = 0.8;

Csb as realvariable;

Ygeneral = Csb * (Fp^0.5)
*(((amul*T(0)*T(0))+(bmul*T(0))+cmul)*1000/rhol(2*0))^0.05;

Csb = gasvelflood  / sqrt(((rhol(2*0))-(rhog(ns)))/(rhog(ns)));

//(gasvel)^2 = (Ygeneral*32.2*1000/Fp/rhog(ns)/corrrhol(2*0)/corrmul(2*0));

sugflood = gasvelflood * 0.3048;
*/

(gasvel)^2 = (Ygeneral*32.2*1000/Fp/rhog(ns)/corrrhol(2*0)/corrmul(2*0));
sugflood = gasvel *0.3048;

sug(ns) = f * sugflood;

DT = (4 * G(ns) * Mgas(ns)/f/1000/sugflood/3.142/rhog(ns))^0.5;
Ygeneral = 0.0238 * (FLG^-0.5666);

//sug(ns) = G(ns) * Mgas(ns)/1000/rhog(ns)/area;

for i in [1:ns-1] do
sug(i) = G(i) * Mgas(i)/1000/rhog(i)/AREA;


endfor

// calculation of pressure drop at flooding
//deltaPflood = 0.115 * (fp^0.7);

//Area of the column, m2
AREA = 3.142*DT*DT/4;
```

```
for i in [1:ns-1] do

//wetted area based on ONDA m2/m3
///*
ONDAaw(i)=ap*(1-exp(-
1.45*((surftenc/surftenl)^0.75)*((rhol(2*i)*sul(2*i)/ap/mul(2*i))^0.1)*((ap*sul(2*i)*sul(
2*i)/gg)^-0.05)*((rhol(2*i)*sul(2*i)*sul(2*i)/ap/surftenl)^0.2)));
// calculation of the gas phase mass transfer coeficient kg in units of kmol/m2.s.Pa

ONDAkg(i)=
CO*((G(i)*Mgas(i)/1000/AREA/ONDAaw(i)/mugas(i))^0.7)*((Scg(i))^0.33)*((ap*dn)^-
2.0)* (ap*Dv(i)/8314/Tg(i));

//wetted area from Wilson (2004)
//awet(i) = ONDAaw(i)+ (ONDAaw(i)*(-6.47 +
(5.9*((rhog(i)*sug(i)/ap/mugas(i))^0.06)) + (8.49e-4*((ap*sul(2*i)*sul(2*i)/gg)^-0.53))
+ (7.28e-4*((rhol(2*i)*sul(2*i)*sul(2*i)/ap/surftenl)^1.13))- (3.97*((ap*dn)^-0.41))));
//awet(i) = ONDAaw(i)* (5.28 - (7.77*((G(i)*Mgas(i)/1000/AREA/ap/mugas(i))^-
0.08))+ (2.07e-9* (((L(2*i)*25.5/1000/AREA)^2)*ap/rhol(2*i) / rhol(2*i)/gg)^-1.54) +
(1.41e-9 * (((L(2*i)*25.5/1000/AREA)/ap/mul(2*i))^1.03)) + (1.09e-3* ((ap*dn)^3)));
//awet(i) =ap * (0.518756 + (0.008482*flowrate*60*0.093/area) + (0.077196 *
sug(i)/0.3048));
//awet(i) = exp(4.54) * ((G(i) * Mgas(i)/1000/area)^0.121) *
((L(i)*25.5/1000/area)^0.148);
//New correlation based on SRP wetted area data

awet(i) = exp(4.733) * ((sug(i))^0.061) * ((L(i)*25.5/1000/area)^0.148);

//calculation of gas phase mass transfer coefficient of the packing kmol/m2.s.Pa

kg(i)= ONDAkg(i)*ONDAaw(i)/awet(i);
//kg(i) = 3e-9;
kga(i) = kg(i) * awet(i);//unit kmol/s.Pa.m3

// calculation of liquid phase mass transfer coefficient of the packing m/s
ONDAkl(i) = 0.0051 * ((mul(2*i)*gg/rhol(2*i))^0.333) *
((L(2*i)*25.5/1000/AREA/ONDAaw(i)/mul(2*i))^0.67) *
((Dl(2*i)*rhol(2*i)/mul(2*i))^0.5)* ((ap*dn)^0.4);

//calculation of liquid phase mass transfer coefficient of the packing m/s
```

```
kl(i) = ONDAkl(i)*ONDAaw(i)/awet(i);
kla(i) = kl(i) * awet(i);
//Factor / awet(i) = height(i) * AREA;
//*/
 //Flux based on the gas phase
///*
Nco2(i) = ((kg(i)*1000 * Pt (i) * loge (Pco2i(i)/Pco2(i))) + Nh2o(i)) * (Pco2i(i) -
Pco2(i))/(Pco2i(i) - Pco2(i) + (Pt(i) * loge(Pco2i(i)/Pco2(i))));

Nco2(i) = KGbig(i)*1000*(Pco2e(2*i)-Pco2(i));


//Nh2o(i) = ((kg(i)*1000 * Pt (i) * loge (Ph2oi(i)/Ph2o(i))) + Nco2(i)) * (Ph2oi(i) -
Ph2o(i))/(Ph2oi(i) - Ph2o(i) + (Pt(i) * loge(Ph2oi(i)/Ph2o(i))));

Ph2oi(i) + Pco2i(i) = Pt(i);

Nco2(i) = kgprime(i) *1000* (Pco2e(2*i) - Pco2i(i));

kgprime(i) = exp(-46.6868 + (-11.5447*ldg(2*i)) + (8197.802/T(2*i)) + (10050.46* kl(i))
+ (0.012346*Pco2i(i)) + (69294.95 * ldg(2*i)/T(2*i))+(-3182533*kl(i)/T(2*i))+(-
6.06135*Pco2i(i)/T(2*i)) +(-87538.9*ldg(2*i)*ldg(2*i)/T(2*i))+(-
2e7*ldg(2*i)/T(2*i)/T(2*i))+(26254990*ldg(2*i)*ldg(2*i)/T(2*i)/T(2*i)));

KGbig (i) = 1 / ((1/kg(i)) + (1/kgprime(i)));
lco2(2*i-1) = lco2(2*i) + (Nco2(i) * awetted(i) *1000);
//lh2o(2*i-1) = lh2o(2*i) + (Nh2o(i) * awetted(i) *1000);
volseg(i) = awetted(i) / awet(i);
volseg(i) = heightseg(i)*AREA;

//*/
endfor

/*
for i in [1:ns] do
cpgas(i) = (cpco2(i) *4184*1000* G(i) * yco2(i)/44) + (cph2o(i) *4184*1000* G(i) *
yh2o(i) /18.02);
Prgas(i) = cpgas(i) * mugas(i)/ thermalk;
kg(i) * 1000 *Mgas(i) * Pco2(i) * (Scg(i)^(2/3)) = hg(i) * (Prgas(i)^(2/3))/ cpgas(i);
Qint(i) = hg(i)* awetted(i) * (T(2*i) - Tg(i)) * 0.000239;
//(L(2*i-1)*cpL(2*i-1)*(T(2*i-1)-Tref)) - Qint(i) = (L(2*i)*cpL(2*i)*(T(2*i)-Tref));
```

```
endfor
*/



//recall dn is in meters

if dn <= 0.015 then
CO = 2.00;
else
CO = 5.23;
endif


if Contactor == "1in Pall Rings" then
dn = 0.025;
ap = 223.5;//Billet
Fp = 48;//AIChE cheresources
surftenc=0.075;
else
if Contactor == "2in Pall Rings" then
dn = 0.051;
ap = 115;
Fp = 20;
surftenc=0.075;


else
if Contactor == "IMTP #25" then
dn = 0.025;
ap = 230;
Fp = 41;
surftenc=0.075;
else
if Contactor == "IMTP #40" then
dn = 0.040;
ap = 145;
Fp = 24;
surftenc=0.075;
else

if Contactor == "CMR #2" then
```

```
dn = 0.051;
ap = 148;
Fp = 80;
surftenc=0.075;
else

if Contactor == "CMR #2A" then
dn = 0.051;
ap = 106;
Fp = 22;
surftenc=0.075;
endif
endif
endif
endif
endif
endif


// rate equations end



nn1 = (k/(k-1))*polyeff;

for i in [0:2*ns] do

L(i) = lco2(i) + lh2o(i) + lamine(i);

ldg(i) = lco2(i)/lamine(i);

endfor

for i in [0:ns-1] do
S(i) = sco2(i) + sh2o(i) + samine(i);
endfor

for i in [0:ns-1] do
lco2((2*i)+1) = lco2(2*i) + sco2(i);
lh2o((2*i)+1) = lh2o(2*i) + sh2o(i);
lamine((2*i)+1) = lamine(2*i) + samine(i);
endfor
```

```
for i in [0:2*ns] do

CpL(i) = 0.888*((cp(1) + (cp(2)*T(i))  + (cp(3) * (T(i)^2))+ (cp(4)*(T(i)^3))+
(cp(5)*(T(i)^4)))*(0.000000239));

endfor

for i in [0:ns-1] do
CpS(i) = (cp(1) + (cp(2)*Ts(i))  + (cp(3) * (Ts(i)^2))+ (cp(4)*(Ts(i)^3))+
(cp(5)*(Ts(i)^4)))*(0.000000239);
endfor


//Mixing operation

 for i in [0:ns-1] do
(L(2*i) * CpL(2*i) * (T(2*i)-Tref)) + (S(i)*CpS(i)*(Ts(i)-Tref)) = L(2*i+1) *
CpL(2*i+1) * (T(2*i+1)-Tref);
endfor

// heat capacity calculation for the gas phase

for i in [1:ns] do
cpco2(i)=(cpc(1) + (cpc(2)*(((cpc(3)/Tg(i))
/sinh(cpc(3)/Tg(i)))^2))+(cpc(4)*(((cpc(5)/Tg(i)) /cosh(cpc(5)/Tg(i)))^2)))*0.000000239;
cph2o(i)=(cph(1) + (cph(2)*(((cph(3)/Tg(i))
/sinh(cph(3)/Tg(i)))^2))+(cph(4)*(((cph(5)/Tg(i))
/cosh(cph(5)/Tg(i)))^2)))*0.000000239;
endfor


cpco2(ns+1):0,fixed;
cph2o(ns+1):0,fixed;

for i in [1:ns] do
Tg(i) = T(2*i);
endfor


// Material balance
```

```
for i in [1:ns] do
lco2(2*i-1) + (G(i+1)*yco2(i+1)) = lco2(2*i) + (G(i) * yco2(i));

lh2o(2*i-1) + (G(i+1)*yh2o(i+1)) = lh2o(2*i) + (G(i) * yh2o(i));

lamine(2*i-1) = lamine(2*i) ;

endfor


yco2(ns+1):0,fixed;
yh2o(ns+1):0,fixed;
dH(ns+1):0,fixed;

//temperature at the interface
Ti([1:ns]) as realvariable(330,free);


// energy balance
for i in [1:ns] do
(G(i+1)*((yh2o(i+1)*(Hvap+(cph2o(i+1)*(Tg(i+1)-
Tref))))+(yco2(i+1)*((dH(i+1)/1000)+(cpco2(i+1)*(Tg(i+1)-Tref))))))+(L(2*i-
1)*cpL(2*i-1)*(T(2*i-1)-Tref))+ Q(i)+ Qcomp(i) + Qx(i)  =(L(2*i)*cpL(2*i)*(T(2*i)-
Tref))+G(i)*(((yh2o(i))*(Hvap+(cph2o(i)*(Tg(i)-
Tref))))+((yco2(i))*((dH(i)/1000)+(cpco2(i)*(Tg(i)-Tref)))));
endfor


act1 as realvariable (0.97752477,fixed);
act2 as realvariable (-0.049949161,fixed);
act3 as realvariable (-31.55650762,fixed);
act([1:ns]) as realvariable;

for i in [1:ns] do
act(i) = act1 + (act2* ldg(2*i)) + (act3 * (1/T(2*i)));
endfor

//equilibrum reboiler assumption
//Pco2(ns)= Pco2e(2*ns);
Ph2o(ns)= act(ns) * ((exp(AA+(BB/T(2*ns))+(CC*loge(T(2*ns)))+
(DD*(T(2*ns)^EE))))/1000);
```

```
Pco2(ns)= Pco2(ns+1) + (meff(ns)*(Pco2e(2*ns) - Pco2(ns+1)));

for i in [1:ns-1] do

//Pco2(i)= Pco2(i+1) + (meff(i)*(Pco2e(2*i) - Pco2(i+1)));
//Ph2oi(i)= (exp(AA+(BB/Ti(i))+(CC*loge(Ti(i)))+ (DD*(Ti(i)^EE))))/1000;
Ph2o(i)= act(i) * ((exp(AA+(BB/T(2*i))+(CC*loge(T(2*i)))+
(DD*(T(2*i)^EE))))/1000);
endfor



/*
for i in [1:ns-1] do
meff(i):0.4;
endfor
*/
Tg(ns+1) : 0,fixed;
Pco2(ns+1):0,fixed;

//Calculation of heat of desorption of solvent based on generic constants
for i in [1:ns] do
dH(i) = (ceq+(2*deq*ldg(2*i)*ldg(2*i)/T(2*i)) + (2*eeq*ldg(2*i)/T(2*i)) +
(feq*ldg(2*i)) )* -1.987;
endfor


// Total pressure on a section
for i in [1:ns] do
Pt(i) = Pco2(i) + Ph2o(i);
endfor

// vapor mole fractions

for i in [1:ns] do

yco2(i) = Pco2(i)/Pt(i);

yh2o(i) = Ph2o(i)/ Pt(i);
```

```
endfor



G(ns+1):0,fixed;

// equilibrium vapor pressure of CO2 expression
for i in [0:2*ns] do
Pco2e(i) = exp(aeq + (beq*ldg(i)) + (ceq/T(i))
+(deq*ldg(i)*ldg(i)/T(i)/T(i))+(eeq*ldg(i)/T(i)/T(i))+(feq*ldg(i)/T(i)));
endfor


//Normalized reboiler duty
Qreboiler = Q(ns)/G(1)/yco2(1);

//compression work

for i in [1:ns-1] do
Wcomp(i) = (G(i+1)*1.987*Tg(i+1)*nn1*(((Pt(i)/Pt(i+1))^(1/nn1))-
1.0))/(1000*compeff);
Qcomp(i)= Wcomp(i);
endfor

Wcomp(ns):0,fixed;
Qcomp(ns):0,fixed;

for i in [1:ns-1] do
Q(i):0,fixed;
endfor



for i in [0:ns-1] do
Ts(i):0,fixed;
S(i):0,fixed;
sco2(i):0,fixed;
samine(i):0,fixed;
endfor
```

```
meff(ns):1,fixed;


for i in [1:ns-1] do
Q(i) : 0,fixed;
endfor

Treb = T(2*ns);

Qkcal = Q(ns);

ldgin = ldg(0);

ldgout = ldg(2*ns);

Tcond = Treb +10;


/*
for i in [1:ns-1] do
//Qx(i) =0;

Qx(i) = UA * ((Tx(i)-T(2*i))-(Tx(i+1)-T(2*i))) / (loge((Tx(i)-T(2*i))/(Tx(i+1)-T(2*i))));

Qx(i) = L(2*i) * CpL(2*i) * (Tx(i+1)-Tx(i));

Txdiff(i) = Tx(i)- T(2*i);

endfor

Qx(ns)=0;

Tx(1) = T(0)+Tapp;

Tx(ns) = T(2*ns);
*/

for i in [1:ns] do
Qx(i) :0,fixed;
endfor
```

```
T(0)+ Tapp = T(2*ns);

L(0) = 0.00378 * flowrate / (0.0255/rhol(0));

LD([0:ns]) as realvariable;

Temp([0:ns]) as realvariable;

Pco2eq([0:ns]) as realvariable;

for i in [0:ns] do
LD(i) = ldg(2*i);
Temp(i) = T(2*i);
Pco2eq(i) = Pco2e(2*i);
endfor

Totalawettedarea as realvariable;
Totalvolseg as realvariable;

Totalawettedarea = sigma(awetted([1:ns-1]));
Totalvolseg = sigma(volseg([1:ns-1]));


heightseg(1):fixed;
for i in [2:ns-1] do
heightseg(i) = heightseg(1);
endfor

Pt(ns):fixed;
for i in [1:ns-1] do
Pt(i) = Pt(i+1) - (f*f*1.63 * heightseg(i));
endfor

// Pump head
Pumphead as realvariable;
// Pump work kcal/s
Wpump as realvariable;
//Equivalent work of the reboiler
Wreboiler as realvariable;
//Equivalent work of internal compression
Wintcomp as realvariable;
// stripperCO2 flow
```

```
stripperCO2flow as realvariable;
Pumpeff as realvariable(0.65,fixed);

stripperCO2flow = G(1) * yco2(1);
totalheightseg as realvariable;

// The terms on the right hand side of the pump head equation are
// The head due to DPstr-abs, head due to height of packing in stripper
// head due to Dpabs-str and  Dp across cross exchanger, sump and above feed point in
both
//absorber and stripper
Pumphead = ((((Pt(1) - 101.325)*1000) / (rhol(0)*gg)) + totalheightseg)+ (((101.325 -
Pt(1))*1000) / (rhol(2*ns)*gg)) + 36.6 ;

totalheightseg = sigma(heightseg([1:ns-1]));

Wpump = ((flowrate * 0.00378541178)* rhol(0)*gg *Pumphead/Pumpeff)*(0.000239);

Wreboiler = (0.75*(Q(ns)*((Tcond - Tcool)/Tcond))) ;

Wintcomp = (sigma(Qcomp([1:ns])));



//Equivalent work , kcal

Weq1 = (0.75*(Q(ns)*((Tcond - Tcool)/Tcond)))   + (sigma(Qcomp([1:ns]))) + Wpump;

//Equivalent work, kcal/gmol CO2

Weq2 = Weq1 / (G(1)*yco2(1));

end
```

Appendix D

Appendices D-1 through D-5 were obtained from The University of Texas at Austin Separation Research Program (UTSRP). The drawings have been reproduced with permission from the UTSRP.

Appendix D-1: Detailed Process Flow Diagram for Pilot Plant

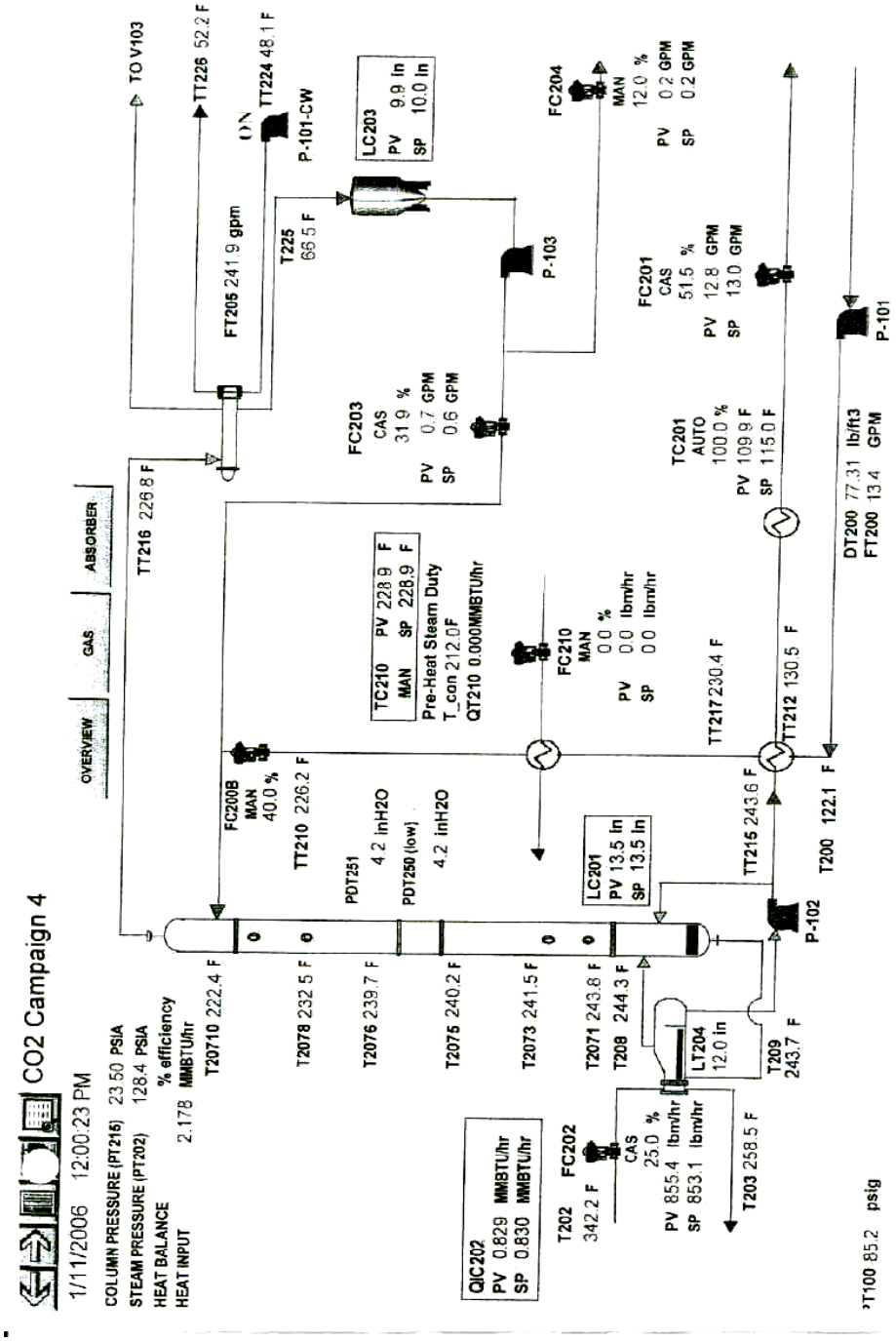

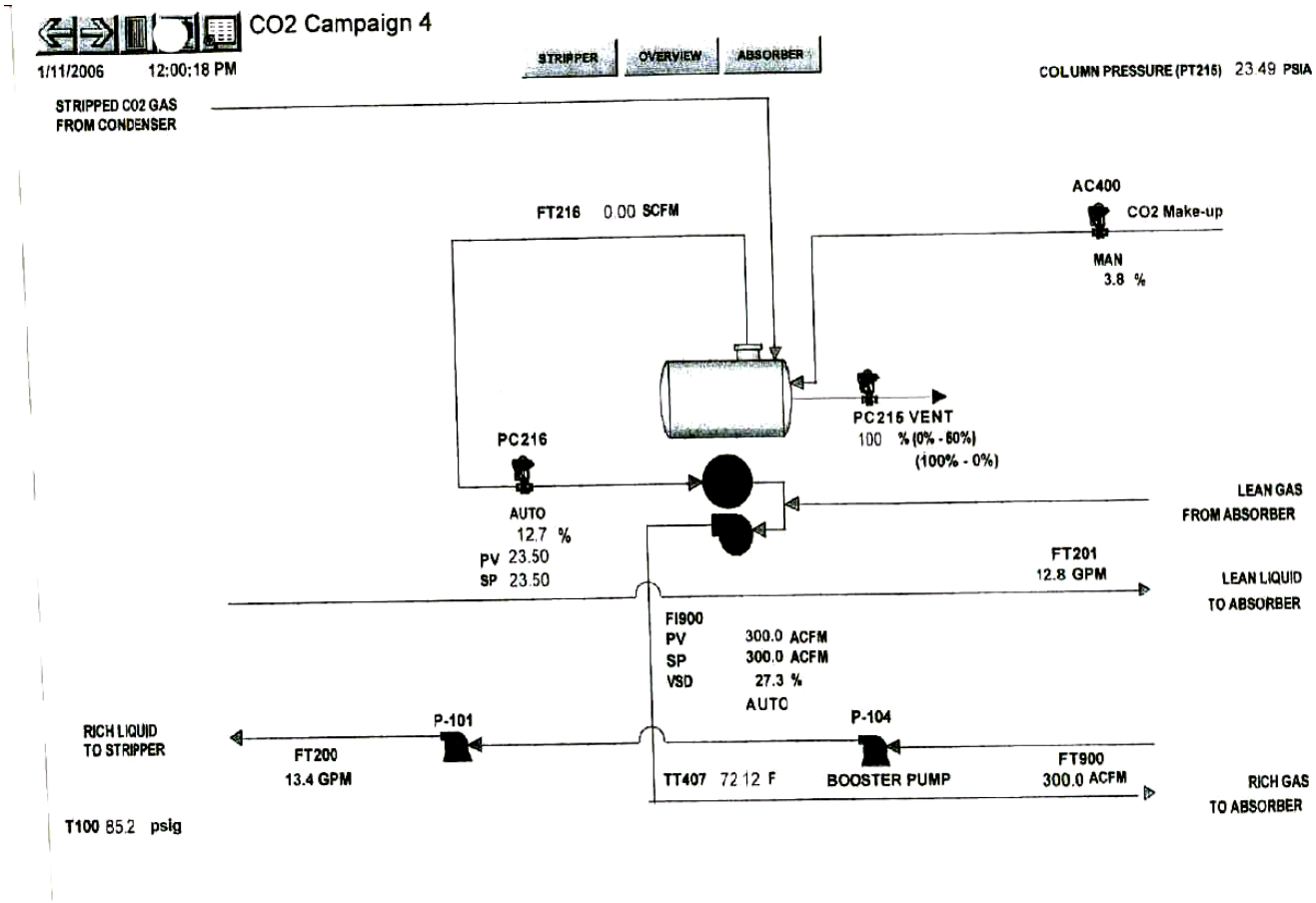
CO2 Campaign 4
1/11/2006 12:00:18 PM
STRIPPER
OVERVIEW
ABSORBER
COLUMN PRESSURE (PT215) 23.49 PSIA
STRIPPED CO2 GAS FROM CONDENSER
FT216 0.00 SCFM
AC400
CO2 Make-up
MAN
3.8 %
PC215 VENT
100 % (0% - 50%)
(100% - 0%)
PC216
AUTO
12.7 %
PV 23.50
SP 23.50
LEAN GAS FROM ABSORBER
FT201
12.8 GPM
LEAN LIQUID TO ABSORBER
FI900
PV 300.0 ACFM
SP 300.0 ACFM
VSD 27.3 %
AUTO
RICH LIQUID TO STRIPPER
P-101
FT200
13.4 GPM
P-104
TT407 72.12 F
BOOSTER PUMP
FT900
300.0 ACFM
RICH GAS TO ABSORBER
T100 85.2 psig

Appendix D-2: Detailed Distributor Drawings

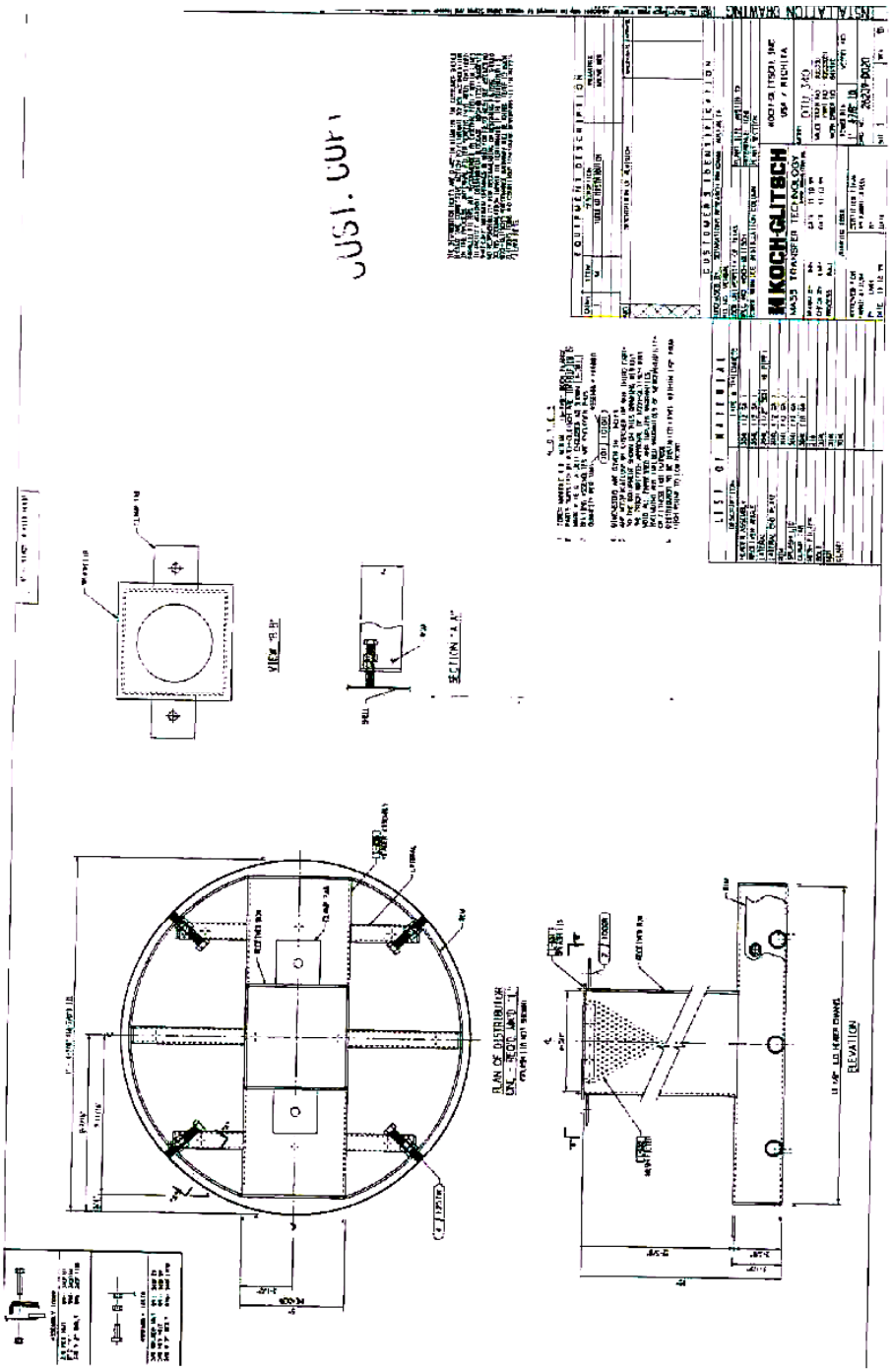

Appendix D-3: Detailed Reboiler and Tube Drawings

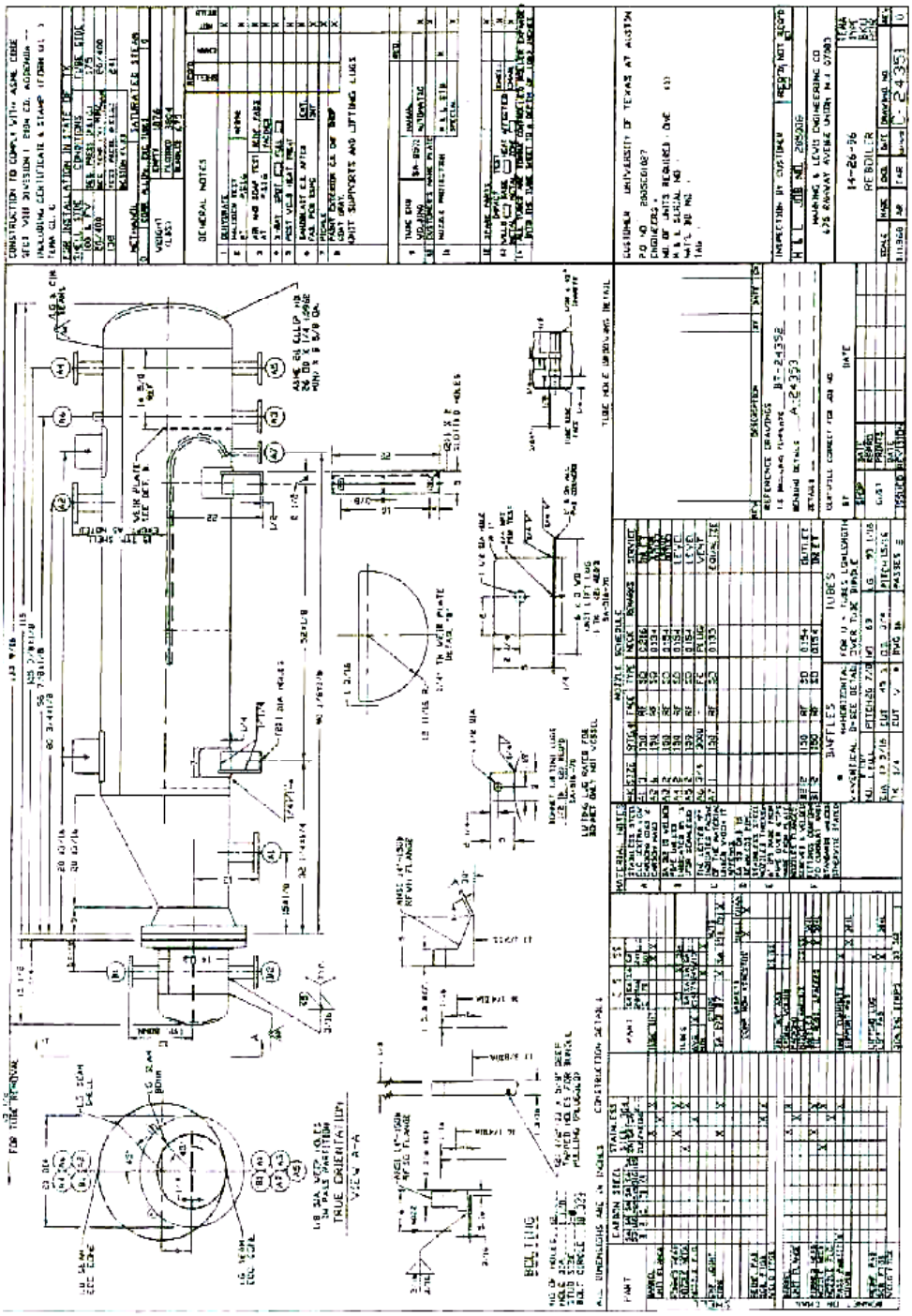

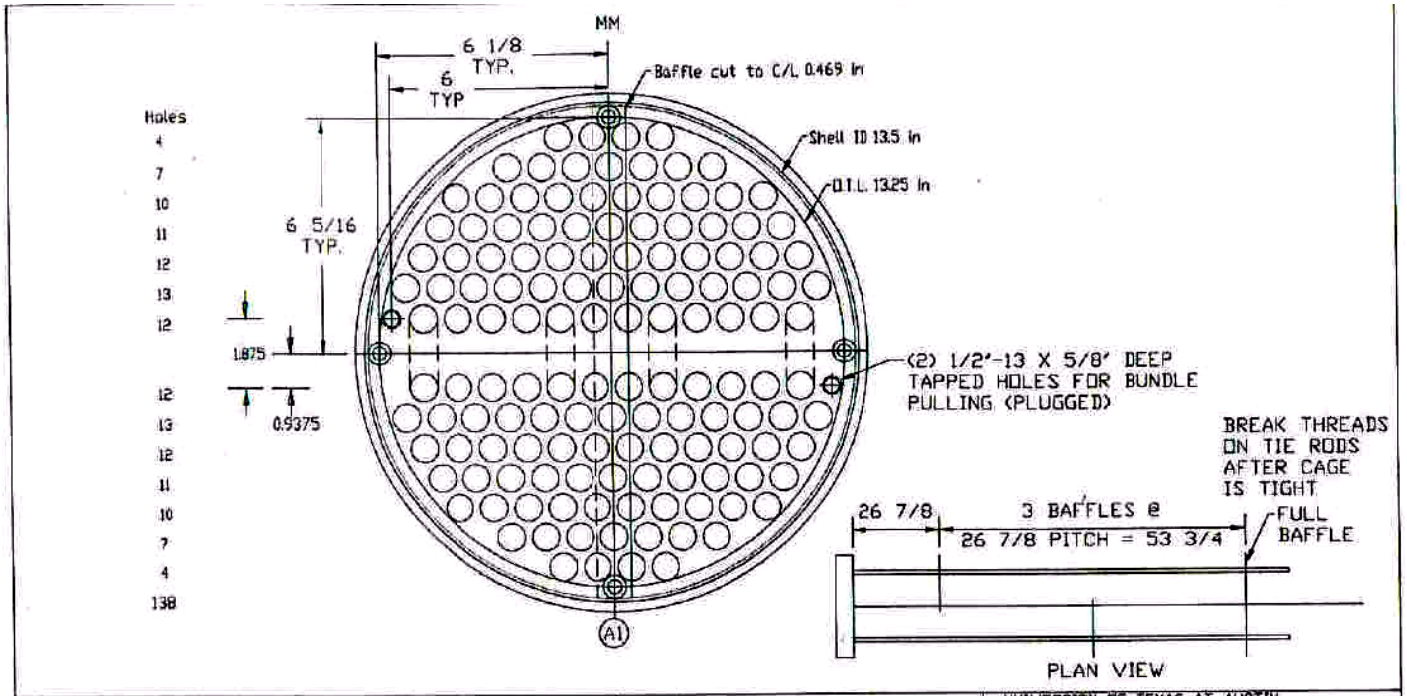

Design Specifications			
Number of Tube Holes	138	Tube Type	U-TUBE
Tube Outside Diameter	0.75 in	Hole Dia	.76562 +.0005 -.0000
Tube Pitch	0.9375 in	Spacer Size	5/8
Tube Pattern	Rotated Tri	Imp. Nozzle	-
Tube Passes	2	Baffle Mat'l	SS-304L
Number of Tie Rods	4	Ht. Ent. Area	.566
Tie Rod Diameter	0.375 in	Ht. Exit Area	----
Baffle Diameter	13.3125 in	Baffle TK.	1/4
Baffle Type	Single Segmental	No. of Baffles	3
Baffle Cut	45%	JOB NO.	205008
		REF DWG. NO.	C-24351

Notes:

Scale: .2736 / 3.6549

Rev.	Date	Description	Dwg	Ckd	Appd

UNIVERSITY OF TEXAS AT AUSTIN
14-26-96 REBOILER
P.O. NO. : 2005C01027
ITEM NO. : H-102-DI

MANNING & LEWIS ENG. CO.
675 Rahway Avenue
Union, NJ 07083

MADE BY AR
CKD. TAR
DATE 3/15/05

Tube Layout

Dwg No. BT-24352 Rev. 0

Appendix D-4:Detailed Cross Exchanger Drawing

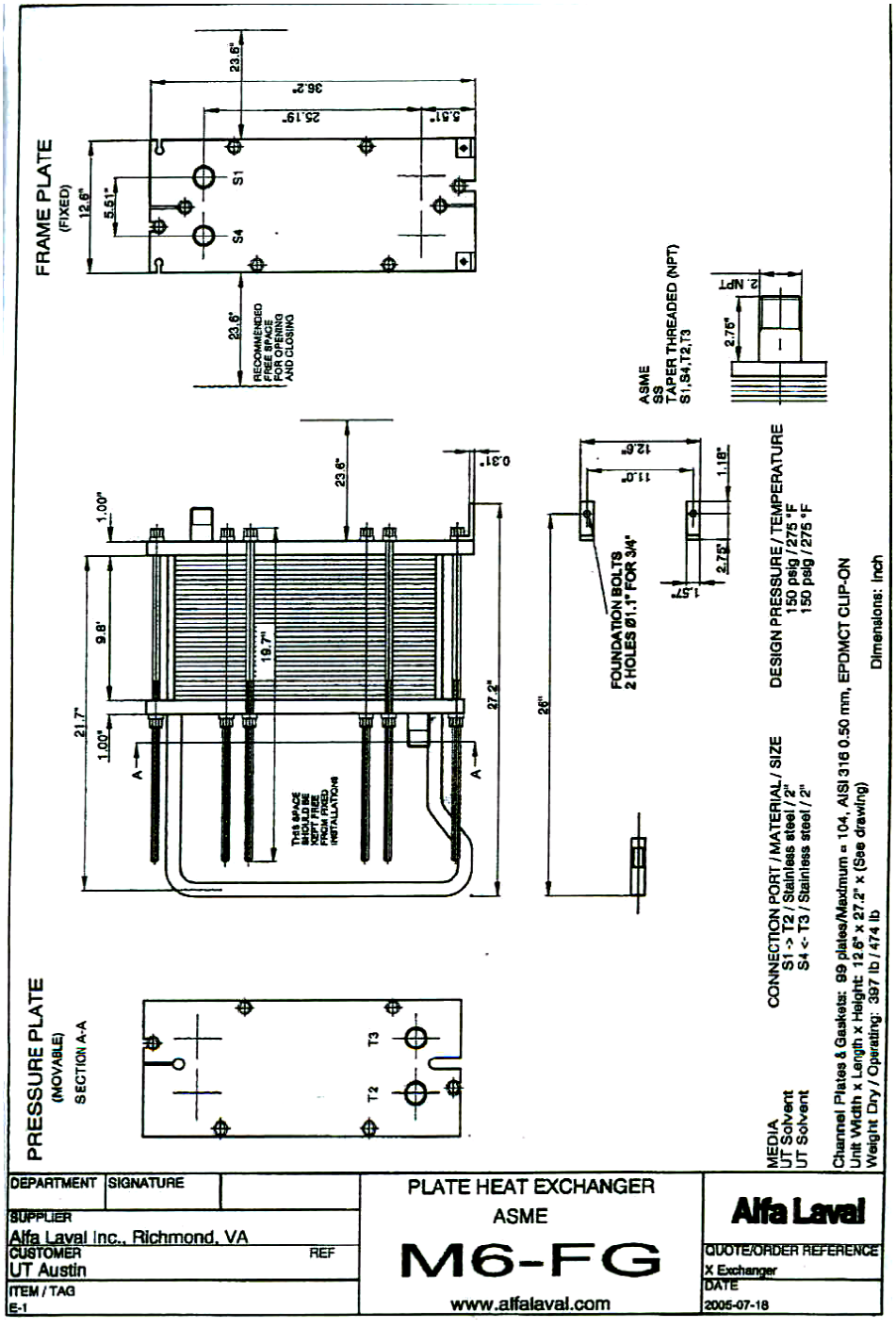

Appendix D-5: Detailed Condenser Drawings

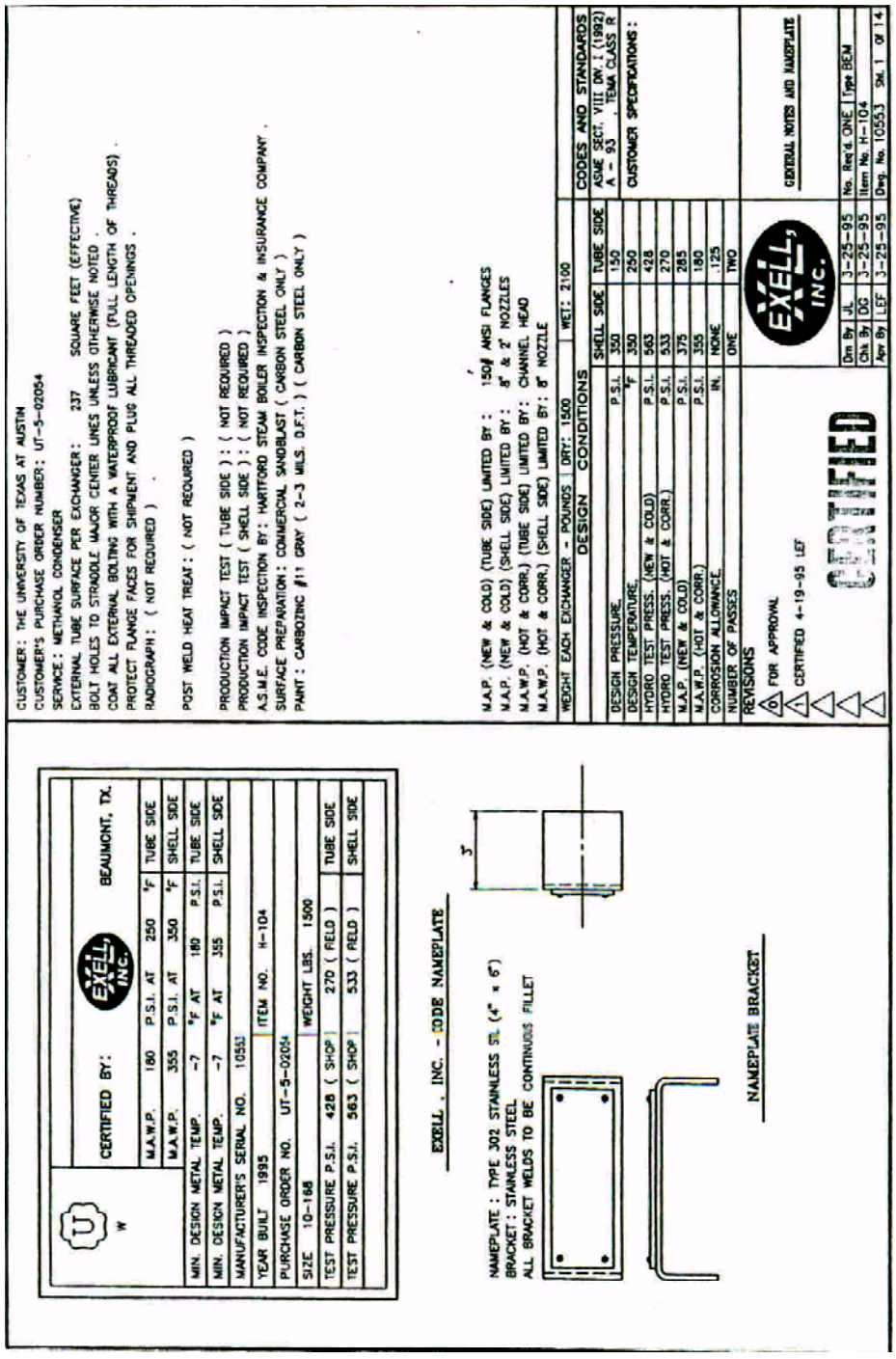

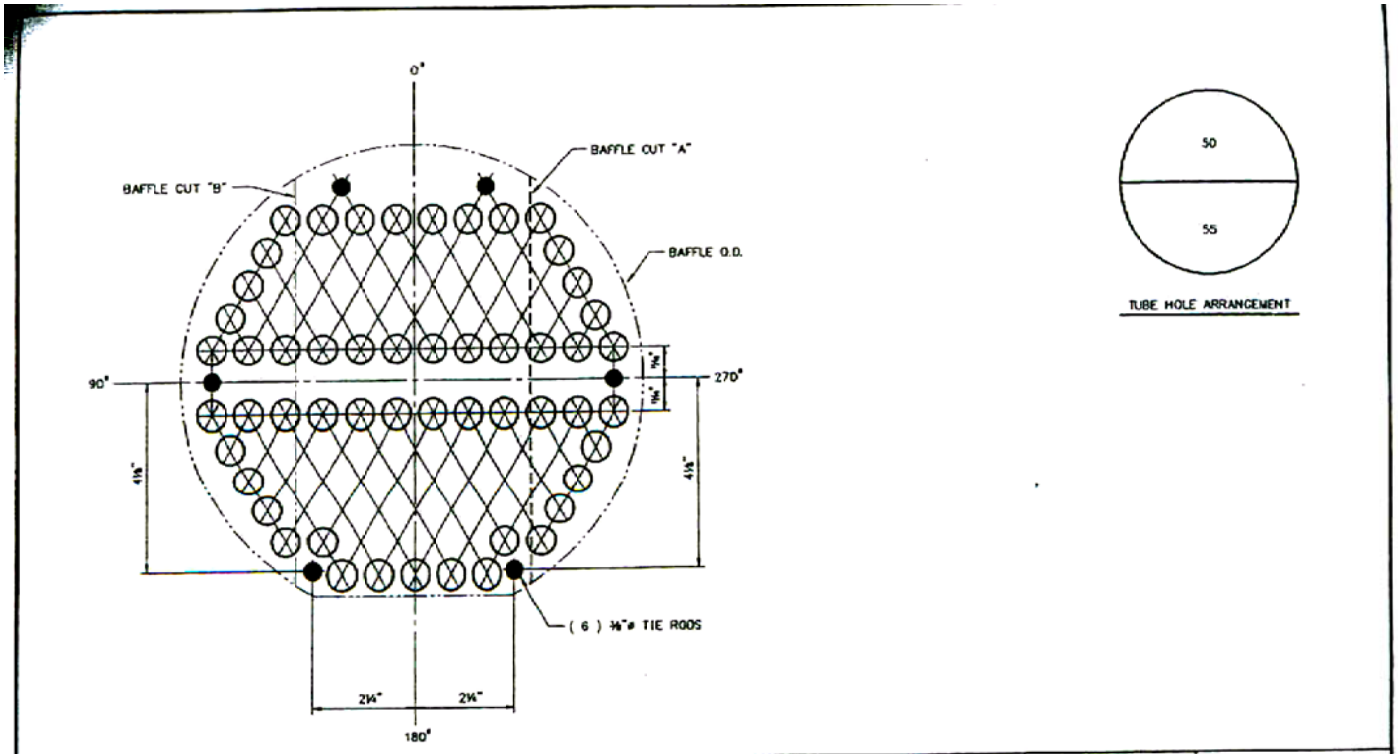
0°
BAFFLE CUT "A"
BAFFLE CUT "B"
BAFFLE O.D.
90°
270°
4⅛"
4⅛"
¾"
¾"
(6) ⅜"ø TIE RODS
2¼"
2¼"
180°
50
55
TUBE HOLE ARRANGEMENT
NOTES
1. NUMBER OF TUBES = 105
2. SIZE OF TUBES = ¾"
3. TUBE PITCH = 1 3/16" TRI.
4. CENTERLINE OF OUTERMOST TUBE = 9.0428"
5. LAYOUT IS VIEWED FROM SHELL SIDE OF TUBESHEET #9
REVISIONS
0 FOR APPROVAL
1 CERTIFIED 4-19-95 LEF
EXELL, INC.
TUBE HOLE LAYOUT
Drn By JL 4-4-95
Chk By DG 4-4-95
Apv By LEF 4-4-95
No. Req'd. ONE Type BEM
Item No. H-104
Dwg. No. 10553 Sht. 7 of 14

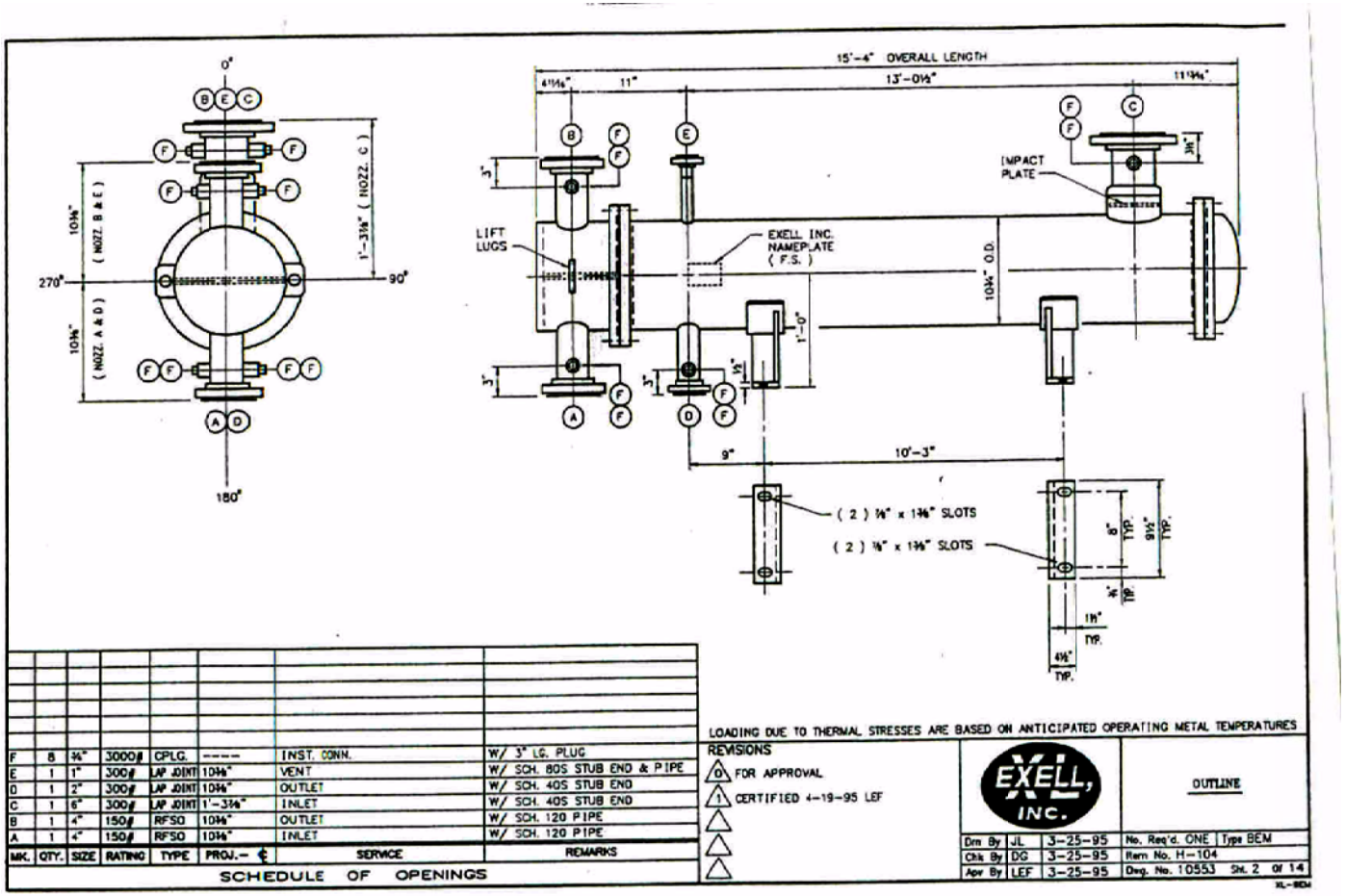

MK.	QTY.	SIZE	RATING	TYPE	PROJ.– ℄	SERVICE	REMARKS
F	8	3/4"	3000#	CPLG.	----	INST. CONN.	W/ 3" LG. PLUG
E	1	1"	300#	LAP JOINT	10 3/4"	VENT	W/ SCH. 80S STUB END & PIPE
D	1	2"	300#	LAP JOINT	10 3/4"	OUTLET	W/ SCH. 40S STUB END
C	1	6"	300#	LAP JOINT	1'-3 3/8"	INLET	W/ SCH. 40S STUB END
B	1	4"	150#	RFSO	10 3/4"	OUTLET	W/ SCH. 120 PIPE
A	1	4"	150#	RFSO	10 3/4"	INLET	W/ SCH. 120 PIPE

SCHEDULE OF OPENINGS

LOADING DUE TO THERMAL STRESSES ARE BASED ON ANTICIPATED OPERATING METAL TEMPERATURES

REVISIONS
0 FOR APPROVAL
1 CERTIFIED 4-19-95 LEF

EXELL, INC.

OUTLINE

Drn By	JL	3-25-95	No. Req'd. ONE | Type BEM
Chk By	DG	3-25-95	Item No. H-104
Apv By	LEF	3-25-95	Dwg. No. 10553 Sht. 2 of 14

Appendix D-6: Sample Calculation of Actual Reboiler Duty

This appendix details a sample calculation for the actual normalized reboiler duty (kJ/gmol CO_2) obtained from the pilot plant tests. The case shown is that for run 5.13. Table 5-6 shows the detailed stripper test results with 5m K^+/2.5m PZ.

The steam rate (QIC202) = 0.8687 MMBTU/hr = 868708.82 Btu/hr

The enthalpy of the rich feed is calculated by:

$\Delta H_{rich} = L_{rich} * C_{p,rich} * (T_{rich} - T_{lean})$

The actual rich solution flow rate is the sum of the absorber rich flow rate (FT200) and the stripper return feed (FT203).

where L_{rich} = FT200 +FT203 (flow rates in gpm)

= (23.86 + 0.46) *60 * 0.13368 * (density of FT200) [=] lb/hr

$C_{p,rich}$ = 0.81 Btu/lb-^oF

$(T_{rich} - T_{lean})$ = 241 – 221 ^oF

A material and energy balance across the mixing point of the absorber rich stream and the stripper water reflux stream calculates the rich stream temperature.

The enthalpy of the lean stream is calculated by:

$\Delta H_{lean} = L_{lean} * C_{p,lean} * (T_{lean} - T_{lean})$

= 0

The sensible heat contribution to the reboiler duty is given as:

$Q_{sensible} = \Delta H_{rich} - \Delta H_{lean}$

The heat consumed in the overhead condenser is calculated from an energy balance around the condenser.

$Q_{cond} = Q_{overhead} - Q_{CO2,overhead} - Q_{H2O\ reflux}$

$Q_{overhead}$ [=] Btu/hr =((FT216*44.01/6.32)*(0.002)*(TT216-T209)) +
(FT216*44.01/6.32*15*3.96566831/44.01/0.0022) +
(((FT203+FT204)*60*0.133680556*62.4*1*(TT216-
T209))+(((FT203+FT204)*60*0.133680556*62.4*10*3.96566831/18.02/0.0022)))
= 383092

FT216 is the CO_2 flow in scfm
TT216 is the Overhead vapor temperature
T209 is the lean solution temperature in ^oF
FT203 is the water reflux rate (gpm)
FT204 is the water that makes it through the condenser with the CO_2

$Q_{water\ reflux}$ [=] Btu/hr = (FT203+FT204)*(60*0.133680556)*62.4*1*(T225-T209)
= -48625

T225 is the condensing liquid temperature (^oF)

$Q_{CO2,overhead}$ = =((FT216*44.01/6.32)*(0.002)*(T225-T209)) +
(FT216*44.01/6.32*15*3.96566831/44.01/0.0022)
= 119924

Q_{cond} = 311793 Btu/hr

The steam rate $Q_{steam\ rate}$ is given by:

$Q_{steam\ rate} = Q_{sensible} + Q_{cond} + Q_{CO2,overhead} + Q_{loss}$

From where the heat loss can be calculated as:

$Q_{loss} = Q_{reboiler} - Q_{sensible} - Q_{cond} - Q_{CO2,overhead}$

Q_{loss} = 197180 Btu/hr

Actual steam rate (measured steam rate –heat loss)

= 671529 Btu/hr

Actual steam (measured –loss)

= 172187 kcal/hr

CO_2 production rate
=FT216*44.01/6.32/0.0022
=88778 g/hr

CO_2 production rate
=2017 gmol/hr

The actual reboiler duty (kJ/gmol CO_2) is given as:

$Q_{actual\ reb\ duty} = Q_{actual\ steam\ rate} / CO_2$ rate

= 85 kcal/gmol CO_2

= 359 kJ/gmol CO_2

Appendix D-7: Rate Model With Structured Packing

This appendix contains the rate model for 5m K^+/2.5m PZ. The model can be used for columns equipped with Montz B1-250 and Flexipac AQ Style 20 structured packing. The characteristics of other structured packing can be added to the model. The code can be obtained from Dr. Gary Rochelle at the University of Texas at Austin.

```
Model Rate Model using structured packing

//declaration of variables
Contactor as ContactorType;
// contactor refers to the different column internals

ns as integerparameter(2);
// ns is the number of segments into which the column has been divided.
// The first segment is the flash segment. This segment is quantified in terms of the height
of a normal
// segment i.e. under conditions where flashing occurs, this segment serves as an
additional segment.

nns as integerparameter;
// nns is the segment at which a side stream is introduced

Solvent as SolventType;
// solvent refers to the different solvent formulations

L([0:2*ns]) as realvariable;
// This is the total solvent rate in mol/s
lco2([0:2*ns]) as realvariable;
// This is the amount of co2 in the solvent in mol/s
lh2o([0:2*ns]) as realvariable;
// This is the amount of water in the solvent in mol/s
lamine([0:2*ns]) as realvariable;
// This is the amount of water in the solvent in mol/s
```

```
ldg([0:2*ns]) as realvariable;
//This is the loading of the solution in mol Co2/mol Alk
//mol Alk is defined as [mol MEA + mol K + mol 2 PZ + mol MDEA + mol KS-1]
ldgin as realvariable;
// This is the rich loading also equal to ldg (0) in mol CO2/ mol Alk
ldgout as realvariable;
// This is the lean loading also equal to ldg (2*ns) in mol CO2/ mol Alk

S([0:ns-1]) as realvariable;
// This is the total side solvent rate in mol/s
sco2([0:ns-1]) as realvariable;
// This is the amount of co2 in the side solvent in mol/s
sh2o([0:ns-1]) as realvariable;
// This is the amount of water in the side solvent in mol/s
samine([0:ns-1]) as realvariable;
// This is the amount of water in the side solvent in mol/s


CpL([0:2*ns]) as realvariable;
// Heat capacity of the solvent
CpS([0:ns-1]) as realvariable;
// Heat capacity of the side liquid stream
Tref as realvariable(298.15,fixed);
// reference temperature in Kelvin

T([0:2*ns]) as realvariable;
// Solvent temperature in Kelvin
Ts([0:ns-1]) as realvariable;
// Side solvent temperature in Kelvin
Treb as realvariable;
// Reboiler temperature in Kelvin
Tcond as realvariable;
// Condensing steam temperature in Kelvin
Tcool as realvariable(313.15,fixed);
// Temperature sink equal to cooling water temperature plus a 10K driving force in
Kelvin
Tx([1:ns]) as realvariable;
// lean solution temperature flowing up the column in the internal exchange configuration
Txdiff([1:ns]) as realvariable;
// temperature difference between solvent temperature and lean solvent flowing up the
column
// in the internal exchnage configuration
```

```
Qkcal as realvariable;
//This is the reboiler duty in kcal
Q([1:ns]) as realvariable;
//This is the heat stream on each segment in kcal
// It represents both heat addition (+) and heat removal (-)
Qreboiler as realvariable;
// This is the normalized reboiler duty in kcal/gmol CO2
// It is the reboiler duty (Qkcal) divided by the CO2 rate in the overhead gas stream
Qx([1:ns]) as realvariable;
// This referes to the heat addition or removal on a segment due to the heat exchange
// as a result of the internal exchange configuration
Qcomp([1:ns]) as realvariable;
// compression heat in kcal



Weq1 as realvariable;
// This is the total equivalent work to the maximum pressure of the stripper in kcal
Weq2 as realvariable;
// This is the normalized equivalent work in kcal/gmol CO2
// It is the equivalent work (Weq1) divided by the CO2 rate in the overhead gas stream
Wcomp([1:ns]) as realvariable;
//work of compression in kcal

G([1:ns+1]) as realvariable;
// This is the gas rate in mol/s
yco2([1:ns+1]) as realvariable;
// This is the CO2 mole fraction in the gas phase
yh2o([1:ns+1]) as realvariable;
// This is the water vapor mole fraction in the gas phase


Pco2e([0:2*ns]) as realvariable;
// This is the equilibrium partial pressure of CO2 in the liquid in kPa
Pco2([1:ns+1]) as realvariable;
//This is the partial pressure of CO2 in the gas phase in kPa
Ph2o([1:ns]) as realvariable;
// This is the partial pressure of water vapor in the gas phase in kPa
Pt([1:ns]) as realvariable(30);
// This is the total pressure on a segment in kPa
// It is equal to the sum of Pco2 and Ph2o
```

```
meff([1:ns]) as realvariable(fixed);
//Murphree efficiency for the reboiler
dH([1:ns+1]) as realvariable;
// heat of desorption of co2 from the amine
R as realvariable(0.08206,fixed);
// Universal gas constant

k as realvariable(1.3,fixed);

nn1 as realvariable;

compeff as realvariable(0.75,fixed);
// compressor efficiency
polyeff as realvariable(0.75,fixed);
// polytropic efficiency


cpco2([1:ns+1]) as realvariable;
// heat capacity of the co2 in the gas phase

UA as realvariable(1,fixed);
// overall heat transfer coefficient


ggeff([1:ns-1]) as realvariable;
// effective gravity in m/s2

//heat capacity coefficients for co2
cpc([1:5]) as realvariable;
cpc(1) : 29370,fixed;
cpc(2):34540,fixed;
cpc(3):1428,fixed;
cpc(4):26400,fixed;
cpc(5): 588,fixed;

cph2o([1:ns+1]) as realvariable;
//heat capacity coefficients for h20
cph([1:5]) as realvariable;
cph(1) : 33363.0,fixed;
cph(2):26790,fixed;
cph(3):2610.5,fixed;
cph(4):8896.0,fixed;
```

```
cph(5): 1169.0,fixed;

// Heat of vaporisation of water for a stage,kcal/gmol
Hvap as realvariable(10.47,fixed);

//Constants for water vapor pressure
AA as realvariable(73.649,fixed);
BB as realvariable(-7258.2,fixed);
CC as realvariable(-7.3037,fixed);
DD as realvariable(4.1653e-6,fixed);
EE as realvariable(2.0,fixed);

// Heat of desorption constants
aeq as realvariable(-4.59244,fixed);
beq as realvariable (34.21513,fixed);
ceq as realvariable (-3834.67,fixed);
deq as realvariable (-1747284,fixed);
eeq as realvariable (-1712091,fixed);
feq as realvariable (8186.474,fixed);


molalK as realvariable (5,fixed);
molalPZ as realvariable(5,fixed);
molalMEA as realvariable(0,fixed);
molaltotalk as realvariable;
co2moles as realvariable;
h2omoles as realvariable;


totalmoles as realvariable;

molaltotalk = molalK + molalPZ + molalMEA;


co2moles = ldgin * molaltotalk;

h2omoles = 1000/18.02;


totalmoles = co2moles + h2omoles + molaltotalk;
```

```
lamine(0) = molaltotalk * (L(0)/totalmoles);


Tapp as realvariable(10,fixed);
// temperature approach in the cross exchanger

Tg([1:ns+1]) as realvariable;

// heat capacity constants for solvent
cp([1:5]) as realvariable;

cp(1) : 276370.0,fixed;
cp(2):-2090.1,fixed;
cp(3):8.125,fixed;
cp(4):-0.014116,fixed;
cp(5): 9.3701e-006,fixed;

// Structured packing variables spec start here


// packing characteristics are specified here
//packarea1, packarea2 and packarea3 are regression constants based on the wetted area
data obtained by the SRP

// Packing factor Fp
Fp as realvariable;

packarea1 as realvariable;
packarea2 as realvariable;
packarea3 as realvariable;

// b is the crimp height
b as realvariable;

//void fraction of the packing
voidfrac as realvariable;

//angle with horizontal for corrugated channel
theta as realvariable;

// characteristic length
ss as realvariable;
```

```
//dry specific surface area of packing
apstr as realvariable;


if Contactor == "Montz B1-250" then
packarea1 = 0.617584;
packarea2 = 0.005441;
packarea3 = 0.036232;
b = 0.0225;
theta = 45;
ss = 0.01645;
apstr = 244;
voidfrac = 0.98;
Fp = 24;
else
if Contactor == "Flexipac AQ" then

b = 0.0388;
theta = 45;
ss = 0.022352;
apstr = 213;
voidfrac = 0.97;
Fp=17;
endif
endif

//Weber number of the liquid
WeL([0:2*ns]) as realvariable;
//Froude number of the liquid
FrL([0:2*ns]) as realvariable;
//Reynold's number of the liquid
ReL([0:2*ns]) as realvariable;

GaL([1:2*ns]) as realvariable;

lratio as realvariable;
Schl([1:2*ns]) as realvariable;

pi as realvariable (22/7,fixed);

//correction factor for total hold up
```

```
Ft([1:ns]) as realvariable;
//dPdzflood , Pa/m
dPdzflood as realvariable(2000,fixed);
//specific wetted area of the structured packing
awetstr([1:ns]) as realvariable;
//dry packing pressure drop
//dpdzdry([1:ns]) as realvariable;
//dpdz actual pressure drop
dpdz([1:ns]) as realvariable;
//hold up dimensionless
holdup([1:ns]) as realvariable;
//liquid phase mass transfer coefficient for structured packing
SRPklstr([1:ns]) as realvariable;// units of m/s
//gas phase mass transfer coefficient for structured packing
SRPkgstr([1:ns]) as realvariable;// units of m/s
klastr([1:ns]) as realvariable;//unit 1/s
kgastr([1:ns]) as realvariable;// unit 1/s

//Effective liquid superficial velocity
Ule([1:2*ns]) as realvariable;
//Effective gas superficial velocity
Uge([1:ns]) as realvariable;
//specific area of structured packing
//apstr as realvariable;

// definition of rate equation variables end here

//rate equations added here

// Constants for calculation of gas phase viscosity
// the constants are from the DIPPR database

//muco2 is the gas phase viscosity of co2, Pa-s
muco2([1:nS]) as realvariable;
amuco2 as realvariable(fixed,2.148e-6);
bmuco2 as realvariable(fixed,4.6e-1);
cmuco2 as realvariable(fixed,2.9e2);
dmuco2 as realvariable(fixed,0);

//muh2o is the gas phase viscosity of h2o - steam, Pa-s
muh2o([1:nS]) as realvariable;
amuh2o as realvariable(fixed,1.7096e-8);
```

```
bmuh2o as realvariable(fixed,1.1146);
cmuh2o as realvariable(fixed,0);
dmuh2o as realvariable(fixed,0);

// binary mixture gas viscosity
mugas([1:nS]) as realvariable;
//constants needed to calculate the viscosity of the binary gas mixture
phi12([1:nS]) as realvariable;
phi21([1:nS]) as realvariable;

// Molecular weights of gases
Mco2 as realvariable(fixed,44.1);
Mh2o as realvariable(fixed,18.02);
//Mgas is the molecular weight of the gas stream
Mgas([1:nS]) as realvariable;
//Pressure of the gas phase expressed in atm
Pgas([1:nS]) as realvariable;

//Universal Gas constant expressed as L atm K-1 mol -1
RR as realvariable(0.08206,fixed);

// Density of the gas phase kg/m3
rhog([1:nS]) as realvariable;

//Diffusivity of gas m2/s
Dv([1:nS]) as realvariable;

//Schmidt Number for the gas

Scg([1:nS]) as realvariable;


//critical constants for co2 and water

Pcco2 as pressure(72.9,fixed);
Pch2o as pressure(220,fixed);
Tcco2 as temperature(304.2,fixed);
Tch2o as temperature(647,fixed);

//density of the  liquid
rhol([0:2*nS]) as realvariable;
```

```
//equivalent weight of PZK expressed as a percent

we as realvariable(22.14,fixed);

//mul is the liquid phase viscosity , Pa-s
mul([0:2*nS]) as realvariable;
amul as realvariable;
bmul as realvariable;
cmul as realvariable;

//viscosity of liquid water Pa-s
muliqh2o([0:2*nS]) as realvariable;
amuliqh2o as realvariable (-5.2843e1,fixed);
bmuliqh2o as realvariable (3.7036e3,fixed);
cmuliqh2o as realvariable (5.8660,fixed);
dmuliqh2o as realvariable (-5.8790e-29,fixed);
emuliqh2o as realvariable (10,fixed);

// Diffusivity of co2 in pure water m2/s
Dco2pureh2o([0:2*nS]) as realvariable;

// Diffusivity of the liquid m2/s
Dl([0:2*nS]) as realvariable;


// Pressure drop at flooding in H2o per ft of packing
deltaPflood as realvariable;

//Total surface area of packing m2/m3
ap as realvariable;

// gas phase mass transfer coefficient from the Onda correlation (1968)
//the unit of kg is kmol/m2.s.Pa

ONDAkg([1:nS]) as realvariable;

//kg for the contactor kmol/m2.s.Pa
kg([1:nS]) as realvariable;

//liquid phase mass tranfer coefficient from the ONDA correlation (1968)
//the unit of ONDAkl is m/s
```

```
ONDAkl([1:nS]) as realvariable;

//kl of contactor m/s
kl([1:nS]) as realvariable;


//column area m2
AREA as realvariable(0.143,fixed);

//constant for kg calculation
CO as realvariable;

// wetted area based on Wilson (2004) experiments

awet([1:nS]) as realvariable;

// nominal diameter of random packing, m

dn as realvariable;

//wetted area from the Onda correlation (1968)
// the unit of ONDAaw is m2/m3

ONDAaw([1:nS]) as realvariable;

//critical surface tension N/m
surftenc as realvariable;

//surface tension of the liquid
surftenl as realvariable(0.04,fixed);

//superficial velocity of the liquid
sul([0:2*nS]) as realvariable;


//correction factor for liq density
corrrhol([0:2*nS]) as realvariable;

//correction factor for liq viscosity
corrmul([0:2*nS]) as realvariable;

//liquid to gas kinetic energy ratio
```

```
FLG as realvariable;

//density of liquid water
rholiqh2o ([0:2*nS]) as realvariable;

//constants in water density equation obtained from the DIPPR database

arh2o as realvariable(1.7863e1,fixed);
brh2o as realvariable(5.8606e1,fixed);
crh2o as realvariable(-9.5396e1,fixed);
drh2o as realvariable(2.1389e2,fixed);
erh2o as realvariable(-1.4126e2,fixed);


// Y axis of Leva GPDC plot

Ygeneral as realvariable;

//Superficial gas velocity m/s
sug([1:nS]) as realvariable;

//Flooding fraction
f as fraction(free,0.8);

//superficial gas velocity at flooding

uo as realvariable;

//Diameter of Tower m

DT as realvariable;
Factor as realvariable(fixed);
height([1:ns]) as realvariable;

//acceleration due to gravity m/s2
gg as realvariable(9.81,fixed);
//New variables
Nco2([1:ns]) as realvariable;
kgprime([1:ns]) as realvariable;
Pco2i([1:ns]) as realvariable;
KGbig([1:ns]) as realvariable;
```

```
Nh2o([1:ns]) as realvariable;
Ph2oi([1:ns]) as realvariable;
volseg([1:ns]) as realvariable;
awetted([1:ns]) as realvariable(10);
heightseg([1:ns]) as realvariable(1.5);
kla([1:ns]) as realvariable;
kga([1:ns]) as realvariable;

// heat tranfer coefficient in the gas phase
hg([1:ns]) as realvariable;
// heat capacity of the gas
cpgas([1:ns]) as realvariable;
//Prandtl number of the gas
Prgas([1:ns]) as realvariable;
//thermal conductivity
thermalk as realvariable (0.02,fixed);
//heat transfer at the interface
Qint([1:ns]) as realvariable;

gasvelflood as realvariable;//ft/s
sugflood as realvariable;

Flowrate as realvariable(fixed);//gallons per sec

Fse as realvariable(0.35,fixed);
klstr([1:ns-1]) as realvariable;
kgstr([1:ns-1]) as realvariable;
SRPawetstr([1:ns-1]) as realvariable;
ffactor([1:ns]) as realvariable;

// friction facor
frictionfactor([1:ns-1]) as realvariable;
// constants for friction factor expression
Afric as realvariable(0.194,fixed);
Bfric as realvariable(212.929,fixed);
// Dry prssure drop
dpdzdry([1:ns-1]) as realvariable;
//pressure drop at preload
dpdzpreload([1:ns-1]) as realvariable;
```

```
// definition of rate equation variables end here

// rate equations start

//calculation of gas phase viscosities

for i in[1:nS] do
muco2(i)= (amuco2*(Tg(i)^bmuco2))/(1+(cmuco2/Tg(i))+(dmuco2/Tg(i)/Tg(i)));
muh2o(i)= (amuh2o*(Tg(i)^bmuh2o))/(1+(cmuh2o/Tg(i))+(dmuh2o/Tg(i)/Tg(i)));
mugas(i)=
(muco2(i)/(1+((yh2o(i)/yco2(i))*phi12(i))))+(muh2o(i)/(1+((yco2(i)/yh2o(i))*phi21(i))));


//calculation of constants in binary gas mixture viscosity equation
phi12(i) = ((1+(((muco2(i)/muh2o(i))^0.5)*
((Mh2o/Mco2)^0.25)))^2)/(2*sqrt(2.0)*((1+(Mco2/Mh2o))^0.5));
phi21(i) = ((1+(((muh2o(i)/muco2(i))^0.5)*
((Mco2/Mh2o)^0.25)))^2)/(2*sqrt(2.0)*((1+(Mh2o/Mco2))^0.5));

// calculation of gas density in kg/m3

Mgas(i)= (yco2(i)*Mco2)  + (yh2o(i)*Mh2o);
Pgas(i) = Pt(i)*0.009869;//This converts the pressure from kPa to atm//
rhog(i)= Pgas(i)*Mgas(i)/RR/Tg(i);



//Calculation of diffusivity of the gas m2/s from BSL
Dv(i)=(((3.64e-
4*((Tg(i)/sqrt(Tcco2*Tch2o))^2.334))*((Pcco2*Pch2o)^(1/3))*((Tcco2*Tch2o)^(5/12))*
sqrt((1/Mco2)+(1/Mh2o)))/Pgas(i))/10000;

//calculation of Schmidt number for the gas
Scg(i)= mugas(i)/rhog(i)/Dv(i);

endfor

amul = (2.79e-7 *we*we)-(2.04e-6*we) + 9.65e-5;
bmul = (-2e-4 *we*we)+(1.37e-3*we) - 7.23e-2;
cmul = (3.63e-2 *we*we)-(0.225*we) + 13.86;
```

```
for i in [0:2*ns] do

// density of the liquid kg/m3
rhol(i)= ((((-1.93e-6*we)-(4.74e-4))*T(i))+(9.787e-3*we)+1.147)*1000;

// viscosity of the liquid Pa-s
// 0.001 is the conversion factor from cP to Pa-s

mul(i)= ((amul*T(i)*T(i))+(bmul*T(i))+cmul)*0.001;

//viscosity of pure liquid water Pa-s

muliqh2o(i) = exp(amuliqh2o+(bmuliqh2o/T(i))+ (cmuliqh2o*loge(T(i))) +
(dmuliqh2o*(T(i)^emuliqh2o)));

//Diffusivity of co2 in pure water
//This is given by Versteeg and van Swaaij(1998)

Dco2pureh2o(i) = (0.0240 * exp(-2122/T(i)))*0.0001;

// calculation of the density of liquid water

rholiqh2o(i) = (arh2o + (brh2o*((1-(T(i)/Tch2o))^0.35)) + (crh2o*((1-
(T(i)/Tch2o))^0.67)) + (drh2o*((1-(T(i)/Tch2o))^1.0))+ (erh2o*((1-
(T(i)/Tch2o))^1.33)))*Mh2o;

// calculation of correction factor for liquid density

corrrhol(i) = (1.7995*(rholiqh2o(i)/rhol(i)))-0.6469;

// calculation of correction factor for liquid viscosity

corrmul(i) = (0.1119*(mul(i)/0.001))+0.6664;

// Diffusivity of co2 in the liquid m2/s
// This is based on the Ratcliff and Holdcroft correlation (1963)
// factor 0.82 proposed by Joosten and Danckwerts (1972)

Dl(i) = Dco2pureh2o(i) / ((mul(i)/ muliqh2o(i))^0.82);

//calculation of the superficial velocity of the liquid
sul(i)=flowrate * 0.00358/AREA;
```

```
endfor


for i in [1:ns-1] do

frictionfactor(i) = Afric + (Bfric/(rhog(i)*sug(i)*ss/mugas(i)));
// the dry pressure drop is in Pa/m
dpdzdry(i) = (frictionfactor(i) *(rhog(i)/ss)* ((Uge(i)/voidfrac/0.7071)^2));
//the preload pressure drop is in Pa/m
dpdzdry(i) - (dpdzpreload(i) * ((1 - ((0.614 + 71.35 *ss)*holdup(i)))^5))=0;


endfor




//for i in [1:ns] do
// calculation of liquid to gas kinetic energy ratio

FLG^2 = (L(2*0)*25.5/G(ns)/Mgas(ns))^2*(rhog(ns)/rhol(2*0));

deltaPpacking as realvariable;

// calculation of the superficial velocity of the gas m/s
Ygeneral = (-0.3148 * loge(FLG)) + 0.7936  ;

f = sug(ns)/sugflood;

//deltaPpacking = f * deltaPflood;

//f = 0.8;

Csb as realvariable;
Ygeneral = Csb * (Fp^0.5) * ((mul(2*0)*1000*2.15)^.05);


Csb = gasvelflood  / sqrt(((rhol(2*0))-(rhog(ns)))/(rhog(ns)));

//(gasvel)^2 = (Ygeneral*32.2*1000/Fp/rhog(ns)/corrrhol(2*0)/corrmul(2*0));
```

```
sugflood = gasvelflood * 0.3048;
for i in [1:ns] do
sug(i) = G(i) * Mgas(i)/1000/rhog(i)/AREA;
endfor
//AREA = ((Flowrate/60) * 0.00378)/sug(ns);

// Y axis for Leva GPDC plot calculation

//Ygeneral = (0.0238 *(FLG^-0.5666));
//endfor
//Diameter of column in m
//DT^2 = (4.0*G(nS)*Mgas(nS)/1000/f/uo/3.142/rhog(nS));
//uo = sug(ns);

//f =deltaPpacking/deltaPflood;

// calculation of pressure drop at flooding
deltaPflood = 1.5;

//Area of the column, m2
AREA = 3.142*DT*DT/4;

//L(0)   * 0.00378 /60  = AREA * sug(ns);
for i in [1:ns-1] do

 //Flux based on the liquid phase
///*
Nco2(i) = ((kg(i)*1000 * Pt (i) * loge (Pco2i(i)/Pco2(i))) + Nh2o(i)) * (Pco2i(i) -
Pco2(i))/(Pco2i(i) - Pco2(i) + (Pt(i) * loge(Pco2i(i)/Pco2(i))));

Nco2(i) = KGbig(i)*1000*(Pco2e(2*i)-Pco2(i));


//Nh2o(i) = ((kg(i)*1000 * Pt (i) * loge (Ph2oi(i)/Ph2o(i))) + Nco2(i)) * (Ph2oi(i) -
Ph2o(i))/(Ph2oi(i) - Ph2o(i) + (Pt(i) * loge(Ph2oi(i)/Ph2o(i))));

Ph2oi(i) + Pco2i(i) = Pt(i);

Nco2(i) = kgprime(i) *1000* (Pco2e(2*i) - Pco2i(i));

kgprime(i) = 0.2 * (exp(-46.6868 + (-11.5447*ldg(2*i)) + (8197.802/T(2*i)) +
(10050.46* kl(i)) + (0.012346*Pco2i(i)) + (69294.95 * ldg(2*i)/T(2*i))+(-
```

```
3182533*kl(i)/T(2*i))+(-6.06135*Pco2i(i)/T(2*i)) +(-
87538.9*ldg(2*i)*ldg(2*i)/T(2*i))+(-
2e7*ldg(2*i)/T(2*i)/T(2*i))+(26254990*ldg(2*i)*ldg(2*i)/T(2*i)/T(2*i))));

KGbig (i) = 1 / ((1/kg(i)) + (1/kgprime(i)));
lco2(2*i-1) = lco2(2*i) + (Nco2(i) * awetted(i) *1000);
//lh2o(2*i-1) = lh2o(2*i) + (Nh2o(i) * awetted(i) *1000);
volseg(i) = awetted(i) / awetstr(i);
volseg(i) = heightseg(i)*AREA;

endfor

/*
for i in [1:ns] do
cpgas(i) = (cpco2(i) *4184*1000* G(i) * yco2(i)/44) + (cph2o(i) *4184*1000* G(i) *
yh2o(i) /18.02);
Prgas(i) = cpgas(i) * mugas(i)/ thermalk;
kg(i) * 1000 *Mgas(i) * Pco2(i) * (Scg(i)^(2/3)) = hg(i) * (Prgas(i)^(2/3))/ cpgas(i);
Qint(i) = hg(i)* awetted(i) * (T(2*i) - Tg(i)) * 0.000239;
//(L(2*i-1)*cpL(2*i-1)*(T(2*i-1)-Tref)) - Qint(i) = (L(2*i)*cpL(2*i)*(T(2*i)-Tref));


endfor
*/



// rate equations end



nn1 = (k/(k-1))*polyeff;

for i in [0:2*ns] do

L(i) = lco2(i) + lh2o(i) + lamine(i);

ldg(i) = lco2(i)/lamine(i);

endfor

for i in [0:ns-1] do
```

```
S(i) = sco2(i) + sh2o(i) + samine(i);
endfor

for i in [0:ns-1] do
lco2((2*i)+1) = lco2(2*i) + sco2(i);
lh2o((2*i)+1) = lh2o(2*i) + sh2o(i);
lamine((2*i)+1) = lamine(2*i) + samine(i);
endfor


for i in [0:2*ns] do

CpL(i) = 0.8888 * ((cp(1) + (cp(2)*T(i))  + (cp(3) * (T(i)^2))+ (cp(4)*(T(i)^3))+
(cp(5)*(T(i)^4)))*(0.000000239));

endfor

for i in [0:ns-1] do
CpS(i) = (cp(1) + (cp(2)*Ts(i))  + (cp(3) * (Ts(i)^2))+ (cp(4)*(Ts(i)^3))+
(cp(5)*(Ts(i)^4)))*(0.000000239);
endfor


//Mixing operation

 for i in [0:ns-1] do
(L(2*i) * CpL(2*i) * (T(2*i)-Tref)) + (S(i)*CpS(i)*(Ts(i)-Tref)) = L(2*i+1) *
CpL(2*i+1) * (T(2*i+1)-Tref);
endfor

// heat capacity calculation for the gas phase

for i in [1:ns] do
cpco2(i)=(cpc(1) + (cpc(2)*(((cpc(3)/Tg(i))
/sinh(cpc(3)/Tg(i)))^2))+(cpc(4)*(((cpc(5)/Tg(i)) /cosh(cpc(5)/Tg(i)))^2)))*0.000000239;
cph2o(i)=(cph(1) + (cph(2)*(((cph(3)/Tg(i))
/sinh(cph(3)/Tg(i)))^2))+(cph(4)*(((cph(5)/Tg(i))
/cosh(cph(5)/Tg(i)))^2)))*0.000000239;
endfor


cpco2(ns+1):0,fixed;
```

```
cph2o(ns+1):0,fixed;

for i in [1:ns] do
Tg(i) = T(2*i);
endfor


// Material balance

for i in [1:ns] do
lco2(2*i-1) + (G(i+1)*yco2(i+1)) = lco2(2*i) + (G(i) * yco2(i));

lh2o(2*i-1) + (G(i+1)*yh2o(i+1)) = lh2o(2*i) + (G(i) * yh2o(i));

lamine(2*i-1) = lamine(2*i) ;

endfor


yco2(ns+1):0,fixed;
yh2o(ns+1):0,fixed;
dH(ns+1):0,fixed;

//temperature at the interface
Ti([1:ns]) as realvariable(330,free);


// energy balance
for i in [1:ns] do
(G(i+1)*((yh2o(i+1)*(Hvap+(cph2o(i+1)*(Tg(i+1)-
Tref))))+(yco2(i+1)*((dH(i+1)/1000)+(cpco2(i+1)*(Tg(i+1)-Tref))))))+(L(2*i-
1)*cpL(2*i-1)*(T(2*i-1)-Tref))+ Q(i)+ Qcomp(i) + Qx(i)  =(L(2*i)*cpL(2*i)*(T(2*i)-
Tref))+G(i)*(((yh2o(i))*(Hvap+(cph2o(i)*(Tg(i)-
Tref))))+((yco2(i))*((dH(i)/1000)+(cpco2(i)*(Tg(i)-Tref)))));
endfor

act1 as realvariable (0.97752477,fixed);
act2 as realvariable (-0.049949161,fixed);
act3 as realvariable (-31.55650762,fixed);
act([1:ns]) as realvariable;

for i in [1:ns] do
```

```
act(i) = act1 + (act2* ldg(2*i)) + (act3 * (1/T(2*i)));
endfor



//equilibrum reboiler assumption
//Pco2(ns)= Pco2e(2*ns);
Ph2o(ns)= act(ns) * ((exp(AA+(BB/T(2*ns))+(CC*loge(T(2*ns)))+
(DD*(T(2*ns)^EE))))/1000);


Pco2(ns)= Pco2(ns+1) + (meff(ns)*(Pco2e(2*ns) - Pco2(ns+1)));


for i in [1:ns-1] do

//Pco2(i)= Pco2(i+1) + (meff(i)*(Pco2e(2*i) - Pco2(i+1)));
//Ph2oi(i)= (exp(AA+(BB/Ti(i))+(CC*loge(Ti(i)))+ (DD*(Ti(i)^EE))))/1000;
Ph2o(i)= act(i) * ((exp(AA+(BB/T(2*i))+(CC*loge(T(2*i)))+
(DD*(T(2*i)^EE))))/1000);
endfor



/*
for i in [1:ns-1] do
meff(i):0.2;
endfor
*/
Tg(ns+1) : 0,fixed;
Pco2(ns+1):0,fixed;

//Calculation of heat of desorption of solvent based on generic constants
for i in [1:ns] do
dH(i) = (ceq+(2*deq*ldg(2*i)*ldg(2*i)/T(2*i)) + (2*eeq*ldg(2*i)/T(2*i)) +
(feq*ldg(2*i)) )* -1.987;
endfor


// Total pressure on a section
for i in [1:ns] do
Pt(i) = Pco2(i) + Ph2o(i);
```

```
endfor

// vapor mole fractions

for i in [1:ns] do

yco2(i) = Pco2(i)/Pt(i);

yh2o(i) = Ph2o(i)/ Pt(i);

endfor


//T(0) + Tapp = T(2*ns);

G(ns+1):0,fixed;

// equilibrium vapor pressure of CO2 expression
for i in [0:2*ns] do
Pco2e(i) = (exp(aeq + (beq*ldg(i)) + (ceq/T(i))
+(deq*ldg(i)*ldg(i)/T(i)/T(i))+(eeq*ldg(i)/T(i)/T(i))+(feq*ldg(i)/T(i))));
Endfor



Qreboiler = Q(ns)/G(1)/yco2(1);

//compression work

for i in [1:ns-1] do
//Wcomp(i) = (G(i+1)*1.987*Tg(i+1)*nn1*(((Pt(i)/Pt(i+1))^(1/nn1))-
1.0))/(1000*compeff);
Wcomp(i) =0;
Qcomp(i)= Wcomp(i);
endfor

Wcomp(ns):0,fixed;
Qcomp(ns):0,fixed;

for i in [1:ns-1] do
Q(i):0,fixed;
endfor
```

```
for i in [0:ns-1] do
Ts(i):0,fixed;
S(i):0,fixed;
sco2(i):0,fixed;
samine(i):0,fixed;
endfor



ldg(2*ns):fixed;

meff(ns):1,fixed;


for i in [1:ns-1] do
Q(i) : 0,fixed;
endfor

//Ts(nns) = T(2*ns) - 2 ;

Treb = T(2*ns);

Qkcal = Q(ns);

ldgin = ldg(0);

ldgout = ldg(2*ns);

Tcond = Treb +10;


/*
for i in [1:ns-1] do
//Qx(i) =0;

Qx(i) = UA * ((Tx(i)-T(2*i))-(Tx(i+1)-T(2*i))) / (loge((Tx(i)-T(2*i))/(Tx(i+1)-T(2*i))));

Qx(i) = L(2*i) * CpL(2*i) * (Tx(i+1)-Tx(i));

Txdiff(i) = Tx(i)- T(2*i);

endfor
```

```
Qx(ns)=0;

Tx(1) = T(0)+Tapp;

Tx(ns) = T(2*ns);
*/

for i in [1:ns] do
Qx(i) :0,fixed;
endfor

T(0)+ Tapp = T(2*ns);

L(0) = 0.00378 * flowrate / (0.0255/rhol(0));

//L(0) /7.082 = lamine(0);

LD([0:ns]) as realvariable;

Temp([0:ns]) as realvariable;

Pco2eq([0:ns]) as realvariable;

for i in [0:ns] do
LD(i) = ldg(2*i);
Temp(i) = T(2*i);
Pco2eq(i) = Pco2e(2*i);
endfor

//for i in [2:ns] do
//Pt(i) = Pt(1);
//endfor

//for i in [2:ns] do
//volseg(i) = volseg(1);
//endfor


// Structured packing equations start here
lratio = 3.617  - (0.12299*(pi/(180/theta))) + (0.001976*((pi/(180/theta))^2)) -
(0.000011167*((pi/(180/theta))^3));
```

```
//Refined model


for i in [1:ns] do
ffactor(i) = sug(i) * sqrt(rhog(i));
endfor


for i in [1:ns-1] do

ReL(2*i) = rhol(2*i) * sul(2*i) * b / mul(2*i);
GaL(2*i) = gg * b*b*b *rhol(2*i) * rhol (2*i)/mul(2*i)/mul(2*i);
Ft(i) *  (ReL(2*i)^0.2) * (voidfrac^0.6) * (1-(0.93*0.9))* ((sin(3.142/4))^0.3) = (29.12 *
((WeL(2*i)* FrL(2*i))^0.15) * (ss^0.359));


WeL(2*i) = (sul(2*i)^2) *  rhol(2*i) * ss / surftenl;
FrL(2*i) = (sul(2*i)^2) /  ss / gg;
holdup(i) = ((4 * Ft(i) /ss) ^(2/3))  * (( 3 * mul(2*i) * sul(2*i) / rhol(2*i) / voidfrac/
ggeff(i)/ sin (pi/4))^(1/3));

ggeff(i) = gg * ((rhol(2*i) - rhog(i))/rhol(2*i)) * (1- (dpdzpreload(i)/dpdzflood));

Uge(i) = sug(i)/(voidfrac/(1-holdup(i))/0.7071);
Ule(2*i) = sul(2*i) /voidfrac/holdup(i)/0.7071;


SRPawetstr(i) = apstr * Ft(i) * Fse;
SRPklstr(i)^2 = 4 * (Dl(2*i) * Ule(2*i)/pi/0.9/ss);
SRPkgstr(i) = 0.054 * (Dv(i)/ss)* ( ((Uge(i) + Ule(2*i))*rhog(i)*ss/mugas(i))^0.8) *
((mugas(i)/Dv(i)/rhog(i))^0.33);

//awetstr(i) =apstr * (packarea1 + (packarea2*flowrate*60*0.093/area) + (packarea3 *
sug(i)/0.3048));

//awetstr(i) = exp(5.289) * ((sug(i))^0.082) * ((L(i)*25.5/1000/area)^0.086);

//awetstr(i) = 0.7*apstr;
(SRPklstr(i) * SRPawetstr(i)/ awetstr(i)) = klstr(i);
```

```
klastr(i) = klstr(i) * awetstr(i);
klstr(i) = kl(i);



SRPkgstr(i) * SRPawetstr(i)/ awetstr(i) = kgstr(i);


kgastr(i) = kg(i) * awetstr(i);
kg(i) * Pt(i) *1000 * Mgas(i) / rhog(i) = kgstr(i);



endfor


Totalwettedarea as realvariable;
Totalwettedarea = sigma(awetted([1:ns-1]));
Totalvolpacking as realvariable;
Totalvolpacking = sigma(volseg([1:ns-1]));

Pt(ns):fixed;

for i in [2:ns-1] do
//Pt(i) = Pt(i+1) - (f*f*1.63 * heightseg(i));
Pt(i) = Pt(i-1) + ((Pt(ns)- Pt(1))/11);
endfor

heightseg(1) :fixed;

for i in [2:ns-1] do
heightseg(i) = heightseg(1);
endfor

// Pump head
Pumphead as realvariable;
// Pump work kcal/s
Wpump as realvariable;
//Equivalent work of the reboiler
Wreboiler as realvariable;
//Equivalent work of internal compression
Wintcomp as realvariable;
```

```
// stripperCO2 flow
stripperCO2flow as realvariable;

stripperCO2flow = G(1) * yco2(1);
totalheightseg as realvariable;

Pumphead = ((((Pt(1) - 101.325)*1000) / (rhol(0)*gg)) + totalheightseg);

totalheightseg = sigma(heightseg([1:ns-1]));

Wpump = ((flowrate * 0.00378541178)* rhol(0)*gg *Pumphead/0.65)*(0.000239);

Wreboiler = (0.75*(Q(ns)*((Tcond - Tcool)/Tcond))) ;

Wintcomp = (sigma(Qcomp([1:ns])));



//Equivalent work , kcal

Weq1 = (0.75*(Q(ns)*((Tcond - Tcool)/Tcond)))   + (sigma(Qcomp([1:ns]))) + Wpump;

//Equivalent work, kcal/gmol CO2

Weq2 = Weq1 / (G(1)*yco2(1));



for i in [1:6] do
awetstr(i) = 0.1*apstr;
endfor

for i in [7:11] do
awetstr(i) = 0.7*apstr;
endfor

end
```

References

. "Wikipedia - the free online encyclopedia." from http://en.wikipedia.org/wiki/.

Alatiqi, I., M. F. Sabri, et al. (1994). "Steady-state rate-modelling for CO_2/amine absorption-desorption systems." Gas Sep. Purif **8**: 3-11.

Alie, C., E. Backham, et al. (2005). "Simulation of CO_2 capture using MEA scrubbing: A flowsheet decomposition method." Energy Conserv. Manag. **46**: 475-87.

Alie, C., L. Backham, et al. (2004). "Simulation of CO_2 capture using MEA scrubbing: a flowsheet decomposition method." Energy Conversion and Management **46**(3): 475-487.

American Institute of Chemical Engineers (2004). Design Institute for Physical Properties

Appl, M. (1982). Removal of CO_2 and/or H_2S and/or COS from gases containing these constituents. US, BASF Aktiengesellschaft.

Aroonwilas, A. (2004). Evaluation of split-flow scheme for CO_2 absorption process using mechanistic mass-transfer and hydrodynamic model. 7th International Conference on Greenhouse Gas Control Technologies. Volume 1: Peer-Reviewed Papers and Plenary Presentations, IEA Greenhouse Gas Programme, Cheltenham, UK.

Aroonwilas, A. and A. Veawab (2006). Cost structure and performance of CO_2 capture unit using split-stream cycle 8th International Conference on Greenhouse Gas Control Technologies. Trondheim, Norway.

Aroonwilas, A. and A. Veawab (2006). Cost,energy consumption and performance of CO_2 capture process using MEA-MDEA and DEA-MDEA. 8th International Conference on Greenhouse Gas Control Technologies. Trondheim, Norway.

Bates, E. D., R. D. Mayton, et al. (2002). "CO_2 capture by a task-specific ionic liquid." J. Am. Chem. Soc. **124**(6): 926-927.

Bishnoi, S. (2000). Carbon Dioxide Absorption and solution equilibrium in piperazine activated methyldiethanolamine. Chemical Engineering. Austin, University of Texas-Austin**:** 270.

Bishnoi, S. and G. T. Rochelle (2002). "Absorption of CO_2 in aqueous PZ/MDEA." AIChE J. **48**(12): 2788-2799.

Bishnoi, S. and G. T. Rochelle (2002). "Thermodynamics of PZ/MDEA/H_2O/CO_2." Ind Eng Chem Res **41**(3): 604-612.

Bosch, H. (1989). Solvents and reactors for acid gas treating, The University of Twente, PhD. Dissertation.

Bullin, J. A., J. C. Polasek, et al. (1983). "How to reduce costs in amine-sweetening units." Chemical Engineering Progress **79**(3): 63-7.

Chen, C. C., H. I. Britt, et al. (1982). "Local composition model for excess Gibbs energy of electrolyte systems. Part I: Single solvent, single completely dissociated electrolyte systems." AIChE Journal **28**(4): 588-96.

Chen, C. C. and L. B. Evans (1986). "A local composition model for the excess Gibbs energy of aqueous electrolyte systems." AIChE Journal **32**(3): 444-54.

Chen, E., G. T. Rochelle, et al. (2006). Pilot plant for CO_2 capture with aqueous piperazine/potassium carbonate. 8th International Conference on Greenhouse Gas Control Technologies Trondheim,Norway.

Cullinane, J. T. (2002). Carbon Dioxide absorption in aqueous mixtures of potassium carbonate and piperazine. Chemical Engineering. Austin, University of Texas-Austin**:** 165.

Cullinane, J. T. (2005). Thermodynamics and Kinetics of aqueous piperazine with potassium carbonate for carbon dioxide absorption. Chemical Engineering. Austin, University of Texas-Austin**:** 295.

Cullinane, J. T., B. A. Oyenekan, et al. Aqueous piperazine/potassium carbonate for enhanced CO_2 capture. 7th International Conference on Greenhouse Gas Control Technologies. Volume 1: Peer-Reviewed Papers and Plenary Presentations, IEA Greenhouse Gas Programme, Cheltenham, UK, 2004.

Cullinane, J. T. and G. T. Rochelle (2004). "Thermodynamics of Aqueous Potassium Carbonate, Piperazine, and CO_2 Mixtures." Fluid Phase Equilibrium **227**: 197-213.

Dang, H. (2000). CO_2 absorption rate and solubility in monoethanolamine/piperazine/water. Chemical Engineering. Austin, University of Texas-Austin**:** 129.

Dang, H. and G. T. Rochelle (2003). "CO_2 absorption rate and solubility in MEA/PZ/H_2O." Sep. Sci. Tech. **38**(2): 337-357.

Desideri, U. and A. Paolucci (1999). "Performance modelling of a carbon dioxide removal system for power plants." Energy Convers. and Manag. **40**: 1899-1915.

Dixon, J. K., M. J. Muldoon, et al. (2005). Tuning ionic liquids for CO_2 gas absorption. AIChE Annual Meeting. Cincinnati,OH,USA.

Draxler, J., G. Stevens, et al. (2004). "The Selection of Absorbents for CO_2 Absorption with Minimum Energy Consumption." Journal of the European Federation of Chemical Engineering: Part A.

Escobillana, G. P., J. A. Saez, et al. (1991). "Behaviour of Absorption/Strpping Columns for the CO_2-MEA System; Modeling and Experiments." The Canadian Journal of Chemical Engineering **69**: 969-977.

Feron, P. H. M. and N. ten Asbroek New solvents based on amino-acid salts for CO_2 capture from flue gases. 7th International Conference on Greenhouse Gas Control Technologies. Volume 1: Peer-Reviewed Papers and Plenary Presentations, IEA Greenhouse Gas Programme, Cheltenham, UK, 2004.

Fisher, K. S., C. Beitler, et al. (2005). Integrating MEA regeneration with CO_2 compression and peaking to reduce CO_2 capture costs, DOE Final Report for Trimeric Corp. subcontract of DOE contract #DE-FG02-04ER84111.

Freguia, S. (2002). Modeling of CO_2 removal from Flue Gas with Monoethanolamine. Chemical Engineering. Austin, University of Texas-Austin**:** 183.

Freguia, S. and G. T. Rochelle (2003). "Modeling of CO_2 Capture by Aqueous Monoethanolamine." AIChE Journal **49**(7): 1676-1686.

Goff, G. S. and G. T. Rochelle (2004). "Monoethanolamine Degradation: O_2 Mass Transfer Effects Under CO_2 Capture Conditions." Industrial & Engineering Chemistry Research **43**(20): 6400-6408.

Goldstein, A. M., E. C. Brown, et al. (1986). "New FLEXSORB Gas Treating Technology for Acid Gas Removal." Energy Process **6**(2): 67-70.

Hilliard, M. D. (2005). Thermodynamics of Aqueous piperazine/Potassium Carbonate/Carbon Dioxide Characterized by Electrolyte MRTL Model within Aspen Plus, M.S.E. Thesis, University of Texas at Austin.

Hoff, K. A., T. Mejdell, et al. (2006). Solvents selection for a post combustion CO_2 capture process. 8th International Conference on Greenhouse Gas Control Technologies. Trondheim, Norway.

Idem, R., M. Wilson, et al. (2006). "Pilot Plant Studies of the CO_2 Capture Performance of Aqueous MEA and Mixed MEA/MDEA Solvents at the University of Regina CO_2 Capture Technology Development Plant and the Boundary Dam CO_2 Capture Demonstration Plant." Ind. Eng. Chem. Res. **45**: 2414-2420.

Imai, N. and K. Ishida Economic Study on CO_2 Capture and Sequestration from PCF Flue Gas. 7th International Conference on Greenhouse Gas Control Technology, Vancouver,Canada,2004

Jassim, M. S. and G. T. Rochelle (2006). "Innovative Absorber/Stripper Configurations for CO_2 Capture by Aqueous Monoethanolamine." Industrial & Engineering Chemistry Research **45**(8): 2465-72.

Jou, F.-Y., A. E. Mather, et al. (1995). "The Solubility of CO_2 in a 30 Mass Percent Monoethanolamine Solution." The Canadian Journal of Chemical Engineering **73**(1): 140-147.

King, C. J. (1966). "Turbulent liquid-phase mass transfer at a free gas-liquid interface." Ind. Eng. Chem., Fundamentals **5**(1): 1-8.

Kirk Othmer Encyclopedia of Chemical Technology, Ed. (2004). Wiley.

Leites, I. L., D. A. Sama, et al. (2003). "The Theory and Practice of Energy Saving in the Chemical Industry: Some Methods for Reducing Thermodynamic Irreversibility in Chemical Technology Processes." Energy (Oxford, United Kingdom) **28**(1): 55-97.

Ma'mum, S., H. F. Svendsen, et al. Selection of new absorbents for carbon dioxide capture. 7th International Conference on Greenhouse Gas Control Technologies. Volume 1: Peer-Reviewed Papers and Plenary Presentations, IEA Greenhouse Gas Programme, Cheltenham, UK, 2004.

McLees, J. A. (2006). Vapor-liquid equilibrium of monoethanolamine/piperazine/water at 35-70^{o}C, The University of Texas at Austin. M.S. Thesis.

Mimura, T., H. Simayoshi, et al. (1997). "Development of energy saving technology for flue gas carbon dioxide recovery in power plant by chemical absorption method and steam system." Energy Conversion and Management **38**(Suppl., Proceedings of the Third International Conference on Carbon Dioxide Removal, 1996): S57-S62.

Mitsubishi Heavy Industries "A feasible new flue gas CO_2 recovery technology for enhanced oil recovery."

Mitsubishi Heavy Industries "Flue gas CO_2 recovery." Trade Publication.

Mock, B., L. B. Evans, et al. (1986). "Thermodynamic representation of phase equilibria of mixed-solvent electrolyte systems." AIChE Journal **32**(10): 1655-64.

Okoye, C. I. (2005). Carbon dioxide solubility and absorption rate in monoethanolamine/piperazine/water. Department of Chemical Engineering. Austin, The University of Texas at Austin,M.S.Thesis.

Onda, K., H. Takeuchi, et al. (1968). "Mass transfer coefficients between gas ad liquid phases in packed columns." Journal of Chemical Engineering of Japan **1**(1): 56-62.

Oyenekan, B. A. and G. T. Rochelle (2005). Modeling of Innovative Stripper Concepts. 8th International Post Combustion CO_2 Capture Network Meeting. Austin,Texas, USA.

Oyenekan, B. A. and G. T. Rochelle (2006). Alternative Stripper Configurations to Minimize Energy for CO_2 Capture. 8th International Conference on Greenhouse Gas Control Technologies. Trondheim,Norway.

Oyenekan, B. A. and G. T. Rochelle (2006). "Energy Performance of Stripper Configurations for CO_2 Capture by Aqueous Amines." Ind Eng Chem Res **45**(8): 2457-64.

Polasek, J. C., J. A. Bullin, et al. (1982). "Alternative Flow Shemes to Reduce Capital and Operating Costs of Amine Sweetening Units." Energy Processing/Canada **74**(5): 45-50.

Posey, M. L., K. G. Tapperson, et al. (1996). "A simple model for prediction of acid gas solubilities in alkanolamines." Gas. Sep. Purif. **10**(3): 181-186.

Rocha, J. A., J. L. Bravo, et al. (1996). "Distillation columns containing structured packings: A comprehensive model for their performance. 2. Mass transfer model." Ind Eng Chem Res **35**: 1660-67.

Rochelle, G. T. (2003). Innovative Stripper Configurations to Reduce the Energy Cost of CO_2 Capture. Second Annual Carbon Sequestration Conference, Alexandria, VA.

Rochelle, G. T., S. Bishnoi, et al. (2001). Research needs for CO_2 capture from flue gas by aqueous absorption/stripping. Austin, The University of Texas.

Rochelle, G. T., G. S. Goff, et al. (2002). Research results for CO_2 capture from flue gas by aqueous absorption/stripping.

Sandall, O. C., E. B. Rinker, et al. (1993). Acid Gas Treating by Aqueous Alkanolamines, Gas Research Insititute**:** 49.

Sartori, G., W. S. Ho, et al. (1985). Gas Treating with Solvents. Separation Technology Symposium, Princeton, NJ.

Sartori, G., W. S. Ho, et al. (1987). "Sterically Hindered Amines for Acid-Gas Absorption." Separation and Purification Methods **16**(2): 171-200.

Sartori, G. and D. W. Savage (1983). "Sterically hindered amines for carbon dioxide removal from gases." Industrial & Engineering Chemistry Fundamentals **22**(2): 239-49.

Sartori, G. and D. W. Savage (1983). "Sterically Hindered Amines for CO_2 Removal from Gases." Industrial & Engineering Chemistry Fundamentals **22**(2): 239-249.

Sexton, A. and G. T. Rochelle (2006). Oxidation products of amines in CO_2 capture. 8th International Conference on Greenhouse Gas Control Technologies. Trondheim,Norway.

Shimizu, S., M. Onoda, et al. (2006). Novel absorbents for CO_2-capture from gas stream. 8th International Conference on Greenhouse Gas Control Technologies. Trondheim,Norway.

Suenson, M. M., C. Georgakis, et al. (1985). "Steady-state and dynamic modeling of a gas absorber-stripper system." Industrial & Engineering Chemistry Fundamentals **24**(3): 288-95.

Suzuki, H., T. Iwaki, et al. (1999). Method for the removal of carbon dioxide present in gases. U.S.P.N. 5,904,908. .

Tobiesen, A., T. Mejdell, et al. (2006). A comparative study of experimental and modeling performance results from the CASTOR Esbjerg pilot plant. 8th International Conference on Greenhouse Gas Control Technologies. Trondheim, Norway.

Tobiesen, A. and H. F. Svendsen (2004). Modeling of desorber:Minimizing the energy demand for solvent recovery. 2nd Trondheim Conference on CO_2 Capture, Transport and Storage.

Tobiesen, F. A. and H. F. Svendsen (2006). "Study of a Modified Amine Based Regeneration Unit." Ind Eng Chem Res **45**(8): 2489-96.

Tobiesen, F. A., H. F. Svendsen, et al. (2005). "Desorber energy consumption in amine based absorption plants." Int. J of Green Energy **2**: 1-15.

USEIA (2006). Annual Energy Outlook 2006 with Projections to 2030, U.S. Energy Information Administration.

USEPA (2006). Inventory of U.S. Greenhouse Gas Emissions and Sinks 1990 - 2004, U.S. Environmental Protection Agency.

Veldman, R. and T. Ball (1991). "Improve gas treating." Chemical Engineering Progress **87**(1): 67-72.

Versteeg, G. F., P. S. Kumar, et al. (2002). "New absorption liquids for the removal of CO_2 from dilute gas streams using membrane contactors." Chemical Engineering Science **57**(9): 1639-1651.

Vickery, D. J., S. W. Campbell, et al. (1988). "Gas treating with promoted amines." Proceedings - Lawrence Reid Gas Conditioning Conference **38**: 1-16.

Weiland, R. H., T. Chakravarty, et al. (1985). "Reaction of acid gases with mixtures of amines." Chemical Engineering Progress **81**(4): 32-6.

Weiland, R. H., M. Rawal, et al. (1982). "Stripping of carbon dioxide from monoethanolamine solutions in a packed column." AIChE Journal **28**(6): 963-73.

Wilson, I. (2004). Gas-liquid contact area of random and structured packing. The University of Texas at Austin, TX.

Yagi, Y., T. Mimura, et al. (2006). Development and improvement of CO_2-capture system. 8th International Conference on Greenhouse Gas Control Technologies. Trondheim, Norway.

Vita

Babatunde Adegboyega Oyenekan was born on May 30, 1977 in Ibadan, Oyo State, Nigeria to Dr. Joseph Adegoke and Anne Adetoun Oyenekan. He graduated from Command Secondary School, Ibadan Oyo State, Nigeria in 1993. He earned a Bachelor of Science degree in Chemical Engineering from The University of Lagos, Nigeria in 1999 graduating with First Class Honors. He was a Chemical, Gas and Process Trainee Engineer with Chevron Nigeria Limited from December 1999 to December 2000. He was admitted to North Carolina Agricultural and Technical University in January 2001 and was awarded the Master of Science degree in December 2003. He was admitted to The University of Texas at Austin in January 2003 to pursue his Ph.D. studies. In the summer of 2005, he worked at Praxair Technology Center, Tonawanda, New York.

Full time employment has been accepted with Chevron Energy Technology Company in Richmond, California.

Permanent Address: 16 Odebunmi Afonka Street, Shasha, Lagos, Nigeria.

This dissertation was typed by the author.